S

OCT 10 2000
STA 4 (S)

ENGINEERING DATA TRANSMITTAL

Page 1 of _____

1. EDT 629783

2. To: (Receiving Organization)	3. From: (Originating Organization)	4. Related EDT No.:
Distribution	Process Engineering	N/A
5. Proj./Prog./Dept./Div.:	6. Design Authority/ Design Agent/Cog. Engr.:	7. Purchase Order No.:
Spent Nuclear Fuel Project	D. R. Duncan	N/A
8. Originator Remarks: Transmittal for approval and release.		9. Equip./Component No.: N/A
		10. System/Bldg./Facility: N/A
11. Receiver Remarks: 11A. Design Baseline Document? [] Yes [X] No		12. Major Assm. Dwg. No.: N/A
		13. Permit/Permit Application No.: N/A
USQ Screening Number: K-00-1242 CSB-00-1274 CVDF-00-1882		14. Required Response Date: ASAP

15. DATA TRANSMITTED

(A) Item No.	(B) Document/Drawing No.	(C) Sheet No.	(D) Rev. No.	(E) Title or Description of Data Transmitted	(F) Approval Desig-nator	(G) Reason for Trans-mittal	(H) Origi-nator Dispo-sition	(I) Receiv-er Dispo-sition
1	SNF-6781	N/A	0	Uranium Pyrophoricity Phenomena and ~~Precition~~ Prediction (FAI/00-39)	S^N, Q	1,2	1	1

16. KEY

Approval Designator (F)	Reason for Transmittal (G)		Disposition (H) & (I)	
E, S, Q, D or N/A (see WHC-CM-3-5, Sec.12.7)	1. Approval	4. Review	1. Approved	4. Reviewed no/comment
	2. Release	5. Post-Review	2. Approved w/comment	5. Reviewed w/comment
	3. Information	6. Dist. (Receipt Acknow. Required)	3. Disapproved w/comment	6. Receipt acknowledged

17. SIGNATURE/DISTRIBUTION
(See Approval Designator for required signatures)

(G) Reason	(H) Disp.	(J) Name (K) Signature (L) Date (M) MSIN	(G) Reason	(H) Disp.	(J) Name (K) Signature (L) Date (M) MSIN
		Design Authority			
		Design Agent			
1	1	Cog.Eng. D.R. Duncan DR Duncan 10/9/00 R3-86			
1	1	Cog. Mgr. J.R. Frederickson J.R. Frederickson 10/9/00 R3-86			
1	1	QA D. W. Smith 48 DW Smith 10/9/00 S2-			
1	1	Safety L. J. Garvin 26 10/10/00 R3-			
		Env.			

18.	19.	20.	21. DOE APPROVAL (if required)
D.R. Duncan DR Duncan 10/9/00 Signature of EDT Originator Date	J.R. Frederickson J.R. Frederickson 10/10/00 Authorized Representative for Receiving Organization Date	J.R. Frederickson J.R. Frederickson 10/10/00 Design Authority/ Cognizant Manager Date	Ctrl. No. N/A [] Approved [] Approved w/comments [] Disapproved w/comments

BD-7400-172-2 (05/96) GEF097

BD-7400-172-1

DISTRIBUTION SHEET

To	From	Page 1 of 1
Distribution	Process Engineering	Date 10/6/00
Project Title/Work Order		EDT No. 629783
Uranium Pyrophoricity Phenomena and Prediction (FAI/00-39)		ECN No. N/A

Name	MSIN	Text With All Attach.	Text Only	Attach./ Appendix Only	EDT/ECN Only
Spent Nuclear Fuel Project					
R. D. Crowe	R3-26	X			
D. R. Duncan (5)	R3-86	X			
J. R. Frederickson	R3-86	X			
L. J. Garvin	R3-26	X			
R. L. McCormack	R3-11	X			
B. J. Makenas	H0-40	X			
C. T. Miller	X3-79	X			
L. J. Olguin	H5-24	X			
A. L. Pajunen	R3-86	X			
J. A. Swenson	R3-11	X			
D. J. Trimble	R3-86	X			
SNF Project Files	R3-11	X			
DOE/RL					
P. G. Loscoe	R3-81	X			
Offsite					
M. G. Plys Fauske & Associates, Inc. 16W070 W. 83rd St. Burr Ridge, IL 60521		X			

SNF-6781
Revision 0

Uranium Pyrophoricity Phenomena and Prediction (FAI/00-39)

Prepared for the U.S. Department of Energy
Assistant Secretary for Environmental Management

Project Hanford Management Contractor for the
U.S. Department of Energy under Contract DE-AC06-96RL13200

Fluor Hanford
P.O. Box 1000
Richland, Washington

SNF-6781
Revision 0
EDT 629783

Uranium Pyrophoricity Phenomena and Prediction (FAI/00-39)

Division: SNF

M. G. Plys
Fauske & Associates

D. R. Duncan
Fluor Hanford

Date Published
October 2000

Prepared for the U.S. Department of Energy
Assistant Secretary for Environmental Management

Project Hanford Management Contractor for the
U.S. Department of Energy under Contract DE-AC06-96RL13200

Fluor Hanford
P.O. Box 1000
Richland, Washington

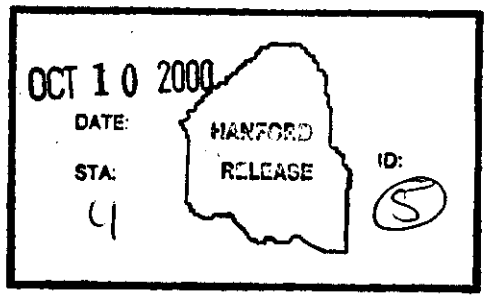

Release Approval

10/10/00
Date

Release Stamp

Approved for public release; further dissemination unlimited

TRADEMARK DISCLAIMER

Reference herein to any specific commercial product, process, or service by trade name, trademark, manufacturer, or otherwise, does not necessarily constitute or imply its endorsement, recommendation, or favoring by the United States Government or any agency thereof or its contractors or subcontractors.

This report has been reproduced from the best available copy.
Available in paper copy and microfiche.

Available electronically at http://www.doe.gov/bridge. Available for a processing fee to the U.S. Department of Energy and its contractors, in paper, from:
U.S. Department of Energy
Office of Scientific and Technical Information
P.O. Box 62
Oak Ridge, TN 37831-0062
phone: 865-576-8401
fax: 865-576-5728
email: reports@adonis.osti.gov(423) 576-8401

Available for sale to the public, in paper, from:
U.S. Department of Commerce
National Technical Information Service
5285 Port Royal Road
Springfield, VA 22161
phone: 800-553-6847
fax: 703-605-6900
email: orders@ ntis.fedworld.gov
online ordering: http://www.ntis.gov/ordering.htm

Printed in the United States of America

Total Pages: 265

FAI/00-39
URANIUM PYROPHORICITY PHENOMENA AND PREDICTION

Submitted To:

Fluor Hanford, Inc.

P.O. Box 1000

Richland, WA 99352

Prepared By:

Martin G. Plys, Michael Epstein, and Boro Malinovic

Fauske & Associates, Inc.

16W070 West 83rd Street

Burr Ridge, Illinois 60521

Tel: (630) 323-8750 Fax: (630) 986-5481

June 2000

Table of Contents

List of Figures

List of Tables

List of Acronyms

AEC	
CCDF	Complimentary Cumulative Distribution Function
CSB	Canister Storage Building
CVD	Cold Vacuum Drying
DOE	U.S. Department of Energy
DUN	Douglas United Nuclear
IE	Ignition Energy
IWTS	Integrated Water Treatment System
MCO	Multi-Canister Overpack
MIE	Minimum Ignition Energy
RH	Relative Humidity
SNF	Spent Nuclear Fuel

Uranium Pyrophoricity Phenomena and Prediction (FAI/00-39)

1.0 PURPOSE AND BACKGROUND

The purpose of this report is to provide a topical reference on the phenomena and prediction of uranium pyrophoricity for the Hanford Spent Nuclear Fuel (SNF) Project with specific applications to SNF Project processes and situations.

Spent metallic uranium nuclear fuel is currently stored underwater at the K basins in the Hanford 100 area, and planned processing steps include: (1) At the basins, cleaning and placing fuel elements and scrap into stainless steel multi-canister overpacks (MCOs) holding about 6 MT of fuel apiece; (2) At nearby cold vacuum drying (CVD) stations, draining, vacuum drying, and mechanically sealing the MCOs; (3) Shipping the MCOs to the Canister Storage Building (CSB) on the 200 Area plateau; and (4) Welding shut and placing the MCOs for interim (40 year) dry storage in closed CSB storage tubes cooled by natural air circulation through the surrounding vault. Damaged fuel elements have exposed and corroded fuel surfaces, which can exothermically react with water vapor and oxygen during normal process steps and in off-normal situations.

A key process safety concern is the rate of reaction of damaged fuel and the potential for self-sustaining or runaway reactions, also known as uranium fires or fuel ignition. Uranium metal and one of its corrosion products, uranium hydride, are potentially pyrophoric materials. Dangers of pyrophoricity of uranium and its hydride have long been known in the U.S. Deparment of Energy (Atomic Energy Commission/DOE) complex and will be discussed more below; it is sufficient here to note that there are numerous documented instances of uranium fires during normal operations.

The motivation for this work is to place the safety of the present process in proper perspective given past operational experience. Steps in development of such a perspective are:

1. Description of underlying physical causes for runaway reactions,
2. Modeling physical processes to explain runaway reactions,
3. Validation of the method against experimental data,
4. Application of the method to plausibly explain operational experience, and
5. Application of the method to present process steps to demonstrate process safety and margin.

Essentially, the logic above is used to demonstrate that runaway reactions cannot occur during normal SNF Project process steps, and to illustrate the depth of the technical basis for such a conclusion. Some off-normal conditions are identified here that could potentially lead to runaway reactions. However, this document is not intended to provide an exhaustive analysis of such cases.

In summary, this report provides a "toolkit" of models and approaches for analysis of pyrophoricity safety issues at Hanford, and the technical basis for the recommended approaches. A summary of recommended methods appears in Section 9.0.

2.0 RUNAWAY REACTION PHENOMENA

Runaway reaction phenomena have been studied and modeled since the early portion of the 20th century, for applications such as predictions of the critical temperature to cause an explosion and understanding of combustion for commercial power production. Good general references on the topic include *Combustion Science* by J. C. Jones and *Thermal Explosion Theory* by P. Gray and P. R. Lee [see References, Sec. 10.0]; these references cite and organize many important papers in the literature. A brief description of runaway reactions, or spontaneous ignition, is provided here to introduce the mathematical models that follow.

Spontaneous ignition may occur in systems with exothermic reactions under the proper conditions. Fundamentally, when the rate of heat generation due to exothermic reactions exceeds the rate of heat loss from a system, the system temperature increases and this feeds back to further increase the reaction rate. Arrhenius reaction kinetics will be explicitly considered, so that reaction rates and power production are an exponential function of the system temperature:

$$R = k \; a \; \Delta H \tag{2-1a}$$

$$k = k_o \; e^{-\Delta E/RT} \tag{2-1b}$$

where R = Reaction power, W,
k = Arrhenius reaction rate, (mass or moles)/(area or volume)/time,
a = Area, m^2, or Volume, m^3, consistent with units of k above,
ΔH = Heat of reaction, J/kg or J/mole, consistent with units of k above,
k_o = Pre-exponential or frequency factor, same units as k above,
ΔE = Activation energy, J/mole,
R = Ideal gas constant (8.314 J/mole/K), and
T = Temperature, K.

Heat losses on the other hand typically increase in a nearly linear manner; for example natural convection heat transfer coefficients are generally a weak power of the temperature difference such as 1/4 or 1/3:

$$L = h(\Delta T) \; A \; \Delta T \tag{2-2}$$

where L = Heat loss power, W,
h = Overall heat transfer coefficient, $W/m^2/K$,
A = System external area, m^2, and
ΔT = Temperature difference from system to ambient, K.

Power production and loss in a reactive system with these characteristics is illustrated in Figure 2-1 as a function of the system temperature. The different power production curves R1 to R3 exemplify systems with the same rate law but with different reactive areas or volumes (depending on the units for k), and the different power loss curves L1 and L2 exemplify changes

in the heat transfer resistance of the system to the ambient temperature for rejection of reaction power. When power production exceeds power loss for any system temperature, for example, R1 is always above L1, a runaway reaction may occur. When power loss exceeds power production for range of temperatures, for example, L1 exceeds R3 for some temperature range, then there is a stable temperature system temperature at which reaction power is rejected in the steady-state to the ambient; it may be shown that the low temperature intersection point is the stable operating temperature.

The critical temperature for incipient runaway exists when the heat rejection curve is tangent to power production curve, as is the case with L1 and R2. A small increase in the reaction area or volume will cause the power production curve to always exceed power loss in this case, as will a small decrease in the heat transfer coefficient or heat transfer area; likewise, decreases in these quantities lead to stable situations. In all cases shown, sustained supply of reactants is assumed because these are steady-state curves; in actual application the supply of one reactant may be limited on a continuing basis due to a low flowrate, low concentration, or diffusion rate limitation, or a reactant may be depleted with time, as is the case with a finite initial amount of fuel.

Figure 2-1: Examples of Thermal Stability and Instability

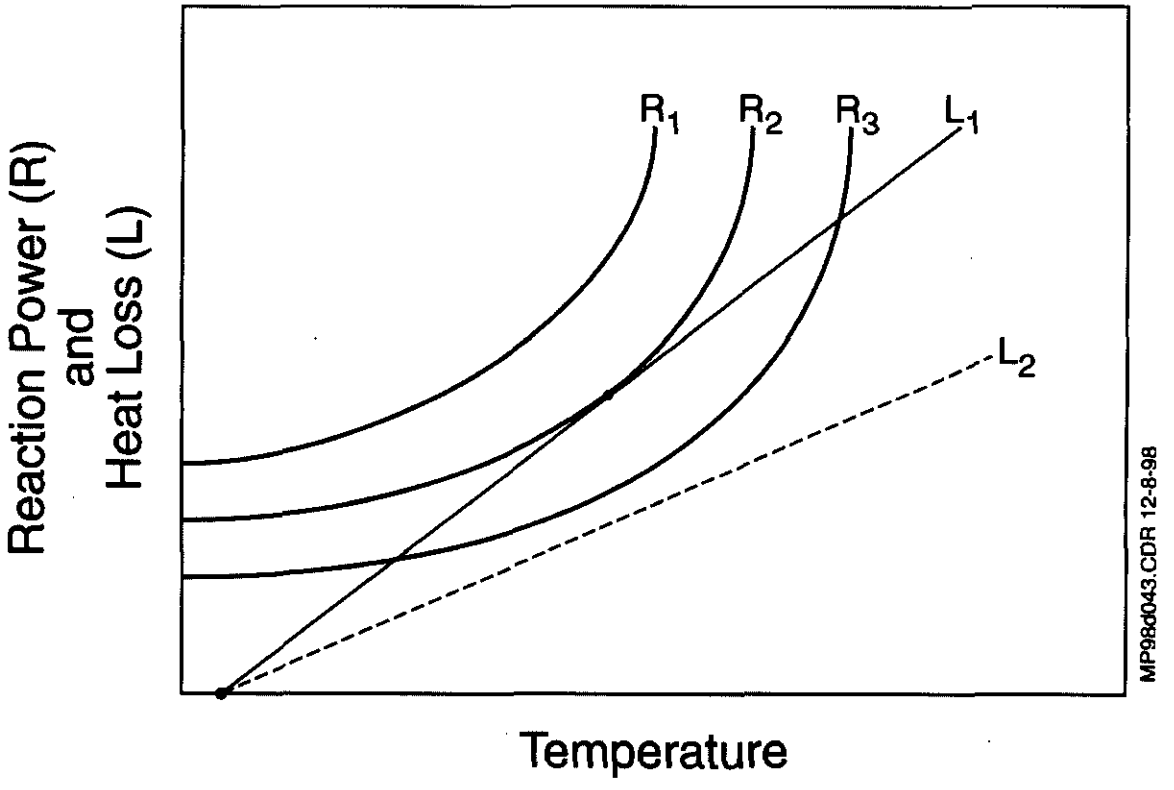

Uranium metal and hydride react with Arrhenius kinetics of the form Equation (2-1) for the temperature range of interest to the SNF Project, between roughly 10°C (in the basins) and 120°C (a central fuel location in a high power MCO during processing or interim storage). Rate laws are covered later in this report but at present it is sufficient to note that the rate is given per unit area available for reaction, that it depends upon whether water vapor, oxygen, or a combination of these gases is the oxidant, and that it may be assumed independent of time. Given the discussion of spontaneous ignition just presented, the statement that these materials are pyrophoric is misleading because the appropriate combination or surface area for reaction, gas available for oxidation, surface area for heat transfer, and overall heat transfer coefficient must exist.

Uranium hydride is commonly referred to as pyrophoric because it is typically found in the form of very small particles, so that it offers a sufficiently high reaction area that ignition of a small quantity can indeed occur at room temperature. Uranium metal in fine form such as thin turnings and tiny chips from machining is likewise a pyrophoricity hazard, but "bulk" metal in larger pieces such as the minimum SNF Project scrap size (1/4 inch) will not ignite until heated to several hundred degrees Celsius. On the other hand, a collection of scrap pieces or fuel elements can offer substantial internal heat transfer resistance, as will be seen below, so that fuel ignition becomes a valid concern when a substantial mass of fuel is assembled and, of course, when sufficient oxidant is available.

3.0 IGNITION THEORY BACKGROUND

3.1 Introduction

Ignition is the process of producing an explosion, a deflagration, detonation, flaming combustion, or smoldering. In many practical situations ignition can be understood on the basis of an Arrhenius reaction approximation for the chemical reaction, rather than some complex branched-chain kinetic mechanism. In this one-step reaction approximation, the rate of chemical reaction is primarily a function of the temperature of the reacting material, and the ignition temperature of the material may be defined as the lowest temperature at which the rate of heat loss is overwhelmed by the rate of chemical heat generation. Statement of an appropriate model for describing ignition requires introduction of an energy balance and the solution of such energy balance equations have been classified as thermal ignition problems. The importance of the dependence of the rate of reaction on temperature distinguishes thermal ignition theory from branched-chain ignitions, which may occur in isothermal systems. Thermal ignition has been discussed in various books and review articles (e.g., [Jones 1993; Frank-Kamenetskii 1969; and Zeldovich, et al. 1985]). The presentations in the last two references are especially extensive.

3.2 Thermal Ignition in Finite Geometry With Uniform Temperature

The concept of thermal ignition can best be approached by first dealing with a reactive solid material of infinite thermal conductivity or a reactive fluid that is so well mixed that its temperature, T, may be assumed to be the same at all locations. If the volume of the material is designated by V, its surface area by A, and if a heat transfer coefficient h is defined for heat loss off its surface, then the amount of heat evolved over the whole surface per unit time by the chemical reaction is

$$V \dot{m}_f''' \Delta H \tag{3-1}$$

and the amount of heat carried away from the surface is

$$hA(T - T_\infty) \tag{3-2}$$

In the above equations:

$\Delta H =$ effective heat of reaction per mass of fuel consumed,

$T_\infty =$ temperature of the ambient that surrounds the reactive material,

and $\dot{m}_f'''$ is the fuel consumption rate (in kg m^{-3} s^{-1}) given by the Arrhenius form

$$\dot{m}_f''' = C \exp\left(-\frac{E}{RT}\right) \tag{3-3}$$

where C = pre-exponential factor,
E = activation energy, and
R = universal gas constant.

The terms in Equations (3-1) to (3-3) may be expressed as an equality

$$h\,A\,(T - T_\infty) = V\,\Delta H\,C \exp\left(-\frac{T_{act}}{T}\right) \tag{3-4}$$

where we introduced the definition of the activation temperature

$$T_{act} = \frac{E}{R} \tag{3-5}$$

It turns out that at the ignition condition (to be defined below) the temperature of the reactive material relative to the ambient temperature, $T - T_\infty$ is small compared with the absolute temperature T_∞. Thus it is convenient to introduce a new dimensionless temperature

$$\theta = \frac{T_{act}\,(T - T_\infty)}{T_\infty^2} \tag{3-6}$$

in which $T_\infty\,\theta/T_{act} = (T - T_\infty)/T_\infty << 1$. Under this condition, it is possible to linearize the exponential term in Equation (3-3) as

$$\dot{m}_f''' = C \exp\left[-\frac{T_{act}}{T_\infty\,(1 + T_\infty\,\theta/T_{act})}\right] \cong C \exp\left[-\frac{T_{act}}{T_\infty}\left(1 - \frac{T_\infty\,\theta}{T_{act}}\right)\right]$$

$$= C \exp\left(-\frac{T_{act}}{T_\infty}\right) \exp(\theta) \tag{3-7}$$

and Equation (3-4) becomes

$$hA\,\frac{T_\infty^2}{T_{act}}\,\theta = V\,\Delta H C \exp\left(-\frac{T_{act}}{T_\infty}\right) \exp(\theta) \tag{3-8}$$

In order to reduce the problem to a minimum number of parameters, new dimensionless parameters are defined

$$T_r = \frac{T_{act}}{T_\infty} \tag{3-9}$$

$$\delta = \frac{V \Delta HC \quad T_r}{h A T_\infty} \exp\left(-T_r + 1\right) \tag{3-10}$$

[Frank-Kamenetskii 1969] introduced the parameter δ and is hereafter referred to as the F-K parameter. Equation (3-8) then becomes

$$\delta = \theta \exp(-\theta + 1) \tag{3-11}$$

The condition of thermal ignition may be now established in a simplified manner. A plot of the F-K parameter δ versus the dimensionless reactive material temperature θ is shown in Figure 3-1. For a fixed value of δ, there are two solutions for the material temperature. The lower temperature, point 1, represents a stable condition since an additional increase in the temperature of the material requires an increase in the value of δ or, equivalently, an increase in the value of the ambient temperature T_∞ (see Equation (3-10)). In contrast, an increase in the temperature from point 2 corresponds to a decreasing value of δ or a reduction in the ambient T_∞. Clearly, the right-hand branch of the curve in Figure 3-1 represents the locus of non-physical solutions. If δ is large enough, there is no corresponding solution for θ; the chemical heat generation rate then always exceeds the heat loss rate, causing θ to increase continually with time. The critical value of θ for the occurrence of ignition may therefore be identified with the maximum value of δ on the δ versus θ plot in Figure 3-1.

Differentiating Equation (3-11) with respect to θ gives

$$\frac{d\delta}{d\theta} = (1-\theta)\exp(-\theta+1) \tag{3-12}$$

The critical condition for ignition is $d\delta/d\theta = 0$ from which we obtain the dimensionless ignition temperature

$$\theta_{ig} = 1.0 \tag{3-13}$$

Substituting this result into Equation (3-11),

$$\delta_{crit} = 1.0 \tag{3-14}$$

which expresses the critical condition for ignition. Referring back to Equation (3-10), we note that the ignition condition depends upon T_∞, the geometry of the reactive material through the ratio V/A, the reaction kinetics through C and T_{act}, and the convective heat transfer regime in the surrounding ambient through h. Clearly, it is not possible to define uniquely an ignition temperature for a given material, as ignition is related to the physical phenomenon of heat transfer.

Figure 3-1: δ Versus θ For Finite Geometry With Uniform Temperature

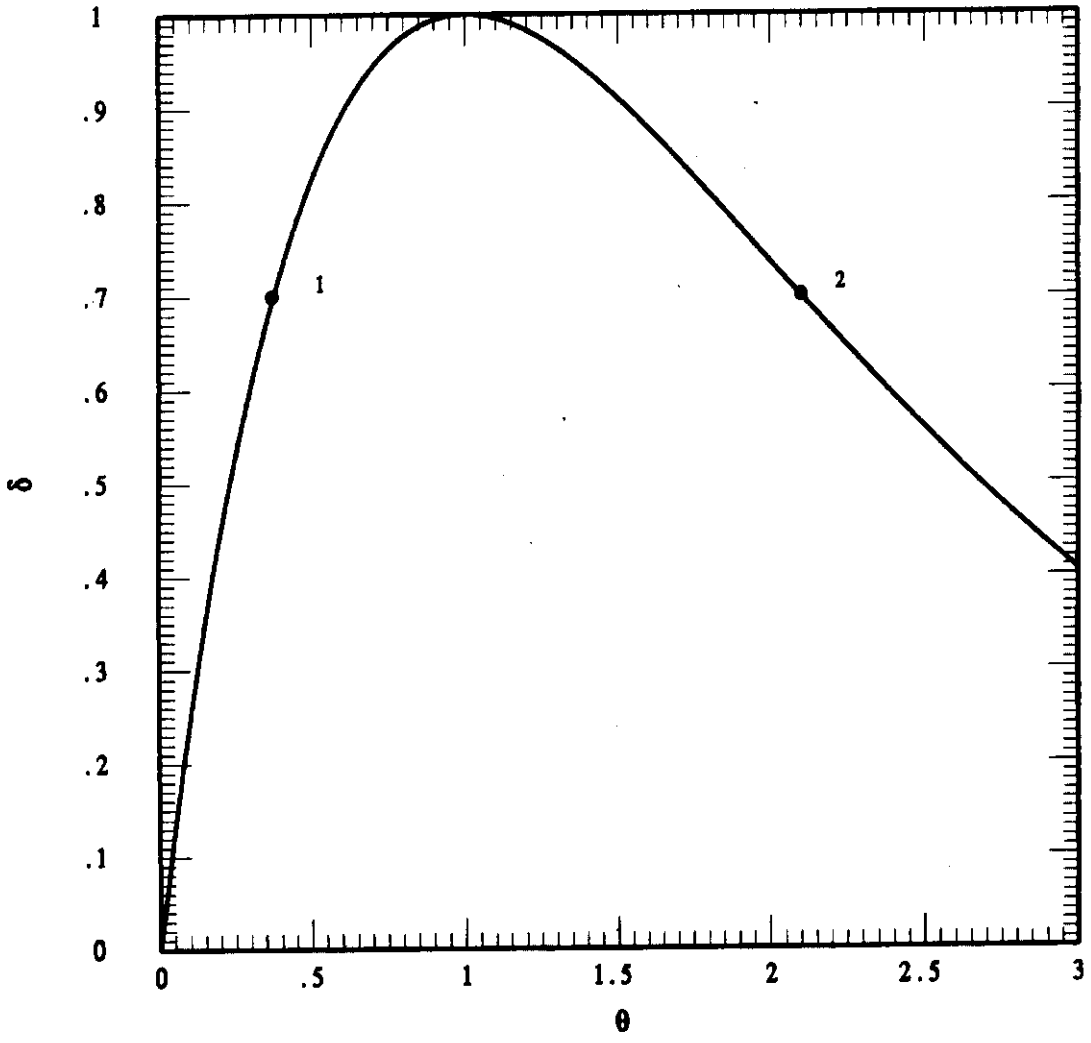

Continuing studies in the theory of thermal ignition have been directed along a number of lines. Usually the objective has been to consider influences of phenomena beyond those contained in Equation (3-10), such as the presence of thermal conduction within the reacting material, reactant/fuel diffusion limitations, non-finite geometry, and the effects of reactant depletion on the ignition temperature. Despite the additional mathematical complexity involved in these studies the ignition condition is still identified with the systems inability to maintain a balance between the chemical heat generation rate and the heat loss rate. In the following two subsections, some additional and more complex thermal ignition problems are discussed. Again, these sections introduce no new physical principles, the basic problems being those of thermal conduction and semi-infinite geometry.

3.3 Thermal Ignition in Finite Geometry With Heat Conduction

3.3.1 Exact Method

In this section, we derive the ignition condition for a reactive slab of thickness 2L subject to a volumetric chemical heating rate given by Equations (3-1) and (3-3). We will assume that the boundaries of the slab are maintained at temperature T_∞. If we locate the origin of our coordinate x at one boundary of the slab, the boundary conditions are

$$T = T_\infty \quad \text{at} \quad x = 0 \tag{3-15}$$

$$T = T_\infty \quad \text{at} \quad x = 2L \tag{3-16}$$

The basic energy balance for the problem is the one-dimensional steady-state heat conduction equation with local heat generation

$$k \frac{d^2T}{dx^2} = -\Delta H \dot{m}_f''' = -\Delta H C \exp\left(-\frac{T_{act}}{T}\right) \tag{3-17}$$

where k is the thermal conductivity of the reactive material. Actually, from symmetry considerations we need only solve the problem over half the slab, i.e., in the segment $0 < x < L$ with the boundary condition given by Equation (3-16) replaced by the adiabatic condition

$$\frac{dT}{dx} = 0 \quad \text{at} \quad x = L \tag{3-18}$$

Two different methods will be used to solve for the ignition condition. These are: (i) the classical Frank-Kamenetskii analysis; and (ii) the so-called constant reaction rate method first introduced by [Thomas and Bowes 1961]. We begin with method (i).

Nondimensionalizing the temperature and the distance x and linearizing in the argument of the exponential of Equation (3-17) in the same manner as in the previous section, one obtains

$$\frac{d^2\theta}{dz^2} = -\delta e^{\theta} \tag{3-19}$$

Equation (3-19) contains two new dimensionless parameters, a new F-K parameter for a heat conducting slab,

$$\delta = \frac{L^2 \Delta H C T_r}{k T_\infty} \exp(-T_r) \tag{3-20}$$

and a dimensionless distance z

$$z = \frac{x}{L} \tag{3-21}$$

Equation (3-19) is subject to the boundary conditions (see Equations (3-15) and (3-18))

$$\theta = 0 \qquad \text{at} \qquad z = 0 \tag{3-22}$$

$$\frac{d\theta}{dz} = 0 \qquad \text{at} \qquad z = 1.0 \tag{3-23}$$

Using the chain rule of differentiation, Equation (3-19) can be expressed as

$$\frac{1}{\delta}\frac{d\theta}{dz}\frac{d}{d\theta}\left(\frac{d\theta}{dz}\right) = -e^{\theta} \tag{3-24}$$

which can be integrated once to obtain

$$\frac{1}{2\delta}\left(\frac{d\theta}{dz}\right)^2 = -e^{\theta} + C_1 \tag{3-25}$$

where C_1 is a constant of integration. Let θ_m denote the maximum dimensionless temperature in the slab. This temperature occurs at the center of the slab (z = 1) where $d\theta/dz = 0$. Thus the integration constant in Equation (3-25) may be evaluated in terms of θ_m to obtain

$$C_1 = e^{\theta_m} \tag{3-26}$$

and Equation (3-25) takes the form

$$\frac{1}{2\delta}\left(\frac{d\theta}{dz}\right)^2 = e^{\theta_m} - e^{\theta} \tag{3-27}$$

Note that the peak temperature θ_m is as yet an unknown quantity.

Equation (3-27) is a separable equation and with the help of the boundary conditions $\theta = 0$ at $z = 0$ and $\theta = \theta_m$ at $z = 1$ may be expressed as a quadrature:

$$\frac{1}{(2\delta)^{1/2}}\int_0^{\theta_m}\frac{d\theta}{\sqrt{e^{\theta_m} - e^{\theta}}} = \int_0^1 dz = 1 \tag{3-28}$$

Solving for δ gives

$$\delta = \frac{1}{2}\left[\int_0^{\theta_m} \frac{d\theta}{\sqrt{e^{\theta_m} - e^{\theta}}}\right]^2 \tag{3-29}$$

Equation (3-29) can be integrated in closed form. The result is*

$$\delta = \frac{e^{-\theta_m}}{2}\left[\ln\left(\frac{1 + \sqrt{1 - \exp(-\theta_m)}}{1 - \sqrt{1 - \exp(-\theta_m)}}\right)\right]^2 \tag{3-30}$$

The above equation provides a value of δ for a given peak temperature θ_m at the center of the slab.

Equation (3-30) is plotted in Figure 3-2. We note that the critical value of δ for ignition of a planar slab is

$$\delta_{crit} = 0.88 \tag{3-31}$$

because no steady-state solutions exist for δ values above 0.88. Thus from the definition of δ, Equation (3-20), we find that ignition is to be expected if the slab half-thickness exceeds the critical value

$$L_{crit}^2 = \frac{0.88\ k T_\infty}{\Delta H C T_r} \exp\left(T_r\right) \tag{3-32}$$

* After considerable algebraic manipulation, Equation (3-30) can be rewritten in the compact form

$$e^{\frac{\theta_m}{2}} = \cosh\sqrt{\frac{\delta e^{\theta_m}}{2}}$$

This is the result that is usually given in the text books on the subject. However in terms of obtaining the ignition condition, there is no particular advantage of this form over Equation (3-30).

Figure 3-2: δ Versus θ_m For a Reactive Finite Slab With Heat Conduction

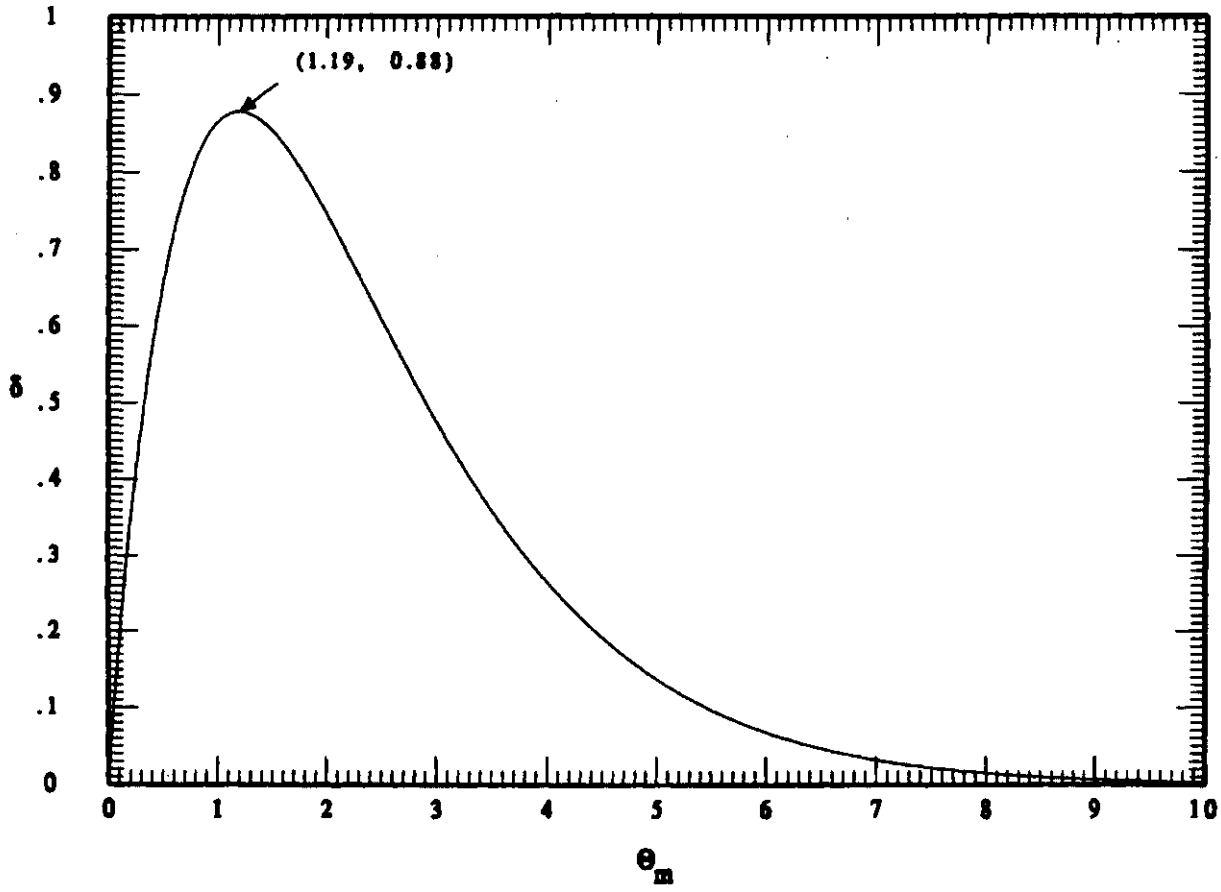

One can also find the critical values of δ for heat-conducting reactive regions of spherical and cylindrical shapes. The results are

$$\delta_{crit} = 2.0 \tag{3-33}$$

for a cylindrical shape and

$$\delta_{crit} = 3.32 \tag{3-34}$$

for a spherical shape, where δ_{crit} in Equations (3-33) and (3-34) is based on the radius of the geometric shape. Thus, for example, the critical radius r_{crit} for a spherical shape is (see Equation (3-32))

$$r_{crit}^2 = \frac{3.32\, k\, T_\infty}{\Delta H C T_r} \exp\,(T_r) \tag{3-35}$$

Returning to Figure 3-2, the maximum pre-ignition temperature rise in the slab is

$$\theta_{m,ig} = 1.19 \tag{3-36}$$

In terms of the physical temperature rise (see Equation (3-6)), Equation (3-36) becomes

$$T_{m,ig} - T_\infty = \frac{1.19\, T_\infty^2}{T_{act}} \tag{3-37}$$

The maximum pre-ignition temperature rise is $1.37\ \frac{T_\infty^2}{T_{act}}$ for the cylinder and $1.60\ \frac{T_\infty^2}{T_{act}}$ for the sphere.

3.3.2 Constant Reaction Rate Method

The principal mathematical difficulty in thermal ignition problems involving heat conduction within the reacting medium is due to the complicated Arrhenius form of the reaction rate function $\dot{m}_f'''$ (T). A conservative but accurate approach to the problem is obtained by assuming that $\dot{m}_f'''$ (T) is spatially uniform and evaluated at the location in the reactive region where the temperature is a maximum, i.e., where $T = T_m$. Note that T_m is initially unknown but readily determined once the heat conduction equation is solved for the temperature distribution in the reactive medium with an assumed spatially uniform heat source. Apparently, the spatially uniform rate of heat generation assumption was first used in one part of a paper by (Thomas and Bowes 1961).

Consider the problem treated in the foregoing, namely, a reactive slab with constant temperature T_∞ at x = 0 and an adiabatic surface at the opposite boundary x = L. For a spatially constant volumetric heat generation rate $\Delta H\ \dot{m}_f'''(T_m)$ in the reactive slab, the solution of Equation (3-17) for the temperature distribution is

$$T - T_\infty = \frac{\Delta H\ \dot{m}_f'''(T_m)}{k}\left(Lx - \frac{x^2}{2}\right) \tag{3-38}$$

Evaluating the above equation at x = L where $T = T_m$ gives

$$T_m - T_\infty = \frac{L^2\ \Delta H}{2k}\dot{m}_f'''(T_m) = \frac{L^2\ \Delta H\, C}{2k}\exp\left(-\frac{T_{act}}{T_m}\right) \tag{3-39}$$

We now introduce the dimensionless quantities given by Equations (3-6) and (3-20) and linearize the argument of the exponential so that Equation (3-39) may be restated as

$$\delta = 2\,\theta_m \exp(-\theta_m) \tag{3-40}$$

which exhibits a maximum when δ is plotted against θ_m. Thus by differentiating Equation (3-40) with respect to θ_m we get

$$\frac{d\delta}{d\theta_m} = 2e^{-\theta_m}(1-\theta_m), \tag{3-41}$$

and the temperature rise at ignition is obtained by setting $d\delta/d\theta_m = 0$ to obtain

$$\theta_{m,ig} = 1.0 \tag{3-42}$$

this approximate result underestimates the exact value of $\theta_{m,ig} = 1.19$ (see Equation (3-36)) by about 16%. By setting $\theta_m = 1.0$ in Equation (3-40), we get the critical F-K parameter at ignition:

$$\delta_{crit} = 0.74 \tag{3-43}$$

which underestimates the exact value 0.88 by 16%. It is important to mention that the 16% discrepancy in δ_{crit} translates to an error of only 8.3% in the critical slab thickness since $L_{crit} = \delta_{crit}^{1/2}$ (see Equation (3-20) or (3-32)).

The constant reaction rate theory is particularly powerful for combined multidimensional geometries and finite-surface heat transfer coefficient (see, e.g., [Epstein, et al. 1996]).

It is appealing at this point to define a unified form of the F-K parameter encountered in the various situations presented above, which will have a consistent form when constant reaction rate theory is applied. First, the reaction rate per unit volume is converted to the product of reactive area per unit volume, A_V, and the reaction rate per unit area by substituting $A_V k_O$ for C in Equation (3-20). Here k_O is the pre-exponential parameter for an Arrhenius rate law for reaction at a surface; it is described in Appendix A that uranium oxidation may be quantified in this manner. Next, the parameter δ, defined by Equation (3-20), is normalized by the value $2/e = 0.74$ which appears in Equation (3-43) to create a modified F-K parameter

$$B = \frac{A_v L \Delta H C T_r}{2k T_\infty \exp(T_r - 1)} \tag{3-44}$$

so the critical value for ignition is

$$B_{crit} = 1 \tag{3-45}$$

Returning to the isothermal reacting medium presented in Section 3-2, the F-K parameter δ of Equation (3-10) becomes identical to the modified parameter B above, upon the substitution

$$\frac{V}{A} = \frac{1}{A_v} \tag{3-46a}$$

$$H = \frac{k}{(L/2)} \tag{3-46b}$$

This physically means that when the general but isothermal shape assumed for Equation (3-10) is viewed as a body with planar geometry, then V/A is the thickness, half that value is the effective conduction thickness for a uniform heat-generating medium, and that the heat transfer resistance to the ambient changes from external to internal.

3.4 Non-Stationary Thermal Ignition Theory and the Minimum Ignition Energy of a Combustible Gas Mixture

The steady-state approach to ignition that was used in the previous subsections, in which ignition was formulated as the condition for the loss of the steady-state, can not be applied to problems involving unbounded regions of reactive material. That is, a slow reaction with balanced heat production and loss at the boundaries cannot be achieved when the reactive medium is infinite in extent. In these situations, the transient term in the energy equation (balance), which represents the rate-of-change of internal energy per unit volume, must be accounted for. An important problem of this type is the determination of the minimum ignition energy (MIE) of a combustible mixture, and this is the subject treated below.

Not many unsteady thermal ignition problems have been solved analytically and, accordingly, the solution presented here is obtained numerically. Since the solution is numerical there is no need to linearize the argument of the exponential in the Arrhenius equation and we may account for additional complications such as fuel gas depletion. However, in order to prevent excessive mathematical and computational difficulties, it is proper to consider that during the short times of interest in the MIE problem there are no convective motions within the gas mixture. The equations for transient heat conduction and gas species diffusion within the mixture then become the starting point of the thermal ignition analysis.

Capacitive spark-type discharges are usually employed to determine the MIE of a combustible gas mixture. In these experiments the energy release approximates a point source and the heating duration may be as little as a fraction of a microsecond. The minimum energy for a stoichiometric gas mixture may be only a few tenths of a millijoule (mj). It is important to note that while sparks have a relatively small energy content, they can ignite a flammable gas mixture because the power density of such sparks is enormous and may exceed 10^{12} W m^{-3}. A diffuse source of energy requires a much higher total energy content to ignite a gas mixture. In this subsection we desire to demonstrate that classical ignition theory can be used to predict the MIE of a combustible gas mixture.

The differential equation of the conduction of heat in a spherically symmetric combustible gas mixture is

$$\rho c \frac{\partial T}{\partial t} = \frac{k}{r^2} \frac{\partial}{\partial r}\left(r^2 \frac{\partial T}{\partial r} \right) + \Delta H \dot{m}_f''' \qquad (3\text{-}47)$$

where ρ, k, c, and ΔH are the density, thermal conductivity, specific heat, and heat of reaction, respectively, of the gas mixture and T is the local temperature. These quantities are assumed to remain constant throughout the reaction zone. The radial coordinate r is measured from the center of the ignition source located at r = 0. The volumetric rate of fuel consumption $\dot{m}_f'''$ (in kg m^{-3} s^{-1}) is given by the Arrhenius form recommended by (Williams 1981) for combustible gas mixtures; namely,

$$\dot{m}_f''' = C Y_{ox} Y_f \exp\left(- \frac{T_{act}}{T} \right) \qquad (3\text{-}48)$$

where Y_{ox}, Y_f are the oxygen and fuel mass fractions, respectively, C is a constant pre-exponential factor, and T_{act} is the activation temperature (= E/R). The mass conservation equations for the fuel and oxygen species are

$$\rho \frac{\partial Y_{ox}}{\partial t} = \frac{\rho D}{r^2} \frac{\partial}{\partial r}\left(r^2 \frac{\partial Y_{ox}}{\partial r} \right) - r_s \dot{m}_f''' \qquad (3\text{-}49)$$

$$\rho \frac{\partial Y_f}{\partial t} = \frac{\rho D}{r^2} \frac{\partial}{\partial r} \left(r^2 \frac{\partial Y_f}{\partial r} \right) - \dot{m}_f''' \qquad (3\text{-}50)$$

where D is an effective, constant oxygen/fuel binary diffusion coefficient in air, and r_s is the constant ratio of the mass of oxygen consumed per mass of fuel consumed. The quantity r_s is determined from the stoichiometry of the reaction.

It is of interest to obtain the solution of Equations (3-47) through (3-50) as the limit of a numerically tractable case in which a finite quantity of heat is liberated over a vanishingly small volume (or "hot spot"). We take this hot spot volume as a sphere of radius R_{HS}, and consider the case of an infinite reactive medium in which the initial temperature is T_{HS} in the hot spot $0 < r < R_{HS}$ and T_0 in the region $r > R_{HS}$. We achieve the solution response to a point source of ignition when R_{HS} is made sufficiently small so that the solution becomes independent of the value of R_{HS}. The remaining initial conditions of interest are

$$Y_{ox}(r, 0) = Y_{ox,0}; \qquad Y_f(r, 0) = Y_{f,0}; \qquad \text{for} \qquad 0 < r < \infty \qquad (3\text{-}51)$$

Equation (3-49) can be removed from consideration in the following manner. Multiplying Equation (3-50) by r_s and subtracting the result from Equation (3-49) yields

$$\rho \frac{\partial}{\partial t} (Y_{ox} - r_s Y_f) = \frac{\rho D}{r^2} \frac{\partial}{\partial r} \left[r^2 \frac{\partial}{\partial r} (Y_{ox} - r_s Y_f) \right] \qquad (3\text{-}52)$$

Thus the quantity $Y_{ox} - r_s Y_f$ obeys a chemical reaction-free equation. By virtue of the initial and boundary conditions represented by Equation (3-51), the only physical solution to Equation (3-52) is

$$Y_{ox} - r_s Y_f = \text{constant} = Y_{ox,0} - r_s Y_{f,0} \qquad (3\text{-}53)$$

In the limit of a stoichiometric mixture, which is considered here, the right-hand side of the above equation is zero and we have

$$Y_{ox} = r_s Y_f \qquad (3\text{-}54)$$

Thus it is only necessary to numerically solve Equations (3-47) and (3-50) with $\dot{m}_f'''$ given by the second-order reaction law

$$\dot{m}_f''' = C r_s Y_f^2 \exp\left(- \frac{T_{act}}{T} \right) \qquad (3\text{-}55)$$

Numerical solutions of Equations (3-47), (3-50), and (3-55) were carried out for a stoichiometric mixture of decane in air. This particular mixture was chosen because it is fairly representative of most hydrocarbon/air pairs and because the kinetic parameters C and T_{act} can be evaluated from the information presented in (Williams 1981). Values for the various physical parameters used in the calculations are given in Table 3-1. The finite difference solution procedure is discussed below.

Table 3-1: Parameter Values Used to Theoretically Determine the MIE of Decane/Air

Thermal Conductivity (air at 1000 K)	$k = 0.068\ W\ m^{-1}\ K^{-1}$
Density (air at 1000 K)	$\rho = 0.352\ kg\ m^{-3}$
Specific Heat (air at 1000 K)	$c = 1140\ J\ kg\ K^{-1}$
Diffusion Coefficient (decane in air at 1000 K)	$D = 1.69 \times 10^{-4}\ m^2\ s^{-1}$
Effective Heat of Reaction	$\Delta H = 4.1 \times 10^{7}\ J\ kg^{-1}$
Kinetic Pre-Exponential Coefficient	$C = 9 \times 10^{8}\ kg\ m^{-3}\ s^{-1}$
Stoichiometric Oxygen-to-Fuel Mass Ratio	$r_s = 3.48$
Activation Temperature	$T_{act} = 1.862 \times 10^{4}\ K$
Initial Stoichiometric Fuel Concentration	$Y_{f,0} = 0.0628$
Initial Mixture Temperature Outside Hot Spot	$T_0 = 20°C$

To calculate the temperature and species concentration profiles we have used a simple first-order finite difference procedure. The hot spot and the surrounding spherical region is divided into concentric spherical shells (or "nodes") of thickness ε. These shells are considered to be perfect conductors. A contact thermal resistance k/ε is assigned to the spherical boundaries between the nodes. Referring to Equation (3-47) the ordinary differential equation for the temperature T_n of arbitrary node n in a reactive gas mixture is

$$\rho c \frac{dT_n}{dt} = \frac{3k}{\varepsilon^2}\left[\frac{(n-1)^2 (T_{n-1} - T_n) - n^2 (T_n - T_{n+1})}{n^3 - (n-1)^3}\right] + \Delta H\ C\ r_s\ Y_{f,n}^2 \exp\left(-\frac{T_{act}}{T_n}\right) \qquad (3\text{-}56)$$

for $1 \le n \le N - 1$, where N equals the total number of nodes. A similar equation can be written for the fuel species concentration Y_f. In all numerical cases the outermost node N was always sufficiently far from the hot spot so that it did not feel the thermal effects of the approaching combustion fronts before the calculation was terminated. The outer surface of node N is regarded as adiabatic. The system of 2N differential equations (species plus energy) is solved by an available subroutine. In order to ensure an accurate numerical solution, the node size ε must be smaller than the thickness δ of a combustion wave. Now, δ ; α/u where u is the velocity of the combustion wave and α is the thermal diffusivity of the reactive medium. It turns out that the node size ε should be less than roughly 10^{-4} m. The node thickness in all the calculations did not exceed 2×10^{-5} m.

In order to determine the MIE of the decane/air system several values of the hot spot radius R_{HS} are selected and for each value the hot spot initial temperature T_{HS} is increased until reaction propagation is predicted. Figures 3-3 and 3-4 show the transition from hot spot cooling (reaction extinction) to reaction propagation (ignition) upon increasing T_{HS} from 25,300 to 25,400°C in a hot spot of radius $R_{HS} = 0.2$ mm*. The initial sensible energy in the hot spot or, equivalently, the minimum ignition energy is then

$$MIE = \frac{4}{3} \pi R_{HS}^3 \rho c (T_{HS} - T_0) = 0.34 \text{ mJ} \quad (3\text{-}57)$$

In order to ensure that this predicted MIE for decane/air is independent of the size of the hot spot, additional calculations were carried out for smaller hot spots of sizes $R_{HS} = 0.04$, 0.1 mm. The predicted MIEs were essentially the same as that given by Equation (3-57). This prediction is in reasonable agreement with the reported MIE measurements of hydrocarbon fuels; namely, MIE = 0.55 mJ for stoichiometric butane combustion (Kuchta 1985) and 0.33 mJ for stoichiometric methane combustion (Zabetakis 1965). From Figure 3-4 we infer a flame speed of 0.34 m s^{-1}. The measured flame speed is 0.3 m s^{-1} (Chemical Handbook 1963).

Figure 3-3: Temperature Profile History Produced by 0.2-mm Radius Hot Spot With an Initial Temperature of 25,300°C, Indicating Reaction Extinction.
Time duration between profiles is 1.6 msec

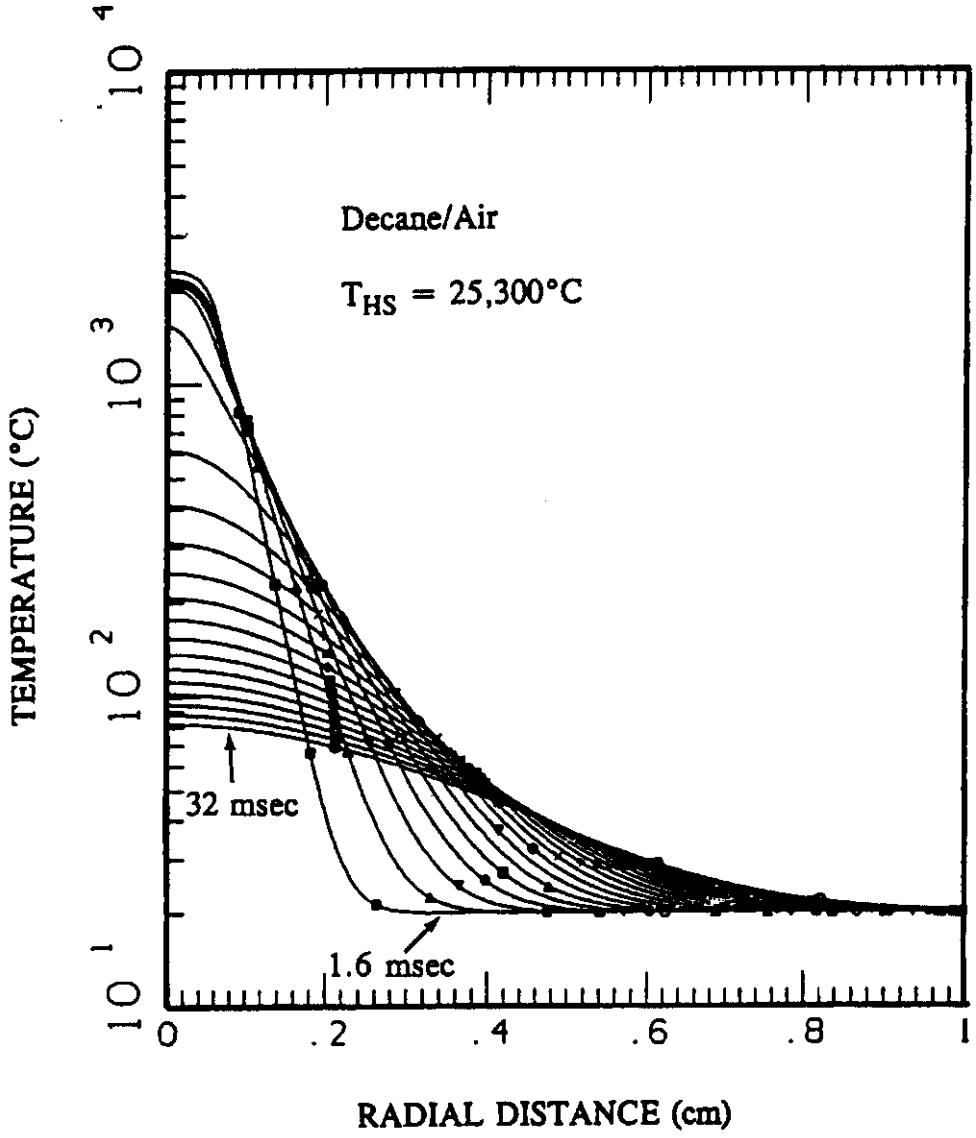

Figure 3-4: Temperature Profile History Produced by 0.2-mm Radius Hot Spot With an Initial Temperature of 25,400°C, Indicating Ignition and Combustion Wave Propagation
Time duration between profiles is 1.6 msec.

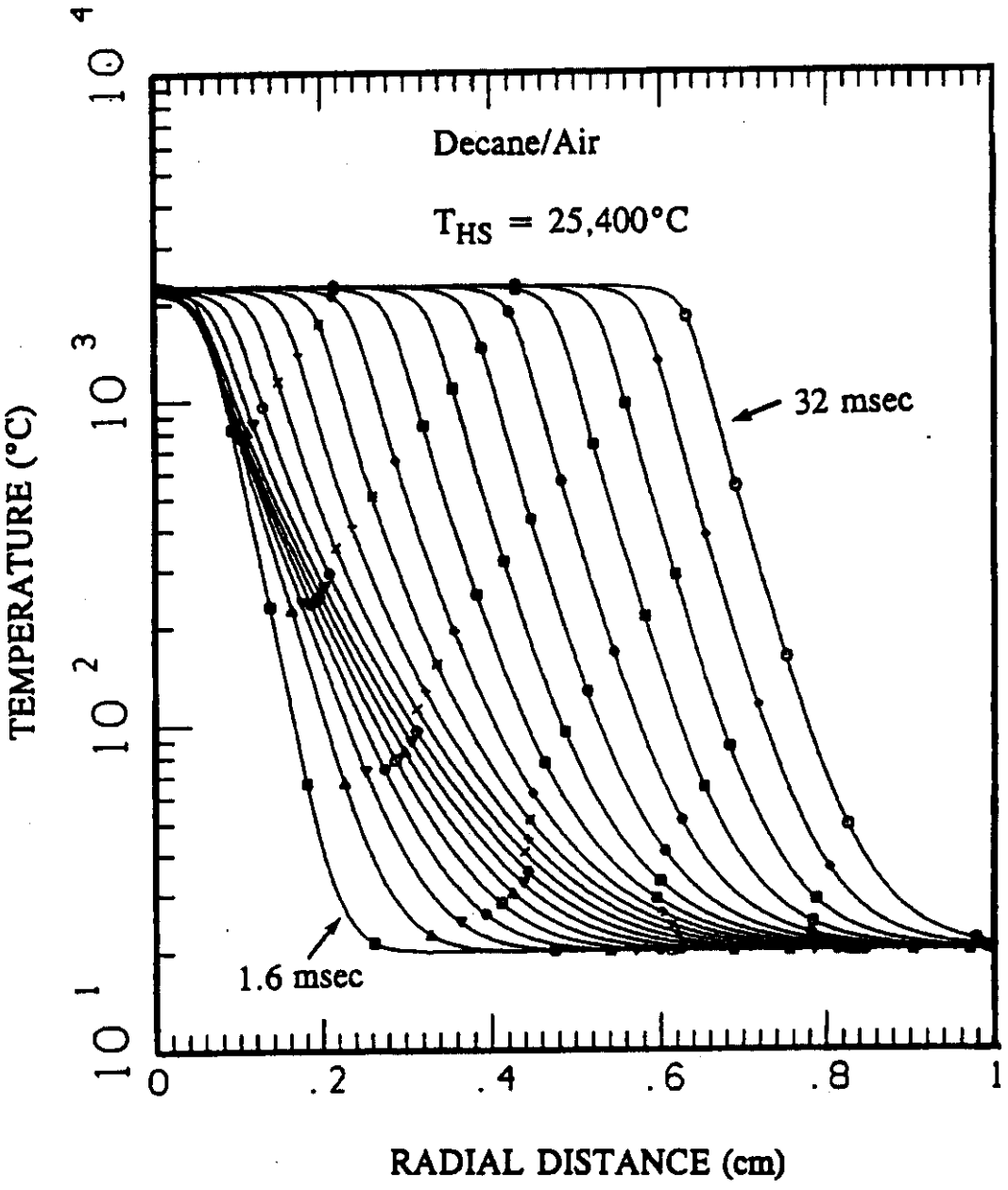

Additional calculations were made with the assumption that the diffusion coefficient D in Equation (3-50) is zero. Interestingly enough, the MIE increased by three orders of magnitude. This demonstrates that the relatively small spark energy for ignition in gases, relative to that of solids, is mainly due to the ability of gaseous fuel and oxygen to diffuse into the reaction zone and replace the fuel and oxygen that has already been consumed.

3.5 Summary

Mathematical methods for prediction of ignition criteria for reactive systems are presented and explained above in preparation for application to uranium metal and spent nuclear fuel. Upon evaluation of steady-state methods, we find that uniform reaction rate theory may be acceptably and (slightly) conservatively applied. A unified ignition criterion, the modified F-K parameter, is presented and will be used in applications.

Transient methods are also presented above in order to demonstrate the efficacy of the technique in meaningful application. Such methods may be applied to uranium metal and spent nuclear fuel as well.

4.0 URANIUM IGNITION THEORY VALIDATION BY COMPARISON WITH EXPERIMENT

Despite the numerous cases of spontaneous ignitions of uranium during storage or processing, only a few laboratory studies of uranium ignition under relatively well defined conditions were reported and only a few attempts were made to confront the experimental results with theoretical analysis relating uranium ignition temperature to the properties of the metal and its environment. Laboratory studies are reviewed below and are used as a means of validating application of ignition theory for uranium systems. The method is then extended in Section 5.0 to plausibly explain ignition experiences, which are less well defined.

4.1 Ignition of Small, Bulk Pieces of Uranium Metal

Baker, et al. (1966) performed uranium ignition experiments using small foils and also presented an analysis that links the ignition temperature with Arrhenius-type oxidation expressions obtained from low-temperature isothermal oxidation experiments. The authors considered both convective and radiative heat losses from a bulk piece of uranium of known surface area "A" and volume V. Thermal conduction within the bulk metal was ignored and therefore a zero-dimensional energy equation was employed. In particular, Baker, et al. (1966) numerically integrated a nonstationary ordinary differential equation, using the exact form of the Arrhenius expression. In their calculations the ambient temperature increased uniformly at the rate of $10°C\ min^{-1}$ in order to simulate the conditions in their experiments, which were performed by placing uranium samples in a flowing oxidizing atmosphere (air or oxygen) within a furnace whose temperature was increased at this rate. Initially, the calculated temperature of the sample lags behind the furnace temperature. At a sufficiently high sample temperature the heat of reaction becomes important and the sample temperature begins to exceed the furnace temperature. At ignition a sharp rise in sample temperature occurs.

If one is only interested in determining the ignition condition and not the temperature-time history of the sample, a steady-state energy balance will suffice. The steady energy balance for a bulk sample of uranium metal undergoing surface-oxidation heating and losing heat from its surfaces by convection and radiation is

$$h(T - T_\infty) + \varepsilon\sigma(T^4 - T_\infty^4) = \dot{m}''_{ox}(T) \bullet \Delta H \qquad (4\text{-}1)$$

where "h" is the convective heat transfer coefficient, σ is the Stefan-Boltzmann constant, ε is the total emissivity of the oxidized surface, ΔH is the heat of reaction (in $J\ (kg\ O_2)^{-1}$), T is the metal temperature, and T_∞ is the ambient (furnace) temperature. Note that the geometric parameters A and V do not appear in the steady-state energy balance given by Equation (4-1). This is because, for a bulk piece of metal, the chemical reaction area is equal to the heat transfer area and, therefore, "A" appears on both sides of the equation and reduces to unity. from both sides of the equation. The solution of Equation (4-1) provides a uranium metal temperature T for a given ambient temperature T_∞. However, above some sufficiently high value of T_∞ there are no solutions to Equation (4-1). This peak ambient temperature is the ignition temperature. Equation (4-1) can be rewritten as

$$hT_\infty + \varepsilon\sigma T_\infty^4 = hT + \sigma\varepsilon T^4 - \dot{m}''_{ox}(T) \bullet \Delta H \qquad (4\text{-}2)$$

The left-hand side of this equation is plotted as a function of T in Figure 4-1 for the following input parameters pertinent to the Baker, et al. (1966) ignition experiments: $h = 21.0\ W\ m^{-2}\ K^{-1}$, $\varepsilon = 0.75$, $\Delta H = 3.4 \times 10^7\ J\ (kg\ O_2)^{-1}$. The McGillivray kinetic rate equation for dry air (see Appendix A) was used in the construction of the curve.

We note from Figure 4-1 that the critical ambient temperature for ignition is 660 K, for no steady-state solutions exist for T_∞ values above 660 K. Figure 4-1 has the shape expected from the introduction to ignition theory presented in Section 3.0. Note also that the predicted temperature of the sample at ignition is about 725 K (452°C) which is about 100°C beyond the 0-350°C temperature range of the data base covered by the McGillivray, et al. (1994) oxidation rate correlation.

Figure 4-1: Solution of Equation (4) With McGillivray, et al., [1994] Oxidation Kinetics ($\rho_{H2O} = 0$)

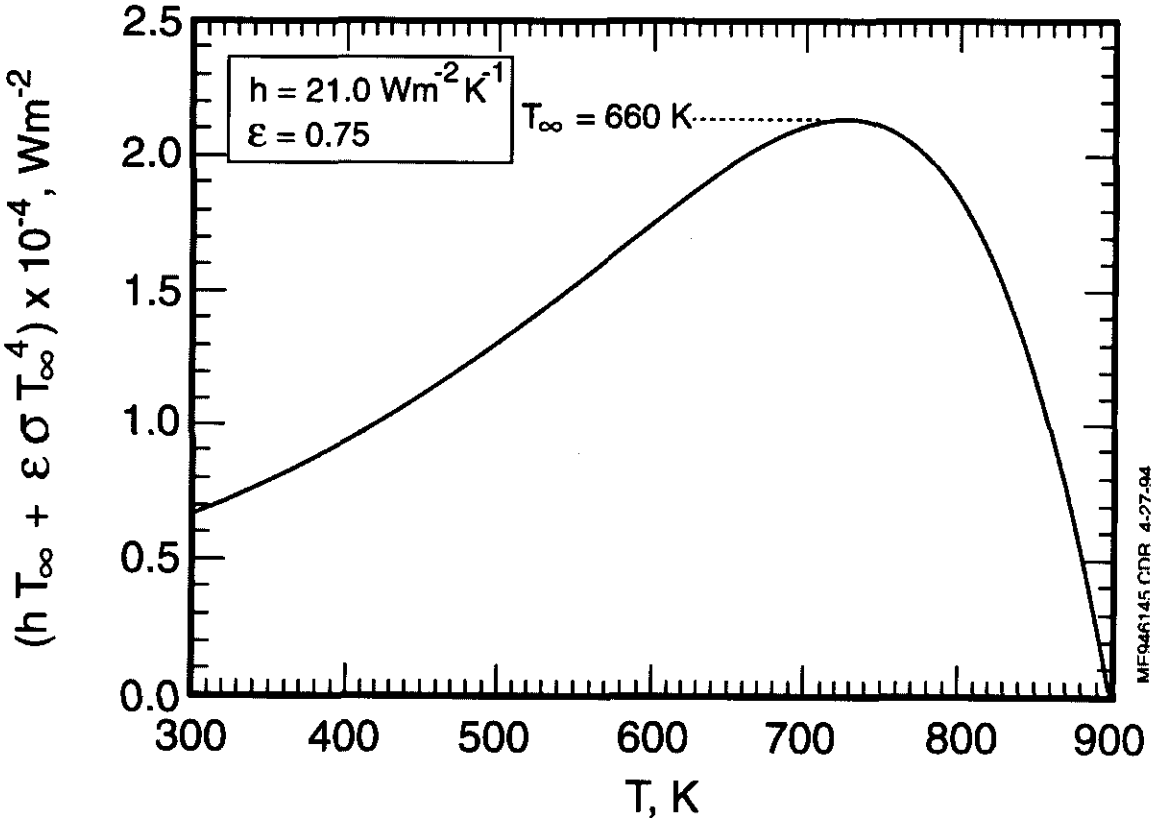

Nevertheless, Figure 4-2 shows that there is good agreement between the theory and most of the ignition data reported by Baker, et al. (1966) for small samples of uranium metal foils. Similar agreement between theory and experiment was reported by Baker and Bingle (1966) using their oxidation rate expression and the nonsteady-state model of sample heatup and subsequent ignition. Calculated ignition temperatures are somewhat higher than experimental values for very thin foils with extremely large specific areas. The reason for this discrepancy is not yet clear.

Last, Equation (4-2) conforms with the F-K parameter of Equation (3-44). For a thin foil, the product $A_v L = 2$ where L is the foil thickness and an effective heat transfer coefficient h_e replaces k/L. The effective heat transfer coefficient is formed by linearizing the radiation term as $h_e = h + 4\varepsilon\sigma T_e^3$. Often assigning $T_e = T_\infty$ is sufficient, but when the sample temperature is well above the ambient, then an approximation such as $T_e = 0.5\,(T + T_\infty)$ where T, the sample temperature at ignition, may be used for an iterative solution.

4.2 Ignition of Uranium Hydride Powder and Uranium Powder

The ignition study discussed in the foregoing dealt only with ignition of uranium metal in bulk. The effects of subdivision of the metal into a powder have been studied by several investigators. The early work of Hartman, et al. (1951) showed that layers of small quantities of uranium and uranium hydride powders ignite at about 100°C and spontaneously at room temperature, respectively. The average particle diameter of the uranium hydride powder was about 2.7 μm (on a particle volume basis), while that of the uranium powder was about 10 μm. Ignition of uranium hydride was noted when the powder mass exceeded 5.0 g. Unfortunately, little additional information was presented by the authors regarding the geometry of the powder and whether or not the air was dry. As mentioned previously, these experiments have been used as evidence of the pronounced pyrophoricity of uranium hydride and in support of the uranium hydride coating mechanism of ignition. However, as we show below, the observed spontaneous ignition of uranium hydride layers are not inconsistent with ignition theory combined with McGillivray, et al's. (1994) oxidation rate law for uranium in moist air.

Figure 4-2: Furnace Temperature at the Onset of Ignition Versus Specific Area of Reacting Uranium Foil (Baker, et al. 1966) (non-protective oxide regime); Comparison With Ignition Theory and McGillivray, et al. (1994) Oxidation Kinetics ($\rho_{H2O} = 0$).

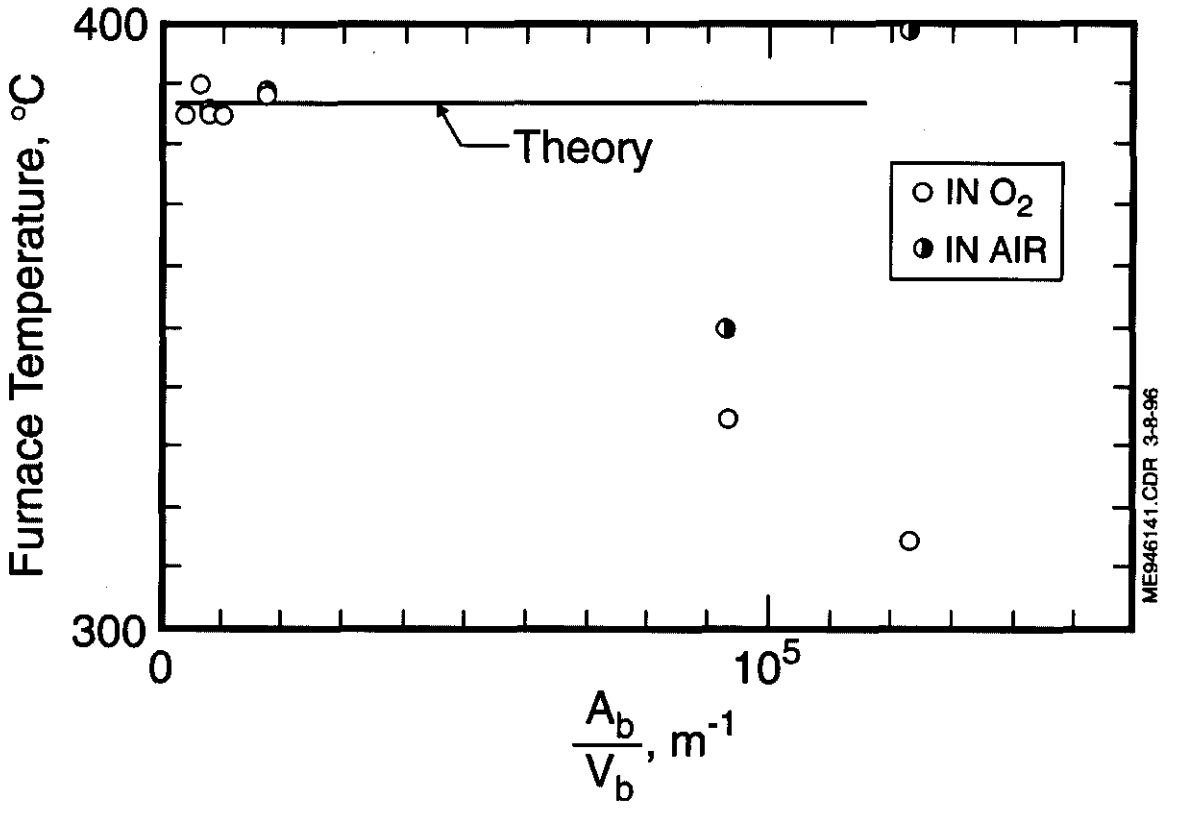

Ignoring the small temperature gradients that exist within a shallow layer of uranium (or uranium hydride) powder we may write the following energy balance between the chemical heat generation rate and the rate of heat loss by natural convection and radiation

$$A_v \, L \, m_{ox} \, (T) \, \Delta H \;=\; h_t \, (T - T_\infty) + \varepsilon \, \sigma \, (T^4 - T_\infty^4) \qquad (4\text{-}3a)$$

$$A_v \;=\; \frac{6\,(1-\phi)}{d} \qquad (4\text{-}3b)$$

where ϕ and L are the porosity and height of the powder layer, respectively, d is the diameter of the spherical (assumed) particles that comprise the powder, T is the temperature of the powder, T_∞ is again the ambient temperature, and h_t is the heat transfer coefficient for turbulent natural convection. The geometric parameters d and L appear in Equation (4-3) because oxidation occurs on the surfaces of the particles interior to the layer while heat loss occurs only at the upper boundary of the layer. The lower boundary is assumed to be adiabatic. Note that the ignition parameter for this system is given by Equation (3-44) with $h_e = k / L$, as discussed for application to Baker's foil experiments.

As was the case with Equation (4-1), if we use Equation (4-3) to plot T_∞ versus T we find a maximum value of T_∞ above which the steady-state heat-balance regime is impossible. The maximum value of T_∞ was determined numerically for two values of the water vapor pressure, zero and 1.5 kPa, corresponding to relative humidities of zero and 60% at an atmospheric temperature of 20°C, and powder depths in the range 1.0 - 10.0 mm. The bed porosity was based on the randomly packed powder value $\phi = 0.4$, the mean particle diameter was taken to be $d = 2.0\ \mu m$, and the oxidation mass flux $\dot{m}''_{ox}$ was calculated using McGillivray's law. Predicted results are shown in Figure 4-3, where the ambient temperature for ignition is plotted against the depth of the layer.

We do not know the temperature or RH of the air on the day in 1951 when Hartmann, et al. at the Bureau of Mines (in Pittsburgh) observed 5 grams of uranium ignite, nor do we know the diameter of the small disc upon which the uranium powder was placed. However, it is reasonable to suppose that the RH in Pittsburgh on any given day exceeds 60%. Thus according to the theoretical results displayed in Figure 4-3, uranium hydride powder of heights in excess of 10 mm undergo spontaneous ignition at room temperature. Five grams of uranium hydride powder placed on a circular surface the size of a dime produces just such a powder. We may conclude that the observed uranium hydride ignition at the Bureau of Mines is not inconsistent with ignition theory. In addition, we may say that for a given metal geometry, uranium hydride does not possess a greater pyrophoric tendency than uranium. Hydriding does result in finely divided reactive metal, however, and this may be the issue with respect to Hanford SNF rather than hydride kinetics.

Figure 4-3: Ignition in Small Powdered Deposits of Uranium Metal or Hydride Predicted With McGillivray, et al. (1994) Oxidation Kinetics

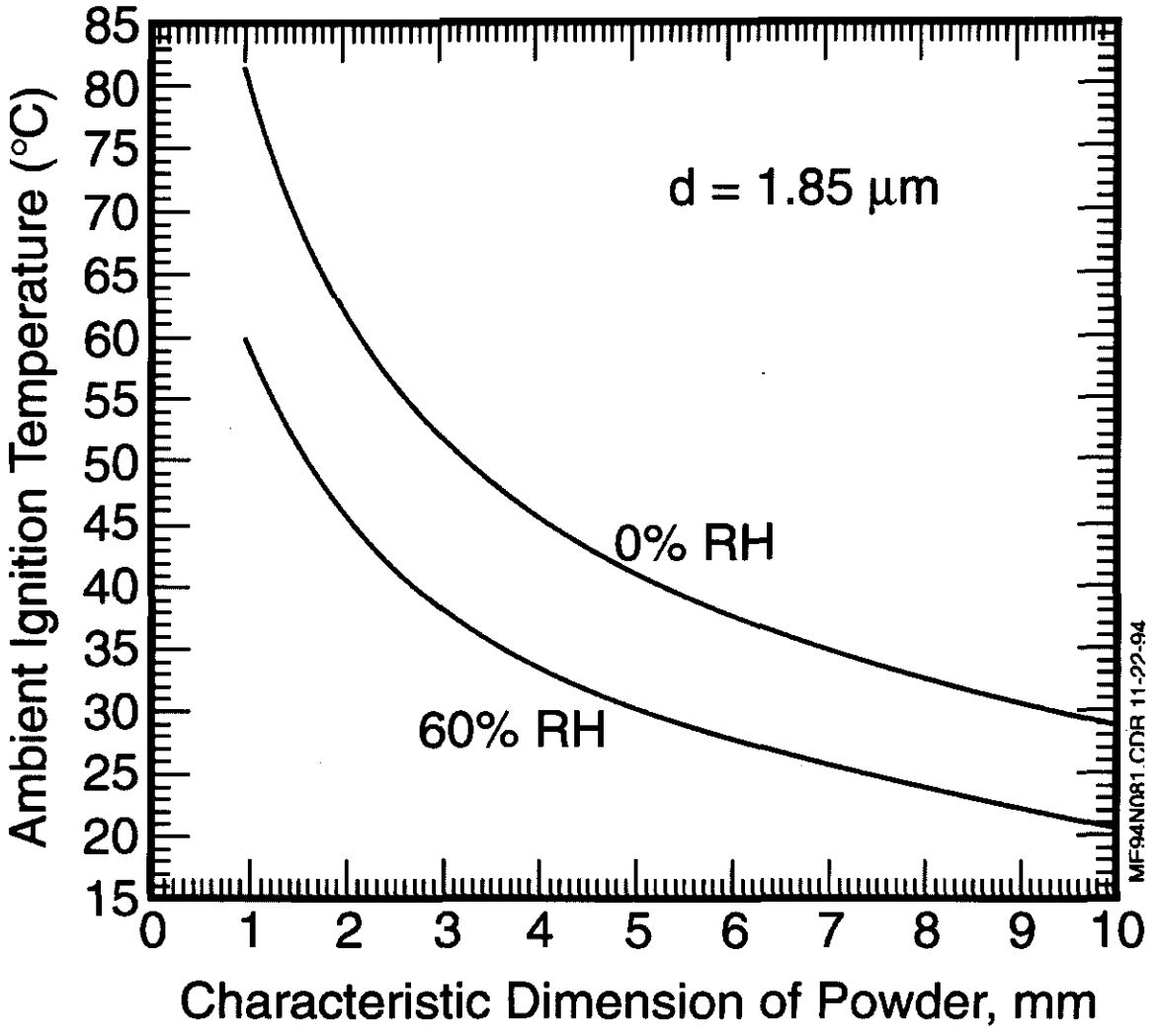

4.3 Tetenbaum, et al. (1962) Uranium Powder Ignition Experiments

The influence of uranium particle size and uranium powder height on ignition temperature was studied by Tetenbaum, et al. (1962). The metal powder charges were placed in stainless steel crucibles of varying diameter in the range 6.35 - 19.05 mm (see Figure 4-4). Powder heights covered the range of 0 - 16 mm. Plots of the measured uranium powder ignition temperature versus powder depth are shown in Figures 4-5 and 4-6 for particle diameters d = 60 μm and d = 840 μm, respectively. The open points in these figures are the measured crucible temperatures at ignition. The ignition temperature was measured by heating the furnace containing the crucible at a known rate in oxygen and recording the temperature of the crucible. Interestingly enough and contrary to intuition and ignition theory, the ignition temperatures were observed to be independent of powder height once a small, critical powder height was exceeded.

No reasonable physical explanation for the trend shown in Figures 4-5 and 4-6 was presented by Tetenbaum, et al., although they attempted to show that their measured ignition temperatures are consistent with an ignition theory in which the chemical heat generated is removed by conduction within a slab whose thickness is equal to the measured critical height of the uranium powder. However, a careful examination of their paper reveals that the reported agreement with theory is based on assigned powder thermal conductivity values involving an order-of-magnitude increase in conductivity for a corresponding increase in particle size from 60 to 1400 μm. This variation in thermal conductivity appears unreasonable when one considers that all the available semi-empirical correlations for predicting effective packed bed conductivity are either particle size independent or show a very weak dependence on particle size. In fact, Swift (1966) measured the thermal conductivity of uranium powder and found that a factor of 30 increase in particle diameter from 30 to 1000 μm results in only a 50 percent increase in powder conductivity. Thus Tetenbaum, et al.'s rationalization of their ignition data must be regarded as unconvincing and the trend of the data in Figures 4-5 and 4-6 remain unexplained. This is unfortunate because the data trends obtained from the apparatus employed by Tetenbaum, et al. have been interpreted to mean that the most important variable affecting the ignition temperature of uranium powder is the specific surface area (surface area per volume or mass of particle). Indeed Schnizlein, et al. (1959) used the data to construct the following correlation between ignition temperature and specific surface area for uranium:

$$T_{ig} = \frac{5562.63}{\log a_m + 8.872} \tag{4-4}$$

where a_m is the surface area per unit mass in $cm^2\ g^{-1}$ and T_{ig} is the ignition temperature in degrees Kelvin. This correlation has been used in a number of evaluations of the susceptibility of uranium metal powder to spontaneous ignition during storage (see e.g. Peacock [1992]). We emphasize here that this correlation should be regarded with caution as it cannot be extrapolated beyond the conditions of the Tetenbaum, et al. experiments.

A straightforward explanation of the data trends shown in Figures 4-5 and 4-6 may be obtained with a two-dimensional model of powder ignition, and this is the subject of the next subsection.

Figure 4-4: Tetenbaum, et al. (1962) Ignition Apparatus

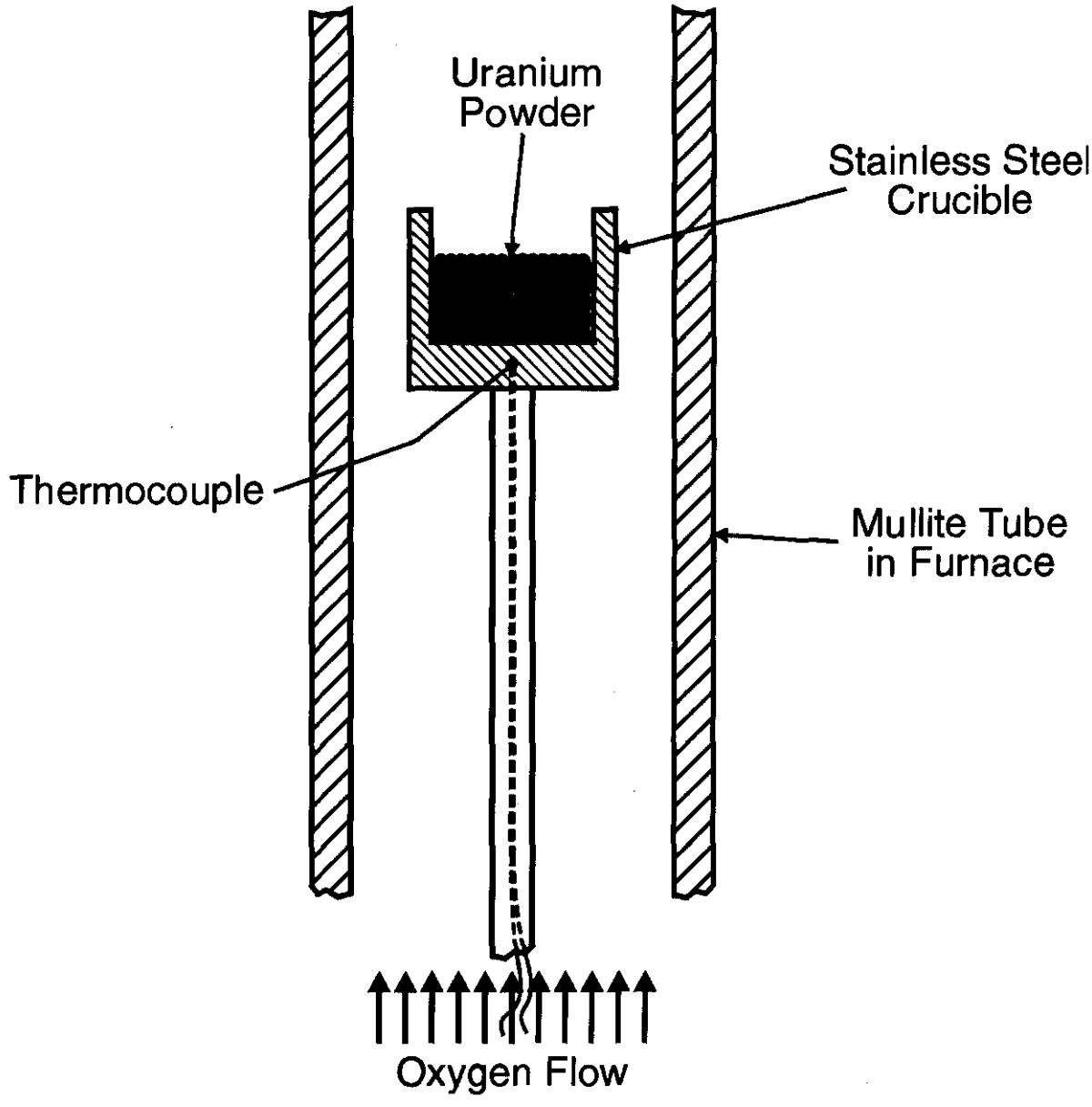

ME947109.CDR 7-22-94

Figure 4-5: Crucible Wall Ignition Temperature Versus Uranium Powder Height in Different Diameter Crucibles - Ignition Theory Compared With Experimental Data of Tetenbaum, et al. (1962)

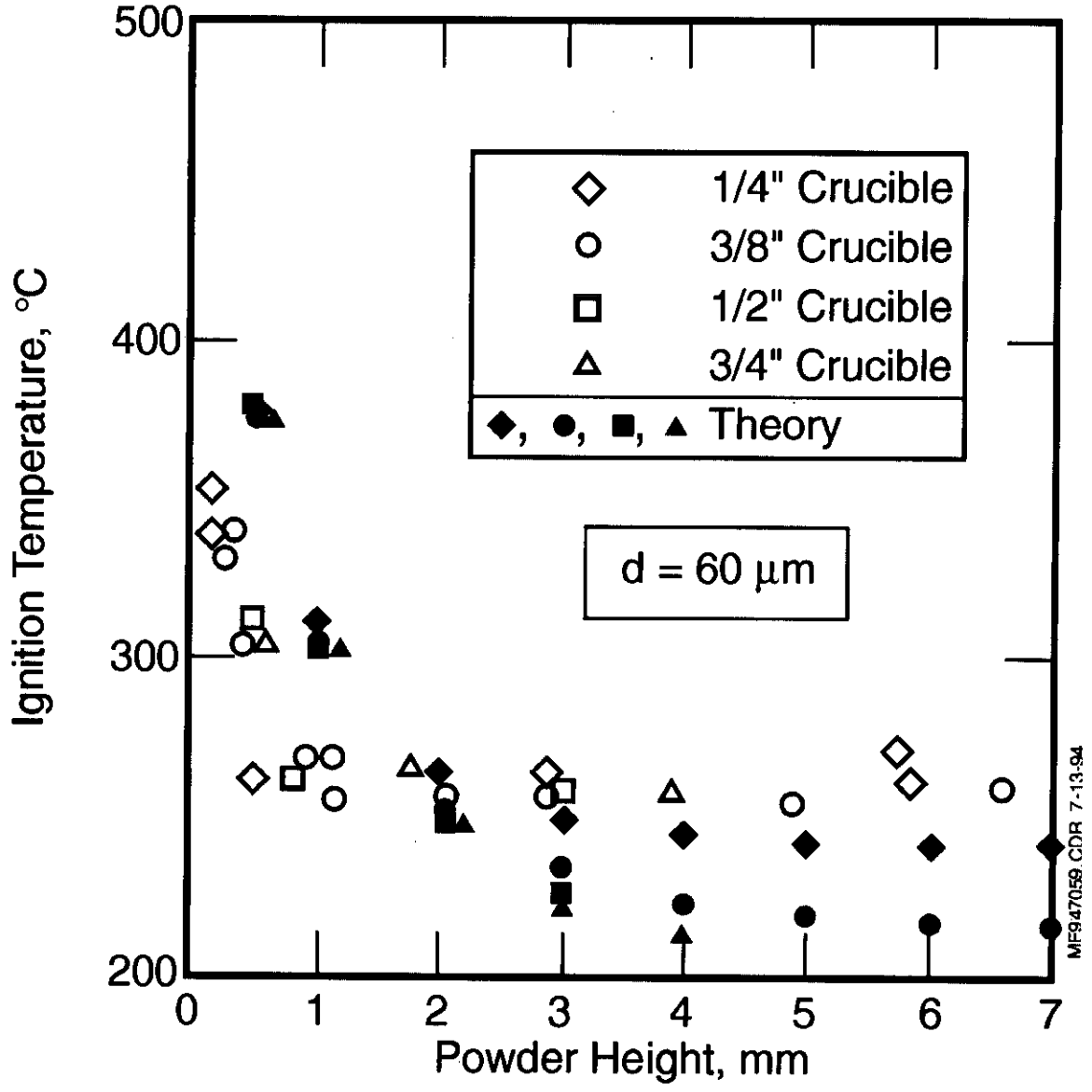

Figure 4-6: Crucible Wall Ignition Temperature Versus Uranium Powder Height in Different Diameter Crucibles - Ignition Theory Compared With Experimental Data of Tetenbaum, et al. (1962)

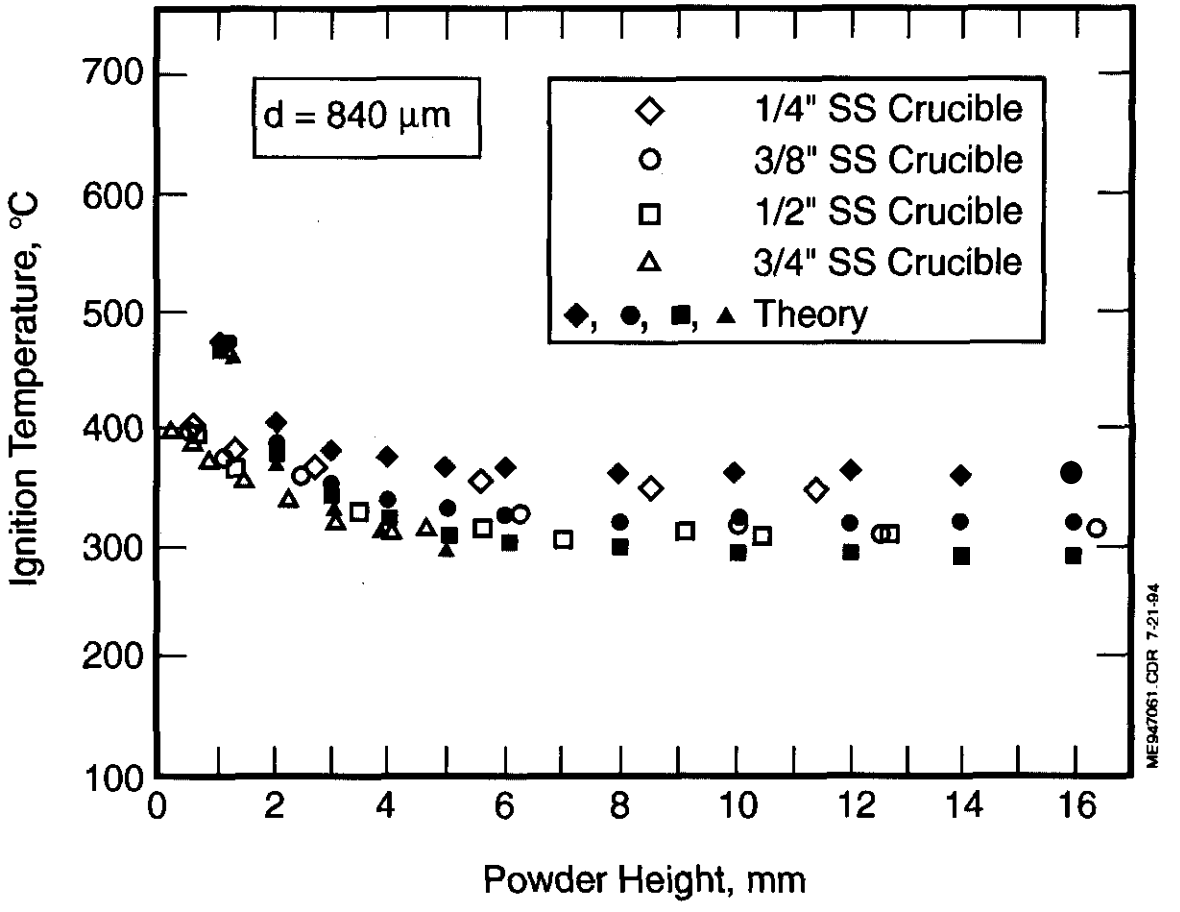

4.4 Interpretation of Tetenbaum, et al. (1962) Uranium Powder Ignition Experiments

The ignition temperature versus powder height trend shown in Figures 4-5 and 4-6 can be explained reasonably well by considering a two-dimensional cylindrically-symmetric temperature distribution in the space occupied by the powder. It is important to recognize that in the Tetenbaum, et al. (1962) experiments, the onset of ignition was determined by monitoring the crucible wall temperature rather than the furnace gas temperature. Thus the only heat loss mechanism to consider in an ignition analysis of these experiments is the conduction of heat through the powder to the crucible wall. Since we do not know the furnace gas (oxygen) temperature at ignition, there is no need to concern ourselves with convective heat transfer from the crucible wall to the flowing oxygen. Accordingly, in the ignition theory presented below, we seek the condition for the sudden impossibility of a steady-state reaction in which the chemical heat production within the powder is balanced by heat conduction through the powder to the crucible walls. We will assume that the temperature of the cylindrical crucible wall is uniform and its value is denoted by the symbol T_w. It is further assumed that no heat loss occurs through the top surface of the powder. This assumption is consistent with the experimental observation that the onset of ignition occurred at the radial center of the powder just below its surface.

The basic equation of the problem is then the equation of steady-state heat conduction in a finite cylinder with local heat generation at the constant volumetric rate $6\,(1-\phi)\,d^{-1}\,\Delta H\,\dot{m}''_{ox}\,(T)$. For constant effective thermal conductivity k_b of the powder "bed", this equation has the form

$$\frac{\partial^2 T}{\partial r^2}+\frac{1}{r}\frac{\partial T}{\partial r}+\frac{\partial^2 T}{\partial z^2} \;=\; -\frac{6\,(1-\phi)\,\Delta H}{k_b\,d}\,\dot{m}''_{ox}\,(T) \qquad (4\text{-}5)$$

where z is the vertical coordinate measured from the bottom of the crucible and r is the radial coordinate measured from the vertical axis of the crucible. The boundary conditions for Equation (4-5) are the constancy of temperature at the crucible walls

$$T\,(r,0) \;=\; T\,(R,z) \;=\; T_w \qquad (4\text{-}6)$$

and the adiabatic condition at the surface of the powder

$$\frac{\partial T}{\partial z}\,(r,L) \;=\; 0 \qquad (4\text{-}7)$$

where R is the radius of the powder (inner radius of crucible) and L is the height of the powder.

The effective thermal conductivity of the uranium powder is estimated here using the Kobayashi (1969) correlation:

$$k_b \;=\; \frac{1.813}{1/k-1/k_m}\left(\frac{k_m}{k_m-1}\,\ell n\left(\frac{k_m}{k}\right)-1\right)+0.0935\,k \qquad (4\text{-}8)$$

where k_m is the thermal conductivity of the uranium metal and k is the thermal conductivity of the interstitial gas. The numerical value of the powder thermal conductivity is estimated using $k_m = 30.0$ W m^{-1} K^{-1}, $k = 0.033$ W m^{-1} K^{-1}, giving $k_b = 0.44$ W m^{-1} K^{-1}. This k_b estimate for powdered uranium falls within the center of the measured k_b values reported by Swift (1966). The Tetenbaum, et al. (1962) experiments employed pure oxygen as the reactive gas so that $\dot{m}''_{ox}(T)$ in Equation (4-5) is given by McGillivray's Law with $p_{H_2O} = 0$; namely

$$\dot{m}''_{ox} = C \exp\left(-\frac{T_E}{T}\right) \tag{4-9}$$

where $C = 10.95$ kg 0_2 m^{-2} s^{-1} and $T_E = 8077.0$ K.

Using the exact method for stationary ignition theory presented in Section 3.3, the F-K parameter for Equation (4-5) is given by:

$$\delta = \frac{6(1-\phi)\,T_E\,R^2\,\Delta H}{T_w^2\,k_b\,d}\,\dot{m}''_{ox}(T_w) \tag{4-10}$$

where the critical value of δ is a function of the height L and radius R of the chemically heated region (powder). Later in Section 4.5, constant reaction rate theory will be employed to derive a modified F-K parameter B whose critical value is B = 1.

The functional relationship δ (L, R) has been determined numerically by Anderson and Zienkiewicz (1974). Approximate algebraic relations for δ (R, L) have been developed by Boddington, et al. (1971, 1982). Their derivation of δ (R, L) for two-dimensional geometries usually involves lengthy evaluations of definite integrals; however, the final expressions for δ (R, L) are algebraic and easy to apply. For the right-circular cylinder, R in Equation (4-10) is replaced by a mean radius R_o given by

$$\frac{3}{R_o^2} = \frac{1}{L^2} + \frac{2}{R^2\left[1 + (R\ /\ L)^2\right]^{1/2}} \tag{4-11}$$

Then, δ is estimated from the following set of algebraic equations:

$$R_s = \frac{3RL}{R+2L} \tag{4-12}$$

$$j = 3\left(\frac{R_o}{R_s}\right)^2 - 1 \tag{4-13}$$

$$\delta = \frac{6(j+3)}{j+7} \tag{4-14}$$

Equations (4-10) to (4-14) can be used to determine the critical crucible-wall temperature T_w above which a uranium powder placed in a crucible will ignite as a function of the diameter of the crucible and the height of the powder bed. Note that Equation (4-10) has to be solved by numerical iteration for T_w once δ has been determined from Equations (4-12) to (4-14).

The calculated crucible temperatures corresponding to uranium powder ignition are plotted as dark data points in Figures 4-5 and 4-6. The calculated values agree reasonably well with the experimental values. The reason that both the measured and theoretical ignition temperature values are independent of height when the powder bed exceeds a critical height can be readily explained. The ignition temperature decreases with increasing powder-bed depth as long as the depth is small compared with the radius of the crucible. When the bed is shallow, most of the heat is conducted downward to the base of the crucible. As the bed depth increases the vertical resistance to heat removal by conduction increases and, accordingly, the ignition temperature decreases. When the bed depth is large enough, however, downward heat conduction is aided by radial heat conduction to the cylindrical crucible wall. The radial distance for heat removal (R) remains constant no matter how deep the powder bed becomes and, therefore, the ignition temperature ultimately becomes independent of powder height.

The insensitivity of ignition temperature to crucible diameter exhibited by both the experimental data and the predictions in Figures 4-5 and 4-6 is due to the fact that the ignition temperature varies only logarithmically with powder radius (see Equations (4-9) and (4-10)) and that the Tetenbaum, et al. experimental program covered a narrow range of crucible diameters.

4.5 Constant Reaction-Rate Theory For 2-D Cylindrical Geometry

The principal mathematical difficulty in thermal ignition problems involving heat conduction within the reacting medium is due to the complicated Arrhenius form of the reaction rate function $\dot{m}''_{ox}(T)$. A conservative but accurate approach to the problem is obtained by assuming that $\dot{m}''_{ox}(T)$ is spatially uniform and evaluated at the location in the reactive region where the temperature is a maximum, i.e., where $T = T_{max}$. Note that T_{max} is initially unknown but readily determined once the heat conduction equation is solved for the temperature distribution in the reactive medium with an assumed spatially uniform heat source.

Consider the problem treated in the previous subsection, namely a reactive right-circular cylinder with constant temperature T_w along the side wall and lower circular boundary and an adiabatic upper circular surface. For a spatially constant volumetric heat generation rate $6(1-\phi)\Delta H\,\dot{m}''_{ox}(T_{max})/d$ in a reactive powder, the solution for the temperature distribution is (Carslaw and Jaeger 1959)

$$T = T_w + \frac{6(1-\phi)\Delta H \dot{m}''_{ox}(T_{max})}{k_b d}\left\{\frac{z(2L-z)}{2} - \frac{16L^2}{\pi^3}\sum_{n=0}^{\infty}\frac{I_0[(2n+1)\pi r/(2L)]}{(2n+1)^3 I_0[2n+1)\pi R/(2L)]}\sin\frac{(2n+1)\pi z}{2L}\right\} \quad (4\text{-}15)$$

where I_o is the modified Bessel function of zero order. Obviously, the maximum temperature occurs at the center of the adiabatic upper surface of the powder. Thus by setting r = 0 and z = L in Equation (4-15) and solving, the result for T_w gives the following relationship between T_w and T_{max}

$$T_w = T_{max} - \frac{6(1-\phi)L^2 \Delta H \dot{m}''_{ox}(T_{max})}{k_b d} \cdot \left\{\frac{1}{2} - \frac{16}{\pi^3}\sum_{n=0}^{\infty}\frac{(-1)^n}{(2n+1)^3 I_0[2n+1)\pi R/(2L)]}\right\} \quad (4\text{-}16)$$

Note that the term in brackets is only geometry-dependent and is constant for a given reactive medium aspect ratio, L/R. As is usual in problems of this type, T_w exhibits a maximum value when plotted against T_{max} and this maximum value is the "wall ignition temperature".

A modified F-K parameter for this problem has the same form as introduced previously but augmented by a geometric form factor f whose value is particular to the cylindrical geometry, constant side and bottom surface temperature, and an adiabatic top:

$$f = 1 - \frac{32}{\pi^3}\sum_{n=0}^{\infty}\frac{(-1)^n}{(2n+1)^3 I_o[(2n+1)\pi R/(2L)]} \quad (4\text{-}17)$$

$$B = \frac{A_v L^2 f C \Delta H T_r}{2 k_b T_\infty \exp(T_r - 1)} \quad (4\text{-}18)$$

again with a critical value B=1.

It is of interest to compare the constant reaction-rate theory described above with the more accurate method of Boddington, et al. (1971, 1982). We note from Figure 4-5 that Boddington, et al's. method results in a predicted ignition temperature of 240°C for a 6.0-mm deep powder of 60 μm particles in a 1/4-inch diameter crucible. Equation (4-16) yields an ignition temperature of 231°C for this powder. This represents less than a 4% deviation from the accurate theory. Note that the constant wall temperature boundary condition provides the most stringent test of the accuracy of the constant reaction-rate theory, as the difference between the two methods vanishes in the limit of surface-convection heat-loss control.

The constant-reaction rate theory is particularly powerful for combined multi-dimensional geometries and finite-surface heat-transfer coefficients. In this situation the method results in very accurate ignition temperature predictions, and the method is conceptually simple compared with the method developed by Boddington, et al. (1971, 1982), and is certainly easier to apply than available numerical techniques (Anderson and Zienkiewicz 1974). In the next section we apply constant-reaction rate ignition theory to a reactive region bounded by a right-circular cylinder with finite-surface heat-transfer coefficients. The results are used to explain the numerous reported spontaneous ignitions of uranium turnings and sintered briquettes placed in drum storage.

4.6 Summary

Evaluations presented above provided confidence in the ability of ignition theory to predict uranium ignitions observed in the laboratory and to explain spontaneous fires that have been experienced during the storage of uranium. In the following sections, we turn our attention to the prediction of the conditions for ignition of Hanford SNF.

5.0 URANIUM PYROPHORICITY INCIDENTS AND INTERPRETATION VIA IGNITION THEORY

5.1 Early Publication History

Pyrophoric behavior of metals used in reactors and defense applications, such as uranium, plutonium, zirconium, and hafnium, is documented in available reports and publications dating from the decade of the 1950's. Apparently, most or all of the material was classified. The earliest clear reference on the topic, AEC Uranium Fire Experience (no author name appears, but this report is sometimes associated with the name of the declassifier, Pearson; see References), dates from 1954 and specifically notes at that time,

> ... perhaps the bulk of the AEC uranium fire experience does not appear to have been recorded and that treatment of the problem to date has been basically confined to uranium fire extinguishment with results that differ with each Operations Office concerned.

The reference goes on to say,

> AEC uranium fires cannot presently be statistically studied due to the absence of recorded information. One contractor (National Lead at Fernald) has experienced upward of 300 such fires in a single month.

The reference describes select incidents in a few sentences apiece, categorizes incidents by type, briefly describes oxidation phenomena, hypothesizes causes for uranium fires, summarizes current mitigation techniques, and proposes a rather detailed research plan to formally understand causes of uranium fires and preventive measures.

Immediately in the literature we may trace a response to AEC Uranium Fire Experience. A literature survey by Robert Hilliard of Hanford on heating of irradiated uranium (Hilliard 1957) cites a classified report by Wally Schultz on ignition of uranium metal in air written only a few months later than the AEC report (Schultz 1955). Hilliard's work goes on to cite data on uranium properties and evaluations of uranium reactions generally from the early 1950's through early 1957. Two articles on the industrial hazard of pyrophoric reactor materials appeared in the December 1956 issue of Nucleonics (see References), motivated by several deaths and serious injuries which had occurred that year in separate incidents with zirconium, uranium, and thorium.

Formal research intended for publication was clearly undertaken subsequent to the AEC report. Hilliard began research on overheating of uranium metal reactor fuels and fission product release, and published a Hanford report in 1959 and a formal journal article in 1961.

At Argonne, Schnizlein, et al. (1959) produced a report on ignition behavior and kinetics of zirconium, thorium, uranium, and plutonium. Tetenbaum et al. (1962) pursued this line of inquiry at Argonne with studies on uranium particle bed ignition; his experiments were described in detail in Section 4.0. The Argonne work continued with publications on burning velocity by

Liebowitz, et al. (1963) and on burning temperatures by Mouradian and Baker (1963). Research at Argonne appears to have concluded with three articles in the Journal of Nuclear Materials comprising two publications by Baker, et al. (1966) and Baker and Bingle (1966), a study of uranium oxidation kinetics (already described in Section 4.0) and a review article on ignition of uranium, and a study of ignition of binary alloys of uranium by Schnizlein, et al. (1966). Baker and Liimatainen (1973) co-authored a review on chemical reactions in nuclear safety for *The Technology of Nuclear Reactor Safety*, the preeminent summary of the topic through the early 1970's.

Accounts of uranium pyrophoricity during storage and processing have recently been given by Abrefah, et al. (1999) and Demiter (1998). The Demiter survey is included as Appendix B. The surveys cover the period 1955-1995 and are essentially updated versions of the much earlier report, AEC Uranium Fire Experience. Douglas United Nuclear (DUN) developed a process for encapsulating metallic uranium scrap in concrete cylinders cast in thin sheet metal cans. A series of tests were performed at DUN to determine the conditions for ignition of the concreted cylinders. The results are reported in Weakley (1980).

As we have already learned the factors which influence uranium pyrophoricity are metal particle size, ambient temperature, ambient moisture content, and heat sources other than oxidation-kinetic heating. Information on one or more of these factors is missing from the documentation of uranium metal ignition incidents. Consequently it is not possible to provide an unambiguous comparison between ignition theory and ignition incidents. However we can demonstrate that the ignition events are compatible with thermal ignition theory.

5.2 Classification of Incidents

A careful reading of the reviews of uranium fire or explosion incidents (Pearson 1954; Abrefah et al. 1999; and Demiter 1998) indicates that the uranium metal ignitions at manufacturing or government sites can be categorized into the following four types:

1. Onset (ignition) of a chemical runaway reaction inside opened drums containing clad uranium fuel elements with exposed uranium surfaces (due to corrosion or sectioning) or uranium scrap consisting of lathe turnings and saw fines. Also ignition of uranium scrap encapsulated in concrete. High ambient temperature and humidity were presumed to be responsible for these ignitions. The runaway ignitions inside drums or concrete cylinders were followed by slow burning similar to a charcoal fire.

2. Explosions inside drums containing corroded fuel elements or metal scrap. An explosion occurred while the drum was being tapped to loosen the lid and at the instant that ambient air entered the drum. Apparently hydrogen gas was also present in the drums that exploded.

3. Ignition of highly corroded fuel elements or defueled, highly porous cladding following accidental dropping onto the floor or during element-to-element contacting under violent shaking conditions in fuel dissolvers or while in transfer trays.

4. Ignition of badly corroded or powdered uranium metal in air at ambient temperature or ignition of accumulated metal powder under water.

We now proceed to show that these ignitions are consistent with thermal ignition theory. We begin with a discussion of Type (1) ignitions inside drums exposed to ambient air.

5.3 Ignition Conditions for Uranium Briquettes or Lathe - Turnings in Drum Storage

Thousands of spontaneous fires have been experienced at room temperature during drum storage of lathe turnings or uranium briquettes made from compacted turnings (Pearson 1954). An appropriate ignition model for these fire experiences would be a packed bed of uranium pieces of given porosity ϕ and specific area A/V, which fills an upright cylindrical drum of radius R and height L. The appropriate energy equation for the reactive cylindrical medium is given by Equation (4-5) where d is now regarded an effective spherical particle size (diameter), which is related to the specific area of the uranium pieces by $A_v = 6/d$. In Equation (4-5), z is the vertical coordinate measured from the bottom of the drum and r is the radial coordinate measured from the vertical axis of the drum.

In order for ignition to occur, the drum lid must be removed. The boundary condition at the exposed upper surface of the debris bed is

$$k_b \frac{\partial T}{\partial z}(r, L) = -h_u \left[T(r, L) - T_\infty\right] \tag{5-1}$$

where h_u is the heat transfer coefficient for combined, linearized "upward" radiation and natural convection and T_∞ is the ambient temperature. Along the cylindrical-side wall of the drum we have the boundary condition

$$k_b \frac{\partial T}{\partial r}(R, z) = -h_s \left[T(R, z) - T_\infty\right] \tag{5-2}$$

where h_s is the heat transfer coefficient for "sideward" directed, combined linearized radiation and natural convection. Heat may be conducted out of the bottom of the drum into the floor. The heat transfer coefficient for this process is denoted by h_d and the relevant boundary condition is

$$k_b \frac{\partial T}{\partial r}(r, 0) = h_d \left[T(r, 0) - T_\infty\right] \tag{5-3}$$

The heat transfer coefficients h_u, h_s, and h_d are discussed below in more detail.

In order to solve Equation (4-5), subject to boundary conditions in Equations (5-1) to (5-3), we invoke the constant reaction-rate theory and assume that chemical heating occurs uniformly throughout the reactive medium at a rate proportional to $\dot{m}''_{ox}(T_{max})$, where T_{max} is the initially unknown maximum temperature within the reactive medium. The solution to Equation (4-5) with uniform internal heating and convection on all boundaries, as given by Equations (5-1) to (5-3) is (Epstein, et al. 1996):

$$T(r,z) = T_\infty + \frac{6(1-\phi)\Delta H}{k_b\, d}\,\dot{m}''_{ox}(T_{max})\left\{L_o\left(\frac{h_d}{k_b}z+1\right)-\frac{z^2}{2}-\frac{h_s}{k_b}\sum_{n=1}^{\infty}\right.$$
$$\left.\bullet\ \frac{\lambda_n\,\beta_n\,I_0(\alpha_n r)}{\alpha_n\,I_1(\alpha_n R)+\frac{h_s}{k_b}I_0(\alpha_n R)}\left[\cos(\alpha_n z)+\frac{h_d}{k_b\,\alpha_n}\sin(\alpha_n z)\right]\right\} \quad (5\text{-}4)$$

where I_0 and I_1 are the modified Bessel functions of zero and first order, respectively. The quantities L_o, α_n, λ_n, and β_n are algebraic functions of the dimensions of the cylinder as follows. Introducing the normalized heat transfer coefficients

$$H_u = \frac{h_u}{k_b}, \qquad H_d = \frac{h_d}{k_b}, \qquad H_s = \frac{h_s}{k_b} \quad (5\text{-}5)$$

Then,
$$L_0 = \frac{L(1+L\,H_u/2)}{H_u + H_d + L\,H_u\,H_d} \quad (5\text{-}6)$$

α_n is the n-th positive root of

$$\tan\alpha_n L = \frac{\alpha_n(H_u+H_d)}{\alpha_n^2 - H_u\,H_d} \qquad n = 1, 2, \ldots, \infty, \quad (5\text{-}7)$$

$$\lambda_n = \frac{2\alpha_n^2}{H_u\,\frac{\alpha_n^2+H_d^2}{\alpha_n^2+H_u^2} + H_d + L\left(\alpha_n^2+H_d^2\right)}, \quad (5\text{-}8)$$

and

$$\beta_n = -\frac{1}{2}\left[\frac{2L\cos\alpha_n L}{\alpha_n^2} + \frac{(\alpha_n L)^2 - 2}{\alpha_n^3}\sin\alpha_n L\right] + L_0 H_d\left[\frac{\cos\alpha_n L}{\alpha_n^2} + \frac{L}{\alpha_n}\sin\alpha_n L - \frac{1}{\alpha_n^2}\right] + \frac{L_0}{\alpha_n}\sin\alpha_n L - \frac{H_d}{2\alpha_n}\left[\frac{2L\sin\alpha_n L}{\alpha_n^2} - \frac{(\alpha_n L)^2 - 2}{\alpha_n^3}\cos\alpha_n L - \frac{2}{\alpha_n^3}\right] + \frac{L_0 H_d^2}{\alpha_n}\left[\frac{\sin\alpha_n L}{\alpha_n^2} - \frac{L\cos\alpha_n L}{\alpha_n}\right] - \frac{L_0 H_d}{\alpha_n^2}(\cos\alpha_n L - 1) \quad (5\text{-}9)$$

The maximum temperature, T_{max}, in the reactive medium (i.e., the cylindrical uranium debris bed) is achieved along the axis of the cylinder and therefore is obtained by setting r = 0 in Equation (5-4) and differentiating the result with respect to z to obtain dT/dz. The location $z = z_{max}$ at which T (0, z) is a maximum is where dT/dz = 0. Identifying z in Equation (5-4) with z_{max}, setting r = 0, and solving the result for T_∞ yields

$$T_\infty = T_{max} - \frac{6(1-\phi)\Delta H}{k_b d}\dot{m}''_{ox}(T_{max})\left\{L_o\left(\frac{h_d}{k_b}z_{max} + 1\right) - \frac{z_{max}^2}{2} - \frac{h_s}{k_b}\sum_{n=1}^{\infty} \bullet \frac{\lambda_n \beta_n}{\alpha_n I_1(\alpha_n R) + \frac{h_s}{k_b} I_o(\alpha_n R)}\left[\cos(\alpha_n z_{max}) + \frac{h_d}{k_b \alpha_n}\sin(\alpha_n z_{max})\right]\right\} \quad (5\text{-}10)$$

If one uses the above equation to plot T_∞ versus T_{max}, T_∞ will pass through a maximum value which is the ignition temperature.

The form of Equation (5-10) may be simplified to

$$T_{max} - T_\infty = \frac{A_v L^2 f \Delta H C e^{-T_E/T}}{2k_b} \quad (5\text{-}11)$$

$$f = \frac{2L_o}{L^2}\left(B_d\frac{z}{L} + 1\right) - \left(\frac{z}{L}\right)^2 - \frac{2B_s}{L^3}\sum_{n=1}^{\infty} C_n\left[\cos(\alpha_n z) + \frac{B_d}{\alpha_n L}\sin(\alpha_n z)\right] \quad (5\text{-}12)$$

where f is the geometric form factor, B_d and B_s are Biot numbers (hL/k), C_n represents the coefficient of the infinite series in Equation (5-10); and the definition of A_v for the contents of the cylinder is employed. The ignition parameter for this system is then given by Equation (4-18), where the form factor f for this case is given by Equation (5-12), and the parameter is normalized so that B=1 is the ignition criterion. Note that f must be evaluated at $z = z_{max}$; this occurs when (df/dz) = 0.

The effects of the specific surface area of the uranium pieces and the size of the storage drum on the ambient ignition temperature are determined numerically without linearization of the reaction power by first seeking the location $z = z_{max}$ where dT/dz is zero and then seeking the maximum value of T_∞ given by Equation (5-4). Two cases are considered; an isolated drum and a drum within an array of drums stored side-by-side. Heat is lost from the isolated drum by convection and radiation off its top and circular side wall. The heat transfer coefficients are estimated to be $h_u = h_s = 9.0$ W m^{-2} K^{-1}, where $h_u = h_t + 4\,\varepsilon\,\sigma\,T_\infty^3$, and $h_s = h_\ell + 4\,\varepsilon\,\sigma\,T_\infty^3$. The radiation component of h_u and h_s is obtained by linearizing the radiation heat flux expression. The drum is assumed to rest on a concrete floor and the appropriate heat transfer coefficient is $h_d = k_{con}/R$, where k_{con} is the thermal conductivity of the concrete (≈ 1.7 W m^{-1} K^{-1}) and R is the radius of the drum. Most of the chemical heat generated within a drum surrounded by other drums is removed by radiation and convection off the top of the stored uranium briquettes. In this case we estimate $h_u = 9.0$ W m^{-2} K^{-1} and assume $h_d = h_s = 0$. The porosity ϕ and thermal conductivity k_b of the briquette or turnings pile are taken to be 0.4 (random packing) and 0.44 W m^{-1} K^{-1}, respectively, for all calculations presented. The atmospheric water vapor pressure is fixed at $P_{H_2O} = 2.0$ kPa and the McGillivray, et al. kinetic rate is used to estimate $\dot{m}''_{ox}(T)$. This value corresponds to an atmospheric RH = 70% at an atmospheric temperature of 23°C (73°F).

The results of the ignition calculations are shown in Figure 5-1 for 30 and 50 gal drums. The radius and height of the uranium briquette bed in a 30 gal drum are R = 0.23 m and L = 0.75 m, while those of the 50 gal drum are R = 0.29 m and L = 0.89 m. It is clear from the figure that spontaneous fires are not likely to occur in isolated drums of stored uranium pieces. However, fires may start at room temperature in one or more drums of a collection of drums stored side-by-side and containing uranium chips, turnings, briquettes, etc. with specific areas greater than about $A/V \approx 3 \times 10^3$ m^{-1}. Fires of this type were common during the 1940s and 1950s, and were most apt to occur on hot humid days (Pearson 1954). Note that uranium turnings are typically 10 to 100 μm thick and therefore have specific areas in the range 10^4-10^5 m^{-1}. Uranium briquettes were made by compacting turnings and producing a sintered metal material of roughly 40% void space. Thus the specific area A/V of stored uranium briquettes may have been of the same order as the A/V values for turnings.

Decay power may be considered in the cylindrical evaluations above by noticing that the volumetric power term under the constant reaction rate approximation is given by

$$Q_v = A_v\,\Delta H\,\dot{m}''_{ox}(T) \qquad (5\text{-}13)$$

Hence, constant volumetric decay power merely augments this term:

$$Q'_v = Q_{dk} + Q_v \qquad (5\text{-}14)$$

where Q_{dk} is decay power per unit volume of the cylinder (i.e., $(1 - \phi)$ times the decay power of spent fuel in the cylinder). A new effective heat loss temperature may be defined as

$$T'_\infty = T_\infty + \frac{Q_{dk} L^2}{2 k_b} \qquad (5\text{-}15)$$

Figure 5-1: Ambient Ignition Temperature Versus Specific Area for Uranium Turnings, Chips, Sintered Briquettes, etc. in Drum Storage

p_{H_2O} = 2.0 kPa.

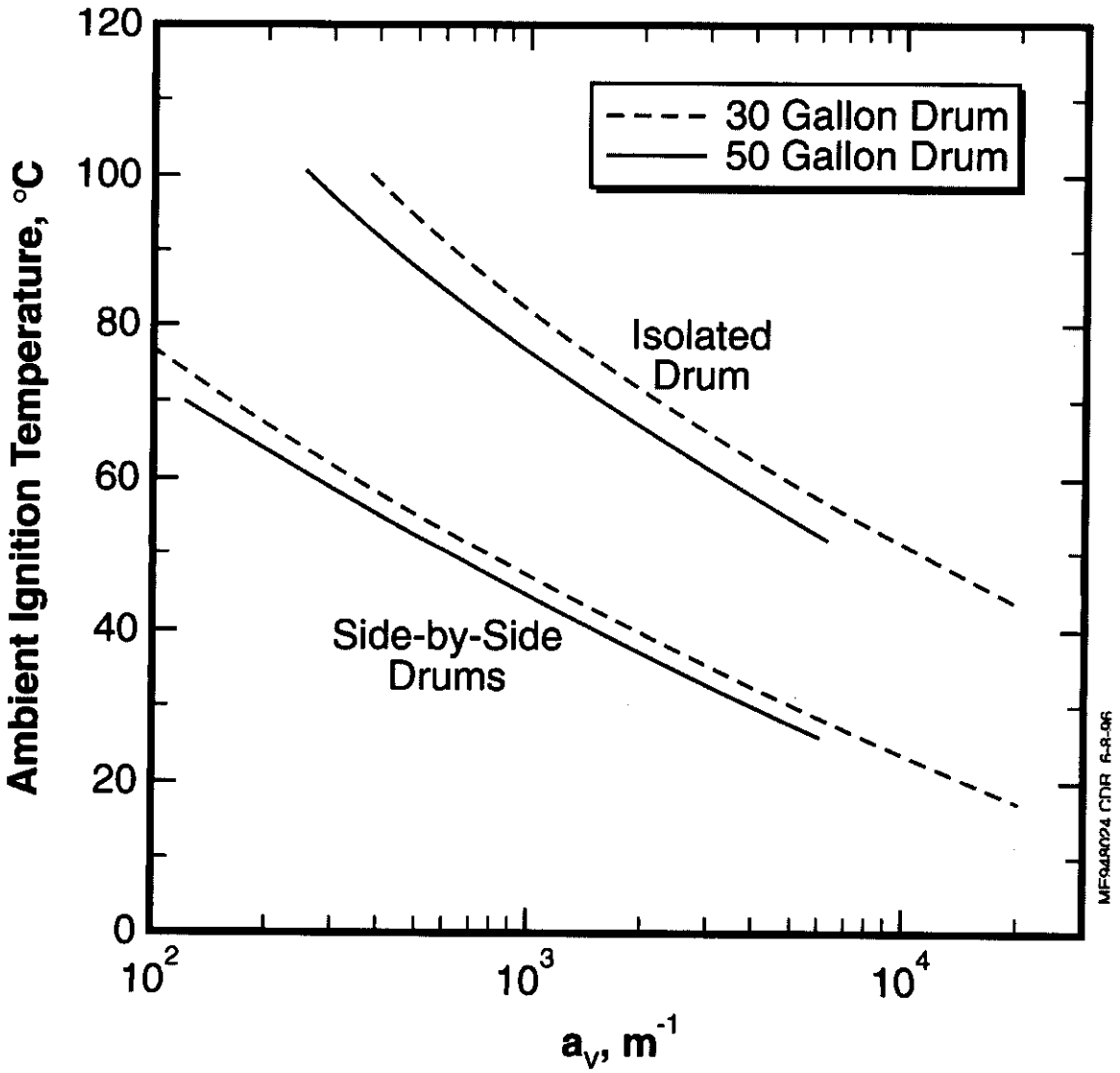

which then allows the form of Equation (5-11) to be retained. The ignition parameter B is the same, except that T_∞ is replaced by its definition in Equation (5-15), and this new value appears in the definition of T_r.

Ignition incidents also occurred in concreted uranium scrap cast into drums (sheet metal cans). Apparently the encapsulated uranium metal reacted with the "free" water in the concrete cylinder. Three different combinations of metal scrap were encapsulated in the concrete cylinders during the autoignition test program performed at DUN (Weakley 1982). These are listed in Table 5-1.

Table 5-1: Mass (in kg) and Size Characteristics of Concreted Uranium Metal Scrap Used in Ignition Tests

Type of Scrap	Average Ratio Fines-to-Chips	Heavy Ratio Fines-to-Chips	Chips Only - Single Chopped	Chips Only - Double Chopped
Fines	4.9	17.9	0	0
Single Chopped Chips	13.3	11.2	12.3	0
Double Chopped Chips	0	0	0	15.4

Unfortunately, the sizes of the fines and chips were not measured and, therefore, a direct comparison of the ignition observations with theory is not possible. However, the theory can be used to predict the sizes of the concrete encapsulated uranium scrap below which ignition occurs. If these predicted sizes are reasonable we may regard thermal ignition theory capable of accounting for the observed ignitions.

The volume of the concrete uranium scrap cylinders in the tests was 0.0275 m^3. The height and/or diameter of the cylinders were not reported. The photographs supplied in Weakley (1982) indicate a cylinder aspect ratio of about unity. Thus the radius and height of the cylinder are estimated to be R = 0.164 m and L = 0.327 m, respectively. The mathematical formalism (Equations (5-4) and (5-10)) derived in the foregoing for predicting ignition conditions in a reactive cylindrical drum of scrap can be immediately applied to the problem of concreted uranium scrap. The thermal conductivity k_b is identified with that of concrete ($k_b = k_{cm}$; 1.7 W m^{-1} K^{-1}) and the oxidation law is assumed to be best represented by the Pearce (1989) oxidation rate correlation for an oxygen free mixture, namely

$$\dot{m}''_{ox} = 119.6 \exp\left(-\frac{6945}{T}\right) \qquad (5\text{-}16)$$

where $\dot{m}''_{ox}$ is in kg O_2 m^{-2} s^{-1} and T is in K. The appropriate heat of reaction that accompanies this law is $\Delta H = 1.67 \times 10^7$ J kg^{-1}. The heat transfer coefficients off the top and sides of the concrete are the same as those estimated for the drum: $h_u = h_s = 9.0$ W m^{-2} K^{-1}. As for the case of the drum, it is assumed that the concrete cylinders in the tests at DUN were placed on a concrete floor; thus, the downward heat transfer is $h_d = k_{con}/R = 10.4$ W m^{-2} K^{-1}.

Another parameter required by the reactive cylinder model is the volume fraction ϕ_m of the encapsulated uranium metal ($1 - \phi$ in Equations (5-4) and (5-10)). The volume fraction can be calculated by dividing the known metal mass by the product of the density of the metal material (1.9×10^4 kg m^{-3}) and the volume of the concrete cylinder (0.0275 m^3). In calculating the volume fractions for the average and heavy fine-to-chip ratio combinations, only the fine components are considered. The larger chip components of the mixture should be less pyrophoric than the fines. The volume fractions for the average and heavy fine-to-chip ratio combinations are then 9.3×10^{-3} and 3.4×10^{-2}, respectively. For the chip only tests the average volume fraction is 2.7×10^{-2}.

The predicted ambient temperatures, T_∞, above which ignition of the encapsulated metal occurs are shown in Figure 5-2 as a function of the characteristic dimension d of the metal scrap. The upper, middle and lower curves refer, respectively, to incipient ignition of the average fine-to-chip ratio cylinders, the chip only cylinders and the heavy fine-to-chip ratio cylinders. The theoretical ignition curves given in the figure do not account for the exothermic hydration process associated with the curing of concrete. The testing at DUN with uranium-free cylinders showed that the internal concrete temperature decays back to the ambient temperature in about 50 hours after casting. Prior to ignition testing, the metal-encapsulated concrete cylinders were cured for at least five days.

The average fine-to-chip ratio cylinders were placed in a 63°C ambient environment for three days. These cylinders did not autoignite. It follows from the theory summarized in Figure 5-2 that the characteristic diameter of the uranium saw fines used in the tests must have exceeded d; 0.48 mm. When the ambient temperature was increased to 97°C, ignition was observed after about 1.0 day. The theory suggests then that the effective diameter of the metal fines was less than about d; 2.5 mm. This predicted size range of the metal fines is consistent with the ignition curve in Figure 5-2 for the heavy fine-to-chip ratio cylinder and the test results. If $0.48 < d < 2.5$ mm for the fines, we anticipate ignition to occur in the heavy fine-to-chip cylinder when the ambient temperature is between 41 and 70°C. Indeed, ignitions of the heavy fine-to-chip ratio cylinders were observed after about two-to-three days in a 63°C environment. These ignitions are judged to be borderline ignitions since they did or did not occur, depending on the method of curing the concrete or whether or not a small fraction (10%) of the fines were concentrated at the center of the cylinder (i.e., unmixed). Thus the effective size of the fine employed in the DUN tests is estimated to be d; 1.5 mm. All the cylinders, including the chips-only cylinders, ignited when placed in a room at 97°C. We infer from this observation and the theoretical chips-only ignition curve in Figure 5-2 that $d \leq 7.0$ mm for the uranium metal chips. The ignition model predicts the expected result that the chips were probably much larger than the fines in the DUN tests.

Figure 5-2: Ambient Ignition Temperature Versus Effective Size of Uranium Metal Scrap Encapsulated in Concrete; Metal Volume Fraction as a Parameter

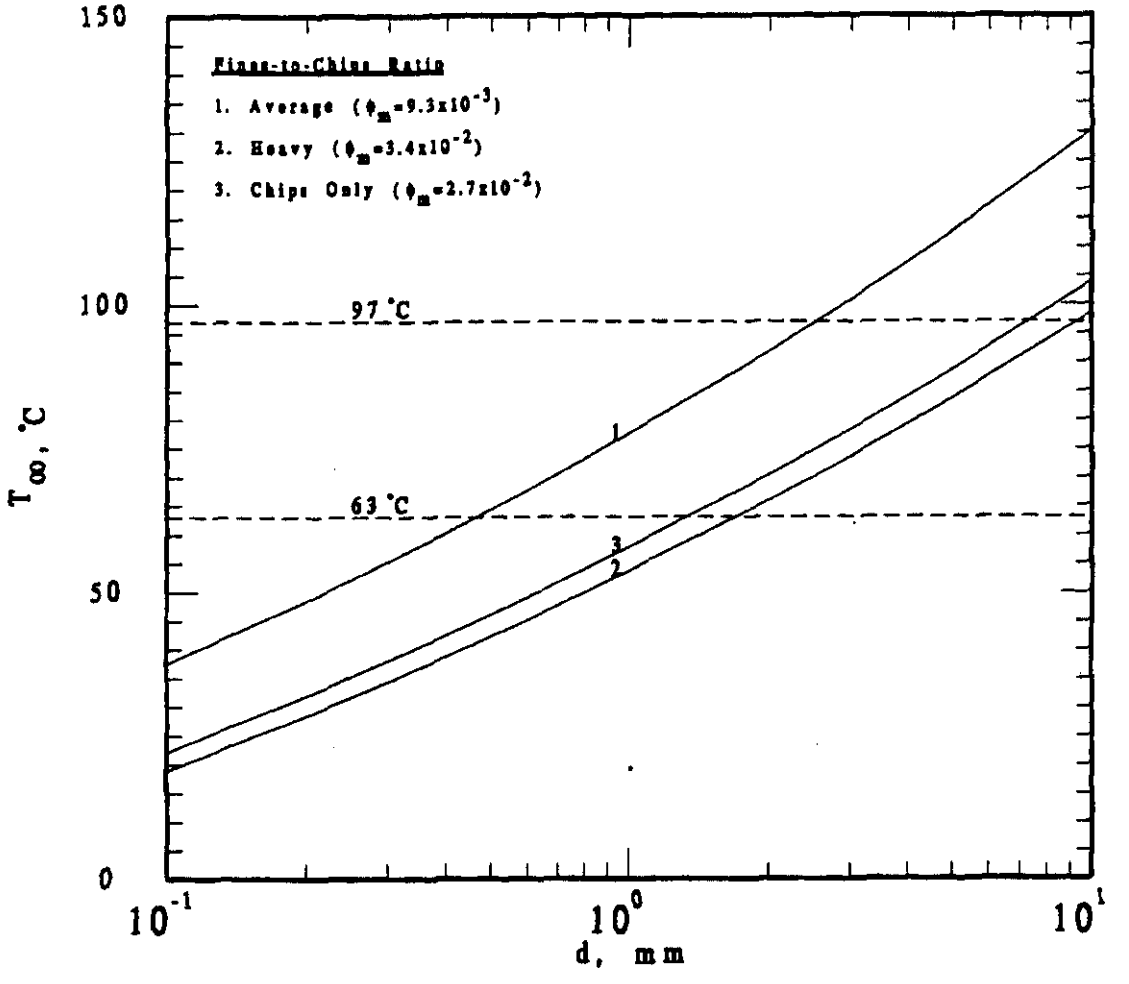

5.4 Explosions Inside Drums Containing Corroded Fuel Elements or Metal Scrap

In this section we present a discussion of Type (2) ignitions. Recall from Section 5.2 that these occur when fuel or scrap is found to be severely corroding in their storage containers. In many reported incidents, flashing of the fuel or explosions occurred when the containers were opened. The flashing was believed to be the spontaneous ignition of uranium or uranium hydride powder, which became suspended due to the mechanical disturbance of opening the container. Suspended uranium powder could also be the cause of the explosions that were reported. Such explosions are known as dust explosions. It is well known that if a settled dust is disturbed, a dust suspension may be formed and ignited by, say, a spark.

Hydrogen gas is usually present inside the containers that store corroded fuel. Flammable hydrogen gas/air mixtures formed upon opening the container may have also been responsible for the reported explosion incidents. We have already demonstrated thermal ignition theory's

ability to predict the ignition of flammable gas mixtures (see Section 3.4). The minimum ignition energy for flammable gas mixtures was shown to be small, only a fraction of a millijoule. The electrostatic potential of a storage drum is such that it can release a spark of energy of about 40 mJ (Britton and Smith 1988). Thus ignition theory provides the understanding of why containers storing corroded fuel or scrap and within which hydrogen buildup occurs are prone to ignite and explode.

Metal dust is also quite flammable and explosive. Depending on the dust concentration, the flame speed may be high and comparable with that in gas deflagrations. The hazard of a uranium dust explosion upon opening a container storing corroded fuel is about the same as a hydrogen explosion. This can be demonstrated through knowledge of the important explosibility characteristics of uranium dust suspensions, namely; the minimum explosive concentration and the minimum ignition energy. This information is apparently not available for uranium metal dust. However, the information can be obtained by appealing to classical thermal ignition theory.

Much like in our previous study of the MIE of a flammable gas mixture (see Section 3.4), we consider a spherical hot spot in a dust cloud within which a high temperature, T_{HS}, is created at zero time. The temperature of the surrounding dust suspension is initially uniform and at temperature T_0. The problem of metal dust ignition is solved by integrating the transient oxygen mass transport and consumption equation, the metal fuel consumption equation, and the transient energy equation in a spherically symmetric coordinate system. These equations are

$$\frac{\partial Y_{ox}}{\partial t} = \frac{D}{r^2}\frac{\partial}{\partial r}\left(r^2\frac{\partial Y_{ox}}{\partial r}\right) - \frac{6\phi_p k_0}{\rho d(1-\phi_p)}\exp\left(-\frac{T_{act}}{T}\right) \tag{5-17}$$

$$\frac{\partial Y_m}{\partial t} = -\frac{6M_p k_0}{\rho_p d M_{ox}}\exp\left(-\frac{T_{act}}{T}\right) \tag{5-18}$$

$$\frac{\partial T}{\partial t} = \left(\frac{k}{\rho c}\right)_{mix}\frac{1}{r^2}\frac{\partial}{\partial r}\left(r_2\frac{\partial T}{\partial r}\right) + \frac{6\phi_p \Delta H k_0}{(\rho c)_{mix} d}\exp\left(-\frac{T_{act}}{T}\right) \tag{5-19}$$

where ϕ_p is the volume fraction of the suspended metal particles, M_p and M_{ox} are, respectively, the molecular weights of the particle material (metal) and the oxidizer gas, Y_{ox} is the mass fraction of oxygen, Y_m is the instantaneous mass fraction of unreacted metal within a representative dust particle, and D is the effective binary diffusion coefficient of oxygen in air and the subscript "mix" refers to the physical properties of the air/metal dust mixture. The product $(\rho c)_{mix}$ is related to ρc for air and $\rho_p c_p$ for the particle material via

$$(\rho c)_{mix} = \rho c(1-\phi_p) + \rho_p c_p \phi_p \tag{5-20}$$

The initial conditions for Equations (5-17) and (5-18) are

$$Y_{ox}(r, 0) = Y_{ox,\infty}; \qquad Y_m(r, 0) = 1.0 \tag{5-21}$$

where $Y_{ox,\infty}$ is the oxygen mass fraction in atmospheric air. The initial condition for Equation (5-19) is

$$T(r,0) = \begin{cases} T_{HS} & 0 < r \le R_{HS} \\ T_0 & R_{HS} < r < \infty \end{cases} \tag{5-22}$$

where R_{HS} is the radius of the hot spot.

The numerical procedure for solving Equations (5-17) to (5-19) has already been discussed in Section 3.4, and will not be belabored here. It should be mentioned though, that when all the oxygen in a computational node is consumed so that $Y_{ox} = 0$ or all the metal is consumed so that $Y_m = 0$ the reaction heating term is shut off by setting $k_0 = 0$. In most of the calculations the hot spot radius was assigned the value $R_{HS} = 0.04$ mm. Based on experience this size is small enough to ensure that the predicted ignition energy (IE) is independent of the size of the hot spot. Nevertheless, some calculations were carried out with $R_{HS} = 0.1$ mm and the results were the same as those with $R_{HS} = 0.04$ mm. Finally, the thermal conductivity, k_{mix}, was identified with that of the gas since the volume of the dust cloud is occupied mainly by air. The values of the parameters used in the calculation are listed in Table 5-2. The Arrhenius law pre-exponential constant and activation temperature are based on McGillivray, et al. (1994), oxidation kinetics in dry air.

Table 5-2: Parameter Values Used to Theoretically Determine the IE of Uranium Metal Dust in Air

Metal particle diameter	$d = 10.0\ \mu m$
Thermal conductivity (air at 1000 K)	$k = 0.068\ W\ m^{-1}\ K^{-1}$
Density of air (at 1000 K)	$\rho = 0.352\ kg\ m^{-3}$
Specific heat of air (at 1000 K)	$c = 1140\ J\ kg^{-1}\ K^{-1}$
Density of metal particle material	$\rho_p = 1.9 \times 10^4\ kg\ m^{-3}$
Specific heat of metal particle material	$c_p = 125\ J\ kg^{-1}\ K^{-1}$
Diffusion coefficient (0_2 in air 990 K)	$D = 1.69 \times 10^{-4}\ m^2\ s^{-1}$
Heat of reaction	$\Delta H = 3.4 \times 10^7\ J\ (kg0_2)^{-1}$
Kinetic Pre-exponential coefficient	$k_0 = 10.95\ (kg0_2)\ m^{-2}\ s^{-1}$
Activation temperature	$T_{act} = 8077\ K$
Initial oxygen mass fraction	$Y_{ox,\infty} = 0.23$
Initial mixture temperature outside hot spot	$T_0 = 293\ K$
Molecular weight of dust particle material	$M_p = 238$
Molecular weight of oxidizer gas	$M_{ox} = 32$

The IE of the uranium metal dust is determined by carrying out a sequence of computational runs during which the hot spot initial temperature T_{HS} is increased until ignition and reaction propagation is predicted. Once the critical hot spot temperature, $T_{HS,crit}$, for ignition is obtained, the ignition energy is calculated using the relation

$$IE = \frac{4}{3}\pi R_{HS}^3 (\rho c)_{mix} (T_{HS} - T_0) \tag{5-23}$$

Figure 5-3 shows the results of the numerical calculations; it contains the IE versus the metal dust volume fraction ϕ_p. Note that the dust volume fraction is readily converted to dust spatial mass concentration m_p, since

$$m_p = \rho_p \phi_p \tag{5-24}$$

The ignition curve in Figure 5-3 shows that the theoretical lower concentration limit to a uranium dust explosion is somewhat less than about $\phi_p = 10^{-5}$ ($m_p = 0.19$ kg m^{-3}). This prediction is in good agreement with the reported minimum explosive concentrations of other metal dusts. For example, the lower limit for aluminum dust is $\phi_p = 1.1 \times 10^{-5}$ (Nagy and Verakis 1983). It was mentioned previously that a spark energy accumulated and released by a storage drum is about 40 mJ. As shown in Figure 5-3, this spark can cause ignition of uranium dust with concentrations in excess of only ϕ_p; 3×10^{-5} (0.57 kg m^{-3}). Even the human body can conceivably produce a static discharge of about 10 mJ, which is sufficient to ignite uranium dusts with concentrations $\phi_p \geq 5 \times 10^{-5}$ (0.95 kg m^{-3}). The MIE of the uranium dust/air mixture is predicted to be about 0.15 mJ (see Figure 5-3). This is less than known MIE values for paraffinic hydrocarbon/air mixtures (0.2 - 0.6 mJ; see Section 3.4). Thus uranium metal dust by itself in air is highly pyrophoric.

When hydrogen gas is present in addition to the dust, the explosibility of the dust is enhanced. An increase in the concentration of hydrogen results in a decrease in the minimum explosive concentration, a decrease in the MIE and an increase in the rate of pressure rise of the dust-gas mixture. That is, the presence of the hydrogen gas can render explosive a dust-H_2 gas mixture at a dust concentration that is below the explosive limit for the dust, and at a H_2 concentration that is below the normal lower explosive limit for the hydrogen. Clearly, tapping open storage drums containing corroded uranium metal is a dangerous business, and from the thermal-theory ignition curve displayed in Figure 5-3, it is no wonder that explosions occurred upon doing so.

Figure 5-3: Predicted Effect of Dust Volume Fraction on Ignition Energy of Uranium Metal Dust in Dry Air; Showing Fuel and Oxide Limited Combustion Regimes

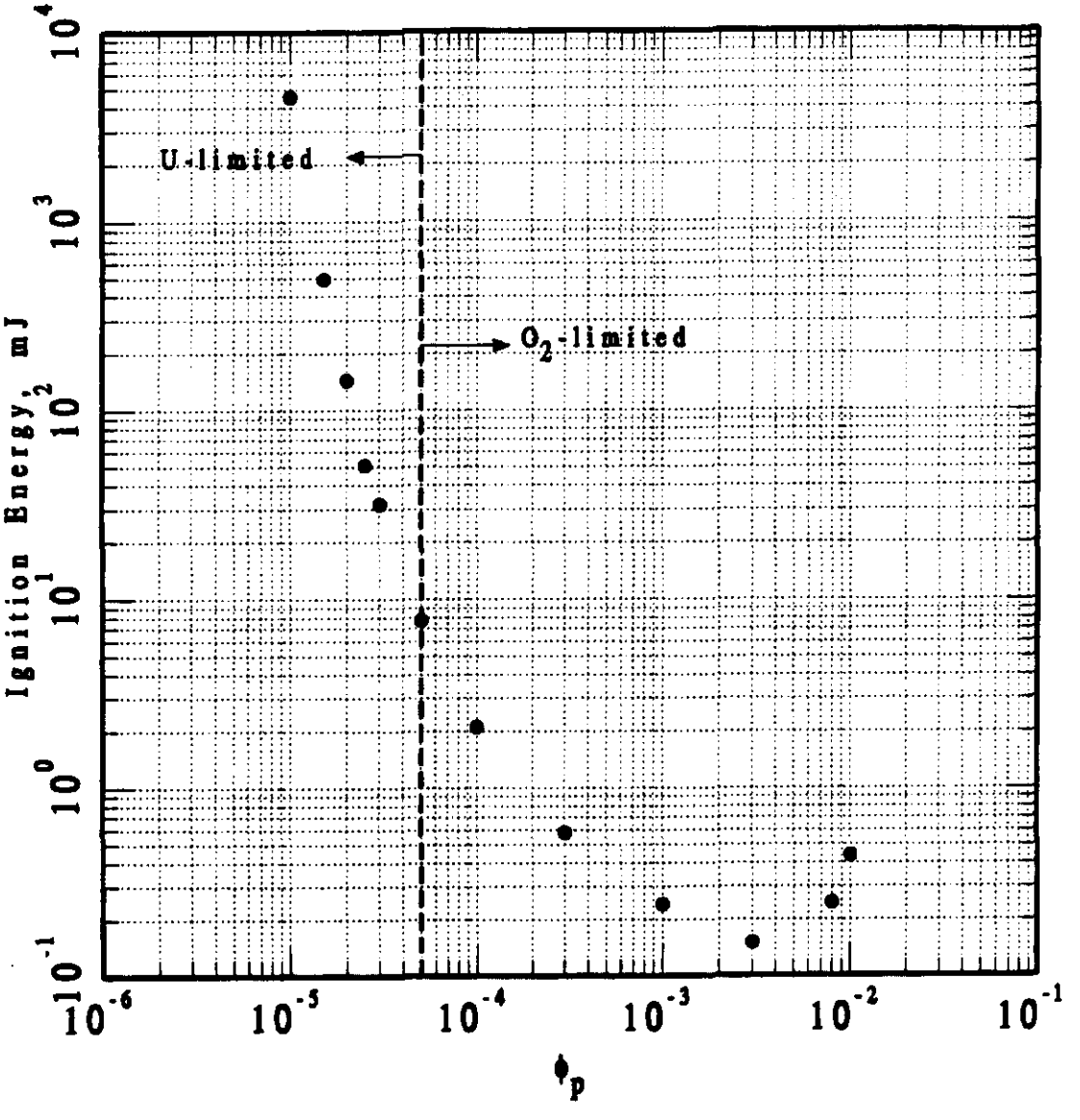

5.5 Ignition of Highly Corroded Fuel Elements Upon Impact

One of the ignition events described by Abrefah, et al. (1999) and Demiter (1998) occurred upon impact of highly corroded fuel elements; specifically a fuel element ignited while shaking against adjacent fuel elements. It is well known that ignitions due to impact result from the rise in temperature in local hot spots at the "point" of impact. There are two independent questions regarding ignition by impact: (1) what is the mechanism through which mechanical energy is converted to hot spot temperature development, and (2) what is the temperature rise necessary to cause ignition? The first questions falls outside the realm of ignition theory as it relates to a difficult area of fluid and solid mechanics. Three potential mechanisms for the formation of impact hot spots are (Bowden and Yoffee 1958): the adiabatic compression of an intervening

layer of gas; the friction of crystals against one another, and viscous heating in plastic flow. The second question regarding the problem of the hot spot temperature (or IE) required to ignite the solid upon impact is handled by the mathematical theory of ignition.

Equations (5-17) and (5-18) may be used to predict whether or not impact hot spots can ignite a highly corroded fuel element. In this case, ϕ_p is identified with the volume fraction of the metal material in the corroded and porous segment of the element involved in the impact. The parameter k_{mix} is now the effective thermal conductivity of the porous fuel matrix. Reasonable numerical values for these quantities are ϕ_p; 0.5 and $k_{mix} = 0.4$ W m^{-1} K^{-1} (see Equation (4-8)). The solutions of the equations indicate that an infinitesimally small source of heat, no matter how energetic, is not capable of producing ignition in a porous but nevertheless dense uranium metal. Thus the required heating of the impacting, corroded fuel rod to ignition must have been accomplished by a large source. The striking of the rods against one another may have produced a metal dust cloud, which surrounded the rod and ignited. This more spatially distributed source of heat with its suspended particles is a high-radiative emitter. It would be of interest to examine the radiative ignition requirements for a highly corroded fuel element. Unfortunately such an effort is well beyond the scope of the present report.

5.6 Spontaneous Ignition of Porous or Powdered Uranium in Air

A common experience is the ignition of porous or powdered uranium metal or metal chips in air after resting uneventfully for several days in an open container. One incident occurred under water. Powder gradually accumulated in a sump under about 25 feet of water. Approximately once a month the powder reacted violently and produced a 30-foot high geyser in the sump. After each event, the sump was cleaned and new powder would accumulate. Obviously the ignition event required a critical volume of powder. This critical volume is easily understood in terms of thermal ignition theory. A gradual increase in volume will eventually result in an unstable situation in which the reaction power production exceeds the heat loss rate from the powder. We already learned in Section 4.0 that thermal ignition theory is capable of predicting ignitions of uranium metal powder under well-controlled laboratory conditions. It stands to reason, then, that all the reported incidents of spontaneous ignition of powdered uranium material (or chips) were classical chemical runaway events that could readily be rationalized by thermal ignition theory if the important parameters were known (particle size, volume of powder, ambient temperature and humidity, etc.).

6.0 IGNITION MODELS FOR SNF APPLICATION

Deterministic ignition models for SNF applications are as follows:

1. Scrap piece ignition: declad, cracked, internally hydrided scrap,
2. Damaged fuel element with declad, cracked, internally hydrided end,
3. Scrap basket in an MCO: with and without fins, and
4. Fuel basket in an MCO.

Deterministic ignition models for SNF applications are of two types. Scrap piece and damaged fuel element models were motivated primarily by concerns of fuel ignition in air. These models can also be used to consider spent fuel currently stored under water at the K Basins and fuel flash incidents reported in France (SGN 1995). Ignition models presume heat transfer to an ambient fluid, which means that air, steam, or water can be considered by an appropriate choice for the heat transfer coefficient. The last two items, fuel basket and scrap models, consider fuel elements and scrap in MCOs during CVD, shipping, and staging.

Ignition models presented in this section are termed deterministic to distinguish the discussion from Section 7.0, which presents probabilistic results. Of course, the starting point for a probabilistic approach is a model derived from stationary ignition theory; probability distributions are applied later. This section derives each model, explains inputs, and shows results parametrically. Appendices contain listings of the models, such as MATHCAD™ files or FORTRAN source codes.

6.1 Scrap Piece Ignition

Figure 6-1 illustrates an internally hydrided scrap piece. Application of stationary ignition theory to damaged fuel geometries assumes that the damage zone is cracked and contains internal hydride. The damage zone has large specific area and greatly enhanced reaction potential.

™ MATHCAD is a registered trademark of MathSoft.

Figure 6-1: Declad, Cracked, Internally Hydrided Scrap Piece

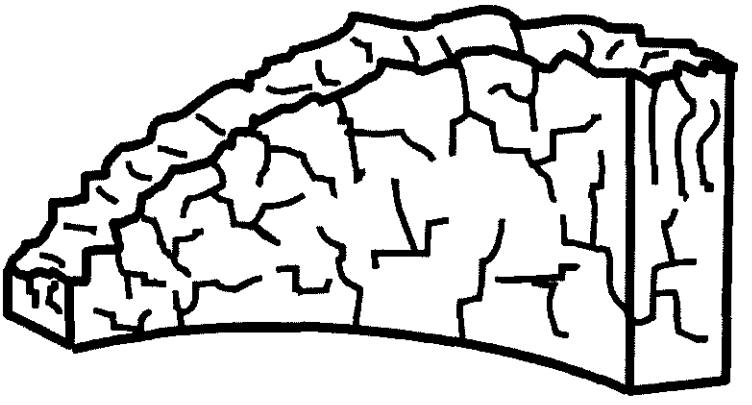

BM986103.CDR 6-30-98

The Arrhenius rate law is the Pearce oxygen-free water vapor law evaluated at saturated conditions (refer to Appendix A). Note that this is the largest Arrhenius rate law available for uranium metal. The rate law is linearized to yield the Frank-Kamenetskii parameter for ignition.

An internally hydrided scrap piece like the one shown in Figure 6-1 can be modeled as a one-dimensional planar slab with internal heat generation. If the thermal resistance is the same on both sides of the piece and one-dimensional conduction is assumed for simplicity,

$$T - T_i = \frac{Q_v b^2}{2k} \tag{6-1}$$

where T is the maximum (centerline) scrap temperature, T_i is the temperature at the scrap surface, b is the fuel element half-thickness, and k is the scrap thermal conductivity. Surface temperature and fluid temperature are related by,

$$T_i - T_f = \frac{Q_v b}{h_f} \tag{6-2}$$

Consequently,

$$T - T_f = \frac{Q_v b}{h_e} \tag{6-3}$$

where the overall heat transfer coefficient, h_e, is

$$h_e = \frac{1}{\frac{b}{2k} + \frac{1}{h_f}} \tag{6-4}$$

In general, the thermal resistance of the scrap is negligible and h_e is practically the same as h_f. As in Section 3.2, use the following expression for volumetric power,

$$Q_v = F A_v C \Delta H e^{-T_r} e^{T_r \theta} \tag{6-5}$$

where F is the hydride volume fraction in the piece, and definitions for reduced temperature ($T_r = T_e/T_f$) and non-dimensional temperature increase ($\theta = (T - T_f)/T_f$)are used to obtain the Frank-Kamenetskii parameter B,

$$B = \frac{F A_v b T_r C \Delta H}{h_e T_f \exp(T_r - 1)} \tag{6-6}$$

Many of the parameters in Equation (6-6) are inherently stochastic or uncertain, and are modeled appropriately by probability distribution functions rather than point-estimates. In Section 7.2, the Frank-Kamenetskii parameter is evaluated probabilistically to find the likelihood of ignition.

6.2 Ignition of a Fuel Element With Damaged End

Consider a fuel element damaged over a length R containing cracks and hydride such that the area per unit volume is A_v, shown in Figure 6-2. Decay and reaction power are either lost by surface convection or conducted axially to a non-reacting portion of the element. The conduction equation for each region is:

$$\frac{d^2 T_1}{dx^2} + \frac{Q_{dk}}{k_1} + \frac{Q_v}{k_1} - \frac{h}{k_1 b}(T_1 - T_f) = 0 \qquad 0 \le x \le R \tag{6-7a}$$

$$\frac{d^2 T_2}{dx^2} + \frac{Q_{dk}}{k_2} - \frac{h}{k_2 b}(T_2 - T_f) = 0 \qquad x > R \tag{6-7b}$$

with boundary conditions:

Figure 6-2: Fuel Element With Declad, Cracked, Internally Hydrided End

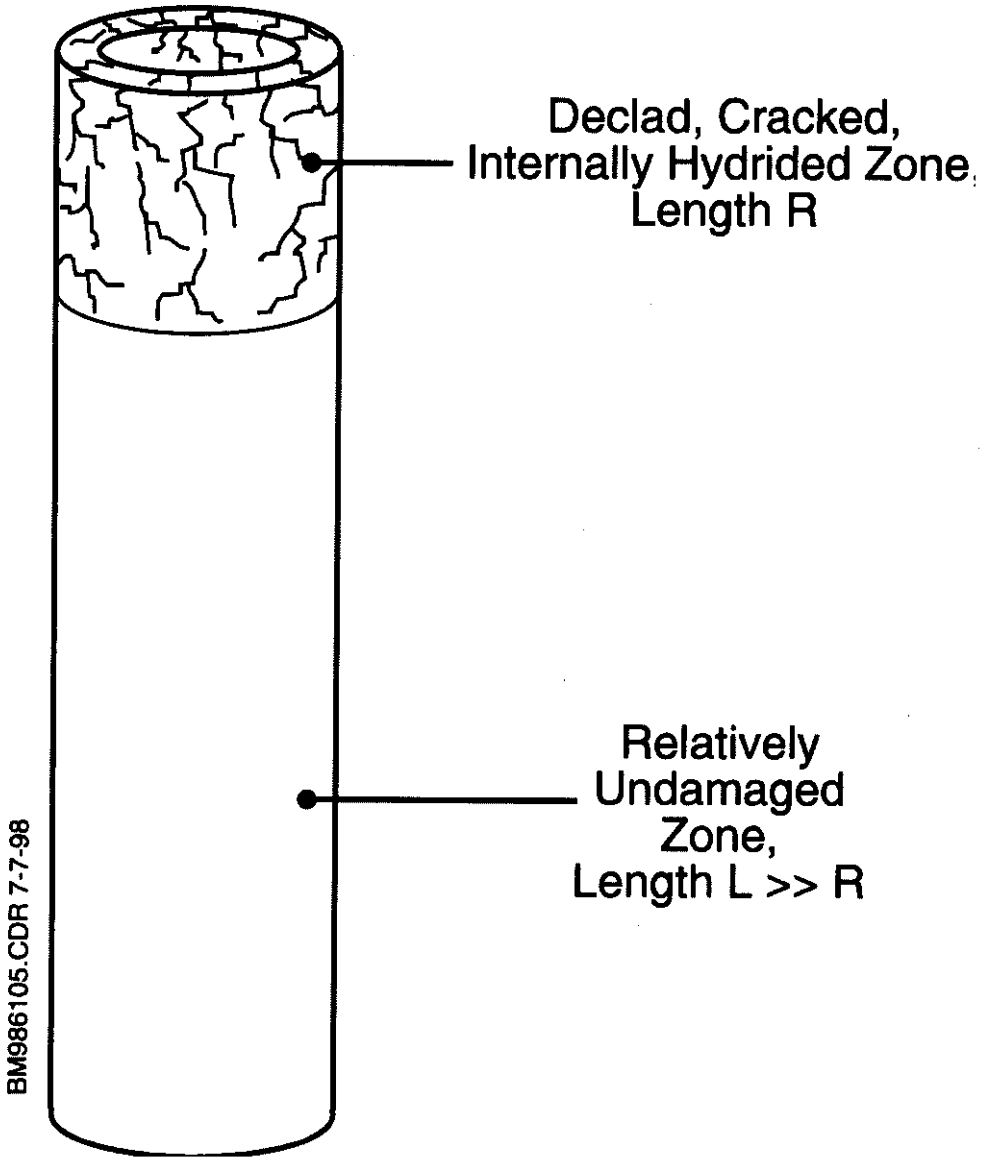

$$\frac{d T_1}{d x} = 0 \qquad \text{at } x = 0, \tag{6-8a}$$

$$\frac{d T_1}{d x} = \frac{d T_2}{d x} \quad \text{and} \quad T_1 = T_2 \qquad \text{at } x = R, \text{ and} \tag{6-8b}$$

$$\frac{d T_2}{d x} \rightarrow 0 \quad \text{as} \quad x \rightarrow \infty. \tag{6-8c}$$

where Q_{dk} is the volumetric decay power (W/m^3), Q_v is the reaction power given by Equation (6–3), h is the heat transfer coefficient to fluid and is uniform over the surface, and b is the element half-thickness. Note both equations have the form

$$T_i'' + q_i - m_i^2 \left(T_i - T_h\right) = 0 \tag{6-9}$$

Also, Q_v is evaluated at an effective average temperature, say either T(x=0) or 1/3 T_R + 2/3 T_o, so q_i is constant.

Solutions satisfying these boundary conditions are:

$$T_1 = T_{q1} - T_{f1} \cosh\left(m_1 x\right) \qquad 0 \le x \le R \tag{6-10a}$$

$$T_2 = T_{q2} + T_{f2} \exp\left(-m_2 \left(x - R\right)\right) \qquad x > R \tag{6-10b}$$

$$T_{q1} = T_f + \frac{Q_{dk} + Q_v}{k_1 m_1^2} \qquad m_1 = \left(\frac{h}{k_1 b}\right)^{\frac{1}{2}} \tag{6-10c}$$

$$T_{q2} = T_f + \frac{Q_{dk}}{k_2 m_2^2} \qquad m_2 = \left(\frac{h}{k_2 b}\right)^{\frac{1}{2}} \tag{6-10d}$$

$$T_{f1} = \frac{m_2 \left(T_{q1} - T_{q2}\right)}{D} \tag{6-10e}$$

$$T_{f2} = m_1 \left(T_{q1} - T_{q2}\right) \sinh\left(m_1 R\right) / D \tag{6-10f}$$

$$D = m_1 \sinh\left(m_1 R\right) + m_2 \cosh\left(m_1 R\right) \tag{6-10g}$$

The maximum temperature is at the end x = 0, where

$$T = T_{q1} - T_{f1} = T_{q1}\left(1-\frac{m_2}{D}\right)+T_{q2}\frac{m_2}{D} = \frac{Q_v\left(1-\frac{m_2}{D}\right)}{k_1 m_1^2}+T_f+\frac{Q_{dk}}{k_1 m_1^2} \quad (6\text{-}11)$$

where the latter result is obtained by noting that $k_1 m_1^2 = k_2 m_2^2$.

By defining an effective sink temperature

$$T_k = T_f + \frac{Q_{dk}}{k_1 m_1^2} \quad (6\text{-}12)$$

an equation analogous to Equation (6-3) is derived:

$$T - T_k = Q_v\left(\frac{1-\frac{m_2}{D}}{k_1 m_1^2}\right) \quad (6\text{-}13)$$

The volumetric power from Equation (6-5) is used with slightly revised definitions

$$T_r = \frac{T_e}{T_k} \quad (6\text{-}14a)$$

$$\theta = \frac{T - T_k}{T_k} \quad (6\text{-}14b)$$

Decay heat proves negligible in relation to oxidation power and $T_k \approx T_f$.

Combining the above equations results in the familiar expression for the maximum temperature, embedded in θ:

$$T_r\,\theta\,e^{-T_r\theta+1} = B \quad (6\text{-}15a)$$

where

$$B = \frac{F A_v \Delta H\left(1-\frac{m_2}{D}\right) C T_r}{k_1 m_1^2 T_k \exp(T_r - 1)} \quad (6\text{-}15b)$$

Equation (6-15b) is evaluated here for the case of N Reactor fuel with the Pearce rate law for steam at 100% RH. Rather than evaluating Equation (6-15b) with sample values to find B, the approach is to find the A_v that leads to ignition for temperatures ranging from 20 to 100°C. The following values apply:

b	=	4.5 mm,
C	=	624,
T_e	=	7529 K,
T_r	=	25.26,
ΔH	=	1.67×10^7 J/kg,
h_f	=	10 W/m^2-K (natural convection to steam),
R	=	3 cm (5% of fuel length),
k_1	=	20 W/m-K,
k_2	=	30 W/m-K, and
F	=	5%.

Note that holding A_v constant and varying F would accomplish the same thing. The results plotted in Figure 6-3 show that for ignition below 50°C, A_v above 1×10^6 1/m is required with F = 5%, or A_v F = 50,000. A reasonable range for F is from 1% to 10% and A_v is expected to have a factor of 3 uncertainty above or below the nominal value 1×10^6 1/m. Therefore, with steady conditions (unlimited reactants) and steam at 100% RH, ignition could occur at relatively low temperatures if fuel damage is extensive.

6.3 Ignition Theory for MCO Fuel Baskets

For MCO fuel baskets, ignition theory is discussed based on two steady-state MCO temperature distribution solutions. The first assumes that the fuel basket can be treated as a single porous, composite medium. In this treatment, effective thermal conductivity is the sum of radiative and composite conductive components. Radiative conductivity depends on emissivities, spacing between fuel assemblies, and the average surface temperature of the fuel assemblies. Composite thermal conductivity is determined by the fuel conductivity, gas conductivity, and fuel basket void fraction. With the effective thermal conductivity in hand, the MCO temperature distribution is found by solving the radial conduction equation with a heat source due to decay and oxidation. Boundary conditions are the ambient temperature outside the MCO and the MCO gas composition.

A second solution calculates individual heat transfer rates from assembly to assembly and from assemblies to the MCO wall, rather than treating the fuel basket as a composite medium. This solution finds 14 fuel element temperatures and seven outer fuel element radiosities (the rate per unit area at which thermal radiation leaves a surface), based on a known MCO wall temperature and gas composition. A solution for fuel element temperature distribution therefore requires detailed matrices for view factors and conduction distances between heat sinks. An iterative scheme generates trial fuel element temperatures until conduction and radiation losses match decay heat and oxidation power.

Figure 6-3: Specific Area to Ignition for a Damaged End With Pearce Rate Law for Steam at 100% RH, 5% of Fuel Length Damaged, and 5% Hydride Fraction

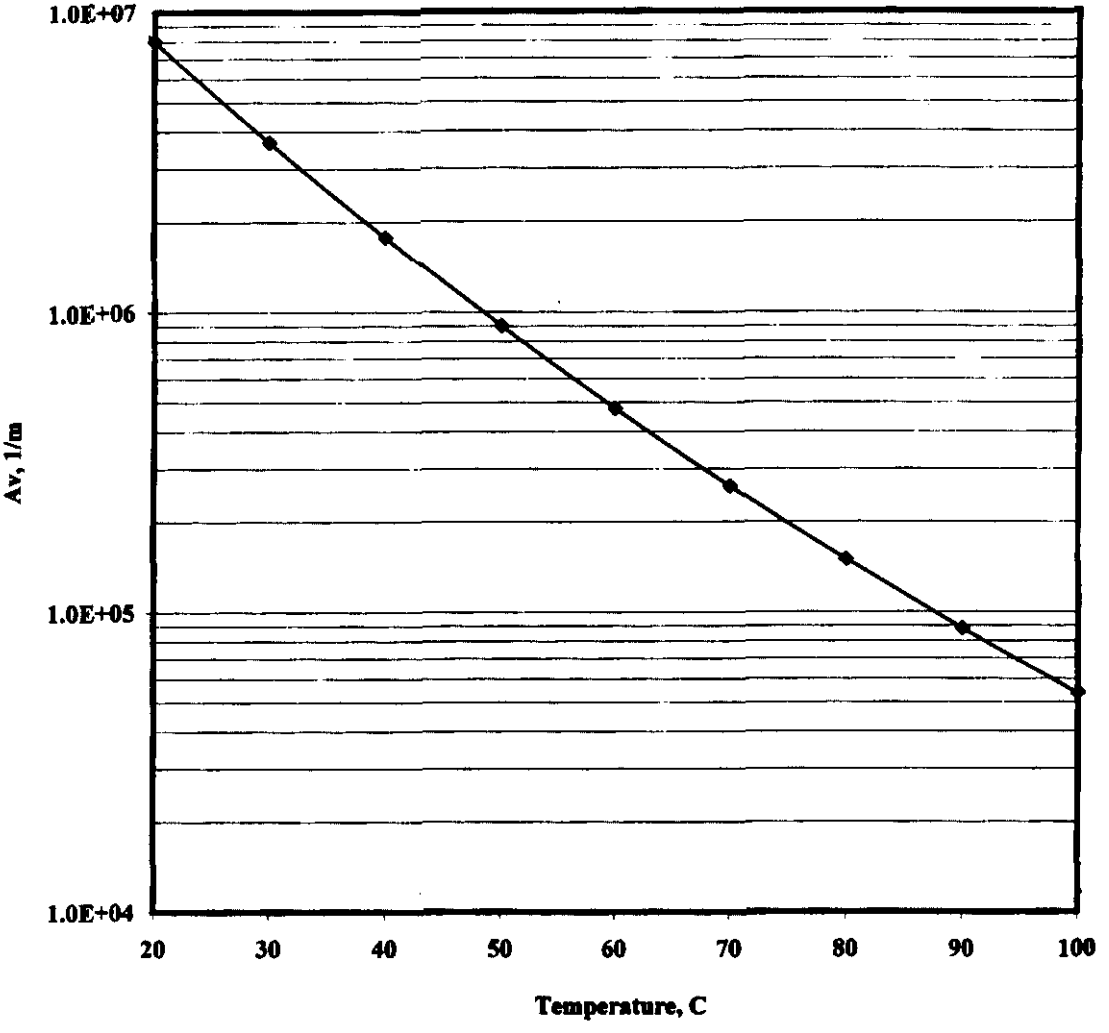

6.3.1 Porous Medium Solution for Fuel Elements Temperature Distribution in the MCO

Ignition theory analysis of fuel baskets loaded in an MCO begins with the following assumptions:

1. There is unlimited reactant available,
2. The fuel oxidation rate is calculated using the relationship published by (McGillivray, et al. 1994) and shown in Appendix A,
3. Reaction rates are calculated at the maximum temperature, which is the so-called constant reaction rate assumption,
4. Axial losses from the MCO are negligible compared to radial losses,
5. Steady-state theory is applied,

6. No account is made of a thick oxide, sludge layer on fuel fragments,
7. The insert and/or dip tube are not accounted for,
8. The MCO contains 54 fuel assemblies in each fuel basket, as shown in Figure 6-4, and
9. The MCO is loaded in a vault tube for storage.

Ignition temperature is defined in terms of the ambient temperature outside the MCO. Ignition is the point at which the heat generated within the MCO due to decay and corrosion cannot be removed from the MCO.

The temperature profile in the MCO is given by the solution of

$$\frac{1}{r}\frac{\partial}{\partial r} k r \frac{\partial T}{\partial r} + Q = 0 \qquad (6\text{-}16)$$

where

$$Q = (1-\phi)\left[q_v + \frac{6}{d} q_r(T)\right] \qquad (6\text{-}17a)$$

$$\frac{6}{d} = \frac{A}{V} \qquad (6\text{-}17b)$$

T = temperature, K,
r = radial coordinate, m,
k = thermal conductivity, W/m/K,
ϕ = porosity, about 0.57,
q_v = decay power, about 2000 W/m^3,
d = effective particle diameter, m,
$q_r(T)$ = Reaction power determined by heat of reaction (3.4×10^7 J/kgO_2) and McGillivray rate law, W/m^2, and
$\frac{A}{V}$ = surface-to-volume ratio, m^{-1}.

Figure 6-4: Mark IV Fuel Basket, from HNF-SD-SNF-DR-003, Rev. 1, Appendix I, MCO Drawings

All dimensions are in inches.

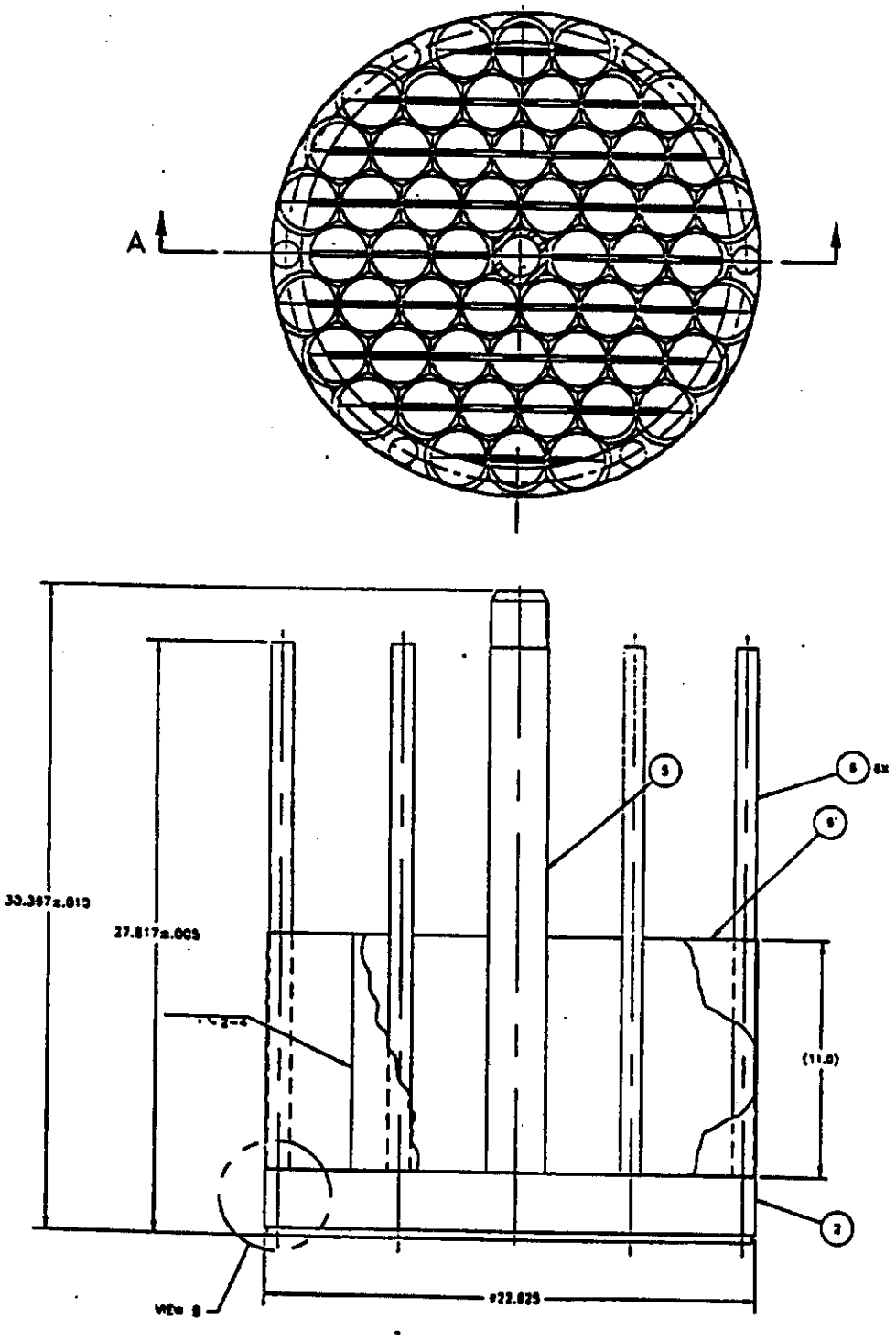

Equation (6-16) is subject to the boundary conditions

$$\frac{\partial T}{\partial r}\Big|_{r=a} = 0 \tag{6-18}$$

$$T\Big|_{r=a} = T_a \tag{6-19}$$

where r = a is the innermost radius at which fuel is found. The ambient temperature is found by considering the continuity relations

$$q''(R) = -k\frac{\partial T}{\partial r}\Big|_R = h_g\left(T_R - T_s\right) + \sigma\varepsilon\left(T_R^4 - T_s^4\right) \tag{6-20a}$$

$$q''(s) = \frac{R}{s}q''(R) = h_a\left(T_s - T_\infty\right) + \sigma\varepsilon\left(T_s^4 - T_\infty^4\right) \tag{6-20b}$$

where r = R is the MCO radius, r = s is the vault tube outer radius, T_s is the vault tube average temperature, T_∞ is the ambient temperature, h_g is the gap heat transfer coefficient, h_a is the ambient heat transfer coefficient, ε is the effective emissivity, and σ is Boltzmann's constant. Note that the controlling heat transfer resistances are gap and ambient convection plus radiation. The temperature gradients across the MCO wall and vault tube are negligible at steady-state.

The ignition condition is found by solving Equations (6-16) to (6-19) for the temperature at r = R:

$$T_a - T_R = \left(\frac{QR^2}{4k}\right)\left[\frac{1}{2}\left(1 - \frac{a^2}{R^2}\right) - \frac{a^2}{R^2}\ell n\frac{R}{a}\right] \tag{6-21}$$

and equating the heat flux

$$q''(R) = \left(\frac{QR}{2}\right)\left(1 - \frac{a^2}{R^2}\right) \tag{6-22}$$

to the expressions in Equation (6-20) to yield T_∞. As usual, successive increasing values of the maximum temperature T_a are employed until the value of T_∞ attains a maximum; this is the ignition threshold.

6.3.2 Model Parameters

The effective conductivity is the sum of radiative and conductive contributions. The radiative contribution is given by

$$k_r = 4\,\sigma\,\varepsilon\,T^3\,\delta \tag{6-23}$$

where T is a mean system temperature and δ is the average spacing between radiating bodies. An estimate for δ is R/4, because there are at most 3 gaps between an element and the MCO wall, plus one gap internal to the inner element. Taking $\delta = 0.075$ m, T = 323 K (a conservative low value), $\varepsilon = 0.7$, $\sigma = 5.67 \times 10^{-8}$ W/m^2/K^4, results in $k_r = 0.40$ W/m/K.

For a composite medium whose continuous phase has a conductivity much less than that of the dispersed phase, the composite conductivity is

$$k_{comp} = k_{cont}\left(1-\alpha^{\frac{1}{3}}\right)^{-1} \tag{6-24}$$

where α is the volume fraction occupied by the dispersed phase, which in this case is the fuel, and k_{cont} is the thermal conductivity of the continuous phase, about 0.03 W/m/K for nitrogen in the temperature range of interest.

There are 54 fuel assemblies nominally present at a cross-section with the following dimensions:

Outer	Outer Diameter (O.D.) Inner Diameter (I.D.)	6.15 cm 4.32 cm
Inner	O.D. I.D.	3.25 cm 1.22 cm

for a total cross-sectional fuel area of 0.12 m^2. The total area containing them has an O.D. of about 0.6 m and an I.D. of about 0.075 m, which yields the following: a basket cross-sectional area of 0.278 m^2, a void area of 0.158 m^2, a porosity (void fraction) $\phi = 0.57$, and fuel volume fraction $\alpha = 0.43$. Thus, the composite conductivity is estimated to be $k_{comp} = 0.12$ W/mK and the total effective conductivity is k = 0.4 + 0.12 W/m/K, or 0.52 W/m/K.

In the gap outside the MCO, the effective heat transfer coefficient is

$$h_g = \frac{k_{gap}}{\delta_{gap}} = \frac{0.03\,\frac{W}{m\cdot K}}{0.0254\,m} = 1.18\,\frac{W}{m^2\,K} \tag{6-25}$$

where again the nitrogen thermal conductivity is used with 1 inch gap clearance on the average. Outside the vault, the Rayleigh number is high enough that turbulent natural convection applies,

$$h_a = 0.062 \frac{k_{air}}{L} \left(\frac{g \beta \Delta T L^3}{\alpha \nu} \right)^{\frac{1}{3}} \qquad (6\text{-}26)$$

where α = thermal diffusivity of air, 3.83×10^{-5} m^2/s,
ν = kinematic viscosity of air, 2.64×10^{-5} m^2/s,
k_{air} = thermal conductivity of air, 0.03 W/m K,
g = 9.81 m/s^2,
L = length scale, m,
β = 1/T, ideally 1/2 ($T_1 + T_\infty$), and
ΔT = $T_1 - T_\infty$.

Note that the length scale, L, appears in both the numerator and the denominator, and thus reduces to unity.

For the baseline geometry, R is identified with the MCO inner radius of 1/2 (23.5 inches) or about 0.30 m. The vault tube outer diameter is 27 inches, and s = 0.34 m. The inner radius is an effective radius where conduction and radiation begin, and this could arguably be taken as the centerline radius of the first fuel elements. A somewhat smaller value of a = 0.04 m, corresponding to the central void, is conservatively used.

Decay power is reported in the range of 78 W/MT to 120 W/MT, so an average of 100 W/MT, or 2000 W/m^3 will be used here. For calculation of the chemical power, a steam pressure p = 2 kPa is appropriate. The chemical rate law used in this analysis is that of McGillivray. Appendix A shows this law in graphical form.

At this point, all geometric, heat transfer, and property inputs are specified, except for the reactive surface-to-volume ratio S/V. For a thin-walled cylinder, S/V is just the inverse of the wall thickness. This is about 220 m^{-1} for decladded but otherwise intact fuel, and from Equation (6-17c) is equivalent to fuel fragments with a mean diameter of 2.7 cm. Fuel fragments of mean size equal to the element thickness of about 1 cm would have S/V $\cdot$ 600 m^{-1}, while half-decladded fuel would have S/V 100 m^{-1}.

Given the above values and S/V = 220 m^{-1}, the ignition temperature (the ambient temperature at incipient runaway) is 38°C, the MCO wall temperature is 82°C, and the fuel maximum temperature is 128°C. This means the radiative contribution to heat transfer was underestimated, so the ignition temperature is also underestimated. Guessing 120°C = 393 K, yields $k_r = 0.72$ and $k = 0.84$ W/m/K. The resulting temperatures at the ignition point are: Ambient, 62°C, MCO wall, 105°C, fuel maximum, 137°C, and the calculation is now consistent. Thus, for the nominal design, an ambient ignition temperature of 62°C is expected. Note that this result is sensitive to the assumed external resistances such as those within the MCO-vault tube gap.

Since the preceding approach requires iteration for k_r, a more elegant approach is to replace k in Equation (6-16) by

$$k = k_{comp} + CT^3 \tag{6-27a}$$

$$C = 4\,\sigma\,\varepsilon\,\delta \tag{6-27b}$$

where $\delta = R / 4$ per the rationale above. The ignition condition of Equation (6-21) then becomes

$$T_a - T_R + C_1\left(T_a^4 - T_R^4\right) = \left(\frac{Q R^2}{4 k_{comp}}\right)\left[\frac{1}{2}\left(1 - \frac{a^2}{R^2}\right) - \frac{a^2}{R^2}\ell n\left(\frac{R}{a}\right)\right] \tag{6-28a}$$

where $$C_1 = \frac{\sigma\,\varepsilon\,\delta}{k_{comp}} \tag{6-28b}$$

FORTRAN source code for ignition analysis (IGMCO) is contained in Appendix C.

6.3.3 MCO Fuel Elements Ignition Analysis Results

Table 6-1 shows results of ignition analysis for a standard MCO containing 54 fuel elements at each level in the stack with the parameters discussed above. The reactive surface area is distributed evenly throughout the MCO, and the exposed area is cast as a failed fuel fraction ranging from fully decladded to an area suggested by estimated corrosion rates in the K East basin (Johnson and Burke 1995). For any given failed fraction, the ignition temperature would be lower if the failed fuel were more concentrated in the center and higher than if the failed fuel were more concentrated at the MCO periphery. It is not very instructive to examine many cases of uneven failure distribution because, for example, concentrating 25% failed fuel at the center would yield a result bounded by the case in Table 6-1 where all fuel is 25% failed.

Table 6-2 shows results for a somewhat different boundary condition on the exterior of the vault tube than considered in the cases of Table 6-1. In Table 6-2, the ignition temperature is listed for cases where all power produced in the MCO is removed by convection from the vault tube with a constant external convective heat transfer coefficient of 5.88 W/m^2/K. This is a better representation of heat transfer in the storage vault, because there is no net radiative loss (each vault tube should radiate to an identical vault tube) and because the average flow conditions in

the vault should not be perturbed by one tube with slightly higher power than expected. The heat transfer coefficient was estimated as a lower bound value given a heat flux of 114 W/m^2 to remove decay power from a vault tube surface at 65.5°C to a vault gas at 46°C. The low bound on the given heat transfer coefficient arises from the use of a high surface to bulk temperature difference for the given heat flux. It is interesting to note that a typical overall heat transfer coefficient for the cases in Table 6-1 is about 8 $W/m^2/K$, and that a high bound for the vault is estimated to be 10 $W/m^2/K$. The ignition temperatures in Table 6-2 followed by an (*) are for this upper bound value.

The results of the analysis, as conservative as they are, indicate that even for a situation of an MCO full of fully decladded fuel that the calculated ambient temperature for ignition is 64°C, assuming that unlimited air access to ALL of the elements exists. For the much more realistic cases where a fraction of the fuel is reactive, the ignition temperature is considerable higher. For reference purposes, the maximum vault ambient temperature is limited to 55°C (131°F). Thus, even for a failed fuel area fraction of 100%, exposed to unlimited air ingress, the ignition temperature is above this temperature. Since the average failed fuel fraction is less than 5%, an ambient ignition temperature above 175°C (350°F) is expected and a substantial margin to ignition would exist.

Table 6-1: Ignition Temperature for MCO Assuming Infinite Medium Heat Transfer

Failed Fuel Fraction (Exposed Area)	A/V (Equivalent)	Ignition Temp. (°C)	MCO Wall (°C)	MCO Max (°C)
1	220	64	109	142
0.75	165	75	119	152
0.45	100	96	139	171
0.25	55	124	165	197
0.1	22	172	212	243
0.05	11	214	255	287
0.014	3	312	360	399

Table 6-2: Ignition Temperature for MCO Assuming Fixed Vault Tube Heat Transfer Coefficient of 5.88 W/m^2K (Conservative Low Value)

Failed Fuel Fraction (Exposed Area)	A/V (Equivalent)	Ignition Temp. (°C)	MCO Wall (°C)	MCO Max (°C)
1.	220	55	106	138
1.*	220	68		
0.75	165	64	116	147
0.45	100	82	134	164
0.25	55	105	158	186
0.1	22	143	199	224
0.1*	22	161		
0.05	11	175	234	257
0.014	3	243	311	331
0.014*	3	270		

* Calculated ignition temperature for a heat transfer coefficient of 10 $W/m^2/K$

6.4 Steady-State Fuel Element Temperature Solution

A second, more detailed approach to ignition conditions requires a steady-state solution for each individual fuel element temperature. A solution scheme iterates for the 14 fuel element temperatures until each of the 14 fuel element energy balances show that losses by conduction and radiation match decay heat and oxidation power. Inputs include volumetric decay heat in the fuel and the thermal conductivity of the interstitial gas. Oxidation power is calculated based on the fuel temperature and user-defined gas composition. Decay heat and oxidation power are conducted and radiated to the MCO wall, which has a boundary condition temperature. Heat transfer to the MCO gas is conservatively ignored.

For a single fuel element, the fundamental equation for steady-state temperature is:

$$Q_{dk} + Q_{ox} = Q_c + Q_r + Q_a \tag{6-29}$$

where Q_{dk} = decay heat,
Q_{ox} = reaction power,
Q_c = gap conduction losses,
Q_r = outer element net radiation losses, and
Q_a = net radiation exchange between inner and outer fuel elements.

Decay heat is an input, and oxidation power is calculated with the Pearce correlation, based on the current fuel element temperature, oxygen concentration, steam partial pressure, and total pressure. Other terms in Equation (6-29) are discussed below.

For a single fuel element, i, conduction losses are written:

$$Q_{cij} = \frac{k_g F_{ij} A_i (T_i - T_j)}{L_{ij}} \tag{6-30}$$

where k_g is the thermal conductivity of the gas, L_{ij} is the conduction distance between heat sink i and heat sink j, F_{ij} is the radiation view factor, and A_i is the surface area of heat sink i. A total of 27 heat transfer paths can be identified.

For each of the seven outer fuel elements and the MCO wall, a new guess for radiosity is generated by:

$$B_i^{new} = \varepsilon_i \sigma T_i^4 + \rho_i \left[\sum B_j F_{ij}\right] \tag{6-31}$$

where σ is the Stefan-Boltzmann constant, ε_i is the emissivity of surface i and ρ_i is the reflectance. With the radiosity known, the net heat loss due to radiation is:

$$Q_{ri} = A_i \frac{\left[\varepsilon_i \sigma T_i^4 - (1-\rho_i) B_i\right]}{\rho_i} \quad (6\text{-}32)$$

Radiation exchange between inner and outer fuel elements is approximated by the expression for radiation exchange between two infinite, parallel flat plates with emissivities ε_i and ε_j:

$$Q_{aij} = \frac{A_i \sigma \left[T_i^4 - T_j^4\right]}{\frac{1}{\varepsilon_i} + \frac{1}{\varepsilon_j} - 1} \quad (6\text{-}33)$$

The iterative solution scheme can be summarized:

1. Guess T_i and B_i, the radiosity.

2. For each of the fuel elements, initialize the total sum heat sources/losses to decay heat:

   $Q_i = Q_{di}$

3. For each of the 27 heat transfer paths, determine the conduction heat transfer rate and update the total sum of heat sources/losses:

   $Q_{cij} = k_g F_{ij} A_i (T_i - T_j)/L_{ij}$
   $Q_i = Q_i - Q_{cij}$
   $Q_j = Q_j + Q_{cij}$

4. For each of the seven fuel outer elements and the MCO wall, determine the new guess for the radiosity:

   $B_i^{new} = \varepsilon_i \sigma T_i^4 + \rho_i [\Sigma B_j F_{ji}]$

5. Once the radiosity is known, determine the net heat loss due to radiation and update the total sum of heat sources/losses:

   $Q_{ri} = A_i [\varepsilon_i \sigma T_i^4 - (1 - \rho_i) B_i]/\rho_i$
   $Q_i = Q_i - Q_{ri}$

6. For each of the seven fuel assemblies, determine the radiation heat transfer rate between the inner and the outer elements and update the total sum of heat sources/losses:

$$Q_{aij} = \frac{A_i \sigma \left[T_i^4 - T_j^4\right]}{\left(\frac{1}{\varepsilon_i} + \frac{1}{\varepsilon_j} - 1\right)}$$

$$Q_i = Q_i - Q_{aij}$$

$$Q_j = Q_j + Q_{aij}$$

7. For each of the 14 fuel elements, determine the corrosion power, $Q_{ox\text{-}i}$, and update the total sum of heat sources/losses:

   $Q_i = Q_i + Q_{oxi}$

8. For each of the 14 fuel elements, determine the new guess for the temperature:

   $T_i^{new} = T_i + Q_i/\lambda\ (m\ c)_i$

   where λ is a relaxation constant, m is heat sink mass, and c is specific heat.

9. If the temperatures and the radiosities have not converged, repeat the procedure starting from Step 2. The scheme converges when no value of Q_i exceeds 0.01 W.

FORTRAN source code (SSTEMP) for the algorithm is shown in Appendix D. Although not shown here, application to stationary ignition theory is simple. For a given set of inputs (decay heat, gas composition, gas thermal conductivity, and total pressure), the MCO wall temperature is increased until a steady-state solution cannot be found.

6.5 Ignition Theory Analysis of Scrap Baskets

Application of ignition theory evolved with scrap basket design. The first application did not consider a copper fin and was therefore similar to the fuel basket application discussed in Section 6.3 (Plys and Malinovic 1997). Numerical results for stationary ignition theory application to scrap baskets without fins are not discussed in detail in this section, however, because scrap basket designs now include copper fins. Discussion of the original scrap basket temperature profile solution is included as a prelude to subsequent applications with copper fins (Plys, et al. 1997). Also, the probabilistic analysis presented in Section 7.0 was based on the original solution without copper fins and was included to illustrate the uncertainty analysis process, even though this design is no longer relevant.

6.5.1 Ignition Theory Analysis of Scrap Baskets Without Fins

If the scrap basket is without a copper fin, the approach to stationary ignition is much like the approach used for the fuel basket in Section 6.3. The equation for temperature profile in the scrap is the same as the temperature profile in the fuel basket using a porous medium approximation; i.e., Equation (6-16). Here, we simply note the differences in the ignition theory application to a scrap basket without a copper fin vis-à-vis the application to a fuel basket in an MCO. These differences involve the effective thermal conductivity, internal natural circulation, and radiative conductivity, and are discussed below.

For the scrap basket, the thermal conductivity is taken as the sum of a composite value for conduction and a term for internal bed radiation. The conduction term given by (Gabor 1970) is a refinement of experimental and analytical work by (Swift 1966):

$$\frac{k_e}{k_g} = 1.813\left(\frac{k_m}{k_m - k_g}\right)\left[\left(\frac{k_m}{k_m - k_g}\right)\left(\ell n \frac{k_m}{k_g}\right) - 1\right] + 0.0935 \qquad (6\text{-}34a)$$

which in the limit $k_m >> k_g$ reduces to

$$k_e = 1.813\, kg\left[\left(\ell n \frac{k_m}{k_g}\right) - 1\right] \qquad (6\text{-}34b)$$

where k_e = effective thermal conductivity, W/m K,
k_m = metal conductivity, W/m K, and
k_g = gas conductivity, W/m K

An alternate model for the thermal conductivity may also be appropriate because the scrap basket porosity may be large:

$$k_e = k_g\left(1 - (1-\phi)^{\frac{1}{3}}\right)^{-1} \qquad (6\text{-}34c)$$

which is the formula for a medium whose continuous phase, here the gas phase, has a thermal conductivity much less than that of the dispersed phase, here the fuel.

The scrap basket porosity and particle size are large enough that internal natural convection is expected. While no solution to the exact problem of a cylindrical, enclosed, heat generating debris bed has been found in the literature, a related problem is described by (Gebhart, et al. 1988). Nusselt numbers in the range of 1.2 to 1.4 are shown for a vertical annular debris bed with adiabatic, impermeable upper and lower boundaries, prescribed temperatures on the inner and outer perimeters, and the appropriate range of aspect ratio and Rayleigh number, though no

correlation is given. For a rectangular enclosure with heat removal on the sidewalls (i.e., net heat transport horizontally, not vertically) and impermeable insulated upper and lower boundaries, with an aspect ratio A = H/R > 1,

$$\frac{k}{k_g} = \frac{1}{\sqrt{3}} \left(\frac{Ra}{A} \right)^{\frac{1}{2}} \tag{6-34d}$$

where

$$Ra = \frac{g \rho H K \beta \Delta T}{\mu \alpha} \tag{6-34e}$$

$$K = \frac{d_p^2 \phi^3}{150 (1 - \phi)^2} \tag{6-34f}$$

= permeability, m^2,
g = acceleration of gravity, m/s^2,
H = height, m,
β = $1/T$ = isothermal compressibility, K^{-1},
ΔT = temperature difference, K,
μ = viscosity, kg/m s,
α = thermal diffusivity, m^2/s, and
d_p = particle size, m.

Values for nitrogen, the limiting gas, are $\mu/\rho = 2 \times 10^{-5}$ m^2/s and $\alpha = 3 \times 10^{-5}$ m^2/s. Using the lowest porosity $\phi = 0.6$, and an average debris size of 0.01 m, yields a permeability of 10^{-6} m^2, which is probably low because it is a laminar value. Using an average temperature of 350 K, a temperature drop of 30 K, and a height of 0.6 m, yields Ra = 840. Because A = H / R = 2, Nu; 12.

Factors that allow the upper bound of the Nusselt number to be larger for a scrap basket are the large particle size which suggests a larger turbulent permeability, the presence of the non-adiabatic MCO lid to enhance convection potential, and the pressure of a void region above the basket contents. Nu = 1 represents conduction, and the effective conductivity may be augmented by the factor k_g (Nu - 1) where Nu is a model parameter. Because the application of equation (6-34d) to the scrap basket is not clear, however, it is conservative to consider the range of 1.2 to 1.4, as discussed above.

The radiative conductivity is given by [Kasparek and Vortmeyer, 1976]

$$k_{rad} = 4 \alpha \varepsilon x T^3 = C T^3 \tag{6-35}$$

$$x = d_p \frac{1 + \frac{\lambda}{\varepsilon}}{1 - \lambda} \tag{6-36}$$

$$\lambda = 1-(1.21)\,(1-\alpha)^{\frac{2}{3}} \tag{6-37}$$

where d_p = effective scrap particle diameter, m, and $\alpha = 1 - \phi$. This formula accounts for transmission of radiation among grey surfaces.

Substituting

$$k = k_e + C\,T^3 \tag{6-38}$$

into Equation (6-16) and applying the boundary conditions in Equation (6-19), yields

$$T_a - T_R + C_1\left(T_a^4 - T_R^4\right) = \left(\frac{Q\,R^2}{4\,k_e}\right)\left[\left(1-\frac{a^2}{R^2}\right) + 2\,\frac{a^2}{R^2}\,\ell n\left(\frac{a}{R}\right)\right] \tag{6-39a}$$

$$C_1 = \frac{\sigma\,\varepsilon\,x}{k_e} \tag{6-39b}$$

The relative contribution of radiation is worth noting by example. The radiative term above can be linearized as

$$C_1\left(T_a^4 - T_R^4\right) \approx \frac{4\,\sigma\,\varepsilon\,x\,\overline{T}^3}{k_e}\left(T_a - T_R\right) \tag{6-39c}$$

so the dimensionless group multiplying the temperature difference is the ratio of radiative to conductive heat transfer. Using $\sigma = 5.67 \times 10^{-8}$, $\varepsilon = 0.5$, $x = 0.025$, $\overline{T} = 333$ K, and $k_e = 0.4$, yields a ratio of 0.26. Thus the radiative contribution is important for helium cover gas and even more important for nitrogen.

The MCO wall temperature is found by continuity of heat flux assuming the simple parallel plate formula for gap heat transfer

$$q''(R) = \sigma\,\varepsilon_g\left(T_R^4 - T_S^4\right) + \frac{k_g}{\delta_g}\left(T_R - T_S\right) \tag{6-40}$$

where ε_g = gap effective emissivity,
T_S = MCO wall surface temperature, K,
k_s = gap gas thermal conductivity, W/m K,
δ_g = gap thickness, m, and

for gap surfaces of emissivities, ε_1 and ε_2, the effective emissivity is

$$\varepsilon_g = \left(\frac{1}{\varepsilon_1} + \frac{1}{\varepsilon_2} - 1 \right)^{-1} \tag{6-41}$$

In summary, ignition theory calculations for a scrap basket without fins are similar to ignition theory calculations for a fuel basket. Differences lie mainly in the determination of the effective thermal conductivity of the scrap. This model has been supplanted by the calculation for a scrap basket design with a fin, which will be presented next. Nevertheless, to illustrate probabilistic approaches, the ignition temperature calculation for scrap baskets without copper fins will be presented in Section 7.1, using probability distributions for selected inputs.

6.5.2 Ignition Theory Application to Scrap Baskets With Copper Fins

An ignition theory model is described here for the case of a scrap basket of modified design in which a copper fin essentially surrounds the scrap in a basket sector. Such a fin is a copper liner running from the center post along the radial spoke supports to the basket rim and continuing along the inside rim. As will be shown below, the copper fin provides an essentially isothermal boundary for scrap. Heat generated in the basket interior is transferred azimuthally to the radial fin and then radially to the peripheral fin where it is conducted across the gap to the MCO wall. The maximum temperature in the scrap lies along the line of symmetry bisecting the 60-degree copper-lined sector, as illustrated in Figure 6-5. Heat generated by scrap inside this point is mostly conducted azimuthally to the radial fin, and heat generated by scrap outside this point is mostly conducted radially to the peripheral fin.

Figure 6-5: Scrap Basket Sector

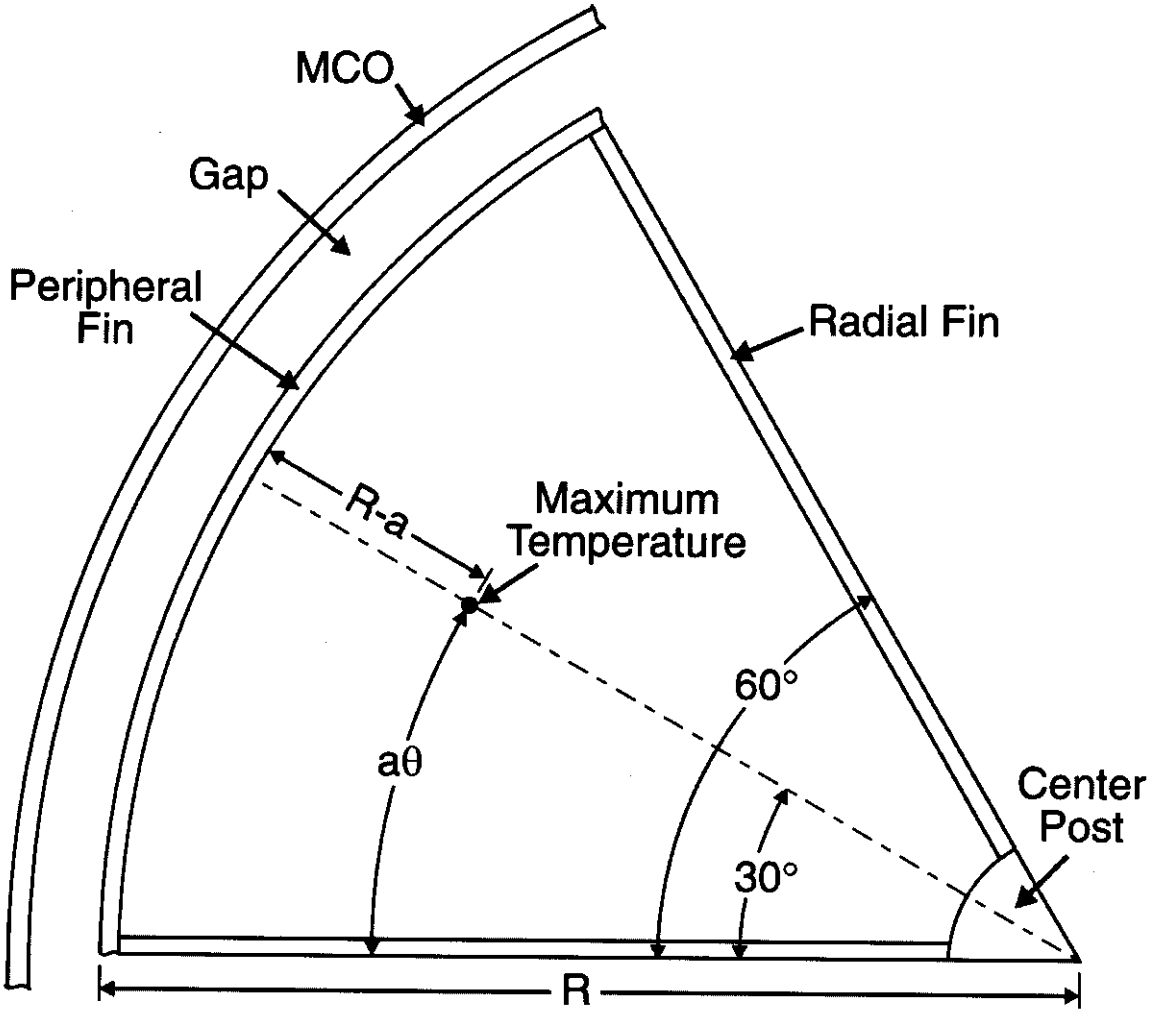

MP974115.CDR 4-22-97

6.5.2.1 Fin Temperature Analysis

Heat transfer in the radial copper fin is described by a modified fin equation

$$\frac{d^2 T}{dr^2} + \frac{q''(r) P}{k A} = 0 \tag{6-42}$$

where P is fin perimeter and A is conduction area. The heat flux q″(r) is due to decay plus reaction power conducted in the θ direction:

$$q''(r) = Q\, r\, \theta \tag{6-43}$$

$$Q = (1-\phi)\left(q_v + \frac{A}{V} q_r(T)\right) \tag{6-44}$$

where θ is the sector symmetry angle of 30° or π/6. The ratio of fin perimeter to conduction area is simply the thickness:

$$\frac{P}{A} = \frac{1}{t} \tag{6-45}$$

so, the conduction equation becomes

$$\frac{d^2 T}{dr^2} + f\, r = 0 \tag{6-46}$$

$$f = \frac{Q\theta}{k\, t} \tag{6-47}$$

The boundary conditions are

$$\frac{dT}{dr} = 0 \qquad r = r_c \tag{6-48}$$

$$T = T_c \qquad r = r_c \tag{6-49}$$

where r_c is the inner radius. This leads to

$$T_c - T_R = \frac{f}{6}\left[R^3 - r_c^2 (3R - 2r_c)\right] \tag{6-50}$$

Using example values from Table 6-3, derived values are f = 434 and $T_c - T_R = 1.63°C$. Thus, for practical purposes, the fin provides a constant temperature boundary condition for azimuthal heat transfer. Note the temperature difference between r = R and another point r = a is given by

$$T_a - T_R = \frac{f}{6}\left[\left(R^3 - a^3\right) - r_c^2\,(3R - 3a)\right] \tag{6-51}$$

so for example, if a = 2/3 R, then $T_a - T_R = 1.17°C$.

Heat transfer in the peripheral copper fin is governed approximately (and conservatively) by the text book solution for a fin with an insulated tip and constant heat transfer coefficient along its length:

$$q = \sqrt{h\,P\,k\,A}\,(T_r - T_\infty)\tanh(m\,L) \tag{6-52}$$

Table 6-3: Example Values

		ASSUMED		
Volumetric Power		Q	2000	W/m^3
Outer Radius		R	0.286	m
Inner Radius		r_c	0.035	m
Symmetry Angle		θ	$\pi/6 = 0.5236$	
Fin Thickness		t	1/4" = 0.00635 m	
Copper Conductivity		k	380	W/m K
Gap (helium) Conductivity		k_g	0.17	W/m K
Gap Thickness	δ_S		0.00476 m	
Scrap Effective Conductivity		k_S	0.5	W/m K
		DERIVED		
Radial Fin Power Term	f =	$\frac{Q\theta}{k\,t}$	434	
Section Perimeter		$L = R\,\theta$	0.1497 m	
Peripheral Heat Flux		q" (R)	281.7	W/m^2
Gap Heat Transfer	h =	$\frac{k_g}{\delta_g}$	35.7	W/m^2 K
Peripheral Fin Parameter	m =	$\sqrt{\frac{h}{k\,t}}$	3.846	
Peripheral Fin Parameter		tanh (m L)	0.5197	
Peripheral Fin Parameter		cosh (m L)	1.171	
Peripheral Fin Parameter		$\sqrt{h\,k\,t}$	9.281	W/m K
Scrap Planar ΔT		$\frac{Q R^2}{2 k_s}$	163.6	K
Effective Heat Transfer Coefficient to MCO	h_{eff}		32.2	W/m^2 K

$$m = \sqrt{\frac{h}{k\,t}} \tag{6-53}$$

$$h = \left(\frac{k}{\delta}\right)_{gap} \tag{6-54}$$

$$L = R\,\theta \tag{6-55}$$

where q denotes the total heat lost assuming it all enters at the fin base, which is conservative. Rearranging for the radial heat flux, noting A = P t,

$$q''(R) = \left(\frac{Q\,R}{2}\right)\left(1 - \frac{r_c^2}{R^2}\right) \tag{6-56a}$$

$$= \frac{q}{R\,\theta\,P} \tag{6-56b}$$

$$= \frac{\sqrt{h\,k\,t}}{R\,\theta}\left(T_R - T_\infty\right)\tanh\left(m\,R\,\theta\right) \tag{6-56c}$$

$$= h_{eff}\left(T_R - T_\infty\right) \tag{6-56d}$$

$$h_{eff} = \frac{\sqrt{h\,k\,t}}{R\,\theta}\tanh\left(m\,R\,\theta\right) \tag{6-56e}$$

For the example parameters, the derived heat flux outward toward the MCO wall is 281.7 W/m^2, and the implied temperature difference from the fin base to MCO wall T_R - T_a is 8.75°C. The temperature drop along the peripheral fin is given by

$$\frac{T - T_\infty}{T_R - T_\infty} = \frac{\cosh\left[m\left(L - x\right)\right]}{\cosh\left(m\,L\right)} \tag{6-57}$$

so, the total drop is given by

$$T_R - T_L = \left(T_R - T_\infty\right)\left(1 - \frac{1}{\cosh\left(m\,L\right)}\right) \tag{6-58}$$

which for the example case is 1.28°C.

6.5.2.2 Hot Spot Analysis

To a good approximation, the maximum temperature in the scrap sector is found by using the quadratic profile for even power generation. The location of the maximum temperature, or hot spot, must clearly lie along the axis of symmetry bisecting a section. Also, it must lie at a distance from the periphery R - a, such that its one-dimensional radial temperature drop is equal to its one-dimensional azimuthal temperature drop along the distance θa. Assuming these one-dimensional profiles may be set equal gives

$$\left(\frac{Q R^2}{4 k_s}\right)\left[1 - \frac{a^2}{R^2} + 2\frac{a^2}{R^2}\,\ell n\,\frac{a}{R}\right] = \left(\frac{Q R^2}{2 k_s}\right)\left(\frac{a^2\,\theta^2}{R^2}\right) + \Delta T_r \qquad (6\text{-}59)$$

where ΔT_r is the temperature drop in the radial fin from r = a to r = R, and k_s is the scrap overall conductivity. Setting

$$\rho = \frac{a}{R} \qquad (6\text{-}60)$$

and

$$\delta = \Delta T_r \left(\frac{Q R^2}{2 k_s}\right)^{-1} \qquad (6\text{-}61)$$

yields an implicit equation for a:

$$\rho^2 = \frac{1 - 2\delta^2}{2\theta^2 + 1 - 2\,\ell n\,\rho} \qquad (6\text{-}62)$$

Note that the heat generation rate Q plays only a minor role in the result through the parameter δ, which is really negligible. Using Table 6-1 values and ΔT_r = 1.2°C from the previous example, yields δ = 0.0073 and ρ = 0.6322, so a = 0.1808 m. The radial conduction distance R - a is thus 0.1052 m and the azimuthal distance is 0.947 m.

From this simplified perspective, the copper fin removes all power generated for r < a, so that the fin is equivalent to a center post of radius r = a.

It is convenient to note that the radial temperature drop is related to the planar drop by a form factor:

$$\Delta T_{rad} = g\,\Delta T_r \qquad (6\text{-}63a)$$

$$g = \frac{1}{2}\left[1-\rho^2+2\rho^2\,\ell n\,\rho\right] \tag{6-63b}$$

This is derived without scrap internal radiation. The actual equation used for the radial temperature drop is derived by (Plys and Malinovic 1997) as

$$T_a - T_R + C_1\left(T_a^4 - T_R^4\right) = g\,\Delta T_r \tag{6-64a}$$

$$C_1 = \frac{\sigma\,\varepsilon\,f_{rad}\,d_p}{k_s} \tag{6-64b}$$

where f_{rad} is a multiplier defined in (Plys and Malinovic 1997) and d_p is the scrap diameter. An approximate solution to check code results is found by linearizing the radiation term:

$$\left(T_a - T_R\right)\left(1+\delta\right) = g\,\Delta T_r \tag{6-65a}$$

$$\delta = \frac{4\sigma\,\varepsilon\,f_{rad}\,d_p}{k_s}\,T_a^3 \tag{6-65b}$$

This formula should slightly overestimate T_a - T_R because T_a is used on the right-hand side.

6.5.2.3 Ignition Temperature Method

The ignition temperature algorithm for a copper-lined scrap basket is as follows:

1. Guess the maximum temperature.
2. Solve for the reaction power and the total volumetric power Q.
3. Solve for the hot spot location r = a.
4. Solve the radial heat conduction equation, including radiation, for the temperature at r = R using an insulated boundary condition at r = a.
5. Evaluate the temperature drop from the peripheral fin to the MCO wall.
6. If the MCO wall temperature passes through a maximum, the ignition point is found. If not, guess a larger maximum temperature and go back to Step 1.

FORTRAN source code for this algorithm (IGMCOFIN) is contained in Appendix E. IGMOCFIN has been validated in (Plys, et al. 1997).

6.5.2.4 Ignition Temperature Calculations for a Scrap Basket With Fins

The IGMCOFIN code was run with the following inputs:

Table 6-4: Input to Ignition Model For a Scrap Basket With Fin			
Porosity	= 0.6	Power W/m^3	= 2000.00
Kin. Rate Mult.	= 3.0	Gap Emiss.	= 0.1800
Emissivity	= 0.7000	Outer Radius	= 0.28600 m
Inner Radius	= 0.035 m	Gap Therm. Cond.	= 0.1700 W/m K
Gap Thickness	= 0.00476 m	Steam Pressure	= 12.000 kPa
Particle Diameter	= 0.0226 m	Nusselt No.	= 1.3000

With the input above, A/V is 265. Two cases were run: one assuming the gas thermal conductivity is that of steam, and another assuming the gas thermal conductivity is that of helium. In either case, the reaction rate is given by the McGillivray correlation with steam pressure equal to 12 kPa. For the helium case, the ambient temperature that leads to ignition (ignition temperature) is 108°C, just below ignition, the maximum temperature in the scrap is 155°C. For the steam case, the ignition temperature is 30°C and the maximum stable scrap temperature is 98°C.

These results show that for a helium-filled MCO, there is considerable margin to ignition even if the reaction area is at an upper bound and the reactant supply is unlimited.

7.0 PROBABILISTIC CALCULATIONS

Many of the preceding ignition theory applications naturally lead to probabilistic calculations that are used in a risk-based approach to demonstrate safety margin. Inputs such as decay power, particle size, and reaction area are truly stochastic, which means probability distribution functions rather than deterministic values describe them. Other inputs such as rate multipliers or emissivities are not necessarily stochastic, but are uncertain due to limited sampling and testing. In these instances, probability distribution functions reflect degrees of belief or confidence more so than inherent randomness.

The Monte Carlo method was chosen to quantify distributions for incipient ignition temperatures resulting from a priori distributions for random parameters and model uncertainty. This method involves selection of successive sets of randomly selected, independent input parameter values to the ignition model and binning of the resulting temperature from each trial. A histogram of the frequency of each ignition temperature is thus created, and statistics such as the mean, standard deviation, and cumulative probability that the ignition temperature lies below a given value can be deduced.

7.1 Probabilistic Calculations for Ignition of Scrap Baskets Without Fins

Stationary ignition theory for a scrap basket without fins has been described in Section 6.5. Input distributions and the resulting histogram for incipient ignition temperature are discussed here (Plys and Malinovic 1997). Source code for these calculations (IGMCOMC) is contained in Appendix F.

Input distributions are shown in Table 7-1. The basis for each distribution is discussed here briefly:

Table 7-1: Input Values			
Parameter	**Distribution Type**	**Value**	**Basis**
Basket Outer Radius	Bright-Line *	0.286 m	22.625" O.D. Basket
Basket Inner Radius	Bright-Line *	0.035 m	2.75" O.D. Tube
Gap Thickness	Bright-Line *	0.00476 m	0.375" = MCO I.D. - Basket O.D.
Gas Conductivity	Bright-Line *	0.16 W/m K 0.022 W/m K	Helium Steam
Decay Power	Triangular	Lo = 140.6 W/m^3 Mid = 1484.0 W/m^3 Hi = 2707.5 W/m^3	7.4 W/mtu 78.1 W/mtu 142.5 W/mtu (Duncan 1997)
Void Fraction	Uniform	Lo = 0.65 Δ = 0.20	(Pajunen 1997)
Rate Multiplier	Uniform	2-5 Optimistic 4-8 Mid-Range 8-12 Pessimistic	Controversial
Scrap Emissivity	Uniform	Lo = 0.40 Δ = 0.40	Metal-to-Oxide Variation Plus Model Uncertainty
Gap Emissivity	Uniform	Lo = 0.18 Δ = 0.07	Steel 0.3 to 0.4 (Duncan 1997)
Reaction Area	Uniform	Lo = 1.0 m^2 Hi = 6.0 m^2	(Plys and Malinovic 1997)
Particle Size	Uniform	Lo = 0.0125 m Hi = 0.0375 m	Criteria for Scrap 1/4" to 3"
Steam Pressure	Uniform	Nominal 4-12 kPa Upset 12-20 kPa	Variation from Saturation at 50°C
Nusselt Number	Uniform	Lo = 1.2 Hi = 1.4	Internal Convection, Section 6.5
* A "Bright-Line" distribution is a point-estimate.			

- Decay Power: (Duncan 1997) states a nominal and upper bound for MCO decay power. The lower bound is the judgement of SNF Project personnel.

- Void Fraction: The lower bound is based on judgment of photographs and videotapes, while the upper bound is based on actual scrap canisters (Pajunen 1997). For reference, fuel baskets are packed to about 57% void, and scrap baskets cannot be packed more efficiently.

- Rate Law Multiplier: The optimistic band values are slightly larger than literature values; the pessimistic band values are an order of magnitude larger than literature values to account for cracking and hydrides; and mid-range values simply fall between optimistic and pessimistic values.

- Scrap Emissivity: Metal and oxide values are 0.5 and 0.7, respectively. To account for uncertainty in the radiation mode, the range is expanded from 0.4 to 0.8.

- Gap Emissivity: For stainless steel, low and high values are 0.3 and 0.4, respectively, which leads to overall values between 0.18 and 0.25.

- Average Particle Size: Scrap pieces are between ¼" and 3", but neither is a reasonable bound because the average size must reflect a reasonable combination of the two. Therefore, ½" is the lower bound and 1.5" is the upper bound.

- Reaction Area: Reaction area was developed in (Plys and Malinovic 1997). Reaction area scales with void fraction, however, so that the smallest void fraction yields the bounding reaction area.

- Nusselt Number: Refer to Section 6.5.

Nine cases were run with the model, corresponding to three ranges of the rate law multiplier and choices of three process conditions as presented in Table 7-2. Process cases considered were normal and off-normal recirculation mode operation (a mostly helium-filled MCO) and normal vacuum mode operation (pure steam at low pressure). Off-normal vacuum mode operation was not considered here because reasonable combinations of parameters exceeding nominal values can lead to prediction of incipient ignition. Figures 7-1 through 7-3 present the probability density functions and cumulative probabilities for the three process cases.

From Table 7-2, it is clear that for optimistic or mid-range choices of the rate law multiplier, a firm safety basis is established for normal recirculation mode operation, but not for the pessimistic multiplier. Off-normal operation and a pessimistic rate law range show a reasonable chance of ignition inception at the current operating temperature. For these recirculation cases, addition of just one percent oxygen would cause reaction poisoning and decrease the rate law by a factor of ten. For the pure steam atmosphere cases, ignition at 50°C is credible for all rate law multipliers as suggested by the deterministic results.

Plotted values of the cumulative probabilities of ignition at 50°C appear slightly higher than table values because of the way plot points are connected.

Figure 7-1: Probability of Ignition Temperature, Normal Operation With Helium, Scrap Basket Without Copper

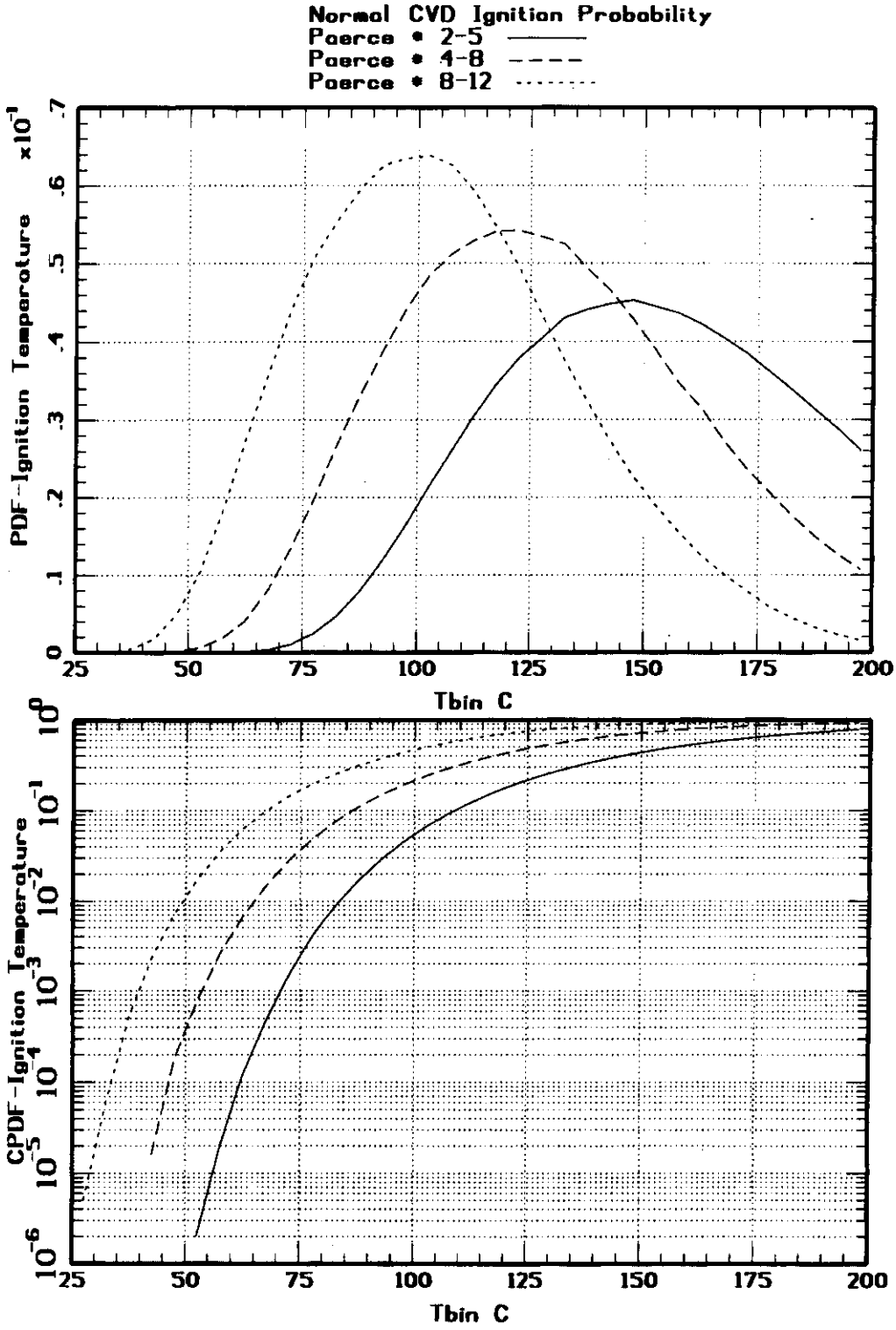

Figure 7-2: Probability of Ignition Temperature, Off-Normal Operation With Helium, Scrap Basket Without Copper

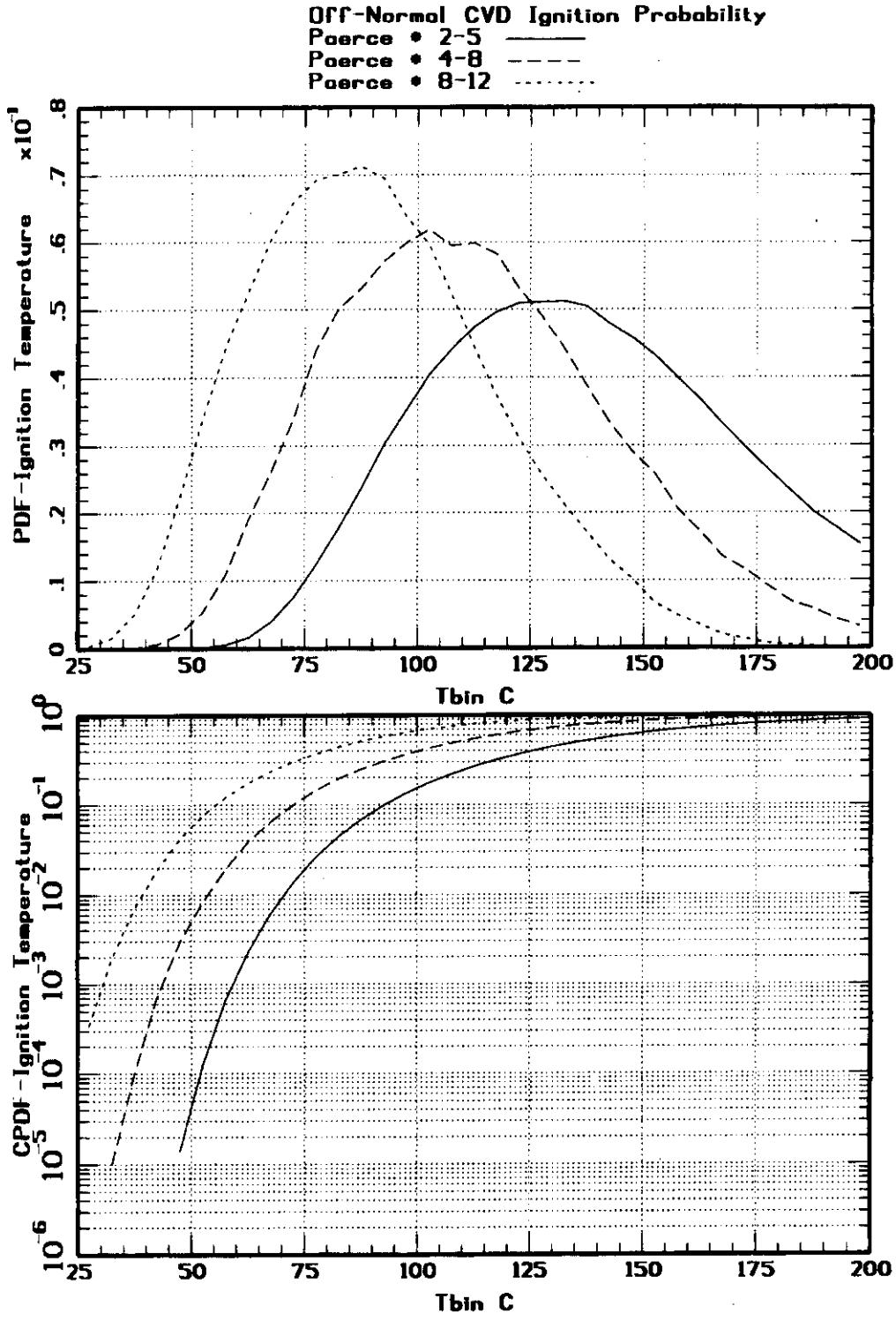

Figure 7-3: Probability of Ignition Temperature, Normal Operation With Steam, Scrap Basket Without Copper

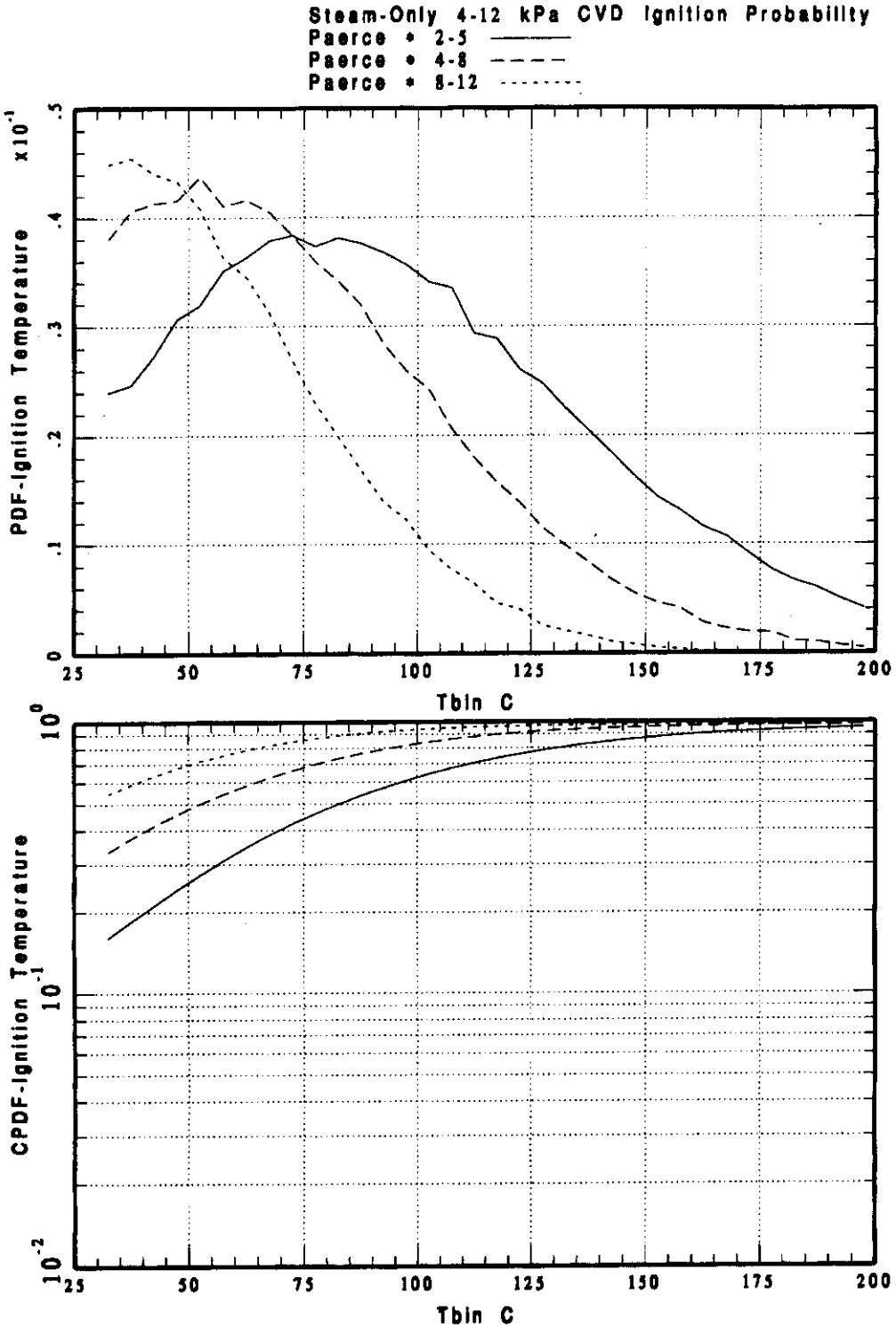

Table 7-2: Probabilistic Ignition Results					
Rate Multiplier	**# Trials**	**P (T < 50°C)**	**P (T < 60°C)**	**P (T < 70°C)**	**T_{avg}**
Normal Recirculation Cases: 4% - 12% Steam					
2 - 5	10^6	$< 10^{-6}$	6.95×10^{-5}	1×10^{-3}	173
4 - 8	10^6	4.74×10^{-4}	4.61×10^{-3}	2.14×10^{-2}	142
8 - 12	10^6	1.23×10^{-2}	4.93×10^{-2}	1.21×10^{-1}	116
Off-Normal Recirculation Cases: 12% - 20% Steam					
2 - 5	10^6	6.20×10^{-5}	1.44×10^{-3}	9.99×10^{-3}	151
4 - 8	10^6	5.55×10^{-3}	2.87×10^{-2}	8.15×10^{-2}	123
8 - 12	10^6	5.86×10^{-2}	1.47×10^{-1}	2.66×10^{-1}	101
Steam Atmosphere: 4 - 12 kPa Steam					
2 - 5	10^5	0.26%	0.33%	0.40%	97
4 - 8	10^5	0.48%	0.56%	0.64%	65
8 - 12	10^5	0.70%	0.77%	0.83%	39

7.2 Probabilistic Analysis of the French Fuel Flash Experience

The French fuel flash expexperience has been described in terms of ignition theory (Plys, Malinovic, and Epstein 1998). A model for decladded fuel with a porous layer describes this experience. The Frank-Kamenetskii parameter is defined in Equation (6-6), except that F = 1 and $b = \delta / 2$, where δ is the porous layer thickness. A probabilistic treatment is shown here to demonstrate that ignition might reasonably be expected in isolated instances, given the random nature of inputs and uncertainties associated with applying stationary ignition theory. An N Reactor fuel example is then presented.

7.2.1 French Fuel Flash Probabilistic Evaluation

A deterministic evaluation shows that B = 0.15, which suggests that some extreme combination of parameters might lead to B = 1.0 or greater. Crystal Ball™, a commercially available software package used for Monte Carlo analyses, was used for analyses presented here. Parameters A_v, δ, h_e, and the rate law coefficient are considered random variables, while other parameters remain at the original point-estimates. Uncertainty in the literature reaction rate is quantified in practice by a multiplicative factor for the coefficient. Probability distributions are as follows:

- Surface-to-volume ratio A_v is a uniform distribution with a minimum of 2×10^5 m^{-1} and a maximum of 1.8×10^6 m^{-1}. This is derived from a value of 6×10^5 m^{-1}, with a factor of 3 uncertainty on either side. With no way of knowing the mode, a uniform distribution is most reasonable.

- Layer thickness, δ, is a triangular distribution with a minimum of 0.5 mm, most probable value of 2 mm, and maximum of 3.5 mm. This is an interpretation of "several millimeters". A minimum layer thickness of 0.5 mm is chosen for a nonzero swollen layer. The average (over inner and outer) fuel element thickness is only 9 mm and the layer thickness must be much less than the fuel element thickness.

- The equivalent heat transfer coefficient, h_e, is a Weibull distribution with minimum of 50 W/m^2-K, most probable value of 100 W/m^2-K, and 99th percentile value of 600 W/m^2-K. The most probable value comes from the point-estimates above; the minimum is based on the pessimistic assumption that the heat transfer is half the point-estimate; and the 99th percentile value comes from assuming that an upper bound is the value for the heat transfer coefficient to the fluid.

- Uncertainty factor for the rate law coefficient had a triangular distribution with a minimum of 0.5, most probable value of 1.0, and maximum of 2.0, to reflect experimental uncertainties in rate law parameters.

Ten thousand trials were obtained for the French fuel Frank-Kamenetskii ignition parameter. Summary statistics from the simulation are as follows:

A complimentary cumulative distribution function (CCDF) shown in Figure 7-4 indicates that with the parameters defined above, ignition occurs (B exceeds 1) about 0.7% of the time. This is in fortuitous agreement with the French experience that 0.5% of the fuel underwent flashing. An appropriate conclusion is simply that ignition is plausible given reasonable variation in controlling parameters; clearly ignition is not predicted unless some combination of nearly worst-case values is chosen, and this has low probability.

Figure 7-4: Complementary Cumulative Probability Distribution for Ignition Parameter of French Fuel

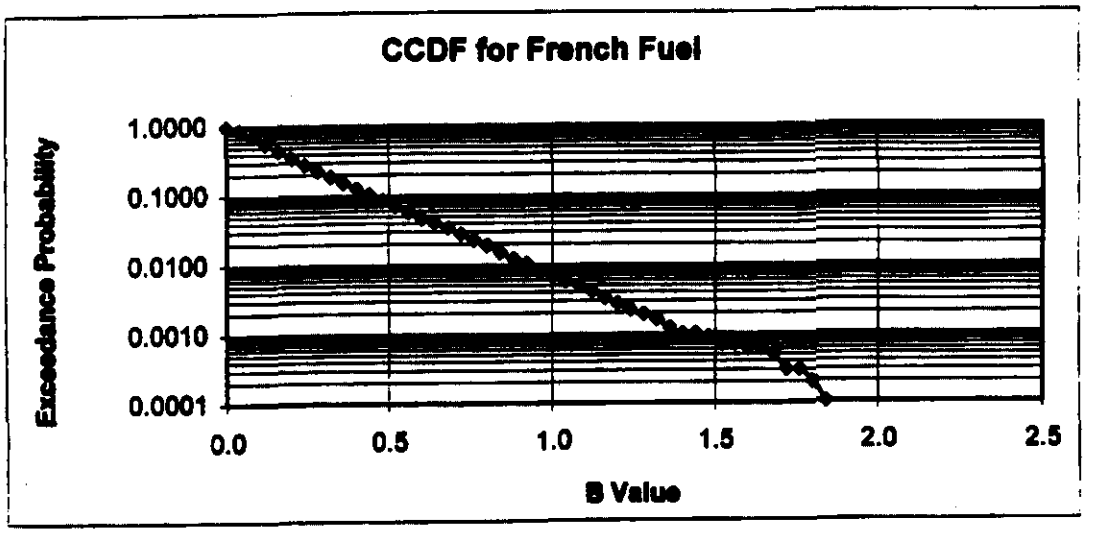

7.2.2 Probabilistic Evaluation on N Reactor Fuel

A calculation similar to the one above for the French fuel was performed for N Reactor fuel. The following point-estimates apply for N Reactor fuel:

A_v	=	1.0×10^6 m^{-1},	
b	=	0.0045 m	(Average fuel half-thickness for outer and inner elements),
C	=	624,	
T_e	=	7529 K,	
T_f	=	298 K	(Ambient water temperature),
T_r	=	25.26,	
ΔH	=	1.67×10^7 J/kg,	
h_f	=	600 W/m^2-K	(Heat transfer to water),
R	=	0.03 m,	(Roughly 5% of fuel length),
k_1	=	10 W/m-K,	
k_2	=	30 W/m-K, and	
F	=	0.05	(Volume fraction of hydride).

Equation (6-15b) shows the Frank-Kamenetskii ignition parameter, B, for a damaged fuel element end. This equation was evaluated with point-estimates, resulting in B = 0.01.

An uncertainty analysis was performed using the following distributions:

- Surface area per unit volume, A_v, is a uniform distribution with a minimum of 3×10^5 m^{-1} and a maximum of 3.0×10^6 m^{-1}. This reflects an estimated value of 1×10^6 m^{-1}, with a factor of 3 uncertainty on either side.

- Fluid heat transfer coefficient, h_f, is a triangular distribution with a minimum of 450 W/m^2-K, a most likely value of 600 W/m^2-K, and a maximum of 750 W/m^2-K. This reflects the usual uncertainty in predicting any heat transfer coefficient based on literature data.

- Damage length, R, is a uniform distribution between 1 cm and 10 cm. Damage lengths less than 1 cm are trivial, while damage lengths greater than 10 cm have not been observed.

- Thermal conductivity in the damaged end, k_1, is triangular with a minimum of 10 W/m-K, most likely value of 20 W/m-K, and maximum of 30 W/m-K. The maximum reflects the undamaged thermal conductivity, while the minimum reflects a pessimistic, factor-of-three reduction.

- Volume fraction of hydride, F, is a uniform distribution between 0.01 and 0.1.

- Rate law multiplier is a triangular distribution with a minimum of 0.5, most probable value of 1.0, and maximum of 2.0, to reflect experimental uncertainty in rate law parameters.

Ten thousand trials were obtained for the N fuel Frank-Kamenetskii parameter. The resulting CCDF for the Frank-Kamenetskii parameter shown in Figure 7-5 indicates that with the parameters defined above, ignition is extremely unlikely.

Curve fits to the output reveal that a gamma distribution is best, based on the Anderson-Darling statistic, regardless of the number of samples used for the test. The Anderson-Darling statistic is preferred because it weights the ends of the distribution more heavily than other goodness-of-fit tests do (Plys, Malinovic, and Epstein 1998). The equation for the gamma distribution is,

$$f(x) = \begin{cases} \dfrac{1}{\beta^{\alpha}\ \Gamma\ (\alpha)}\ x^{\alpha-1}\ e^{-\frac{x}{\beta}} & \text{for } x > 0,\ \alpha > 0, \text{ and } \beta > 0 \\ 0 & \text{elsewhere} \end{cases} \tag{7-1}$$

where α and β are related to mean and standard deviation, as follows:

$$\mu = \alpha\beta \tag{7-2a}$$

and

$$\sigma^2 = \alpha\beta^2 \tag{7-2b}$$

For a mean of 0.01928 and standard deviation of 0.01547, $\alpha = 1.604$ and $\beta = 0.011842$. Evaluating the inverse of the gamma function shows that B = 0.19 has an exceedance probability of 1×10^{-6}. Exceedance probability for B = 1.0 is zero for any practical purpose and flashing cannot be expected, even for thousands of fuel elements.

Figure 7-5: Probability Density Function for Ignition Parameter of K Basins Damaged Element.

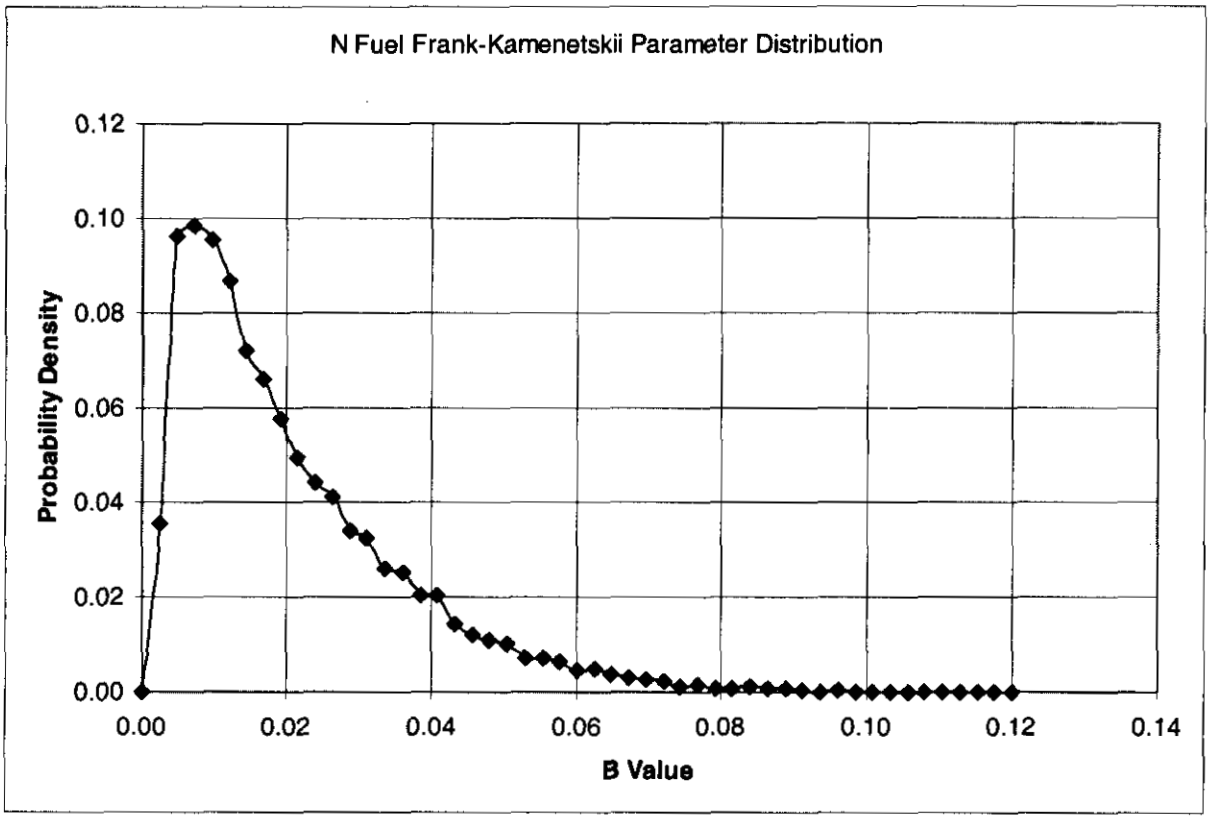

8.0 TRANSIENT ANALYSIS

Transient solutions have not been considered heretofore. Previous sections determined incipient conditions for ignition and merely noted that the time to attain these conditions offers considerable margin. This section considers three examples of transient calculations: (1) hydride layer burnout and impact on damaged fuel ignition potential, (2) K Basins Integrated Water Treatment System (IWTS) Settlers, and (3) application of the HANSF code, which is an integrated tool for considering phenomena inside an MCO such as fuel oxidation, convection, and radiative heat transfer and the potential for radionuclide release.

8.1 Hydride Layer Impact on Damaged Fuel Potential

Uranium hydride pyrophoricity has been mentioned in Sections 2.0 and 5.2. A time-dependent consideration is motivated by concerns regarding the impact of hydride surface layers. Uranium hydride may be present in corrosion layers formed on damaged fuel surfaces during under water storage, or it may be present as a coherent layer due to exposure to hydrogen during dry storage.

8.1.1 Hydride Layers

Consider a mostly oxidic layer of extreme thickness and hydride content:

δ = Layer thickness = 10 μm = 10^{-5} m,
ρ = Layer density = 8,000 kg/m^2,
f = Hydride fraction = 0.25, and
A_v = Area per unit volume hydride
= 5×10^6 m^{-1}.

The effective area enhancement factor for reaction, given the initial area implied by the unreacted hydride, is

$$F_{ho} = f \delta A_v = 12.5 \quad (8\text{-}1)$$

For a hydride layer created in dry storage, choosing f = 1.0 and δ = 20 μm = 2×10^{-5} m, yields an effective area enhancement of F_{ho} = 100.

While in these cases the initial reactive area is high, the amount of reactant is limited, so the amount of energy available to heat up underlying fuel is limited. The hydride layer is in thermal contact with its metal fuel substrate, which is declad both inside and outside on a damaged end, and has the following properties:

ρ_f = fuel density, 19,000 kg/m^3,
c_f = fuel specific heat, 120 J/kg, and
b = fuel half-thickness, 0.0045 m.

For simplicity, the heat of reaction of the metal with water vapor is used and the ratio of oxygen weight gained to hydride weight consumed is needed:

ΔH = heat of reaction, 1.67×10^7 J/kgO_2, and
μ = net molecular weight (O_2 minus 3/2 H_2) gain/molecular weight UH_3 consumed = 29/241.

With this information, the adiabatic temperature rise of the damaged end is

$$\Delta T_{ad} = \frac{\rho f \delta \mu \Delta H}{\rho_f c_f b} = 3.9°C \quad (8\text{-}2)$$

for a partially hydrided corrosion layer. For a hydride layer formed in dry storage, using example values mentioned above, the result is $\Delta T_{ad} = 31°C$.

Thus, despite high area enhancements, the limited amount of hydride reactant may not be sufficient to cause underlying base metal to undergo a thermal excursion. This is addressed by a transient analysis.

8.1.2 Hydride Layer Transient Model

The kinetic rate law for hydride reaction is chosen here as the Pearce oxygen-free law:

$$w'' = k_o p^{1/2} \exp\left(-\frac{T_E}{T}\right) \quad (8\text{-}3)$$

where w'' = Weight gain, kgO_2/m^2 s,
k_o = 0.05939 kgO_2/m^2 s kPa$^{1/2}$,
p = H_2O pressure, kPa,
T_E = Normalized activation energy,
= 4936.7 K, and
T = Reaction temperature, K.

For spherical hydride particles, the area is reduced as mass is depleted:

$$\frac{A}{A_o} = (1-\alpha)^{2/3} \quad (8\text{-}4)$$

where A/A_o is the fractional area for reaction and α = hydride reacted fraction.

A mass balance on hydride in the layer is:

$$\frac{d\alpha}{dt} = \frac{A_v}{\rho\mu}(1-\alpha)^{2/3}\, w''(T) \tag{8-5}$$

The time of hydride consumption is therefore given for an isothermal system by

$$\int_0^1 (1-\alpha)^{2/3}\, d\alpha = \int_0^{t^*} \frac{A_v\, w''}{\rho\mu}\, dt \tag{8-6}$$

$$t^* = \frac{3\rho\mu}{A_v\, w''} \tag{8-7}$$

At T = 75°C = 348 K and p = 12 kPa, $w'' = 1.42 \times 10^{-7}$ kgO_2/m^2 s, and using previous corrosion layer values yields $t^* = 4{,}066$ seconds, or somewhat greater than one hour.

Note that all the hydride in the layer is assumed to have access to oxygen. For a combination of thick enough layers and high enough temperatures, reactant depletion can occur in the layer. In this case, the diffusion equation can be used to estimate the reacting layer depth.

The hydride model is coupled with a finite-difference model for the underlying fuel substrate and the remainder of the fuel element. These models are contained in a MATHCAD file in Appendix G.

8.1.3 Transient Results

Results of complete transients for combined hydride layer and metal surface reactions appear in Figure 8-1. A hydride surface area enhancement factor and an underlying metal rate law multiplier are assigned to various cases as shown. A damage length of 10 cm and undamaged length of 56 cm are used. A view factor of 0.26 is selected for heat loss from the element because the inner portion of the perimeter gains heat from the inner element, and because part of the element views equal or higher temperature elements.

For hydride layer area enhancements considered here, hydride reactions do not lead to runaway, but merely decrease the time required to achieve a steady-state axial temperature difference. Note that a high enhancement factor can overshoot the steady-state, however.

Figure 8-1: Temperature Rise During Hydride Layer Reaction for Various Ambient Temperatures, Steam Partial Pressures, and Metal Rate Multipliers

Fig. 8-1Temperature Rise During Hydride Layer Reaction for Various Ambient Temperatures, Steam Partial Pressures, and Metal Rate Multipliers. F= x + y means the initial rate law multiplier F is the sum of a sustained term 'x' from internal hydride or any other reason, and a depleting term 'y' due to the surface hydride. Curves arranged top to bottom by peak value in order listed below figure.

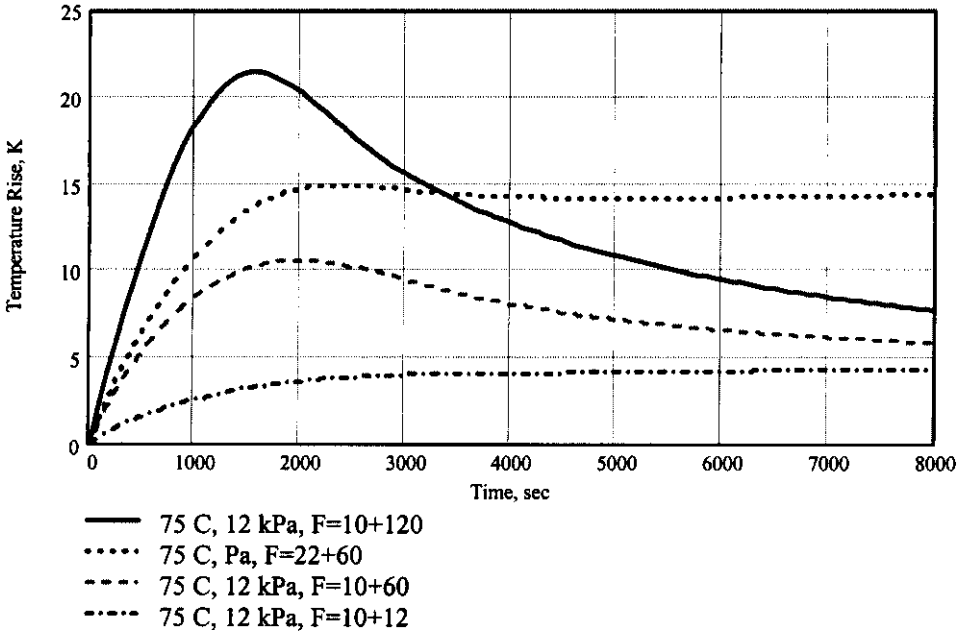

8.2 IWTS Metal-Water Reaction Rate Evaluation

The IWTS is designed to remove particulate and dissolved impurities from K Basins water to maintain water quality specifications during fuel removal operations. Primary components include three submersible pumps, a knock out pot, particulate settlers, deep bed filters, ion exchangers, and water distribution piping. IWTS settlers receive particulate not retained within the knock out pot, which is by definition below 0.5 millimeters in size. This particle size distinction clearly renders thermal stability of the settlers less likely than that of the knock out pot when all other factors are equal.

On the other hand, it is difficult to imagine mechanisms that create a large quantity of metallic particulate this small, and this size range is characteristic of oxidic canister sludge. Thus, best judgement is simply that the metal fraction of settler particulate will in practice be low, and certainly lower than that of the knock out pot. Two additional factors complicate analysis of thermal stability of particles in the settlers, and tend to skew the analysis toward overly conservative inputs and results: first, since IWTS settlers are not instrumented, an analysis of the settler must consider a relatively full settler; second, because of the large density difference between metallic and oxidic particles, metallic particles will preferentially settle in the upstream (entry) portion of the settler - a selective mechanism for concentration of metallic particulate in one portion of the settler.

8.2.1 Ignition Theory Analysis

A lumped parameter approach considers removal decay heat and oxidation power by conduction in a long cylinder (Plys and Malinovic 1999):

$$Q_{dk} + Q_{rx} = \frac{k}{L} A_s (T - T_w) \qquad (8\text{-}8)$$

where Q_{dk} is decay heat, Q_{rx} is oxidation power, V is settler debris volume, A_s is settler debris heat transfer area, T is centerline temperature, T_w is wall temperature, and L, effective length, is ½ the radius.

Given the above discussion, the stability figure-of-merit used above for the knock out pot, the Frank-Kamenetskii parameter, is modified to replace the term $f * L^2$ by $½ R^2$. This means that no credit is taken for axial conduction away from a zone of metallic particulate, and in cross section the settler pipe containing this material is nearly full.

The average particle diameter at the inception of thermal stability in the settlers is shown in Figure 8-2 as a function of metal mass fraction for various bed thermal conductivities. Tolerable particle sizes are smaller for a given metal mass fraction in the settlers versus the knock out pot because of the larger settler diameter and the potential length of a settled region of metallic particles. Thus, thermal stability of the settlers relies either upon the fact that its feed solids will be mostly oxidic, or that particles can deplete during loading.

8.2.2 Settler Transient Particle Depletion Model

Particles accumulate in the settler over the course of fuel cleaning; a time scale of at least one year. As shown earlier, particles smaller than about 0.25 mm diameter should be completely reacted over this time scale. The heat transfer resistance is very small when particles begin to accumulate, and it increases to the limiting value used above in the steady-state evaluation when the settler is full. Thus, it is reasonable to consider a transient problem in which the settler is slowly filled with particles, which may slowly react and reject heat through a small but increasing heat transfer resistance.

The evolution of the particle size distribution is given by a simplified form of the traffic equation, where the corrosion velocity is constant for all particle sizes (Plys and Malinovic 1999):

$$\frac{\delta n(r,t)}{\delta t} = S(r) + U(t)\frac{\delta n(r,t)}{\delta r} \qquad (8\text{-}9a)$$

Figure 8-2: Settler Example Transient Calculation

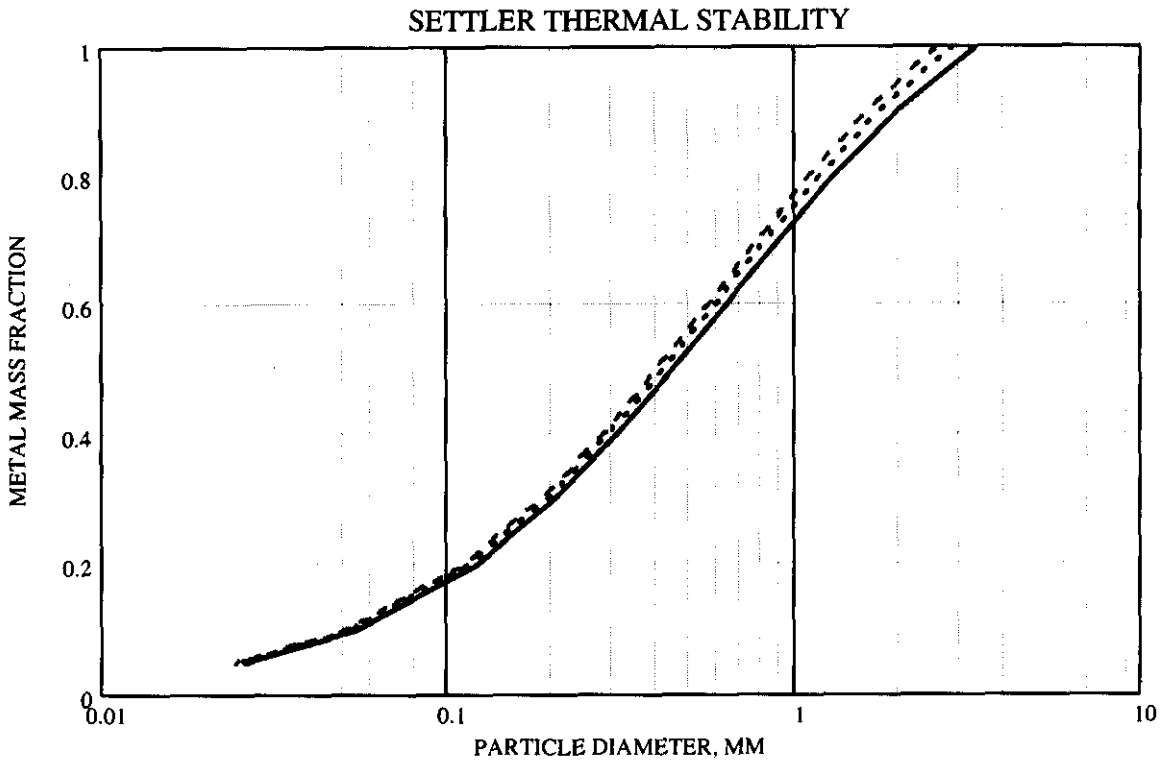

Relationship between particle diameter, mm, and metal mass fraction for incipient runaway in a nearly-filled 20" diameter settler: Unstable above curves, stable below curves. Effective thermal conductivity varied from 3 W/m/K (top) to 2 W/m/K (bottom); ε = 30%.

$$U = \frac{238}{32}\left(\rho_m^{-1}\right)\dot{m}''_{ox}(T) \qquad (8\text{-}9b)$$

where $n(r, t)$= Number of particles of size range within dr of r,
$S(r)$ = Source rate (constant with time), and
$U(t)$ = Corrosion velocity.

An effective numerical approach is to apply the sectional method and write a mass balance for "bins" of defined radius range. Properties associated with bins are:

N_i = Number of particles in bin i,
Δr_i = Size range of bin i,
S_i = Source rate to bin i,
r_i = $\sqrt{r_{\ell i}\, r_{hi}}$, = Average radius of bin i,
A_i = $4\pi r_i^2$, = Reactive surface area of a single particle,
V_i = $\frac{4}{3}\pi r_i^3$, = Volume of a particle in bin i, and
$r_{\ell i}$, r_{hi} = Low and high radii of bin i.

Particles in a bin react to produce oxide, decrease in size, and eventually move to the next lower radius bin. The metal source to a bin is given by

$$S_i = \rho_m\, \eta\, \dot{V}\, s_i \qquad (8\text{-}10)$$

where $\dot{V}$ = Volumetric rate of material addition, m^3/s,
s_i = Incoming particle distribution, number per unit bin volume, $\#/m^3$,
ρ_m = Metal density, kg/m^3, and
η = Metal volume fraction.

Hence the overall particle balance for bin i is:

$$\frac{dN_i}{dt} = S_i + U\left[\lambda_{i+1} N_{i+1} - \lambda_i N_i\right] \qquad (8\text{-}11)$$

where
$$\lambda_i \equiv -\frac{A_i}{V_i - V_{i-1}} \qquad (8\text{-}12)$$

A particle source rate may be defined which fills the settler over a given duration and accounts for expansion of metal as it oxidizes:

$$\dot{V} = \frac{A_x (1-\varepsilon)}{\tau}\left[1-\eta+\frac{\rho_m}{\rho_o}\eta\right]^{-1} \quad (8\text{-}13)$$

where A_x = Settler cross-sectional area, m^2, and
τ = Time to fill settler, seconds.

As noted above, the oxide volumetric addition rate is found by multiplying the feed rate by the oxide volume fraction, and the metal source rate (number of metal particles per bin per unit time) is found by multiplying the feed rate by the metal volume fraction and dividing by the volume of a single particle in a given bin. Source particle volume distributions are obtained by normalizing a truncated log-normal particle size distribution with the indicated sample mean and standard deviations. Note that a large value of the mean will cause large particles to be added, which take longer to deplete than small particles, while a small value of the mean will cause smaller particles to be added, which have larger initial reaction area than large particles but deplete more quickly.

A dynamic equation for temperature is not required because the thermal response time is on the order of hours, while the filling time is on the order of a year. Therefore, a steady-state version of the lumped parameter equation used for the knock out pot may be used here. The heat transfer resistance used for calculations considers an effective length for conduction, which is the smaller of: (a) half the height of the particles, or (b) one-third the diameter, in accord with the knock out pot resistance used earlier. Thus the resistance grows to a maximum value in this model more quickly than the settler is filled, and the temperature is conservatively high.

An approximation in the model described above is that all particles are at the same average or lumped temperature. In reality new particles are added to the top of the settled particle bed, and a more elaborate solution would require following the particle size distribution at various coordinates, but this only is meaningful if a temperature gradient is also used.

8.2.3 Settler Depletion Calculations

Transient results of settler filling and particle reaction were calculated for rate law multipliers of 3 or 10, various source distributions, a metal mass fraction of 50% to 100%, and a settler fill time of one year. Cases are summarized in Table 8-1. In all cases results are stable; a discontinuity in the temperature occurs when the heat transfer resistance attains a maximum. Note although the temperature increases with time, the values shown are steady and the final value is the maximum to be attained. An example transient calculation is shown in Figure 8-3, for Case 2 of Table 8-1.

Particle number distributions attain a steady distribution in a period of time predictable by dividing the mean radius by the corrosion velocity. Note that larger source particles lead to higher long-term reaction area and power because of their longer depletion time. Also, the rate law multiplier has little influence on results, because it changes the depletion time, so the product of area times multiplier remains relatively unchanged.

These calculations indicate that particle depletion during the long duration of settler filling provides thermal stability, because the reacting area is limited. This conclusion is even true for unusually large particles, 100% metal, and a rate law multiplier of 10.

Table 8-1: Transient Settler Particle Addition and Oxidation Results [1]. All Temperatures are Stable.

Case	Source Distribution Parameters [2] and Mean Radius [3]	Metal Mass Fraction μ and Rate Multiplier ξ	Maximum Reaction Area, A, (m^2), Final Temperature, T, (°C), and Peak Reaction Power, Q_r, (W)	Comments [4]
1	r = 20 μm μ_s = 50 μm σ_s = 50 μm	μ = 0.5 ξ = 3	A = 105 m^2 T = 20°C Q_r = 27 W	Smallest particle sizes, steady-state ≈ 0.12 year.
2	r = 43 μm μ_s = 100 μm σ_s = 100 μm	μ = 0.5 ξ = 3	A = 100 m^2 T = 20°C Q_r = 26 W	Intermediate particle sizes, steady-state ≈ 0.25 year.
3	r = 142 μm μ_s = 300 μm σ_s = 200 μm	μ = 1.0 ξ = 3	A = 180 m^2 T = 20°C Q_r = 58 W	Large Particles, steady-state ≈ 0.75 year.
4	r = 142 μm μ_s = 300 μm σ_s = 200 μm	μ = 1.0 ξ = 10	A = 62 m^2 T = 22°C Q_r = 53 W	Steady-state ≈ 0.25 year Higher ξ causes faster depletion, but same steady reaction rate
5	r = 185 μm μ_s = 400 μm σ_s = 200 μm	μ = 1.0 ξ = 3	A = 180 m^2 T = 22°C Q_r = 59 W	Unrealistically large particles, steady-state ≈ 0.8 year.

(1) Time to fill settler = 1 year in all cases.
(2) Truncated log-normal with r_{max} = 250 μm.
(3) Geometric mean to yield A/V = 3/r for source.
(4) Steady-state time = time to deplete particles at mean radius.

Figure 8-3: Example Settler Transient Calculation: Temperature and Reactive Surface Area History (top), Particle Size Distribution History (bottom)

Temperature and reactive area: Discontinuity in T when height = 2/3 diameter

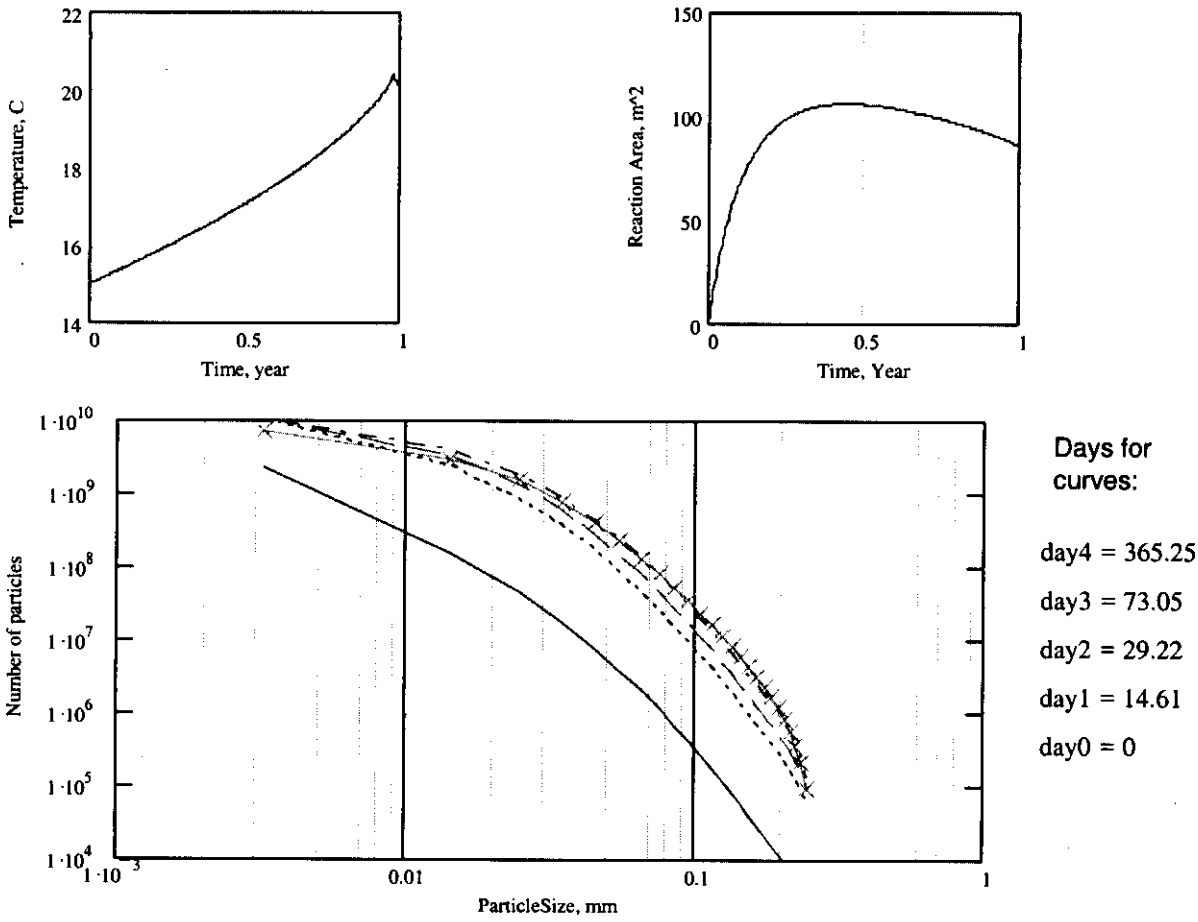

Particle size distributions for increasing times from lower (solid) to upper (crosses) curves

8.3 The HANSF Code

The HANSF code is an integrated model considering MCO phenomena such as fuel oxidation, convective and radiative heat transfer, and the potential for fission product release (Plys, et al. 1999). HANSF accounts for generic phenomena such as gas and aerosol transport between regions (between the MCO and, say, an operating area), aerosol agglomeration and deposition, and heat transfer to structures, including evaporation/condensation. It has been used for all phases of spent fuel disposition, including CVD, transportation, staging, and storage (Plys, et al. 1998). Discussion here is limited to a brief introduction of HANSF capabilities, description of MCO, fuel, and scrap nodalization, and the results of two sample cases for normal CVD.

8.3.1 Code Description

Integral accident assessment combines models for reaction kinetics (uranium oxidation) with models for temperature distributions in the fuel and other heat sinks, fission product release, and vapor and aerosol transport/deposition. Fuel or scrap basket ignition would drive releases by increasing MCO pressure beyond the set point for the MCO rupture disk. The subsequent blowdown would entrain freshly oxidized uranium oxide and release radionuclides to operating areas and/or the site, depending on the accident scenario.

Integral assessment with HANSF addresses the limitations of stationary ignition theory noted in Section 3.2, namely the inability to consider the presence of conduction within the reacting material, reactant/fuel diffusion limitations, complex geometry, and the effect of reactant depletion. HANSF considers factors such as differences between fuel baskets (free water content and reactive areas), non-uniform distributions for water content, damage (reactive area) hydriding, air ingression scenarios, and loss of MCO cooling. Despite the addition of these complexities, ignition is still determined by a balance between oxidation power and decay heat to a lesser extent, and heat losses via conduction and radiation to MCO walls, lid, and bottom. For conditions that lead to ignition, HANSF analysis provides the time to ignition and defines the interval for mitigating actions.

HANSF is comprised of generic phenomenological routines that handle familiar thermo-dynamic and heat transfer functions not unique to MCO application, and MCO-specific routines. HANSF generic phenomenological capabilities include:

- Multiple-compartment representation,
- Pressure driven and counter-current gas flows,
- Gas and aerosol transport between compartments,
- Vapor-aerosol equilibrium,
- Aerosol deposition due to gravitational sedimentation, impaction, etc., and
- Heat transfer to structures.

MCO phenomena provide rates-of-change for the generic routines. For example, MCO routines for oxidation provide sources to heat sinks (fuel elements), which are used by generic routines to calculate temperature profiles. Routines for phenomena unique to MCO applications are as listed below:

- Oxidation of fuel,
- Hydriding\dehydriding,
- Uranium oxide hydrate decomposition,
- Heat transfer in the fuel basket,
- Heat transfer in the scrap basket,
- Evaporation and condensation,
- Radiolysis, and
- Nitriding.

Details are contained in (Plys, et al. 1999) and only highlights are presented here. In most HANSF applications for ignition conditions and timing, hydrate decomposition, radiolysis, and nitriding have proved to be second-order effects. The remaining items are the major components of the balance between oxidation power and decay heat, and heat removal to the MCO walls, lid, and bottom.

8.3.2 Nodalization and Assumptions

An MCO interior may be modeled as consisting of anywhere from one to five tiers, where a tier is a fuel basket or scrap basket or represents more than one basket in a single "lumped" basket. For example, in Figure 8-4, the MCO interior can be modeled as five gas spaces, one for the scrap basket and one for each fuel basket. In this manner, HANSF can consider variations between fuel and scrap baskets, or variations between fuel baskets. These gas volumes communicate via flow areas set by the user through generic junction inputs. Forced flows into or out of MCO gas volumes can be imposed, so as to model vacuum drying and helium purge.

In the base model, fuel basket, MCO wall, and cask wall are nodalized radially as illustrated in Figure 8-5. Thermal analysis can efficiently take advantage of symmetry, such that the fuel may be represented by 14 heat sinks in a 30° sector of the MCO. Thus, seven pairs of heat sinks are used to represent the portions of seven fuel assemblies located in that sector. Within the 30° MCO sector, heat transfer from fuel assembly to fuel assembly, and from the fuel assemblies to the MCO wall, is found by solution of conduction and thermal radiation networks. A scrap basket is modeled in a pseudo-one-dimensional manner illustrated in Figure 8-6, by modeling two-dimensional heat transfer as a combination of azimuthal and radial flows. The exact solution for the two-dimensional scrap temperature distribution may be well-represented by identifying the dominant heat flow paths as either azimuthal or radial.

8.3.3 HANSF Results

HANSF results for two CVD simulations are discussed here to show code capabilities and the importance of reactant depletion. The two cases discussed here consider the normal CVD process, with indefinite vacuum drying and helium purge. MCO nodalization is as discussed in the previous section and nominal parameters for CVD runs are shown in Table 8-2. Results presented here use the basic input values with sensitivity reaction rate law multipliers of 22 (Case VC1A22) and 50 (Case VC1AR50). Many other normal and off-normal CVD cases have been considered in (Plys, et al. 1998), for example, and the case identifiers VC1A22 and VC1AR50 come from this reference.

Figure 8-4: MCO Control Volumes and Flowpaths

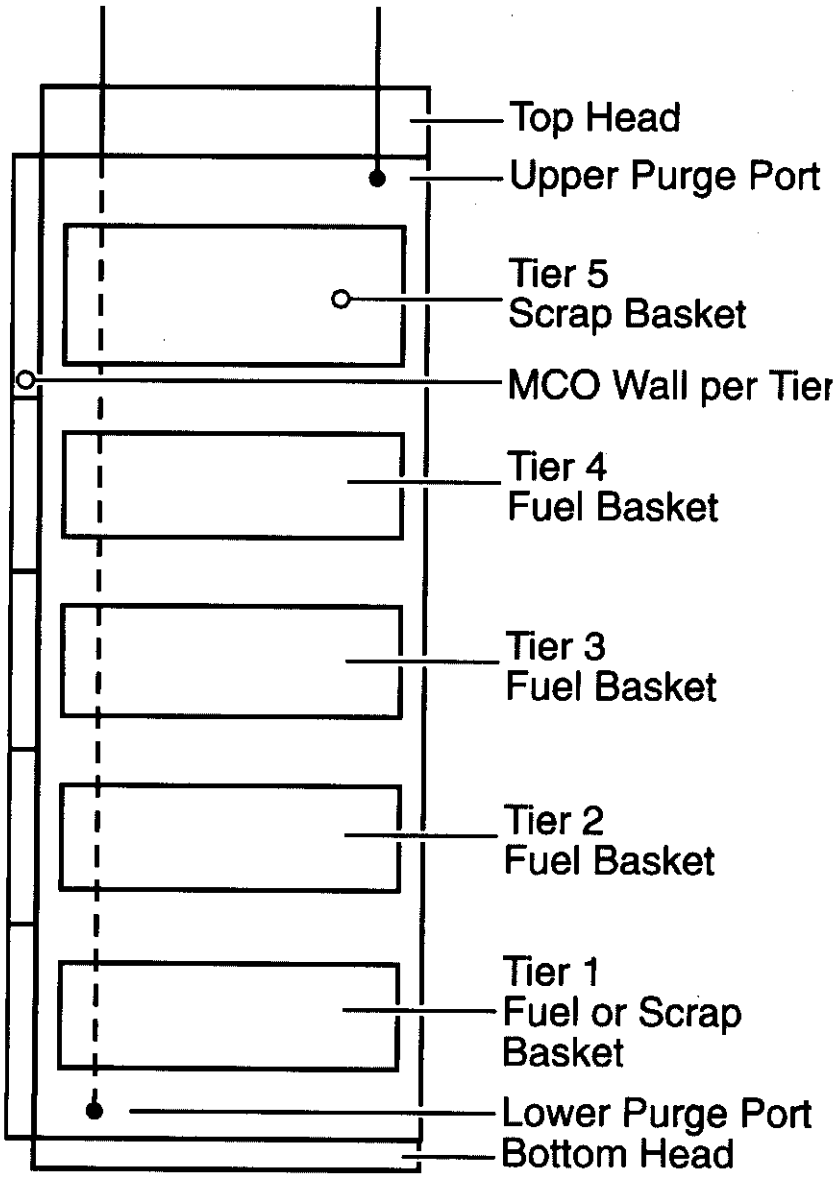

Figure 8-5: Pin-by-Pin Nodalization Scheme

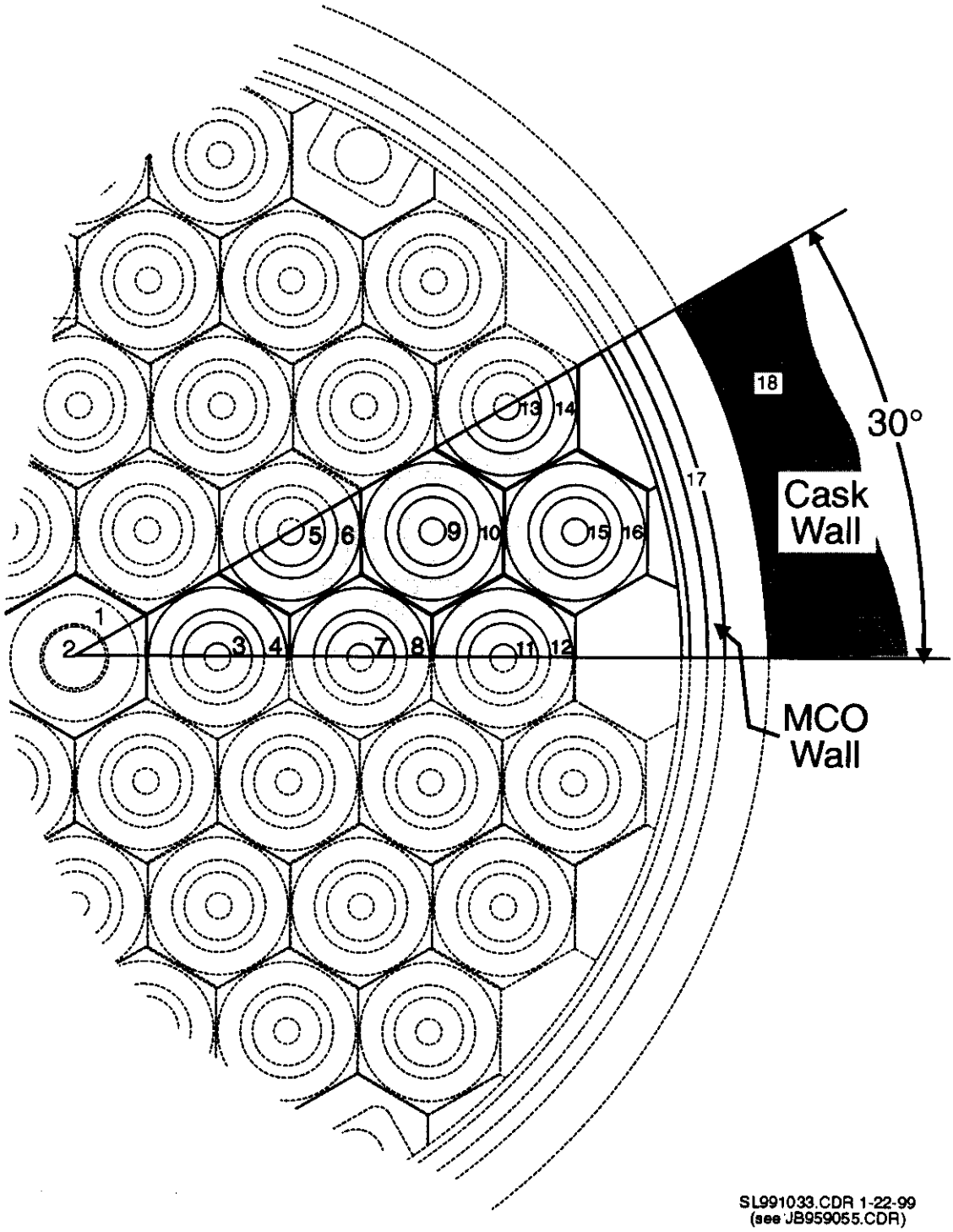

Figure 8-6: Sample Scrap Basket Nodalization

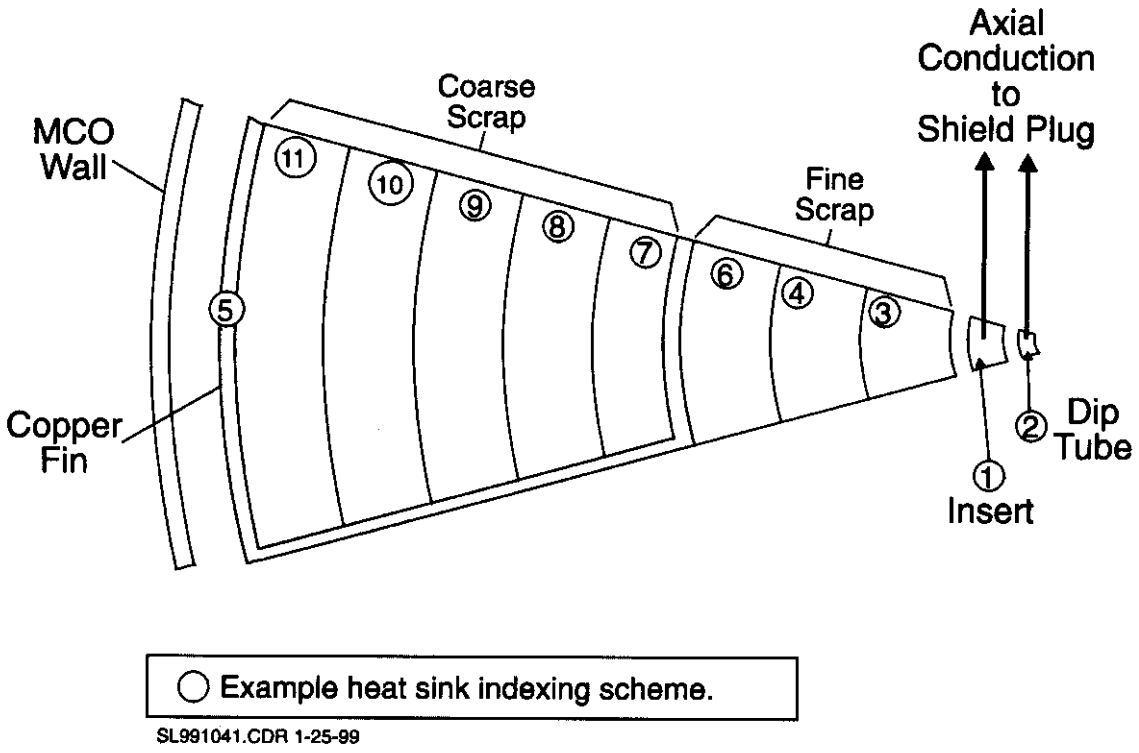

Table 8-2: Basic Simulation Input Values.	
Decay Power	776 W/MCO bounding
Scrap Mass	980 kg
Fuel Mass (per basket)	1357 kg
Scrap Reaction Area	4.5 m^2 bounding
	1.7 m^2 nominal
Fuel Reaction Area (all)	3.5 m^2 bounding
	0.2 m^2 nominal
Reaction Rate Law	Pearce x 10 baseline
	Pearce x 22 (sensitivity)
	Pearce x 50 (sensitivity)
Hydride Rate Contribution	Pearce x 12 nominal
Scrap Water Inventory (CVD)	1.5 kg
Fuel Water Inventory (CVD)	6 kg/basket bound
	0.1 kg/basket nominal
Scrap Hydrate Water	0.41 kg bounding
	0.055 kg/m^2 reactive area nominal
Fuel Hydrate Water	0.40 kg bounding
	0.0055 kg/m^2 reactive area nominal
MCO Free Volume	0.5 m^3
Fuel Emissivity	0.7
MCO Emissivity	0.25
Pump Flow Rate (CVD)	35 cfm
Helium Injection (CVD)	1.6 cfm
CVD Ambient, Pre-Shipping	41°C upset conditions
Start of Shipping	Noon
CSB Service Ambient	41°C upset conditions

Figure 8-7 shows some of the more important results for Case VC1A22, which is considered first. Complete sets of plots for the two cases are presented in Appendices H (Case VC1A22) and I (Case VC1AR50). Plots show gas concentrations, scrap and fuel temperatures, mass of steam and hydrogen purged, and MCO pressure.

Due to evaporation, scrap and fuel temperature decline from an initial temperature of 50°C, but temperatures increase upon local dryout. For the scrap basket, local dryout occurs after about three hours, and for the top fuel basket, which has the nominal inventory of 0.1 kg, dryout occurs almost immediately. A complicated pattern of decreases and increases in temperature is observed for fuel in the remaining baskets, due to the interplay between local and evaporative cooling and radiative and convective heating from the MCO wall inward toward the central fuel elements. The MCO pressure decreases to 12 kPa, which corresponds to saturation at 50°C, and decreases further as evaporation cools the water-bearing surfaces.

Hydrogen is produced by reaction of water vapor with fuel, and about 50 grams are produced by the time of dryout and a bit more is produced in the long run. Note that scrap temperatures reach a maximum during the oxidation period, as expected. At equilibrium, there is little temperature difference across the scrap basket, but there is a temperature difference of about 20°C across the dry fuel basket. Oxidation lasts for about 11 hours, as evidenced by plots for helium and steam concentrations that show steam depletion and complete inerting at just under 11 hours. In summary, for Case VC1A22, peak scrap temperature is 65°C, peak fuel temperature is 83°C, and 50 grams of hydrogen are produced at dryout.

Case VC1AR50 is just a variation of Case VC1A22, with rate law multiplier increased from 22 to 50. Important results are shown in Figure 8-8. The overall progression is similar to that for Case VC1A22, although scrap temperatures and fuel peak temperatures are slightly higher. For Case VC1AR50, peak scrap temperature is 70°C, peak fuel temperature is 88°C, and 70 grams of hydrogen are produced at dryout.

Figure 8-7: Selected Results for Case VC1A22
Gas concentration, scrap basket temperatures, fuel basket temperatures, and total gas mass purged.

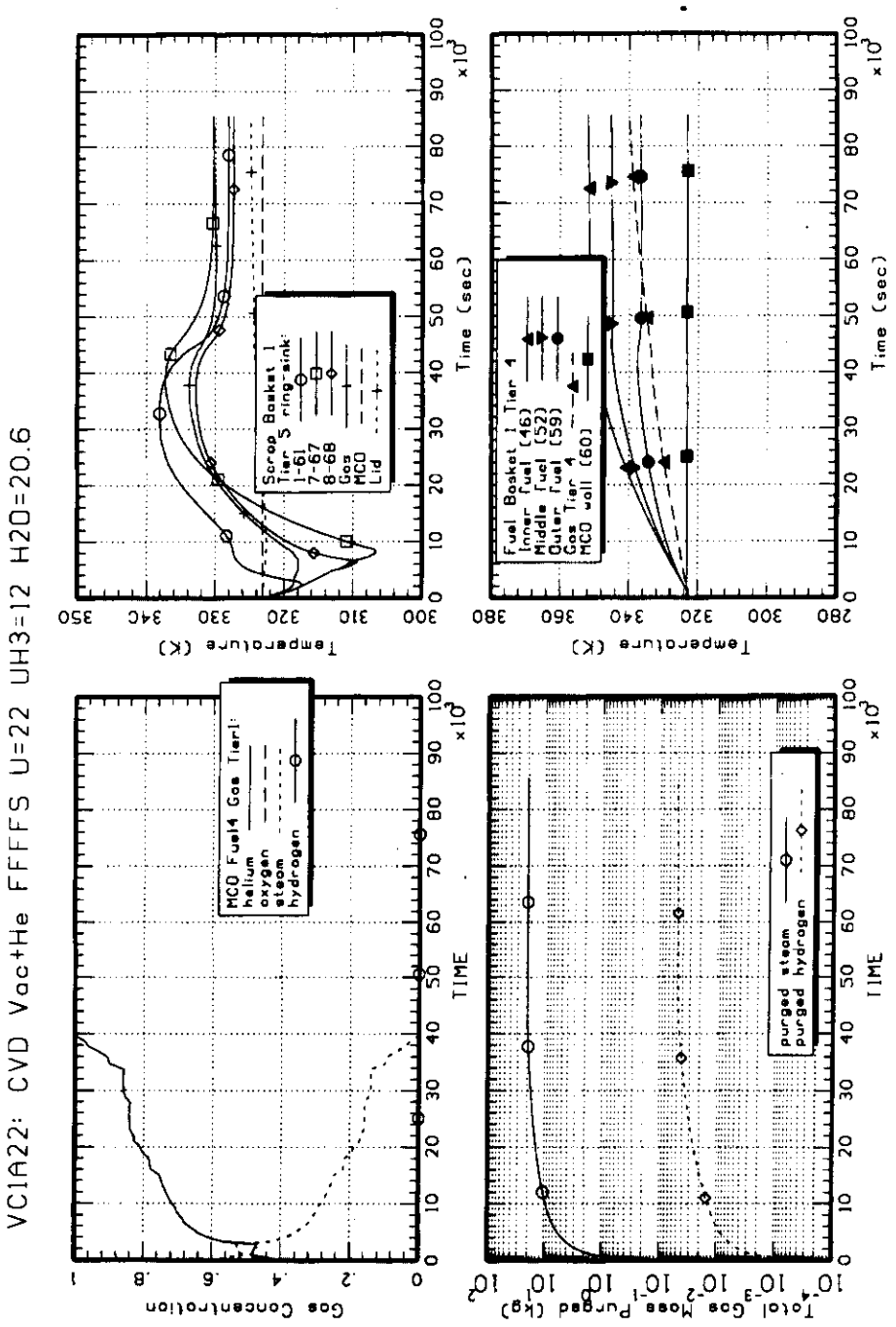

Figure 8-8: Selected Results for Case VC1A50R
Gas concentration, scrap basket temperatures, fuel basket temperatures, and total gas mass purged.

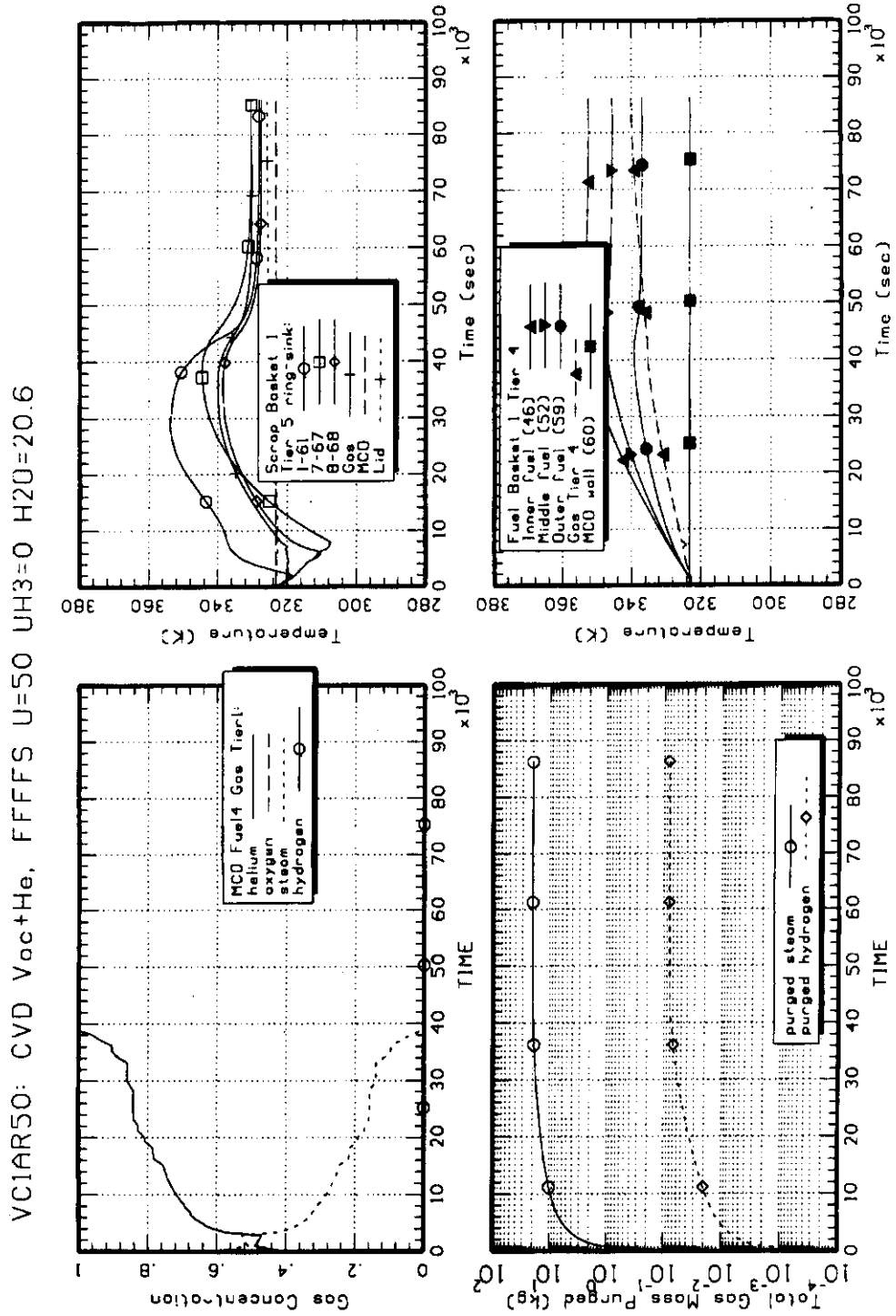

In conclusion, neither case results in a thermal excursion despite rate law multipliers far larger than the baseline value, peak temperatures are relatively benign, and normal CVD shows wide margin to thermal excursion. The oxidation period is limited by vacuum helium purge and steam depletion, and scrap temperatures decline after oxidation ends.

9.0 SUMMARY

The phenomenon of pyrophoricity has been studied for chemical process safety and its mathematical formulation, ignition theory, is well established in the literature. An introduction to runaway and modeling of ignition is provided here in Sections 2.0 and 3.0.

We have applied ignition theory to experiments conducted with uranium powders and foils using recently available kinetic rate laws, and found that results can be explained and understood, where before these results were not quantified and were on occasion misinterpreted (Epstein, et al. 1996). Also, documented experience suggests that the rate law for metal oxidation in air is applicable to uranium hydride. Experimental validation is discussed in Section 4.0, and this sets the stage for interpretation of historical observations of pyrophoricity incidents summarized in Section 5.0.

Examples of applications to SNF process safety are given in Sections 6.0, 7.0, and 8.0, in increasing order of complexity. It is usually desirable that a process be designed to be inherently safe against the possibility of a pyrophoric event, which means that in the steady-state heat produced from decay power and chemical reactions is all removed by conduction and convection to the surroundings. Therefore, a steady-state thermal stability analysis resulting in an ignition criterion is typically applied for safety evaluation, and examples are given in Section 6.0. Usually there is uncertainty in parameters used for the steady-state evaluation; for example, there is scatter in kinetic rate law data, and there is uncertainty inherent in estimating the thermal transport properties of heterogeneous media. Sensitivity or uncertainty analyses are easy to perform with the steady-state ignition criterion, as shown in probabilistic evaluation examples of Section 7.0.

Following the philosophy described here, transient analyses are typically not necessary for normal process safety assessment, but they are useful for analysis of off-normal conditions. Exceptional cases are described in Section 8.0, where examples are given that benefit from considering transients, and examples of process simulation are provided.

A key lesson learned is that the relatively simple ignition criterion obtained from constant reaction rate theory is both appropriate for safety analysis and easy to use. This technique is sufficiently accurate for safety analysis and is somewhat conservative, as demonstrated in Sections 3.0 and 4.0. This technique is appropriate for safety analysis because, as described above, steady-state thermal stability is highly desirable, as is the ability to conduct uncertainty analysis. Therefore, this report ends with a summary of the recommended method, and includes sufficient information to analyze common situations without resort to complex solutions.

9.1 Recommended Method

The recommended ignition criterion is:

$$B = \frac{A_v \, f \, L^2 \, \xi k_o \, \Delta H \, T_r}{2 \, k_{eff} \, T_{lin} \exp\left(T_r - 1\right)}$$

$$\begin{aligned} B &> 1 \quad \text{Ignition} \\ B &= 1 \quad \text{Incipient Ignition, Stability Criterion} \\ B &< 1 \quad \text{No Ignition} \end{aligned} \tag{9-1}$$

and parameters used in the criterion are evaluated as follows.

A_v is the reaction area per unit volume in the reactive medium of characteristic size L. A common situation is for a porous particle bed, in which A_v is related to an average reacting particle size:

$$A_v = \frac{6\,(1-\phi)}{d} \tag{9-2}$$

where ϕ is the porosity. Note that if particles are not all metal, the formula above should be multiplied by metal volume fraction.

The geometric form factor f = 1 for one-dimensional planar geometry, in which case L is the conduction distance through the reactive medium. For example, in a reacting slab convecting on both sides, L is the half-thickness. The value f = 1/2 applies to one-dimensional cylindrical geometry, in which case L = R, the radius of the reacting medium. For two-dimensional cylindrical geometry, form factors are given in Section 9.2 below. Note that these characteristic lengths are for the reacting medium and not any external packaging, which is considered later.

An Arrhenius rate law is assumed in the ignition criterion. Consistently defined rate law parameters are:

$$w''\left[\text{kg } O_2 \,/\, m^2 \,/\, s\right] = \xi \, k_o \exp\left(\frac{-T_E}{T}\right) \tag{9-3}$$

where ξ is a reaction rate law multiplier to consider uncertainty, k_o is the Arrhenius law pre-exponential factor which provides the units of the result, and T_E is the normalized activation in Kelvin (activation energy divided by ideal gas constant). The enthalpy of reaction ΔH is in units of J/kgO_2.

A reduced temperature is related to the Arrhenius parameters and the linearization temperature:

$$T_r = \frac{T_E}{T_{lin}}$$
$$T_{lin} = T_\infty + \frac{Q_v f L^2}{2 k_{eff}} \quad (9\text{-}4)$$

The linearization temperature is simply the ambient temperature for heat loss T_∞ in the absence of decay power. When there is decay power (or some other volumetric power source in the medium besides the reaction described by the kinetic law), the linearization temperature represents the maximum temperature in the absence of reactions.

The effective thermal conductivity k_{eff} includes resistance internal to the reacting medium, k_m, and external heat transfer resistance quantified by h_{eff}, the effective overall heat transfer coefficient, W/m^2-K,

$$k_{eff} = k_m \left(1 + \frac{2 k_m}{h_{eff} L} \right)^{-1} \quad (9\text{-}5)$$

For an isothermal case, $k_{eff} = k_m$. The effective conductivity is derived as extension to the isothermal boundary case by simply requiring continuity of heat flux. If there is an external heat source to the reacting boundary, such as solar radiation, the average value can be added and a new expression derived. Thermal radiation external to the reacting surface should be considered to augment pure conduction when the external heat transfer coefficient is evaluated.

For cases in which application of the formula above is not clear, an equivalent formula may be derived using the techniques presented in preceding sections. Essential steps are:

1. Write the heat conduction equation and obtain a solution for the maximum temperature minus a known temperature; see for example Equation (4-16) or (5-10).

2. Apply the Frank-Kamenetskii approximation,

$$e^{-T_E/T_m} \simeq e^{-T_r} e^{T_r \theta} \quad (9\text{-}6)$$

$$e\,\theta = \frac{(T_m - T_{lin})}{T_{lin}} \quad (9\text{-}7)$$

3. Rearrange the equation so that terms containing the maximum temperature are all on one side, and constant terms are all on the other, in the form:

$$T_r \theta e^{-T_r \theta + 1} = B \qquad (9\text{-}8)$$

When the ignition parameter B is defined in this manner, the left-hand side attains a maximum at B = 1, which is the ignition criterion.

A more brute force approach may be used when simultaneous relations allow the most convenient solution for the maximum temperature. This was followed for example in Section 6.3.1, where the temperature profile across a rod array was conjoined with exact expressions for boundary heat losses. In this case, a simple algorithm is used to numerically find the maximum physically possible value of the maximum medium temperature. The ambient temperature is incrementally increased, and other temperatures are found in succession. Both the resulting maximum temperature and the ambient heat losses pass through a maximum at the ignition condition, as shown in Figures 3-2 and 4-1.

Appendix A contains a summary of kinetic rate laws for low-temperature uranium reactions in various atmospheres. "Low temperature" means generally below 100 to 200°C, a range of interest for practical problems in material handling and processing.

9.2 Examples of Recommended Method

9.2.1 Uranium Hydride Ignition

An example for application of the method is to understand observations of uranium hydride powder ignition by (Hartman, et al. 1951). Such an evaluation was presented in our earlier work (Epstein, et al. 1996) using the exact constant rate solution without the Frank-Kamenetskii approximation, but with a model equation neglecting internal heat transfer resistance, and using the full McGillivray correlation, which cannot be simplified as described above. Here we employ Equation (9-1) above directly using the following parameter values:

Bed thermal conductivity k = 0.4 W/m/K typical of uranium metal beds,
h = 5 $W/m^2/K$ typical of natural convection plus thermal radiation for the temperature range of interest,
ϕ = 0.4 porosity typical of a random bed,
$\Delta H = 3.4 \times 10^7$ J/kgO_2 for U oxidation with O_2, and
d = 1.85 micron particle size per Hartman's distribution.

These conductivity and porosity values are recommended for most analyses of powders, filings, or turnings. Particle size depends upon the material in question.

Predicted results are shown in Figure 9-1 for dry air (label McGillivray Dry), humid air using three times McGillivray (McGillivray Humid) which is typical of 40 - 60°C range (see Figure A-6), and humid air using Ritchie's correlation, which is also independent of RH. Note,

the higher activation energy used by Ritchie leads to its result spanning results obtained using McGillivray. Due to the difference in activation energies between correlations, and the simplicity in using a constant rate law multiplier to interpolate between dry and saturated conditions, this approach is recommended for common use. Note that general uncertainty based on scatter in rate law data also justifies this simplified approach.

The result shown here is very close to our earlier comparison (see Figure 4-3). The calculation file that produced Figure 9-1 is reproduced in Appendix J.

9.2.2 2-D Cylindrical Geometry: Ignition of Uranium Scrap in Drum Storage

Here the method for two-dimensional cylindrical geometry derived in Section 5.3 is simplified for ease of use in common situations. The solution given by Equations (5-4) through (5-12) is numerically quite complicated. For example, the axial location of the maximum temperature z_m must be found by setting the derivative of Equation (5-4), $(df/dz_m) = 0$ in order to use Equation (5-12), and in order to solve either equation the infinite series must be evaluated. This is a valuable equation, however, because it provides the solution for independent values of the heat transfer coefficient on the bottom, side, and top of a cylindrical scrap container. By setting the heat transfer coefficient to either very small or very large values, limiting adiabatic or isothermal boundary conditions are emulated on any surface.

Figure 9-1: Ambient Temperature, °C, as Function of Powder Depth, mm, for Ignition of Small Deposits of Fine Uranium Metal or Hydride for Various Kinetic Rate Laws, particle diameter 1.85 micron

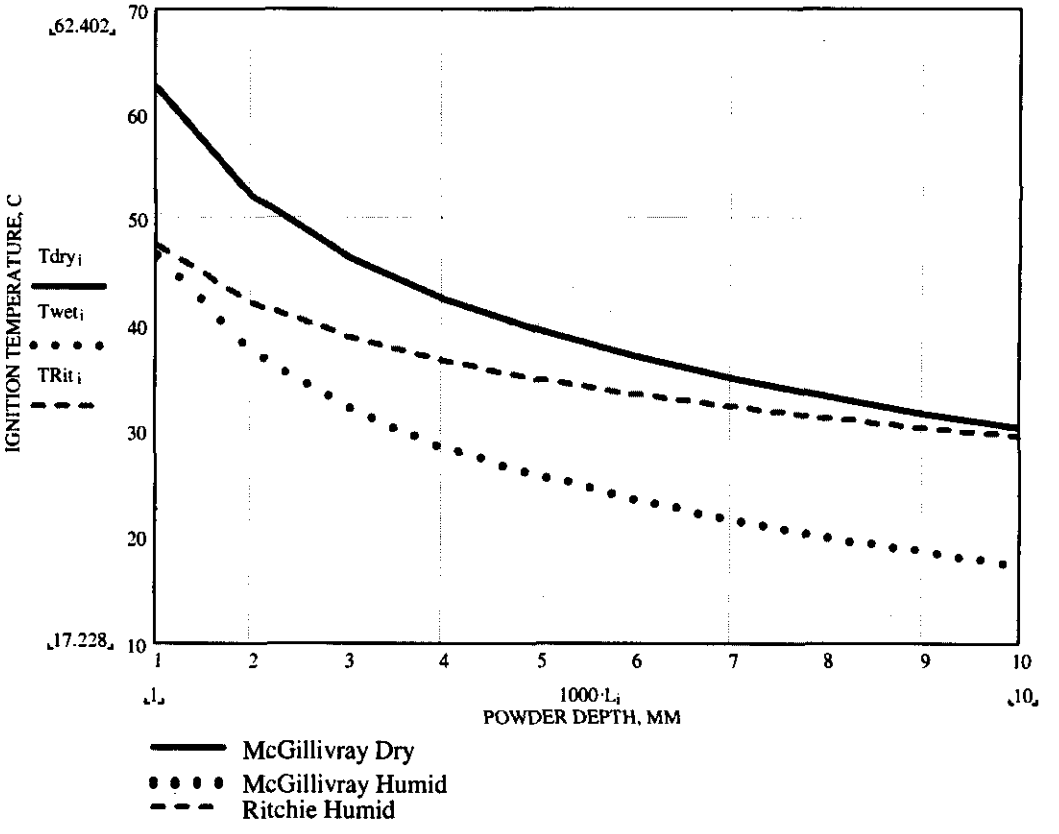

Figure 9-2: Values of Geometric Form Factor "f" of Equation (9-1) for Various Canister Radii R and Aspect Ratios R/L, Isolated Scrap Drums

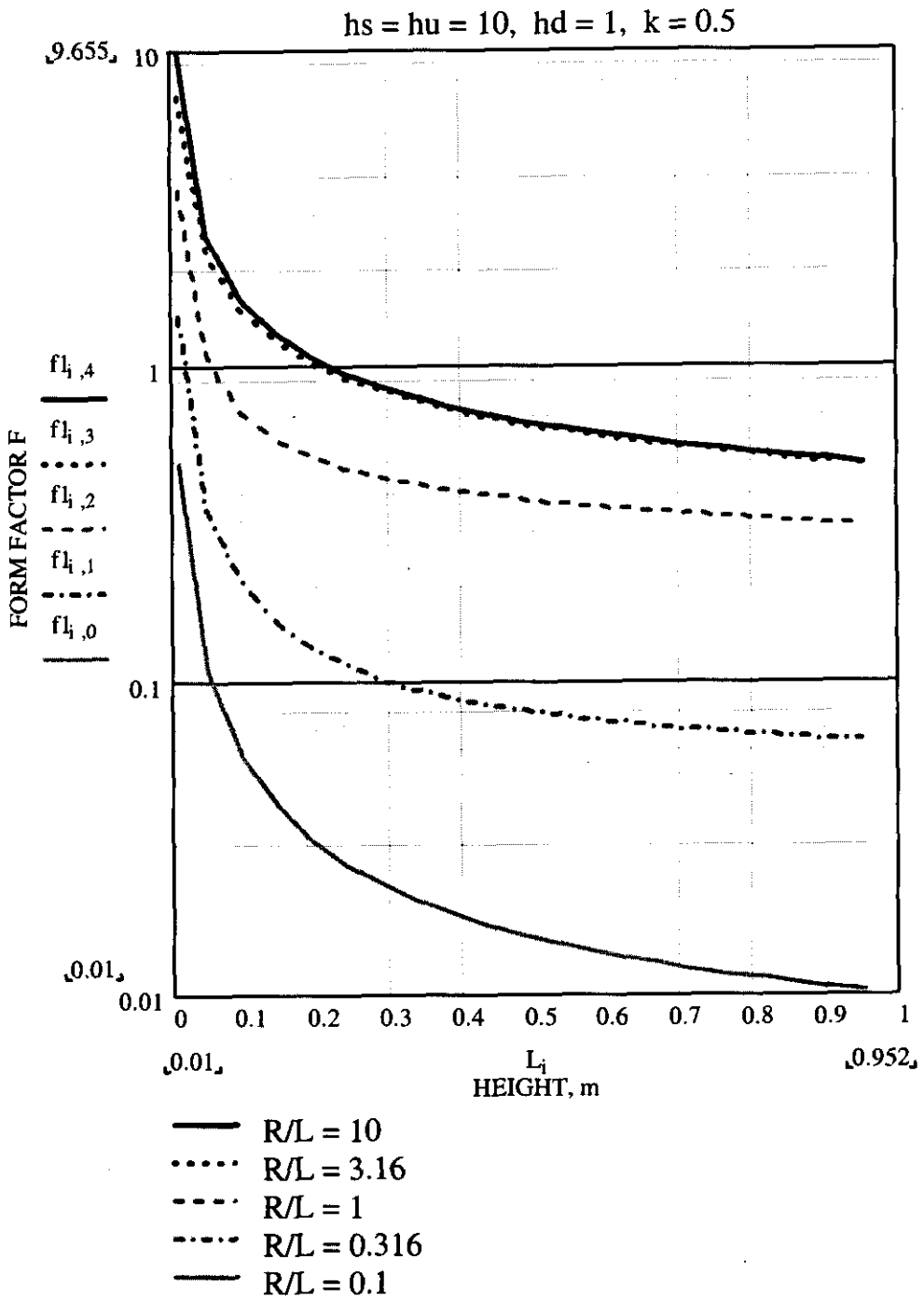

Figure 9-3: Values of Geometric Form Factor "f" of Equation (9-1) for Various Canister Radii R and Aspect Ratios R/L, Side-by-Side Scrap Drums

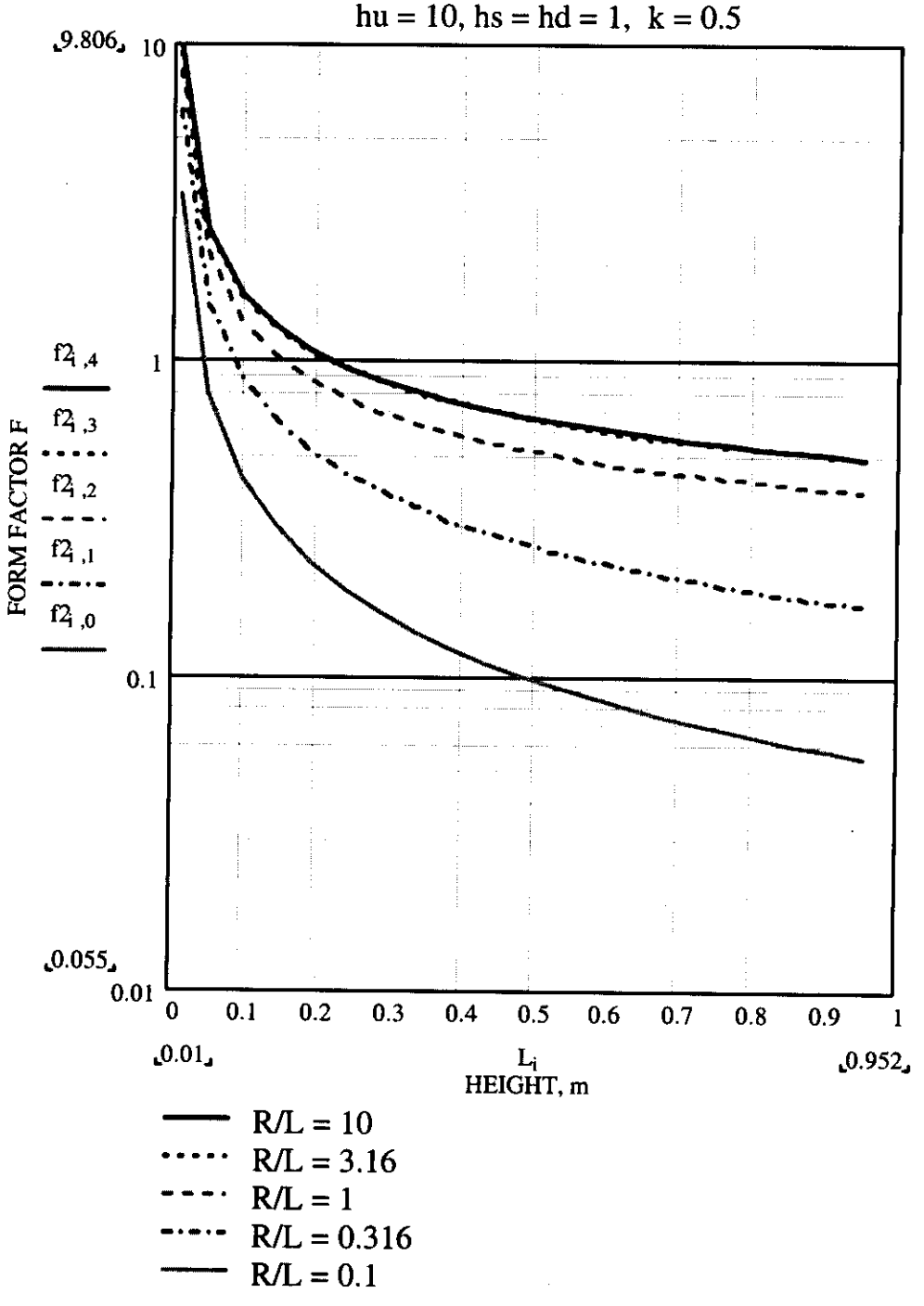

As described in Section 5-3, the ignition parameter in Equation (9-1) can be used if the cylinder height is identified as L, and the form factor is evaluated. Values of the form factor pertinent to typical drum storage in air are shown in Figures 9-2 and 9-3 for cases of an isolated drum and side-by-side drums, respectively. In each case, the upward heat transfer coefficient is 10 $W/m^2/K$ and the downward heat transfer coefficient is 1 $W/m^2/K$ (nearly insulated, small downward conduction loss). An isolated drum has free convection on its side, hence h = 10, while side-by-side drums radiate to one another and have lower natural convection, hence h = 1 is used to distinguish these cases. Values of the form factor are given in each figure for decreasing values of R/L, and note that for R/L greater than about 3, the value is nearly independent of the ratio because conduction is nearly all axial. Note the range of R/L is varied from flat pancake through a tall cylinder.

In Figure 9-4, a form factor chart is given for underwater application. For this chart, convection to water occurs on the drum sides and top, and the bottom is essentially insulated. Thermal conductivity of material in the drum is consistent with that of a debris bed of particles and water. A heat transfer coefficient of 300 $W/m^2/K$ is used for underwater convection.

For a 50 gallon drum, appropriate values are R = 0.29 m and L = 0.89 m. From Figures 9-2 and 9-3, the form factor for an isolated drum is f = 0.065 and that for side-by-side drums is 0.17. A scrap porosity of $\phi = 0.4$ and thermal conductivity of 0.5 W/m/K (consistent with the form factor figure) are used with the McGillivray dry kinetics multiplied by a factor $\xi = 3$ to account for typical humidity. This is all the information required to use Equation (9-1) to calculate the relationship between effective scrap particle size and ambient ignition temperature, shown in Figure 9-5. These results are nearly the same as those of Figure 5-1, but are obtained expeditiously through the form factors and the simple ignition criterion. Note the side-by-side drum ignition temperature in Figure 5-1 is about 10 degrees lower than that of Figure 5-9. This is because the form factor used for Figure 9-5 is about a factor of 3 lower than is obtained when the sideward and downward boundaries are truly adiabatic. The calculation file used for this example is given in Appendix J.

Figure 9-4: Values of Geometric Form Factors "f" of Equation (9-1) for Various Canister Radii R and Aspect Ratios R/L, Under Water Storage Convecting Sideward and Upward, Insulated Bottom

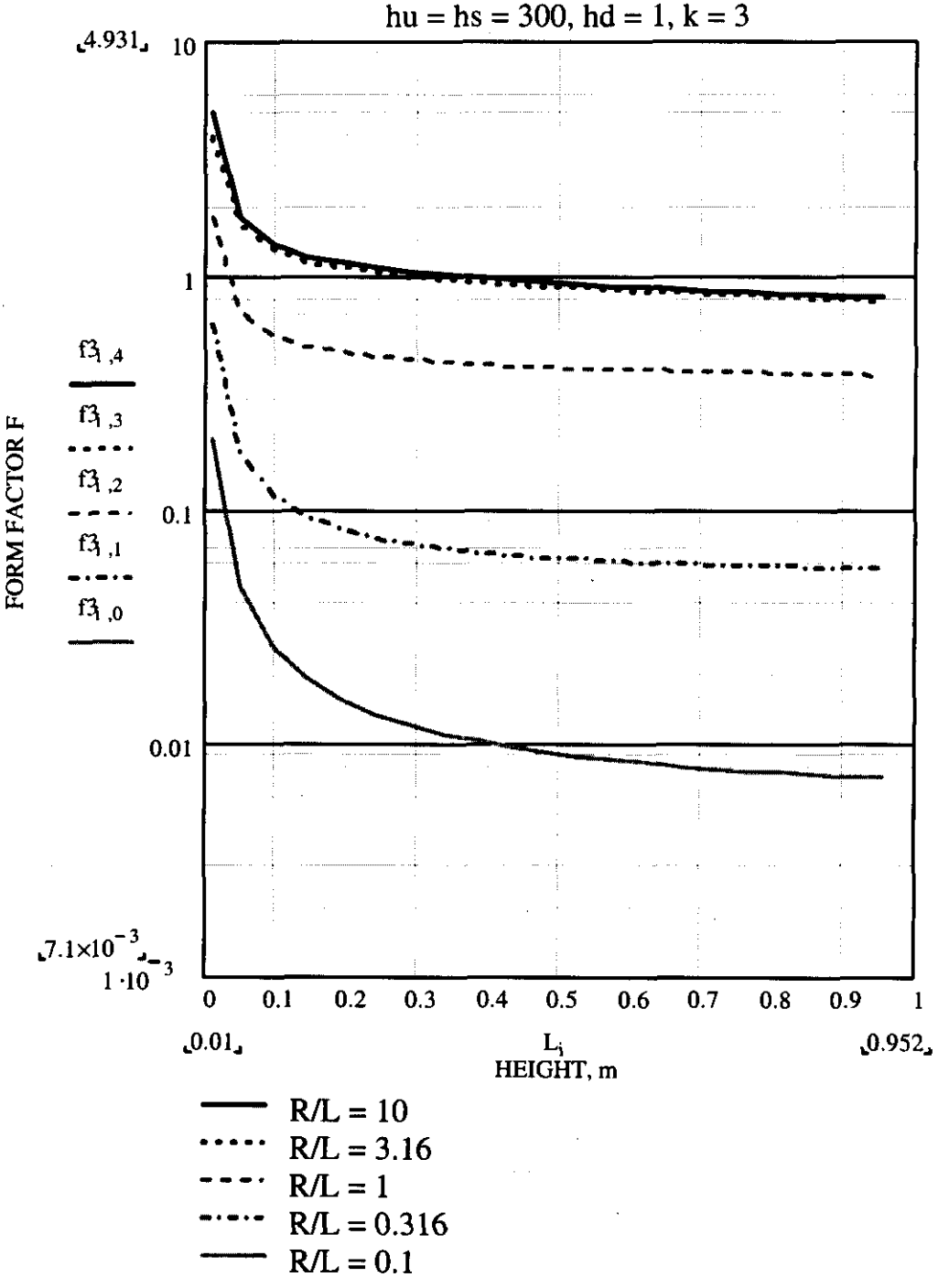

Figure 9-5: Ambient Temperature for Ignition of Isolated (solid) and Side-by-Side (dash) 50 Gallon Drums with Uranium Metal Scrap for Various Average Scrap Sizes, mm

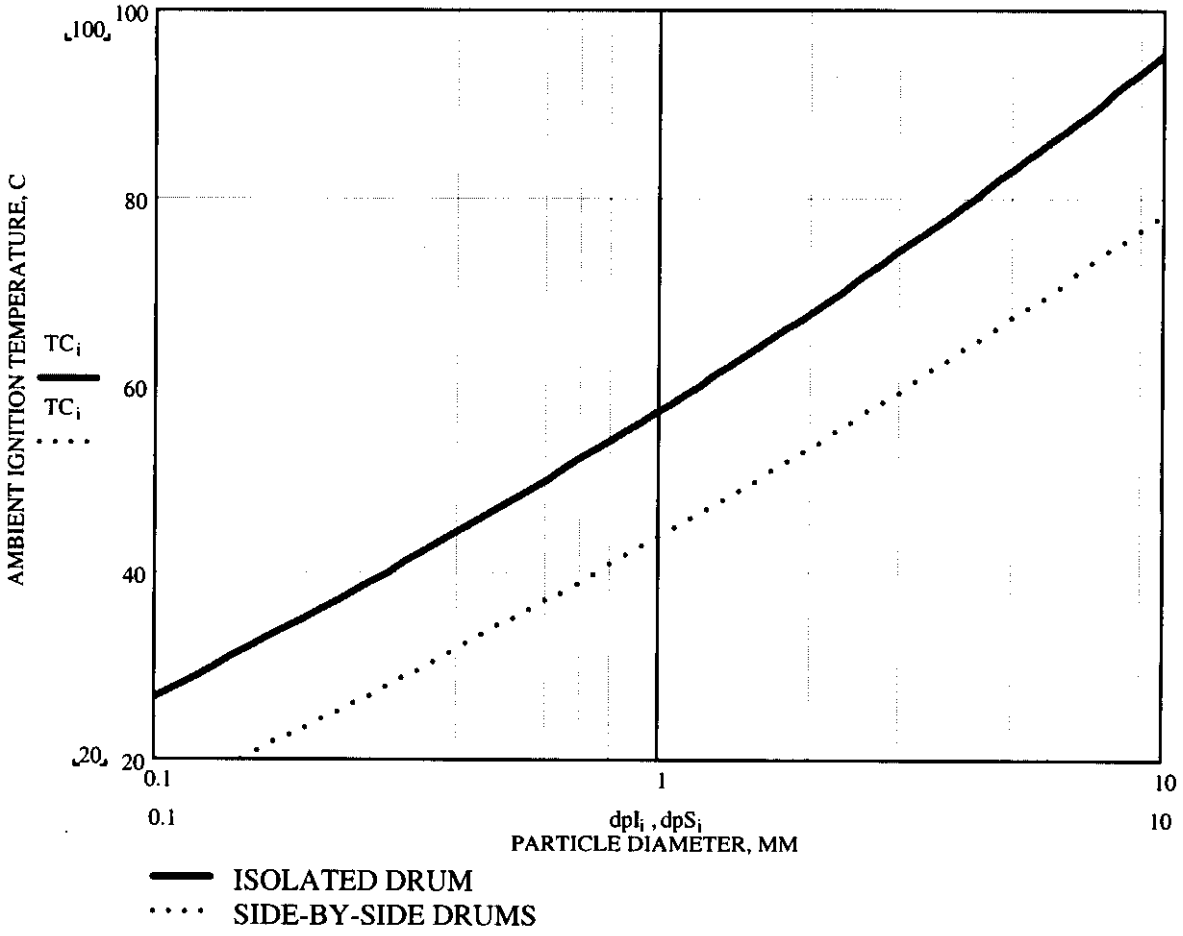

9.3 Model Cross-Reference

A summary of ignition formulas and examples, for which there are closed-form examples, appears in Table 9-1. For more complex situations, the general method described in Section 9.1 and examples of Section 6.0 should be consulted.

Table 9-1: Summay of Ignition Formulas

1-D Exact Method	
	Slab Equation (3-32) Cylinder Equation (3-34) Sphere Equation (3-33)
1-D Constant Rate Method	
	Slab Equations (3-43) and (3-32) or Equation (9-1), f = 1 Cylinder Equation (9-1), f = 1/2
2-D Exact Method	
	Cylinder, constant T_w Equations (4-10) to (4-14)
2-D Constant Rate Method	
	Cylinder, constant T_w Equations (4-17), (4-18) Cylinder, convective boundaries Equations (5-11), (5-12) or Equation (9-1), f from Figures 9-2 to 9-4

10.0 REFERENCES

Abrefah, J., et al., 1999, *Analysis of Ignition Testing on K-West Basin Fuel*, PNNL-11816, UC-602, Pacific Northwest National Laboratory, Richland, Washington.

Anderson, C. A., and O. C. Zienkiewicz, 1974, *Spontaneous Ignition: Finite Element Solutions for Steady and Transient Conditions*, J. Heat Transfer, 96, pp. 398-404.

Baker, L., Jr., and J. D. Bingle, 1966, *The Kinetics of Oxidation of Uranium Between 300 and 625°C*, Journal of Nuclear Materials, Vol. 20, pp. 11-21.

Baker, L., Jr., and R. C. Liimatainen, 1973, *Chemical Reactions*, Argonne National Laboratory, Argonne, IL, and Office of Atomic Energy Affairs, Department of State, Washington, D.C., Chapter 17 of "The Technology of Nuclear Reactor Safety," Volume 2, Reactor Materials and Engineering, Editors Thompson, T. J., and Beckerley, J. G., The Massachusetts Institute of Technology (M.I.T.) Press, Cambridge, MA.

Baker, L., Jr., J. G. Schnizlein, and J. D. Bingle, 1966, *The Ignition of Uranium*, Journal of Nuclear Materials, Vol. 20, pp. 22-38.

Boddington, T., P. Gray, and D. I. Harvey, 1971, *Thermal Theory of Spontaneous Ignition: Criticality in Bodies of Arbitrary Shape*, Philos. Trans. R. Soc. London, Ser. A, 270, pp. 467-506.

Boddington, T., P. Gray, and S. K. Scott, 1982, *Temperature Distributions, Critical Conditions, and Scaling for Exothermic Materials Under Different Boundary Conditions*, J. Chem. Soc., Faraday Trans., 77, pp. 813-823.

Bowden, F., and Yoffee, 1958, Initiation and Growth of Explosions in Liquids and Solids, Cambridge Monographs on Physics, Cambridge University Press.

Britton, L. G., and J. A. Smith, 1988, *Static Hazards of Drum Filling. Part 1: Actual Incidents and Guidelines; Part 2: Electrostatic Models: Theory and Experiment*, Plant/Operations Progress 2, pp. 53-56.

Carslaw, J. S., and J. C. Jaeger, 1959, *Conduction of Heat in Solids*, 2nd Edition, Oxford University Press.

Chemical Engineers Handbook, 1963, 4th edition, McGraw-Hill, New York, pp. 9-32.

Demiter, J. A., 1998, *Hanford N-Fuels Pyrophoricity Documentation Evaluation for the Spent Nuclear Fuels Project*, COGEMA Engineering Corporation, Letter Report to D. R. Duncan, COGEMA-98-529, July 1. (Included in Appendix B)

Duncan, D. R., 1997, *Spent Nuclear Fuel Project Technical Databook*," HNF-SD-SNF-TI-015, Rev. 2, Fluor Daniel Hanford, Inc., Richland, Washington.

Epstein, M., W. Luangdilok, M. G. Plys, and H. K. Fauske, 1996, Nuclear Safety 37, pp. 12-16.

Frank-Kamenetskii, D. A., 1969, Diffusion and Heat Transfer in Chemical Kinetics, Plenum Press, New York.

Gabor, John D., 1970, *Heat Transfer to Particle Beds with Gas Flows Less Than or Equal to That Required for Incipient Fluidization*, Chemical Engineering Science, Vol. 25, pp. 979-984.

Gebhart, B., Y. Jaluria, R. L. Mahajan, and B. Sammakis, 1988, *Buoyancy-Induced Flows and Transport*, Hemisphere, New York.

Gray, P., and P. R. Lee, 1967, *Thermal Explosion Theory*, Comprising Vol. 2 of Oxidation and Combustion Reviews, C.F.H. Tipper, Editor, Elsevier Publishing, New York.

Hartman, et al., 1951, *The Explosive Characteristics of Titanium, Zirconium, Thorium, Uranium, and their Hydrides*, U.S. Bureau of Mines, Report of Investigation 4835, U.S. Department of Interior, December.

Hilliard, R. K., 1957, *Effect of Heating Irradiated Uranium: A Literature Survey*, Hanford Atomic Products Operations, HW-52753, November.

Johnson, A. B., and S. P. Burke, 1995, *K-Basin Corrosion Program Report*, WHC-EP-0877, September.

Jones, J. C., 1993, *Combustion Science: Principles and Practice*, Millenium Books, an Imprint of E. J. Dwyer, Newtown, Australia.

Kasparek, G., and D. Vortmeyer, 1976, Warmestrahlung in Schuttungen aus kugelin mit vernachlassigbarem Warmeleitwiderstand, Warme-und Stoffubertragung, Vol. 9, pp. 117-128, Springer-Verlag.

Kobayashi, M., 1969, Ph.D. Thesis, Northwestern University, Evanston, IL.

Kuchta, J. M., 1985, *Investigation of Fire and Exploseion Accidents in the Chemical, Mining and Fuel-Related Industries - A Manual*, Bureau of Mines Bulletin 680.

Liebowitz, L., et al., 1963, *Burning Velocities of Uranium and Zirconium in Air*, Nuclear Science and Engineering, Vol. 15, pp. 395-403.

McGillivray, G. W., D. A. Geeson, and R. C. Greenwood, 1994, *Studies of the Kinetics and Mechanism of the Oxidation of Uranium by Dry and Moist Air - A Model for Determining the Oxidation Rate Over a Wide Range of Temperatures and Water Vapor Pressures*, Journal of Nuclear Materials, 208, pp. 81-97.

Mouradian, E. M., and L. Baker, Jr., 1963, *Burning Temperatures of Uranium and Zirconium in Air*, Nuclear Science and Engineering, Vol. 15, pp. 388-394.

Nagy, J., and H. C. Verakis, 1983 Development and Control of Dust Explosions, Dekker, New York.

Pajunen, A. L., 1997, *Estimated Fuel Inventory Loaded in Fuel and Scrap Baskets*, HNF-SD-SNF-CN-012, Rev. 0, Hanford, Richland, Washington.

Peacock, H. B., 1992, *Pyrophoricity of Uranium*, Report WSRC-TR-92-106, Savannah River Laboratory, March.

Pearce, R. J., 1989, *A Review of the Rates of Reaction of Unirradiated Uranium in Gaseous Atmospheres*, CEGB Report RD/B/6231/R89, Central Electricity Generating Board, Berkeley Nuclear Laboratories, United Kingdom.

Pearson, H. E., 1954, *1954 - AEC Uranium Fire Experience*, HAN-64841, Hanford, Richland, Washington, September 17.

Plys, M. G., and B. Malinovic, 1997, *Risk-Based Assessment of Fuel Reaction Potential During CVD*, FAI/97-31, Fauske & Associates, Inc., Burr Ridge, Illinois.

Plys, M. G., et al., 1997, *Simulation of Cold Vacuum Drying With Modified Scrap Baskets*, FAI/97-48, Fauske & Associates, Inc., Burr Ridge, Illinois. (Released by the SNF Project as HNF-SD-SNF-CN-023, Rev. 0, *Thermal Analysis of Cold Vacuum Drying of Spent Nuclear Fuel*, 1999.)

Plys, M. G., B. Malinovic, and M. Epstein, 1998, *French Under Water Fuel Flash Incidents and K-Basins Fuel Application*, FAI/98-75, Rev. 2, Fauske & Associates, Inc., Burr Ridge, Illinois. (Released by the SNF Project as HNF-2786, Rev. 0, *Assessment of Potential for Rapid Ignition of Submerged N Reactor Fuel*, 1998.)

Plys, et al., 1998, *Simulation of Normal and Off-Normal Multi-Canister Overpack Behavior*, FAI/98-33, Rev. 3, Fauske & Associates, Inc., Burr Ridge, Illinois. (Released by the SNF Project as HNF-2256, Rev. 2, *Simulation of Normal and Off-Normal MCO Behavior*, 1998.)

Plys, M. G., and B. Malinovic, 1999, *IWTS Metal-Water Reaction Rate Evaluation*, FAI/99-26, Fauske & Associates, Inc., Burr Ridge, Illinois. (Released by the SNF Project as SNF-4266, Rev. 0, *IWTS Metal-Water Reaction Rate Evaluation*, 1999.)

Plys, M. G., et al., 1999, *Hanford Spent Nuclear Fuel Safety Analysis Model HANSF 1.3.2: User's Manual*, FAI/99-74, (Rev. 3 of FAI/98-40), Fauske & Associates, Inc., Burr Ridge, Illinois. (Released by the SNF Project as SNF-3650, Rev. 2, *HANSF 1.3.2 User's Manual*, 1999.)

Schnizlein, J. G., et al., 1959, *Ignition Behavior and Kinetics of Oxidation of the Reactor Metals U, Zr, Pu and Th, and Binary Alloys of Each*, Report ANL-5974, Argonne National Laboratory, April.

Schnizlein, J. G., L. Baker, Jr., and J. D. Bingle, 1966, *The Ignition of Binary Alloys of Uranium*, Journal of Nuclear Materials, Vol. 20, pp. 39-47.

Schultz, W. W., 1955, *Ignition of Uranium Metal in Air*, HW-34441, January 13, cited by R. K. Hilliard, 1957.

SGN, 1995, *SGN Review on Spent Nuclear Fuel Project*, Report to WHC on Retrieval and Conditioning of Hanford N-Reactor Fuel, SGN Reseau Eurisys #2398A, Rev. 0, July. (Included in SNF-2786, Rev. 0, *Assessment for Potential of Rapid Ignition of Submerged N Reactor Fuel*, 1998.)

Swift, D. L., 1966, *The Thermal Conductivity of Spherical Metal Powders Including the Effect of an Oxide Coating*, Int. J. Heat Mass Transfer, 9, pp. 1061-1073.

Tetenbaum, M., et al., 1962, *Uranium Powder Ignition Studies*, Nucl. Sci. Eng., 14, pp. 230-238.

Thomas, P. H., and P. C. Bowes, 1961, "*Thermal Ignition in a Slab with One Face at a Constant High Temperature*," Trans. Faraday Soc. 57, pp. 2007-2017.

Weakley, E. A., 1980, *Interim Report on Concreted Uranium Fines and Chips Billet Curing Tests - A Basis for Resuming Shipment of Concreted Uranium Scrap Billets*, UNI-1454, United Nuclear Industries, Inc., May.

Weakley, E. A., 1982, *Interim Report on Concreted Uranium Fines and Chips Billet Curing Tests - A Basis for Resuming Shipments of Concreted Uranium Scrap Billets*, Report UNI-1454, United Nuclear Industries, Inc.

Williams, F. A., 1981, *A Review of Flame Extinction*, Fire Safety Journal 3, pp. 163-175.

Zabetakis, M. G., 1965, *Flammability Characteristics of Combustible Gases and Vapors*, Bureau of Mines Bulletin 627.

Zeldovich, Y. B., G. I. Barenblatt, V. B. Librovich, and G. M. Makhviladze, 1985, The Mathematical Theory of Combustion and Explosions, Plenum Publishing, New York.

APPENDIX A URANIUM METAL AND HYDRIDE REACTION RATES

A.1 INTRODUCTION

Data and correlations for uranium metal reactions with air and water vapor at temperatures below 300°C are summarized here. More complete literature information may be found in (Colmenares 1984) and specific references cited here, and a more complete discussion of N Reactor fuel reaction rates may be found in Pajunen (1999) and Trimble (1999).

The abundance of literature data exist for U-H_2O, U-Air, and U-H_2O-Air systems. In application, it is assumed that replacing nitrogen in air or dilution of water vapor by any other (relatively) non-reacting gas does not affect the rate. For example, data for the U- H_2O reaction rate may be taken with a mixture of He and H_2O.

It is simply assumed that uranium hydride, UH_3, reacts with the same rate per unit area as the metal; there simply are no open literature data to support any difference.

A.2 REACTION PHENOMENA

The U-O_2 and U-H_2O reactions may be written:

$$U + 2\,H_2O \rightarrow UO_2 + 2\,H_2$$

$$U + O_2 \rightarrow UO_2$$

These reactions are stoichiometric expressions and their use is conservative for estimates of heat generation, hydrogen generation, and oxygen depletion rates.

Rate data are usually expressed in terms of weight gain per unit area per unit time. This unambiguously provides a measure of the rate of oxygen addition to the corrosion product, but the reaction stoichiometry must be defined in order to infer the rate of oxidation of uranium metal, and a density must be assumed to infer the speed of a corrosion interface. The reaction rates follow a linear rate law; i.e., the rate gain per unit area per unit time is generally a constant, as discussed below. This is because the oxide corrosion layer has half the theoretical density of the metal, so that stress causes the corrosion layer to slough off after it attains a thickness of one to several microns.

The reaction rate is significantly higher for U- H_2O than for a mixture of U- H_2O-Air or for U-Air. Figure A-1 illustrates the effect of oxygen concentration on reaction rate at 100°C for various water vapor pressures (Colmenares 1984). Reaction rate increases markedly as oxygen partial pressure falls from 0.1 kPa to 0.01 kPa; e.g., for water vapor pressure equal to 13.3 kPa, reaction rate increases by a factor of 12. Above 0.05 kPa or so, oxygen partial pressure has little effect on reaction rate. A practical implication of this data is that air ingression can poison the $U + 2\,H_2O$ reaction.

In the absence of oxygen, hydrogen is produced by the reaction with water vapor, but in the presence of non-negligible amounts of oxygen, per Figure A-1, no hydrogen is produced. Net oxygen depletion occurs before water vapor reactions, as illustrated by the data of [McD. Baker, et al., 1966] in Figure A-2. Figure A-2 shows that the water vapor concentration remains constant, while oxygen concentration decreases linearly. Steam concentration decreases precipitously after oxygen is depleted, and hydrogen production increases greatly.

A.3 REACTION RATE DATA AND CORRELATIONS

A number of experimental investigations and derived reaction rate laws appear in the literature for unirradiated, uncorroded U metal reacting with O_2 or H_2O alone and U with both O_2 and H_2O. The literature shows wide variation between rate laws for U-O_2, U-H_2O, and U-H_2O-O_2 (or U-H_2O-Air).

Figure A-1: Effect of Oxygen Concentration on the Uranium-H_2O (v) Reaction (O_2 + H_2O (v) + N_2 Mixtures) at 373 K
Total pressure = 101 kPa.

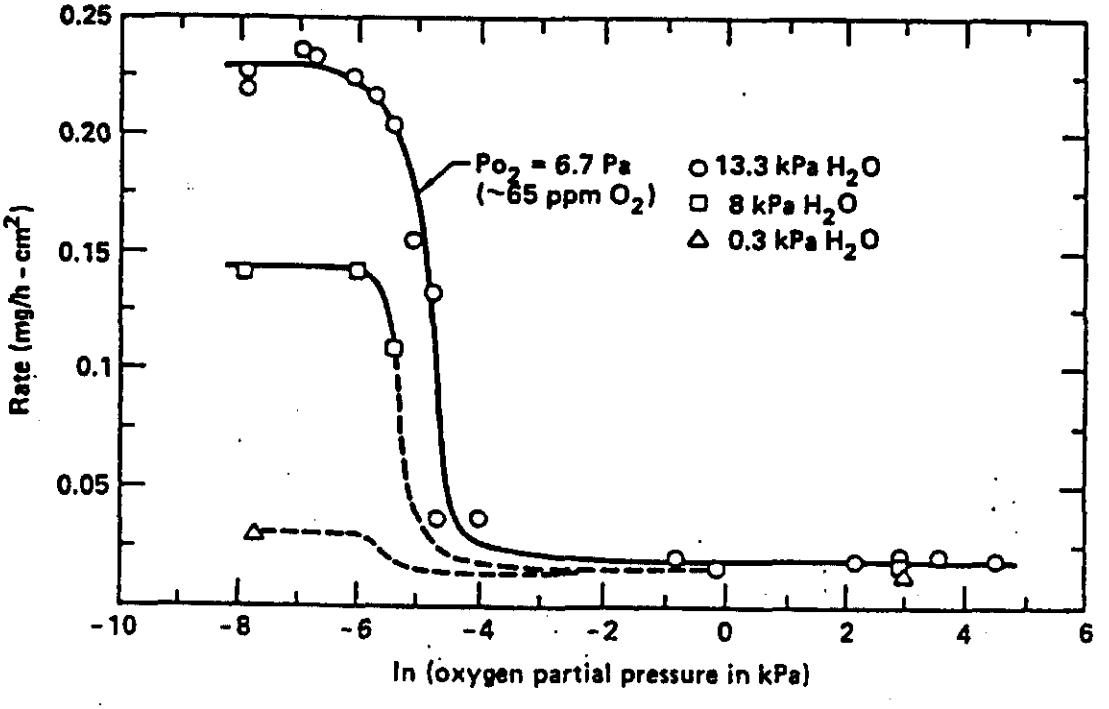

Figure A-2: Variation of Gas Composition With Time in (McD. Baker, et al. 1966) U-O_2.H_2O Experiments

x = H_2O o = O_2 • = H_2

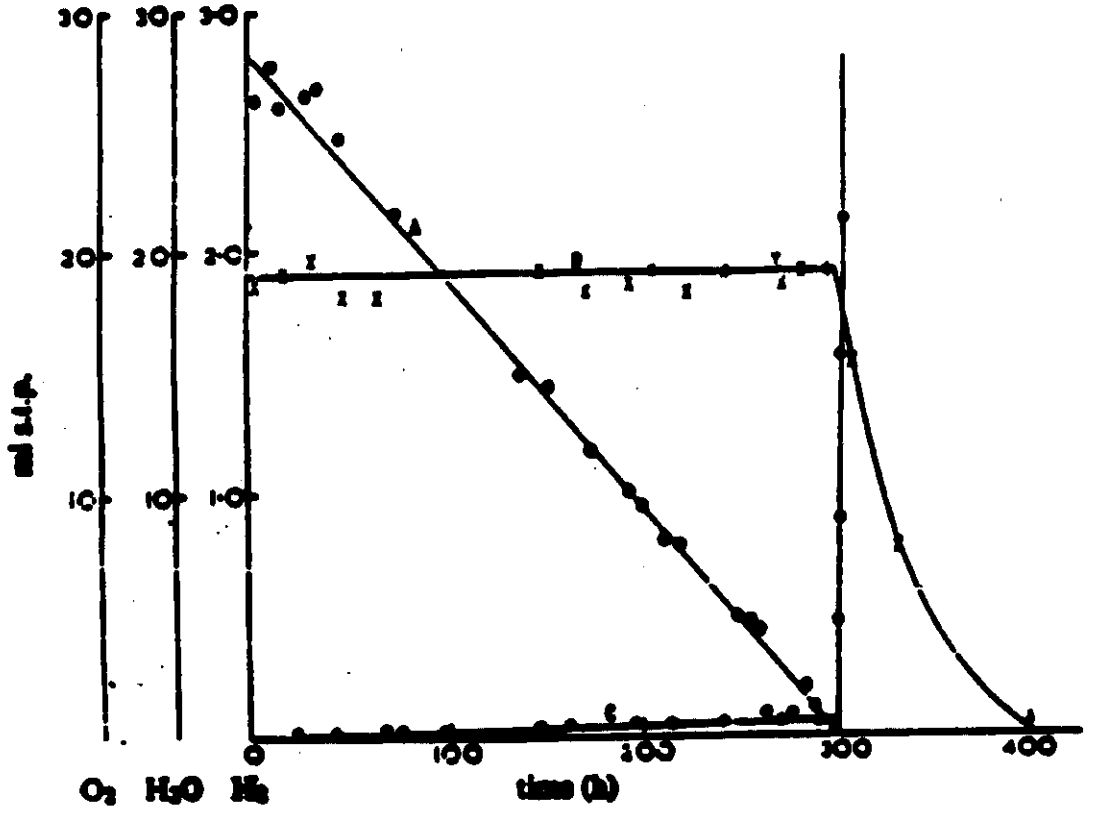

The McGillivray correlation (McGillivray, et al. 1994) can be used for steam and oxygen conditions, and is a function of temperature and steam partial pressure:

$$W'_{O2} = \frac{0.4195 \frac{P_{st}}{1000} \exp\left(-\frac{6432}{T}\right)}{1 + 2.48 \times 10^{-7} \frac{P_{st}}{1000} \exp\left(\frac{5327}{T}\right)} + 10.95 \exp\left(-\frac{8077}{T}\right) \frac{kg\,O_2}{m^2 \cdot s} \quad \text{(A-1)}$$

where P_{st} is the partial pressure of steam in Pa and T is temperature in K. Note that the McGillivray correlation uses units of kg O_2/m^2 s. Oxygen weight gain as a function of steam partial pressure is plotted in Figure A-3. For selected temperatures, oxygen weight gain was calculated assuming steam partial pressure varies from 0.1 Pa (dry conditions) to saturation.

Figure A-4, taken from (Pearce 1989), compares correlations and data for U-H_2O (oxygen-free) and U-H_2O-Air (100% RH) systems. Figure A-5, which is also taken from (Pearce 1989), contains data for unsaturated U-H_2O-Air (< 100% RH). Based on a linear regression of all the available data, Pearce reports the following correlation for oxygen-free conditions, steam partial pressure up to 1 atmosphere, and temperatures in the range between 20 and 350°C:

$$W''_{O2} = 10^{\left[4.33 - \frac{2144}{T} + 0.5\,\ell og\left(\frac{P_{st}}{1000}\right)\right]} \frac{mg \cdot O_2}{cm^2 \cdot hr} \qquad \text{(A-2)}$$

where T is temperature in degrees K and P_{st} is steam partial pressure in Pa. In moist air, with conditions of 100% RH and temperatures less than 100°C, weight gain is expressed by:

$$W''_{O2} = 10^{\left[8.33 - \frac{3730}{T}\right]} \frac{mg \cdot O_2}{cm^2 \cdot hr} \qquad \text{(A-3)}$$

Figure A-3: Oxygen Weight Gain as Function of Steam Partial Pressure

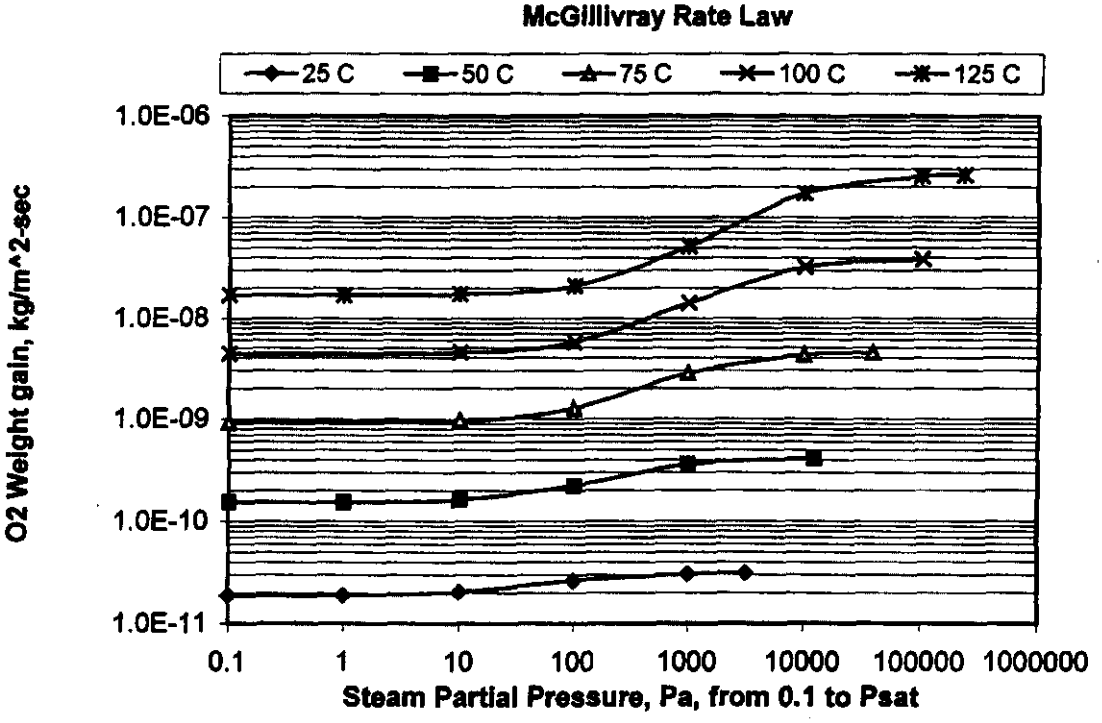

Figure A-4: Rates of Reaction at 100% RH in the U-H_2O and U-O_2-H_2O Systems

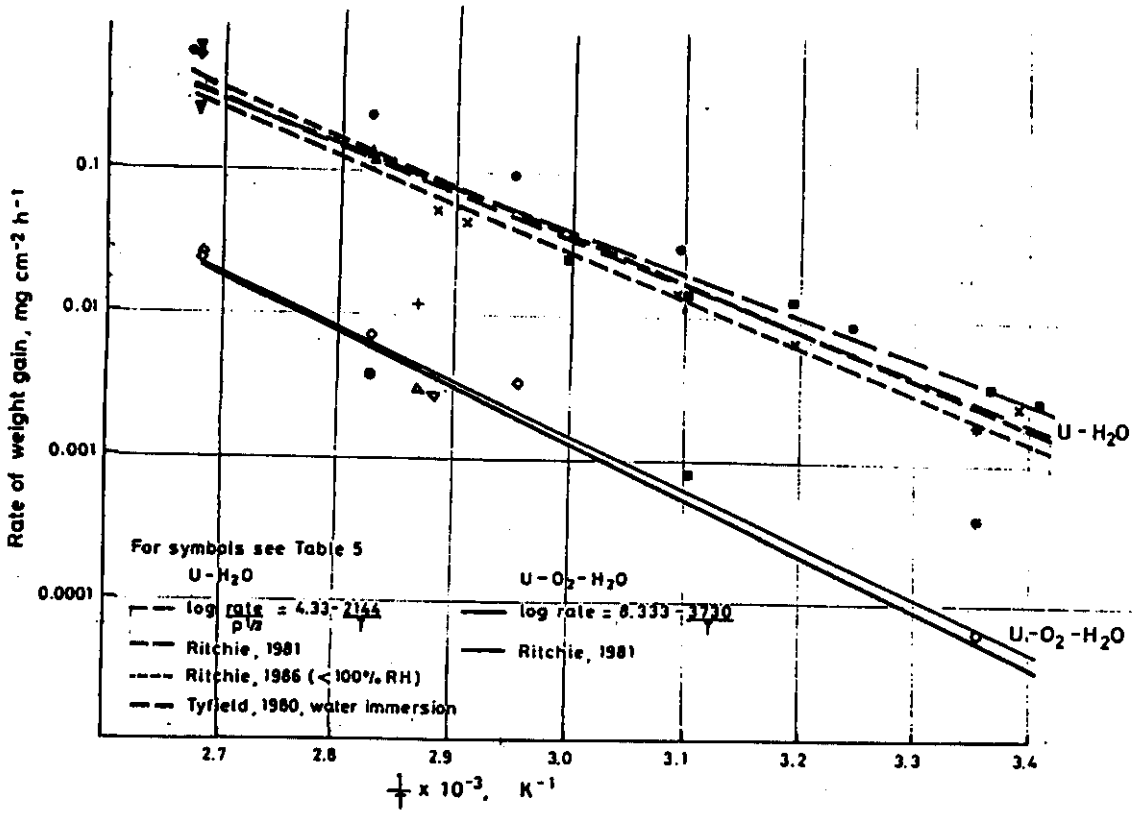

Figure A-5: Variation of Reaction Rate With Water Vapor Pressure, U-O_2-H_2O System

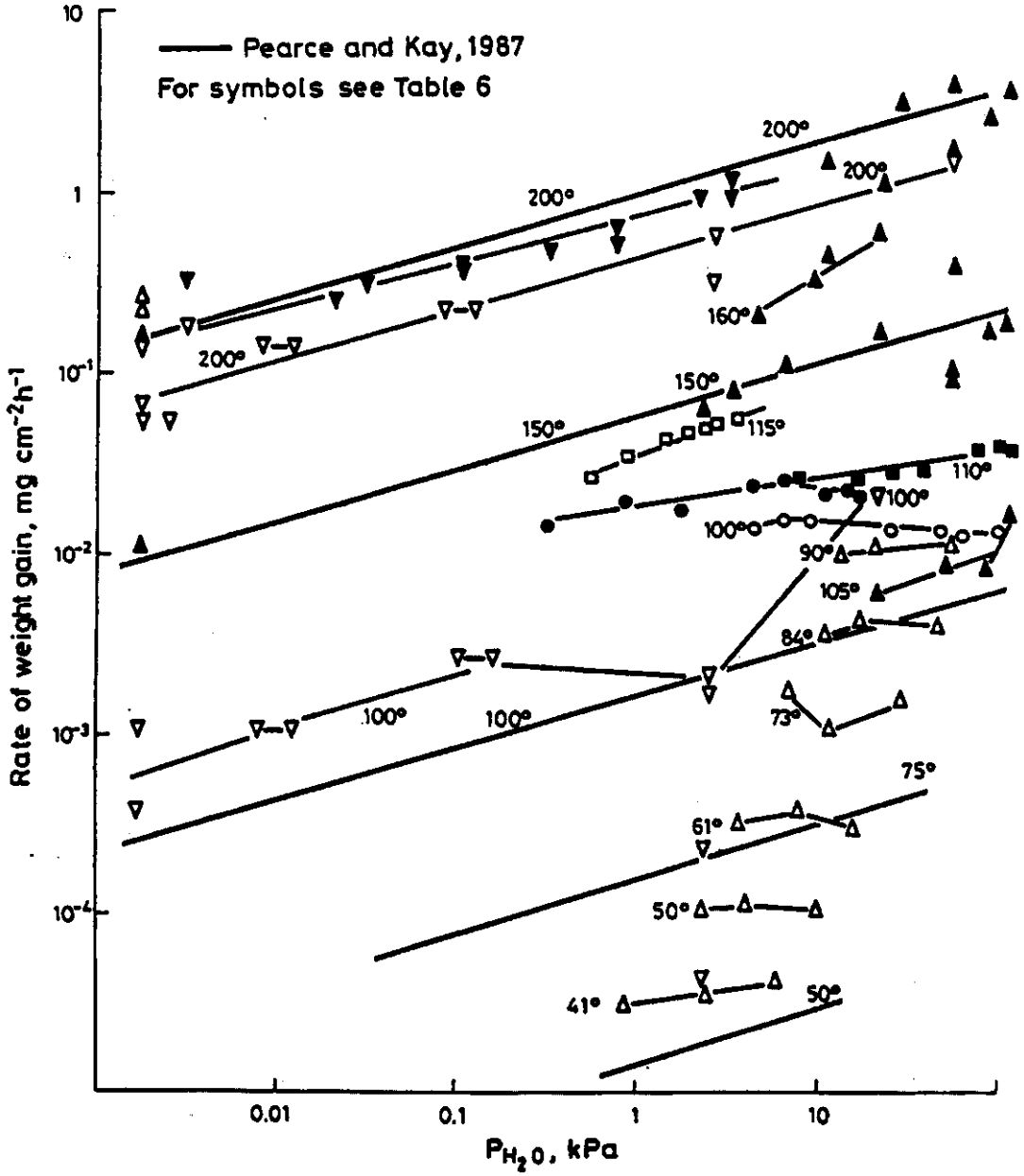

Low temperature literature correlations for uranium reactions in various gaseous atmospheres are summarized in Table A-1 and Figure A-6. The correlations are presented in consistent units, and all but the McGillivray correlation for non-zero water vapor follow the Arrhenius form required for simplified ignition theory formulas. When the water vapor pressure appears in a correlation, the pre-exponential is multiplied by the water vapor pressure factor in the table, i.e., k_o is replaced by ($k_o P^n$).

Table A-1: Literature Correlations for U Metal With Various Gases
In all cases, T is Temperature in Kelvins, P is Pressure in Kilo Pascals, and the Rate is Provided in $kgO_2/m^2/s$

A. Correlation Following $R = k_o P^n \exp(-T_E / T)$

Correlation	k_o, ($kgO_2/m^2/s$)	T_E, (K)	n
Pearce, Oxygen-Free Water Vapor	0.0594	4,937	0.5
Pearce, 100% RH, In Air, T < 100°C	598.0	8,589	0
Pearce, < 100% RH, In Air, T < 192°C	$1.023 \cdot 10^5$	11,490	0.3
Ritchie, < 75% RH, In Air, T < 100°C	$2.111 \cdot 10^8$	13,280	0
McGillivray, Dry Air	10.95	8,077	0

B. McGillivray Correlation for U-H_2O-Air

$$R = \frac{0.4195\, P \exp\left(\frac{-6432}{T}\right)}{1 + 2.48 \times 10^{-7}\, P \exp\left(\frac{5327}{T}\right)} + 10.95 \exp\left(\frac{-8077}{T}\right) \frac{kg\, O_2}{m^2 \cdot s}$$

The McGillivray correlation for dry air can be used directly. For cases with RH between 10% and 90%, the dry McGillivray correlation can be multiplied by a factor that is independent of RH, and ranges from about 2 at 30°C to 8 at 100°C. From the Pearce correlation with variable RH, the pressure is only taken to the 0.3 power, so over this RH range the Pearce result would only vary by a factor of 2.

Note that the Pearce correlation cannot be used for very low RHs, for it cannot fall below the dry air value. In the temperature range shown, and for the range of RHs mentioned, the effect of water vapor pressure is arguably small, and in fact, Ritchie chose to neglect this variation as seen from the table. The activation energies used by Pearce and Ritchie for moist air are higher than those for 100% humid or dry air; hence, these two curves non-physically cross their limiting cases. This reinforces the recommendation above, that for moist air and typical ambient humidity, the McGillivray dry air law multiplied by a factor of about 3 or 4 is suitable for most calculations.

Figure A-6: Comparison of Literature Correlations for U Metal Reactions, Weight Gain kgO_2/m^2 s. Gases are Pure H_2O (Pearce oxy-free, + symbol), Air at 100 % RH (Pearce 100% RH, solid line), Dry Air (McGillivray dry, xx symbol), and Several Correlations for Air with 75% RH (see legend)

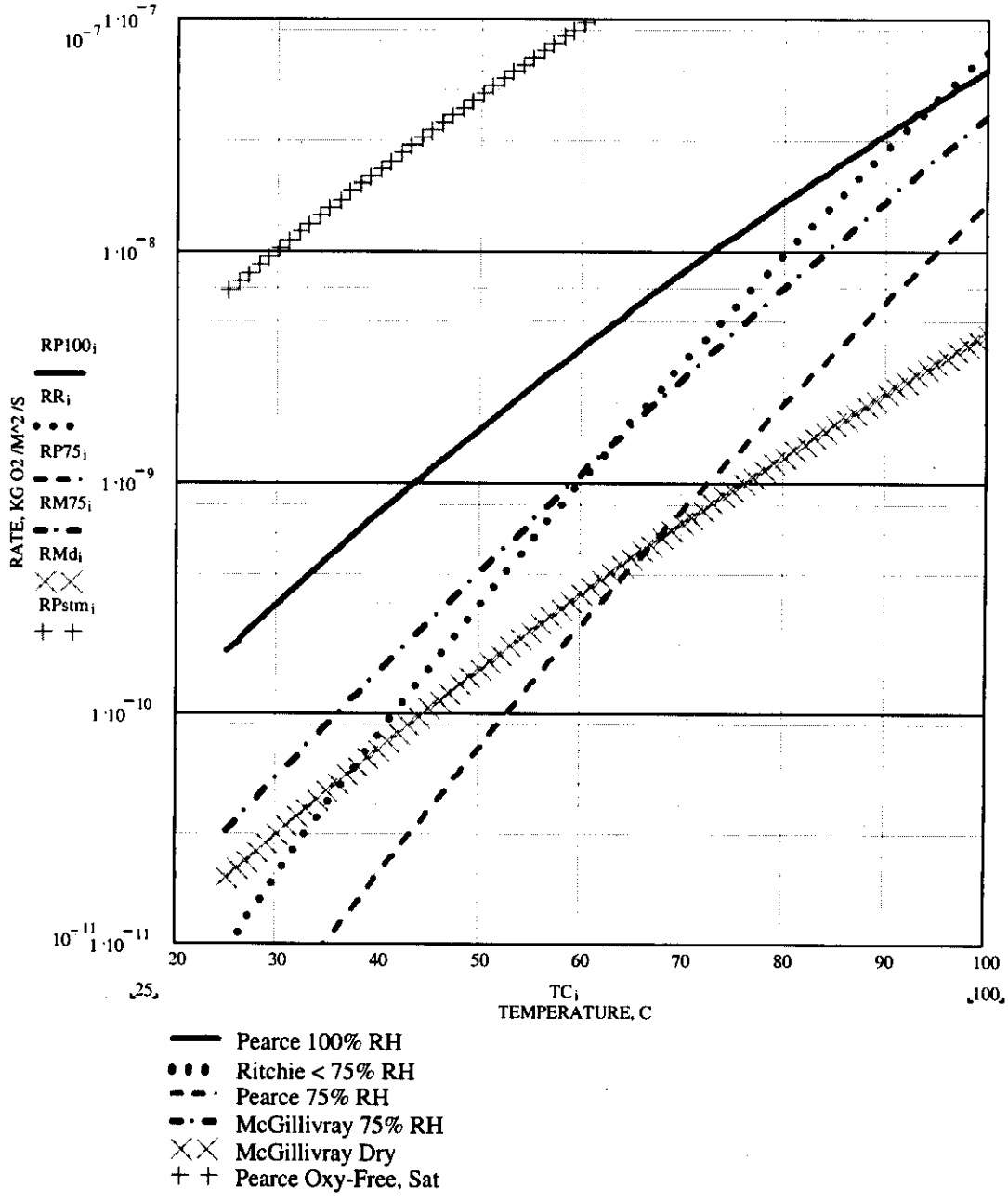

A.4 REFERENCES

Colmenares, C. A., 1984, *Oxidation Mechanisms and Catalytic Properties of the Actinides*, Prog. Solid St. Chem., Vol. 15, Great Britain, Pergamon Press Ltd., pp. 257-364.

M. McD. L. N. Baker, Less, and S. Orman, 1966, *Uranium + Water Reaction*, Transactions of the Faraday Society, Number 525, Vol. 62, Pt. 9, September.

McGillivray, et al., 1994, *Studies of the Kinetics and Mechanism of the Oxidation of Uranium by Dry and Moist Air*, Journal of Nuclear Materials, 208, North-Holland, pp. 81-97.

Pajunen, A. L., 1999, *Uranium Oxidation Rate Summary for the Spent Nuclear Fuel Project*, HNF-4165, Rev. 0, Duke Engineering and Services Hanford, Richland, Washington.

Pearce, R.J., 1989, *A Review of the Rates of Reaction of Unirradiated Uranium in Gaseous Atmospheres*, CEGB Report RD/B/6231/R89, Central Electricity Generating Board, Berkeley Nuclear Laboratories, United Kingdom.

Trimble, D. J., 1999, *Oxidation Kinetics of K Basin Fuel*, HNF-4206, Rev. 0, Duke Engineering and Serivces Hanford, Richland, Washington.

APPENDIX B COGEMA-98-529

COGEMA ENGINEERING CORP.

July 1, 1998 COGEMA-98-529

Mr. D. R. Duncan
Principal Engineer
DE&S Hanford, Inc.
Post Office Box 350
Richland, Washington 99352

Dear Mr. Duncan:

HANFORD N-FUELS PYROPHORICITY DOCUMENTATION EVALUATION FOR THE SPENT NUCLEAR FUELS PROJECT

An evaluation was conducted for the Spent Nuclear Fuel (SNF) Project to determine the value of uranium pyrophoricity documentation (specific focus was Hanford historical documents related to N-fuels) in providing information and data to bound underwater spent N-fuel ignition/burning events and provide background on uranium pyrophoricity in general.

Documentation was collected from SNF Project files, previous researchers, the 333 Building uranium file, and the Declassified Document Tracking System (DDTS); evaluated as to its significance to the SNF N-fuel uranium ignition/burning issue, and listed chronologically on the attached table (Enclosure 1). A large file on the pyrophoricity of uranium/zirconium dating back to the 1940s (maintained by E. A. Weakley at the 333 Building prior to his retirement) was, unfortunately, not located. A listing of contacts made to gain information is included as Enclosure 2.

To rate the value of documents, relative to the SNF Project needs, a document value rating system was established (Enclosure 3). A document rated #1 provided no information to the SNF Project, while a document rated #5 would provide specific data, with credible and referenced information concerning pyrophoric studies or incidents of aged, irradiated, N-Basin stored N-fuels. The evaluation found no documents providing information at the #5 rating. Summaries were written for several documents. Those with summaries are noted on the table by an asterisk and are included as Enclosure 4.

The Declassified Document Tracking System (DDTS) was searched, using 19 key name identifiers, for documents relating to underwater spent N-fuel ignition/burning information. Of the several hundred documents listed, 37 were identified significant to the SNF Project, and were ordered. Of the documents ordered, 24 have been evaluated and added to Enclosure 1, eight documents have not been received, three classified documents will not be declassified, and two documents were drafts of previously listed documents.

P.O. Box 840
Richland, Washington 99352-0840
Phone (509) 372-3572 • Fax (509) 372-3169

D. R. Duncan
Page 2 of 2
July 1, 1998

COGEMA-98-529

Several Hanford 300 Area fuel production documents concerning uranium turnings and fines are provided in the literature listing. While these documents and accident reports provide general uranium and zirconium metal information, none is relative to incidents with aged, irradiated, water-stored N-fuels.

Several documents offer specific theoretical and testing data concerning uranium or uranium/zirconium pyrophoricity in several conditions and states. The data is valuable in establishing an ignition model, but no specific data has come from experimentation and testing with long-term, basin-stored N-fuel. Several references are listed for European fuel studies, but the fuel is of differing types and compositions from that of N-fuel, and all studies deal with newly irradiated fuel (~ up to three years old).

This completes the search for, and evaluation of, Hanford historic uranium fuel pyrophoricity documentation, including industry general uranium pyrophoricity documentation, pertinent to bounding N-fuel, underwater uranium ignition/burning events for the SNF Project. All known sources of information have been examined for data relating to this subject. Should you have any additional questions, please contact me on 376-9671.

Sincerely,

Mr. James A. Demiter
Principal Scientist

cmr

Enclosures (4)

cc: J. R. Frederickson, DE&S Hanford, Inc.
M. G. Plys, Fauske & Associates, Inc.

Table B-1: Documents on Uranium/Zirconium Pyrophoricity (Relative value to N-fuels at K-Basin) [COGEMA 98-529]					
Author	**Document Number**	**Title**	**Date**	**Comments**	**Priority Value**
Ballinger, R,G. (MIT)	JRF-98-005	Rapid Reactions in Basin. Memo prepared by R.G. Ballinger of Spent Nuclear Fuel Technical Assistance Group (TAG), entitled "Fuel [Flashes] and Burning Issues." Pages 6	3/23/98	No evaluation required.	1
Shen, E.J.	HNF-1894	K-Basins Fuel Ignition Issues, Pages 15.	12/97	No evaluation required.	1
Abrefah,J., H.C. Buchanan, S.C. Marschman	SNFCT97:0 32	Highlight Report: Hydrogen Released from Corroded/Damaged K-West Spent Nuclear Fuel in Vacuum. Pages 13.	3/97	Provides hydrogen release data from heated SNF samples; both UH_3 decomposition and U RXN with moisture liberated hydrogen.	1
Abrefah,J., H.C. Buchanan, S.C. Marschman	SNFCT97:0 04	Draft highlight Report: Oxidation Kinetics of K-West Spent Fuel in Dry Air. Pages 12.	11/96	No evaluation required.	1
Thorton,TA, J. Abrefah, SC Marschman	SNFCT96:0 57:R00	Highlight Report: Ignition Test Results on KW SNF Element SFEC10-4366 End Samples. Pages 13.	96	Provides supporting data that damaged SNF ignites 200-300° C lower than intact SNF.	1
Bolt, A.L.	Memo to A.L. Pajunen	N-Fuel Hydrogen and Oxygen in the Canister Overpack. Pages 3	10/31/96	No evaluation required.	
Abrefah, J., W.M. Gerry, S.C. Marschman	SNFCT97:0 06	Highlight Report: Ignition Testing of As-Cut and Conditioned SNF Samples. Pages 11.	10/96	Provides ignition temperature for three spent fuel specimens that exhibit corrosion degradation. Temperature is ~300° C lower.	1
Cooper, T.D., E. Cramer, T. Thornton	Draft Report	Pyrophoricity and Ignition of Bulk Uranium Metal. Pages 17.	8/9/96	Draft, not released.	2
Willey, D.M.	AEA Fax No. 001 513 648 5754	Uranium Hydride Hazard Experience at AEA-Windscale. Pages 4	7/25/96		2
Merkling, G. Reddick	Email Merkling to Zaman	Comments on Draft CVD Product Criteria from G Reddick (copy of markup attached)	7/18/96	No evaluation required.	1
		SNFP Gas Generation from N-Fuel in Multi-Canister Overpacks	7/96	No evaluation required.	1
		SNFP Estimate of Volatile Fission Products Release from Multi-Canister Overpacks	7/96	No evaluation required.	1
		SNFP Surface Area Estimates for N-Reactor Fuel in the K-East Basin	7/96	No evaluation required.	1
		SNFP Photon Heat Deposition Calculations for Hydrogen Generation within Multi-Canister Overpacks	7/96	No evaluation required.	1
		SNFP Detonation Phenoma of Hydrogen /Oxygen in Spent Fuel Containers	5/96	No evaluation required.	1
		SNFP Recommended Reaction Rate Constants for Corrosion of N Reactor Fuel	5/96	No evaluation required.	1
Reddick, G.W.	Telephone Conference call	G. Reddick and Michael Jump Re: N Reactor fuel processing incidents at NFS in the late 1960s. Pages 2.	3/18/96	No evaluation required.	1
Epstein,M., W. Luangdilok, MG Plys, HK Fauske	Nuclear Safety Vol. 37, No. 1 Jan-Mar 1966	On Prediction of the Ignition Potential of Uranium Metal and Hydride. 16 Pages.	1/96	No evaluation required.	No Eval. Req.
Haschke, JM	LA-13069-MS	Reactions of Plutonium and Uranium with Water: Kinetics and Potential Hazards. Pages 4	12/95	Only 3 text pages - incomplete text? Provides UH_3 formation and RXN data	3
SGN Reseau Eurisys	NT 02630 00 0007 Rev.A	Technical Note: Review of SGN's knowledge concerning uranium hydrides. Pages 16.	12/95	No evaluation required.	1

Table B-1: Documents on Uranium/Zirconium Pyrophoricity (Relative value to N-fuels at K-Basin) [COGEMA 98-529]

Author	Document Number	Title	Date	Comments	Priority Value
Hands, Brian	BNFL - R&D Dept. Sellafield , UK	"Corrosion of Metallic Uranium Fuel During Pond Storage," pages 13.	1995	Viewgraph presentation only.	1
Lasserre, Veronique & Roux, Patrice	NUMATE C - SGN (K-Basin SNFP)	French Experience in Metallic Uranium Fuel Handling - Presentation. Pages 16	7/11/95	No evaluation required.	1
SGN Reseau Eurisys	2398A, Rev. 0	SGN Review on Spent Nuclear Fuel Project, Pages 38.	7/95	No evaluation required.	1
BNFL , UK Group	R&D Report 0326	Contract No. MRY-SWV-383520, "A Summary of BNFL's Experience in the Storage and Handling of Spent Metallic Fuel - Addendum: Summary of reference paper contents," pages 26	April 1995	See write-up	3/4*
Addison, CWE	BNFL	Storage and Corrosion of Spent Metal Fuel-UK Experience and its Implications for DOE Spent Nuclear Fuel Management. Pages 6	12/94		2
Solbrig, C.W., Krsul, J.R., Olsen, D.N.	ANL-	"Pyrophoricity of Uranium in Long-Term Storage Environments," Proceedings of Conference on DOE Spent Nuclear Fuel. Pages 5	12/94	Fernald drum reactions. See write-up	2*
Makenas, B.J.	WHC, Nuclear Fuel Evals. -Internal Memo to R. Omberg	Trip Report, BNFL and Atomic Energy Authority Sellafield Site Visit, 10/11-13/94	10/19/94	No information.	1
Sautman, M.T.	DNFSB-Memo	Fernald Environmental Management Project-Uranium/Thorium Interim Storage Safety Review Trip Report	9/29/94	Results of audit of FEMP. Discussion is as result of two drum incidents. No data	1
Weber, J.W.	WHC-SD-SNF-SARR-001	Review of Consequences of Uranium Hydride Formation in N-Reactor Fuel Elements Stored in the K-Basins. Pages 76.	9/94	Postulated accident analyses, consequences for bounds of safety evaluation	1
Epstein,M., W. Luangdilok, M.G.Plys, H.K Fauske	FAI/94-76	K- Basin Severe Accident Analysis: Fuel Heatup and Ignition Potential. Pages 118.	8/94	No evaluation required.	No Eval.. Req.
Marchetti, Sal	Fluor Daniel, Inc. 94-02A-FC-050 for DOE, Idaho Falls Office	Articles on Hydrides/Pyrophoricity of Fuels, SNF Storage Survey 1. Energy Daily, Monday, 06/13/94 2. EG&G Ltr, 06/13/94 w/BNFL Attachments of 06/02/94 pages, apx 70	07/06/94	General information on BNFL fuel experience	2
Porten, D.E., Crowe, R.D.	WHC-SD-SNF-RA-001, Rev 0	Accident safety analysis re *K-Basin Safety Analysis Report WHC-SD-SNF-SAR-001*, pages 64	1994	No useful data; development of accident safety analysis	1
Martz, JC, Haschke, JM, & Stakebake, JL	J. of Nucl. Materials 210 (1994) pgs 130-142	"A Mechanism for Plutonium Pyrophoricity," pages 12	Jan. 1994		
McGillivray, GW, DA Geeson, RC Greenwood	J of Nuclear Materials 208 (1994) 81-97	Studies if the Kinetics and Mechanism of the Oxidation of Uranium by Dry and Moist Air, A model for determining the oxidation rate over a wide range of temperatures and water vapour pressures	9/1/93	Overall rate expression for the air oxidation of uranium.	2

Table B-1: Documents on Uranium/Zirconium Pyrophoricity (Relative value to N-fuels at K-Basin) [COGEMA 98-529]

Author	Document Number	Title	Date	Comments	Priority Value
Wood, D.H., Snowden, S.A., Howe, H.J., Jr; Thomas, L.L., Moon, D.W., Gregg, H.R., Miller, P.E.	Journal of Nuclear Materials, SSDI 0022-3115(93) E0292-11?	Letter to the Editors regarding the chemistry of metallic uranium stored in steel drums, pages 3	07/26/93	LLNL drum explosion incident	1*
Fisher, D and Knight, S	AEA-D&W-0566	Study, "B30 Bottled Fuel Opening Option Study," prepared at Windscale, Seascale, Cumbria (UK) CA20 1PF, pages apx 150	April 1993	See write-up.	4*
Dir. Office of Nuclear Safety	DOE/NS-0013, Issue No. 93-1	"Fire, Explosion, and High-Pressure Hazards Associated with Waste Drums and Containers," pages 4	02/93	Fernald incident of 8/92, also refers to a Hanford incident. Proposed method to vent over pressurized drums.	1
Bruch, B.F.	WEMCO:PM&A(SE): 92-065	Technical Aspects of the June 17, 1992 Drum Explosion Incident at the Fernald Environmental Management Project, pages 4	08/31/92	pages 2,4,6 missing. Probably a 2-sided page document, copied as 1-sided.	
Thorton, T.A.	PNL Draft Report (not officially released)	A Summary of some Uranium Metal fuel Ignition Incidents and Their Relevance to K-Basin SNF Processing and Interim Storage		Information used in write-ups.	3/4
Swanson, J.L.	PNL	Project Plan for the PNL Activities Regarding Characterization of Irradiated N-Fuel	4/92	No copy	1
Peacock	WSRC-TR-92-106	Pyrophoricity of Uranium WSRC-TR-92-106, pages 12	3/92	Uranium ignition bases: mainly specific surface area, also temp & particle size	3
Swanson, J.L.	PNL - Letter to R.J. Thompson of WHC	Review of WHC-SD-NR-TA-009, pages 4	12/4/91	Also has one pg. Article, "Fire danger at North Wales nuclear store," from *New Scientist*, 03/02/91	1
Ryan, J.L.	PNL - A letter report for WHC	"Review of Information Pertinent to the Oxidation (Burning) of Irradiated N-Reactor Fuel," pages 33	12/91	Summary and review of literature.	2
Swanson, J.L.	PNL, - Letter to WHC R.J. Thompson,	Another letter re: Review of WHC-SD-NR-TA-009, (See letter of 12/04/91)	09/13/91	Review of Schmidt (91)	1
Siemer, JM	WHC-SD-NR-PHA-001	"Preliminary Hazards Analysis of K-Basin Fuel Encapsulation and Storage." Pages 82	9/11/91	No data, development for HAZOP study.	1
Schmidt, J.P.	WHC-SD-NR-TA-009	"An Assessment of the Potential for energetic uranium Hydride Reactions Occurring during K Basin Irradiated Fuel Handling Activities," pages-5	8/14/91	Generalizations. A specific PHA assessment. Poorly referenced, some general U information. See write-up	1*
Swanson, J.L.	PNL letter to R.J. Thompson, WHC	"Potential Safety Problem in Handling of Stored Fuel", pages 3	08/08/91	Review of Schmidt (91)	1
Schumacher, J.J.	NRFS 90-05 Event Fact Sht. WHC	"333 Building Duct Fire," in Metrology Lab at N Reactor Fuel Fabrication facilities. Pages 5	08/06/90		
Weakly, EA	Event Fact Sheet	"Analysis of Uranium in Drums from 340-B Building," pages 4	04/10/90	Uranium chips stored in drums three years - no incident.	1
Swanson, JL	PNL-6609, UC-711	"Recent Studies Related to Head-End Fuel Processing at the Hanford PUREX Plant," pages apx 120	August 1988	See write-up	1*

Table B-1: Documents on Uranium/Zirconium Pyrophoricity (Relative value to N-fuels at K-Basin) [COGEMA 98-529]					
Author	**Document Number**	**Title**	**Date**	**Comments**	**Priority Value**
Tyfield, SP	Nucl. Energy, 1988, 27, No. 2, Apr., pages 91-98	"Corrosion of reactor grade uranium in aqueous solutions relevant to storage and transport," by CEGB Berkeley Nuclear Labs, pages 8	April 1988	See write-up	4*
Pearce, R.J., P. Kay	TPRD/B/09 55/R87	The Reactions of Uranium with Moist Hydrogen. Pages 39.	10/87	Deals with N-fuels dissolution mainly. Summarizes cited literature. Good references in Chapters 6, 7, and 9.	2
Swanson, J.L., et al.	PNL-5708/UC-70	Laboratory Studies of Shear/Leach Processing of Zircaloy Clad Metallic Uranium Reactor Fuel. Pages 101.	12/85	No specific information - only general statements. Good references. Sect 6 & Sect. 10 - Values and data. See write-up	2*
Best, T.L.	UNC-2307	"Procedures for Reporting Accidental Losses for Ruptured Fuel," pages 3	04/07/83	N-Reactor nuclear material control for documenting ruptured fuel element SNM loss.	1
Bloom, JW	UNC Report re: UO 82-24,	CORRECTIVE ACTION #3 This letter and report lists recommendations generated by the subject at 333 Bldg	03/10/83	This and JE Lyttle's report deal with the same incident at 333Bldg , Hanford Site.	1
Lyttle, JE	UO No. 82-24	Final Report, "Unusual Occurrence Report No. 82-24 - Peel Test Saw Exhaust Duct Fire," pages 8	11/15/82	Uranium fines exhaust duct fire in 333 Building.	1
Moore, R.H.	PNL Draft	Analysis of the Safety and Technical Performance of the UNC Nuclear Industries Concretion Process. Pages 35.	8/25/82	Concreted U/Zr fines & turnings in billets. Gives ratio of U/Zr to concrete and history of three billet fires. See write-up.	3*
Smallwood, D	UNC , UE No. FM 82-4	Undesirable Event Report re: Uranium fines igniting at 333 Bldg, pages 2	07/16/82	Ignited uranium fines in 333 Building.	1
Galioto, T.A	UNC Occurrence Report UO 82-05	"Uranium Concrete Billet Autoignition" Occurrence report regarding an unusual occurrence at 303K Bldg. in 300A of Hanford Site, pages 9.	03/13/82		
E.R. Johnson and Associates, Inc.	ORNL/Sub-81/ 31066/1	Consolidated Fuel Reprocessing Program, "Review of the Operating History of the Nuclear Fuel Services, Inc., West Valley, NY, Irradiated Fuel Processing Plant.", pages 8	09/81	NFT fuel reprocessing waste generation; only chapter 8.0 - NOTE: cc:Mail message dated 6/14/95 is attached.	1
Bechtold and Kummerer	TRAC 0231	Bechtold and Kummerer to Paris, KE Fuel Basin visual Fuel Inspection, UNC Nuclear Industries, Richland, WA	7/13/81	No copy	
Ritchie, A.G.	J. of Nuclear Materials 102 (1981) 170-182	A Review of the Rates of Reaction with Oxygen and Water Vapour at Temperatures up to 300°C - pages 12	5/20/81	Corrosion of uranium by oxygen and water vapor at 20-100 degrees C. Partial text only.	
Bloch, J & Mintz, M.H.	J. of the Less-Common Metals, 81 (1981) 301-320	Kinetics and Mechanism of the U-H Reaction (*Nuclear Research Centre Negev-U. Of Negev, Israel).* pages 12	2/12/81 (Revised 6/2/81)	Model development of uranium hydride growth at the hydride-metal interface.	3
Kratzer, W.K.	UNC, UNI-1543	Basis for a Revision to Safety Analysis Report, 105-KW Fuel Storage Facility, Radionuclide Control, pages 13	06/17/80	Some good corrosion data on broken fuel at 105-KW	3
Lyttle, JE	Occurrence Rpt UO-79-27 - UNC Nuclear Ind.	"Fire in 3712 Warehouse Building," 300 Area, Fuels Production Department. Pages 6	07/23/79	Concreted U/Zr fines & turnings fire in 3712 building.	1
Kirk, W.R.	U.E. No. 77-2	Fuels Production Division - Unusual Event Report re: incident at 304 Bldg in 300 Area of Hanford Site, 1 page	08/08/77	Actual person who discovered condition was A.E. Brown	

Table B-1: Documents on Uranium/Zirconium Pyrophoricity (Relative value to N-fuels at K-Basin) [COGEMA 98-529]					
Author	**Document Number**	**Title**	**Date**	**Comments**	**Priority Value**
Brown, V	PAWP/111/ 41/P4/SAC/ 76/P6	"Summary of Some Incidents Involving Uranium Fires," by Safety Assessment Group. Pages	May 76	Paper reports on uranium fire incidents in USA, France, etc. See write-up.	2*
Unruh, C.M.	BNW (PNNL) Occurrence Report 75-BNW-12	"Pressurization of Depleted Uranium Turnings Drum 306-W," (300 Area) pages 7	09/15/75		
Levitz,N.M., B.J. Kullen, M.J.Steindler	ANL-8139	Management of Waste Cladding Hulls. Part I. Pyrophoricity and Compaction. Pages 57.	2/75	Fuel cladding waste handling, compaction, and storage for waste repository.	1
Condon, J.B.	J. of Physical Chemistry, Vol. 79, #4. (392-396)	Calculated vs. Experimental Hydrogen Reaction Rates with uranium *(Union Carbide Corp, Nuclear Div. Oak Ridge, TN)*- pages 8	8/22/74		2
Condon, JB and Powell, GL	Y-DA-5317	Paper submitted by Oak Ridge Y-12 Plant to Conference on Metallurgy of Uranium Alloys. Pages 51	12/21/73	The reaction kinetics of hydride formation and hydrogen embrittlement in the uranium-hydrogen system. Some pages missing.	3
Raab, G.J.	ARH-2492	Receipt and Storage at T Plant of Ruptured N Reactor 94-Metal Fuel Form Nuclear Fuels Services. Pages 12.	5/15/72	Safety document only for receiving ruptured N-fuel from NFS and storing in T-plant. No data	1
Schulz, W.W.	ARD-2351	Shear-Leach Processing of N-Reactor Fuel — Cladding Fires, pages 35 (including 2 page article "Zircaloy Surface Explosions on N-Fuel Samples," dated 6/11/65)	2/15/72	N-Reactor fuels manufacturing, NFT reprocessing of N-fuel from 1966-71, & cladding fires during dissolution due to sensitized Be weldments. See write-up	3*
Musgrave, J.E.	Journal of Nuclear Materials 43 (1972) p155-163	"A Theory of Burning Curve Ignition of Nuclear Metals," pages-9	1/17/72	Burning curve ignition theories and variables of nuclear metals: uranium and plutonium	3
Schmidt, J.P.	DUN-5020	"Non-Uniform corrosion Performance of Tapered-Base Cans in Fuel Lot KG431LR At KW Reactor," pages 3	11/05/68	Corrosion evaluation of one lot of fuel elements fabricated with tapered-base cans and irradiated in KW-Reactor concluding corrosion percentages are within K Reactor limits.	1
Guay, A.E.	DUN-4034	"RIF History of N Fuels Failures," pages 66	03/22/68	Computer pages showing data (time, date, tube power, pressures, and temperatures) for each N-Fuel element that failed. No written text. No value.	1
Traxler, F.C.	DUN-3955	"Fission Product Release Rate from Aluminum Clad Uranium Fuel," pages 11	03/22/68	Evaluates the release of fission gases Cs, I, Kr, and Xe from irradiated, full-size aluminum clad fuel elements from 400 to 1100 C in air and steam atmospheres.	1
Matheison, W.E., and Nicholson, G.A.	ARH-214	"PUREX Chemical flowsheet Processing of aluminum-Clad Uranium Fuels," pages 41	02/14/68	The PUREX flowsheet data for processing aluminum-clad fuel elements with U-235 enrichments less than 0.95%.	1
Leggett, R.D. and Kemper, R.S.	BNWL-CC-1444 Pt2 RD	Rough Draft of, "Status of Metallic Uranium Fuel Technology," pages 188	12/05/67	A synopsis of N-Reactor including three appendices only: Appendix A, N-Reactor Fuel Design; Appendix B, N-Reactor Fuel Fabrication; and Appendix C, Fuel Element Irradiation Performance. Gives program and testing summations which were specific to successful operation of N-Reactor.	1

Table B-1: Documents on Uranium/Zirconium Pyrophoricity (Relative value to N-fuels at K-Basin) [COGEMA 98-529]

Author	Document Number	Title	Date	Comments	Priority Value
Pearce, R.J.	R&D Dept. Berkeley Nuclear Labs	The Ignition of Uranium Part 1, A Literature Survey, pages 19	1966 or 67	Many generalizations in the survey of unknown data.	2
Baker, MM, LN Less, S Orman	Transactions of the Faraday Society, No.525, Vol. 62, Part 9	Uranium + Water Reactions, Part 1 and 2. Pages 18.	9/66	Effects of temperature, RH, and pH on uranium + water reactions.	3
Baker, L., JG Schnizlein, JD Bingle	J of Nuclear Materials, Vol 20 (1966) 22-38	The Ignition of Uranium. Pages 17.	2/28/66	Provides uranium ignition temps for small cubes, foils, and wires. No data on U/$H_2$0/Zr RXNs, UH_3, or aged fuel. See write-up.	3*
Cornell, D.L.	Hanford APO, RL-GEN-1120, Hanford Code C-44	N-Reactor Fuels Process Significant Events 1960 - 1966, pages 3	08/29/66	Tech. Library does not have copy. Only have Appendix III - pages 51 & 52. Documents 300 Area uranium oxide burner fires (4) and two fines/soot fires. See write-up.	2*
Johnson, A.B. Jr (BNW) and Hammond, J.E. (DUN)	BNWL-CC-1795	"Behavior of an Unirradiated Aluminum-Clad Uranium Fuel Element in a Simulated Failure Experiment," pages 32	12/20/65	An out-of reactor experiment to simulate process tube coolant flow loss. This experiment came as an investigation following an actual loss-of-coolant incident in a process tube at KW-Reactor. The experi-ment investigates interactions of the Zircaloy-2 process tube, aluminum fuel jacket, uranium core, and steam environment at 850 C.	1
Backman, G.E.	HW-84619	Summary of Environmental Contamination Incidents at Hanford, 1958-1964	4/12/65	Notes two fuel element discharge fires from ruptured fuel at 105KE and one at 105KW. Also noted are stack curie release info.	2
US- AEC	Summary Report WASH-1052 (Metal ignition and burning section only)	Nuclear Safety Research and Development Program. Pages 11.	11/64	A summation of several studies (no references). Much on fission products release, and Pu metal. Work done or to be done at ANL, BNFL, and ORNL.	2
Pensinger, DL (a)	Letter to HP Kraemer	Letter informing of fire, "Zirconium and Uranium Fire at Oxide Burner," 1 page	09/04/64	Drum of uranium turnings ignited. Gives weight of turnings, when drum was filled, and U enrichment. See write-up.	3*
Mishima, J.	HW-83668	"A Review of Research on Plutonium Releases During Overheating and Fires," pages 21	08/64	A review of literature on plutonium oxidation and ignition and general fire release parameters and data.	1
Pensinger, DL (b)	Letter to HP Kraemer	Letter informing of fire, "Zirconium and Uranium Fire at Oxide Burner," 1 page	07/31/64	Bucket of uranium containing 20 lbs. of fines atop 10 lbs of turnings ignited.	2
Evans, T.W.	HW-79040	"N Fuel Failure Behavior and the Role of the PRTR Rupture Loop in the N Fuel Failure Testing Program," pages 30	09/30/63	This document discusses contributions of the PRTR rupture loop installation in N-Reactor at a time when N-Reactor is over 80% complete, most fuel failure testing is complete, and R&D budgets are shrinking.	1

Table B-1: Documents on Uranium/Zirconium Pyrophoricity (Relative value to N-fuels at K-Basin) [COGEMA 98-529]					
Author	**Document Number**	**Title**	**Date**	**Comments**	**Priority Value**
Blasewitz, A.G.	HW-77654	"Radiographic Examination of Production Fuels," pages 8	05/17/63	Eliminate radiography, the lease valuable inspection technique, as a method of inspecting fuel end closures for an annual cost savings of $80K.	1
Gittus, J.H.	TN799.U7. G536	Metallurgy of the Rarer Metals-Uranium, London, Betterworths. Pages 14.	1963	Not sure if complete?	3
Zima, G.E.	HW-66930	Recent Zirconium Fire Experience at Hanford and the General Zirconium Fire Problem. Pages 9.	9/29/60	Zr-2 fires while machining C-Reactor process tubes. See write-up.	2*
Maffei, H.P.	HW-66911	"Failure of Coextruded Zircaloy-2 Clad Uranium Fuel Elements During Static Autoclave Testing," pages 4	09/27/60	Failure of coextruded Zircaloy-clad uranium fuel element during autoclave testing prior to reactor exposure.	1
Harmon, M.K.	HW-66850	Redox Dissolver Incident - Comprehensive Report. Pages 75.	9/13/60	Operational and production slanted. No specific data on fire or uranium fuel. Shows potential damage of water, HNO_3, and Uranium metal RXN. See write-up.	2*
Zima, G.E.	HW-62442, UC-25, Metallurgy & Ceramics	Hanford APO report, "Pyrophoricity of Uranium in Reactor Environments," pages 73	1/22/60	Probably the best Hanford summation of uranium/zirconium pyrophoricity but it is slanted toward reactor safety. The work is a result of reactor discharge fires. See write-up	3/4*
	Reactor Handbook	Reactor Handbook, Second Edition, Volume I, Materials, Interscience Publishers, Inc. New York, 1960 pp 127-133 pages - 7	1960	No copy	
Evans, T.W.	HW-62797	Post-Discharge Aqueous Corrosion of Failed Uranium Fuel Elements. Pages 8.	11/59	Failed uranium fuel storage evaluation for two month period only.	1
Hopkinson, BE	Corrosion Technology	Corrosion of Unalloyed Uranium By Water. Pages 5.	11/59		2
Swanson, J.L.	HW-62109	"An Estimation of the Explosion Hazard During Reprocessing of Metallic Uranium Fuel Elements Metallurgically Bonded to Zircaloy Cladding," pages 9	09/30/59	Dissolution of U-Zr alloys in nitric acid produces explosive residues of UZr_2. This explosive residue will not be formed when ammonium fluoride is added to the decladding step.	1
Schnizlein, J.G., et al	Argonne National Lab. - ANL-5974	An AEC R&D report, "Ignition Behavior and Kinetics of Oxidation of the Reactor Metals U, Zr, Pu and Th, and Binary Alloys of Each," pages apx 195	4/59		
Notz, K.J., Mendel, M.G.	J.Inorg. Nucl. Chem, Vol 13	X-ray and Kinetic Study of the Hydrogen Reduction of gamma -UO_3, pages 10	2/16/59		
Geering, G.T. and Worlton, D.C.	HW-57814	"Clad Splitting In Defective Zircaloy-2 Clad Uranium,"	10/16/58	Twenty-two Zircaloy-2 clad uranium fuel rods from Nuclear Metals, Inc. showed blistering or splits at areas where ultrasonic testing had indicated unbonded areas. A loose black powder, analyzed as UN and UO_2, was found under the blister that ruptured.	1
Evans, T.F.	HW-56403	"Continuous Pilot Plant Dissolution of Aluminum-Jacketed Uranium Fuel elements in Nitric Acid," pages 19	07/30/58	Operational characteristics of a 5-inch diameter tower experimental dissolver yielding dissolution rates of 50-60 lb U/hr for aluminum-jacketed fuel elements in HNO_3	1
Claudson, T.T.	HW-56832	Effect of Clad Stiffness Upon the Corrosion Rate of Uranium. Pages 7.	7/17/58	Short-term corrosion study calls for further study - no data useful.	1

Table B-1: Documents on Uranium/Zirconium Pyrophoricity (Relative value to N-fuels at K-Basin) [COGEMA 98-529]					
Author	**Document Number**	**Title**	**Date**	**Comments**	**Priority Value**
Aronson, S & Clayton, J.C.	J. Inorganic Nuclear Chem. 1958, Vol. 7	Kinetics of the Reduction of U_4O_9 in Hydrogen, pages 8	4/14/58		
Book, H.E.	HW-54351	Preliminary considerations Regarding Burning Slug Incidents, pages 4	01/02/58	Burning uranium slugs during reactor discharge.	1
Miller, N.R. and Kratzer, W.K.	HW-53226	"Production Test IP-119-A Irradiation of aluminum Jacketed Wafered Uranium Fuel Elements in the KER Test Facility," pages 11.	11/19/57	A production test proposing high temperature (250-300 C) corrosion testing for the NPR program of aluminum clad, Al-Si bonded, wafered, I&E uranium elements during irradiation at the 1706 KER Facility at KE-Reactor. No data.	1
Wyman, W.L.	HW-49857	"Projection Fuel Element Autoclave Rupture Test," pages 12	04/26/57	Autoclave testing (170 C and 100 psig) of fuel element rail support systems to determine which fuel support system will cause the least damage to process tubes at fuel rupture.	1
Smith, M.L.	HW-48013	A Survey of the Pyrophoricity Hazards of Rupture Fuel Elements, pages 11.	1/28/57	Reduce breakage of ruptured fuel slugs by developing better discharge techniques.	2
Gardner, H.R. and Riches, J.W.	HW-43543	"The Effect of Uranium Hydride Distribution and Recrystallation on the Tensile Properties of Uranium," pages 34	01/09/57	The effect of uranium hydride distribution, hydrogen concentration, variations in cooling rate, and recrystallization of beta-quenched uranium all have effect on tensile properties of uranium. However, the magnitude of the effects are rather small and may not be important.	1
Smith, R.B. (b)	Nucleonics, Vol. 14, No.12, pgs 28-33, Dec 1956	"Pyrophoricity - A Technical Mystery Under Vigorous Attack", pages 6	12/56	See write-up.	2*
Gardner, H.R., Riches, J.W.	HW-43428	"The Effect of Cooling Rate on the Nucleation and Growth of Beta-Uranium Hydride in Metallic Uranium," pages 28	10/12/56	The Jominy end quenching technique was used to study structural (in this case growth characteristics and nucleation of beta-uranium hydride) changes in the metal as a function of cooling rate using beta-heat treated uranium dingot metal specimens. For cooling rates ranging from 0.002 to 300 C/sec., the size of the hydride precipitate increased, and the number de-creased, with decreasing cooling rate. As many as 500 hydride inclusions per square millimeter can be formed at cooling rates of 6 to 20 C/sec. Metallographic examination also showed over 90% of the hydride inclusions form at grain boundaries. No relationship is made to irradiated fuel hydride formation.	3
Hoage, J. H.	HW-23562	"Material Loss in Ruptured Fuel Elements." Pages 1.	06/19/56	Examination of 130 ruptured fuel elements provided data that 9.5 ± 0.5 lbs were lost in ruptures, or 520 lbs. of fuel material.	2

Table B-1: Documents on Uranium/Zirconium Pyrophoricity (Relative value to N-fuels at K-Basin) [COGEMA 98-529]

Author	Document Number	Title	Date	Comments	Priority Value
Schultz, W. W., et al.	HW-32365	"Explosion Hazards in the Nitric Acid Dissolution of Uranium-Zirconium Alloy Fuel Elements," pages 8	07/20/56	Dissolution of Zr-U alloys containing low percentages is Zr in HNO_3 produces an explosive intermetallic compound - UZr_2.	1
Smith, R.B. (a)	TID-8011 AEC- The Industrial Atom	A Monograph entitled, "The Fire Properties of Metallic Uranium," pages 12	04/12/56	See write-up.	2*
Atwood, J.M., Hall, R.B, Nelson, S.L.	HW-40115	Recirculation Loop Slug Rupture Incident at 100-H, pages 10	11/22/55	Hanford 100-H reactor fuel slug rupture.	1
General Electric Co., Hanford Atomic Products Operation	HW-35942	Quarterly Technical Activities Report, Fuel Technology Sub-Section - January - March 1955, pages 5	4/3/55	Only Table of Contents, and pages 4.21 and 4.22 included.	
Schultz, W.W.	HW-34441	"Ignition of Uranium Metal in Air," pages 1.	01/13/55	Uranium ignition data in 50% O_2 - 50%Ar is provided. For "aspirin" sized pieces of uranium, ignition of unirradiated samples occurred at approximately 400 C, while irradiated samples ignited at approximately 320 C.	2
Pearson, H.E.	HAN-64841	1954 - AEC Uranium Fire Experience,	9/17/54	A research proposal document. Some good early information but with few references and several in 1943. It lacks depth and specifics about old U fuel and water RXNs. It states: "AEC Uranium Fires Cannot Presently be Statistically Studied Due to the Absence of Recorded Information."	2
General Electric Co., HAPO	HW-30780	"Evaluation of Uranium Hydride Compact Slugs," 17 pages	02/04/54	Fifty experimental slugs were manufactured from decomposed uranium hydride powder and compared to standard uranium production metal slugs. The pressed uranium powder slugs compared poorly to the uranium metal slugs.	1
Hartman et al.	US Bureau of Mines - Report 4835	The Explosive Characteristics of Titanium, Zirconium, Thorium, Uranium, and their Hydrides - Report of Investigation 4835, US Department of Interior	12/51	No copy	
Jones, K. & King,R.E.	Technical Department - AEC, 3-2026	Report on Production Test No. 314-11-M, Study of Abnormal Pyrophoric RU Rods, pages 3	4/4/45	This report deals with same event as Mr. Schier's 3/5/45.	1
Schier, R.J.	Atomic Energy Commission 3-1786	Metal Fabrication Study - Study of Abnormal Pyrophoric Rods - PT-314-11-M	3/5/45	Uranium "pyrophoric rods" extrusion yield and useability.	1

* Denotes a write-up on the document has been completed and is attached.

Historical Search for Hanford Spent Fuel, Metallic Uranium, and Zirconium Pyrophoricity Documentation - Contacts Listing

4/30/98
Called Ev Weakley (946-1365), Thurman Cooper (373-2543), and Mark Benecke (376-0002) and got no answers.

5/1/98
Able to get with retired Hanford employee Everett (Ev) Weakley (946-1365) and discuss if he had left a file of uranium/zirconium fire incidents with supporting documentation. He indicated he had developed a file over the years, going back to the 1940s, of uranium and zirconium fires and accident information that should be in the possession of Mark Benecke or Jerry Bishop. The file had Hanford specific data as well as other DOE sites, U.S., and foreign data. He retired in 1994 and indicated he was called back when the depleted uranium turning drums (618-4 BG) were discovered north of 300 area. He is a valuable information source for operational history of the 300 area uranium work. I will try to obtain the documentation file from Mark or Jerry.

5/4/98
Called Tom Thornton (373-6668) to see if he had copies of some of the references in his "A Summary of Some Uranium Metal Fuel Ignition Incidents and Their Relevance to K-Basin SNF Processing and Interim Storage" document.

5/4/98
Got with Mark Benecke at home to discuss the location of the Ev Weakely file. Mark said he had a file that he may have given to FFTF personnel, but he couldn't remember. He said Chuck Compestine (376-3311) an old 33 Building HPT may have some information also. Mark would look at work tomorrow for the file and call me back. Mark's work phone is 376-0002.

5/5/98
Called Scott Barney (373-2419) to see if he had any files on uranium/zirconium pyrophoricity work he may have done in the past to support Hanford fuels programs. Scott indicated he had never done any fuels work and remembered only literature searches conducted for SNF. I indicated I would talk to Thurman Cooper for any documentation or work results to support SNF uranium/zirconium reactivity.

5/5/98
Mark Benecke called and said he had found a file about uranium/zirconium fire and accident incidents. He indicated I could copy what I needed. He is still unsure about another file he

thought existed that also summarized all such incidents and may have been specific to Hanford. I urged him to continue to look for the file. I will pick up the one file before 12:30 pm this date and copy relevant documentation tonight.

5/5/98
Called Thurman Cooper and Chuck Compestine - no answer

5/6/98
Thurman Cooper (373-2543) returned my call. He had only been involved in the one uranium pyrophoric document and thought it had been released as an SD. I said I only had a draft and could he please check to see if the document was finalized. He called back and indicated the document was never released as an SD by was only at the draft stage. He was not familiar with others who had worked the uranium/zirconium pyrophoric issue for SNF.

5/6/98
Called Tom Thornton again about references; no answer.

5/6/98
Mark Benecke returned my call and said he had found another file on uranium pyrophoric issues dated from 1962 to 1966. He would look through it and see what was really in it. Mark called back and FAXed me an appendix from the only document that seemed to meet our needs. The other items in the file were incident reports from the 300 Area. The appendix from document "N-Reactor Fuels Process Significant Events 1060-1966" listed 13 events. Four were oxide burner (303M) Building incidents, six were alarms or false alarms, one was a fire in the exhaust ductdue to soot accumulation, one was a failure of the acid transfer line between 313 and 333 Buildings, and one was a belt sander caused uranium fire because the sander wasn't kept clean of fines. I will get the document anyway; it is RL-GEN-1120 by D.L. Cornell, 52 pages. Mark also thought about who he could have given the EV Weakley U/Zr pyrophoricity file to and came up with Al Pitner.

5/6/98
Called Al Pitner (376-9539) and left message. Also called Chuck Compestine (376-3311) back and got no answer.

5/6/98
Al Pitner called back and said he knew nothing about the file from Ev Weakley. I believe it might be worth getting Ev Weakley back and talk about incidents he recalls. Copies can be made of reference lists from several sources and highlight the ones with a bearing on N-Fuels SNF program as we talk about them.

5/7/98
Called Chuck Compestine and he indicated during his time at 333 complex (1979-1984) he remembers about six fires. He indicated there is a big file that has all of the information and pictures. I asked him to look for the file since he would know where it is and what it contains. I informed him that Mark Benecke loaned out a large file and can't remember to whom. Chuck hopes they are not the same file but does have his fears. Chuck will look for the file and call me back. Chuck, off the top of his head, recalls: the sander fire about 1991, the 3712 building fire from concreting uranium fines in the fall of 1979 (pictures in file), a 303K building fire from curing concrete containing uranium fines in 1981-82, and two fires from uranium dust in ducts.

5/7/98
Called Tom Thornton with no answer, Called Susi Heinisch to see if she can locate him. She was not aware of a Tom Thornton in the building; she will check and call me back. In the mean time, I will send a cc:mail to Tom asking for references from his summary document. (No tom Thornton on cc:mail.)

5/7/98
Susi Heinisch called back and said they believe Tom Thornton got laid off last year.

5/7/98
Called Tom Thornton's home phone (627-0246) and his wife indicated he was working in Las Vegas for Framatome doing N-Reactor fuel acceptance for Yuca Mountain. His number in Vegas is 702/295-4483.

SPENT NUCLEAR FUELS PROJECT N-FUELS PYROPHORICITY, IGNITABILITY, AND UH_3 FORMATION AND REACTIVITY REFERENCES VALUE RATING
May 28, 1998

1 - A reference with no specific data, relative to Hanford N-Fuels, concerning pyrophoricity, ignitability, storage, uranium/zirconium oxidation reactions at Hanford or other DOE complex sites, foreign sites, or domestic sites. This category would include safety documentation, assessments, and analysis conducted with specific, provided information to bound a certain condition.

2 - A reference providing general information on uranium/zirconium reactivity, general uranium accident information, uranium pyrophoricity and ignition temperatures and bounds, and UH_3 formation and reactivity. These references will not include information relevant to Hanford stored N-Fuels.

3 - A reference that provides specific data concerning uranium/zirconium metal pyrophoric nature and accidents providing material amounts, size, weight, surface area, pore size, particle size, conditions, temperatures, humidity, etc. A laboratory study concerning the nature of uranium/zirconium metal pyrophoricity , ignitability, hydride formation and reactivity that provides empirical data in specific detail to define the bounding conditions, limit, extent, and consequences of the experiment with repeatability to tabulate or graph the outcome. The data may be developed through tests with unirradiated or limited irradiated fuel testing.

4 - A reference of specific data, as with category three (3), but with data specific to irradiated fuel of other types (non-Hanford N-Fuels) from foreign (i.e. - BNFL) or domestic/ DOE sites. The irradiated fuel work need not be of a similar age to that of Hanford N-Fuels, i.e.- over 15 years in pool storage.

5 - A reference providing specific data with direct information concerning pyrophoric irradiated fuel incidents relevant to the type, condition, or age of K-Basins N-Fuel storage.

COGEMA-98-529

ENCLOSURE 4

Summaries from Documents Listed on Table in Enclosure 1

Consisting of 35 pages,
Including cover sheet

The Fire Properties of Metallic Uranium

Smith, R.B. (a) 4/12/56
Priority Value = 2

In a facility for the manufacture of metallic uranium powder, some of the powder accumulated in a sump under about 25 feet of water. The powder would accumulate for about a month, then suddenly and spontaneously react violently, producing a "30 ft high geyser" in the sump. After subsidence and cleanout new powder would accumulate for another month or so, and the violent reaction would be repeated.

Key points/unknowns:
- Explosive reaction occured under water
- Sump water oxygen-equilibrated
- Unknown chemical composition of powder
- No explanation of 'critical volume' effect

A series of fires had occured in 55-gallon drums containing metallic uranium chips stored in air. On one occasion during the inspection of the contents of a drum, an investigator observed nothing out of the normal (ambient temperature, chips quiescent) but was nevertheless warned by an experienced operator to "stand back" from the drum. Moments later a 25 foot high column of flame shot up from the drum and the contents became incandescent.

Key points/unknowns:
- Drum contents quiescent just before explosion
- No mechanical perturbance noted
- Uranium chips stored in air environment
- Unknown hydride chemistry of chips after air storage
- Unknown duration of storage
- No mention in reference of whether other fires occurred only when drums were opened

The Fire Properties of Metallic Uranium

Smith, R.B. (a) 4/12/56
Priority Value = 2

Two batches of uranium metal powder were successfully experimentally treated with carbon tetrachloride to render them non-pyrophoric. When a third, slightly larger, batch of the same powder was treated in the same way, it exploded violently and severely injured the experimenter.

Key points/unknowns:
- Expectation of passivation becomes sensitization instead
- Quantity of powder may have been the key factor
- No explanation of handling method was given

Some scrap uranium metal was 'oxidized' for shipment. After shipment the 'oxidized' material spontaneously ignited when the package was opened and the contents exposed to air, consuming the container packing material. "Pieces of burning metal" were observed in the package.

Key points/unknowns:
- Preoxidation was obviously incomplete
- Spontaneous ignition
- Method of 'oxidation' unknown

Specimens of low density, porous (about 15 g/cc) uranium metal spontaneously ignited in air at ambient temperature after resting uneventfully for several days on a shelf.

Key points/unknowns:
- Spontaneous ignition of highly porous uranium metal
- Unknown degree of corrosion
- Unknown storage condition (canned?, open?)

The Fire Properties of Metallic Uranium

Smith, R.B. (a) 4/12/56
Priority Value = 2

Stainless steel cans containing loose, dry uranium metal chips had been stored uneventfully for about 6 months at ambient air conditions on a shelf. The area of the shelf then was accidentally heated to about 105F for a short period. The overheating was stopped, the cans checked and found to be unaffected, and the area apparently returned to normal entering a weekend. After the weekend the cans were found to contain burn holes and about 6% of the uranium had been oxidized.
Key points/unknowns:

- Slight overheating apparently induced accelerated reaction
- Not all the uranium oxidized, despite apparent unlimited air supply
- Unknown chemical composition of uranium

Pyrophoricity - A Technical Mystery Under Vigorous Attack

Smith, R.B. (b) 12/56
Priority Value = 2

In 1951 at Oak Ridge Y-12 some zirconium powder, originally stored in wooden barrels which had deteriorated, was intentionally wetted with water and repackaged in steel drums. Several years later one of these drums was observed to display a black powder similar to carbon dust. Shortly after this observation, this drum spontaneously exploded with red fire, smoke billowing to over 100 ft, and a pronounced concussion blast. Two people were killed and a third seriously injured. Later, during controlled oxidation of the remaining drums, and in spite of extensive precaution, another drum exploded.

Key points/unknowns:
- Powder observed was probably zirconium hydride
- Ignition initiator unidentified
- Unknown purpose of wetting powder

During removal of the top of a one gallon, polythene-lined, metal can containing zirconium powder known to be contaminated with about 16% water, the can exploded in a ball of flame accompanied by a concussion wave. Two people were killed and two others seriously injured.

Key points/unknowns:
- Unknown ignition initiator
- Unknown source or purpose of water contamination

Pyrophoricity - A Technical Mystery Under Vigorous Attack

Smith, R.B. (b) 12/56
Priority Value = 2

Three unirradiated, flat, 1/4" thick uranium fuel plates - made by powder metallurgical techniques - were found to have become extremely swollen. The swelling was attributed to incomplete decomposition of uranium hydride (presumably the material precursor for the uranium metal plate) during hot pressing. This subsequently resulted in a buildup of hydrogen pressure within the plate, swelling it to nearly the shape of a rod. One day after discovery of the swollen plates, one of them spontaneously "exploded and took off like a rocket".

Key points/unknowns:
- Hydrogen gas ignition identified as source of explosion
- Plates extensively swollen as a result of internal hydrogen pressure

For an extensive period of time no fire problem had been experienced at a facility for the storage of scrap zirconium in physically segregated open bins. Then several days after a heavy rain in May 1955 one bin caught fire with flames shooting to 100 ft in the air. Several non-adjacent bins then caught fire and before long all bins were burning, ultimately resulting in the virtually complete consumption of the zirconium. The heat generated was intense enough to thermally ignite wood and crack windows over 150 ft away.

Key points/unknowns:
- Initiator of ignition undetermined
- Fire uncontrollable once started
- Unknown whether hydride played a role

Pyrophoricity of Uranium in Reactor Environments

Zima, G.E. 1/22/60
Priority Value = 3/4

The document provides a summary of uranium pyrophoricity work, at Hanford and other DOE sites. The work, however, is the result of reactor spent fuel discharge fires at Hanford. Included, with substantial references, are uranium corrosion data; UH_3 formation and reactivity data; uranium-hydrogen reaction product ranges; effects of aluminum on uranium reactivity; and uranium physical properties, dynamics, and chemistry.

The intent of the document was to "review some of the current information relative to the pyrophoricity of uranium and to attempt to identify some aspects of its troublesome phenomenon which can support further investigation". "The fortunately low incidence of metallic uranium fuel element fires, up to the present, does not suffice as an adequate base for extrapolation to future operations because of existing uncertainty with respect to both causative mechanisms and fire control techniques".

The chemical reactivity of metallic uranium has been manifested in pyrophoric behavior and oxidation reactions of explosive violence. At least one compound, UH_3, has demonstrated comparable reactivity and there is indication that some pyrophoric sensitization can be acheived by certain alloying elements.

The experience at Hanford reactors suggests conditions which tend to reduce the fuel element fire hazard. These are:

1. Minimizing the in-core residence time of a fuel element with a cladding defect which permits uranium corrosion.
2. Employment of removal and discharge techniques which do not contribute to the deterioration of the fuel element.
3. Minimizing the time interval between fuel discharge and entry into the retention basin.
4. Installation of permanent modifications to the fuel discharge area.
5. Development of a practicable quench gas or inert foam blanket for use during discharge operations.

The determined factors affecting pyrophoricity are:

a. The inherent reactivity of the active substance and the heat release per volume of reacting material.
b. The specific area (A^*_p) of the reacting particles.
c. The physical and chemical coupling among reacting particles.
d. The rate of exposure of active material.
e. Subsidiary heat producing reactions, such as the combustion of hydrogen.
f. The cooling and oxidizing potentials of the environment.

The pyrophoric factors related to uranium were found to be:

a. The U-air reaction satisfies the ignition requirements for reactivity and heat release over a wide range of environmental conditions. In uranium/water reactions the hydrogen generated can augment the hazard potential either as free H_2 or in the compound UH_3.
b. The effects of irradiation on the pyrophoricity of uranium remains obscure.
c. Aluminum, in small concentrations, has shown an ability to significantly lower the ignition temperature of massive uranium.
d. Helium has been found effective in inhibiting and quenching uranium and UH_3. ignition.

REDOX Dissolver Incident Comprehensive Report

Harmon, M.K. 9/13/60
Priority Value = 2

This report provides an of the REDOX uranium dissolver fire incident. The incident, caused by allowing approximately 50% of the bare, irradiated fuel slugs in the dissolver to become above the water surface, resulted in failure to the inner dissolver stainless steel shell from the burning uranium slugs and an over-pressurization in the dissolver which blew the lid off.

The evaluation of the incident concluded the first-cut dissolution fuel had etched surfaces higher in area-to-unit weight ratio then that of original fuel surfaces. The uncovered metal fuel gradually heated by the decay of fission products. The poor heat transfer caused the fuel surface temperature to rise from about 80° to about 150° C. At these temperatures, the reactions with oxygen and saturate water vapor atmosphere in the dissolver became significant. The fission decay heat and the heat of reaction continued to about 300° C where oxidation reactions proceed rapidly dependent on reacting gases penetration of the oxide scale. Ignition then occurred by oxide scale interaction with nitric acid or frictional movement. The fire was enhanced by sudden uranium hydride exposure of the etched fuel surface to the oxidizing gases.

At the time of the incident the dissolver was filled with 10.98 tons of irradiated fuel of which 5.5 tons was not covered with the water/acid solution. The aluminum-clad (E-metal) fuel had undergone its first decladding cut (addition of 50 to 100 lbs of 60 N of HNO_3 per minute). It is reported that the dissolver solution reached its final specific gravity for the cut prior to completing acid addition. The resulting raw metal solution was then removed from the dissolver and about 400 gallons of water were added to the dissolver. (Normal operating level for the dissolver was 1,050 gallons.) The dissolver was then allowed to remain idle due to lack of storage space for additional raw metal solution. The 5.5 tons of fuel had been exposed to the moist air of the dissolver for about 30 to 36 hours. During the resultant uranium fuel fire and overpressurizations, the facility ventilation system had a 300-fold increase in gamma activity for approximately two hours.

About 10:00 am on April 17, the temperature of the dissolver and silver reactor inlet began to rise. The seal pot was blown and vacuum reading were sporadic. These activities seemed to cycle throughout the day until process parameters were all again under control at 7:40 pm. At that time 60 % HNO_3 addition was started. The reaction in the dissolver became so violent that the acid addition was shut off after only 20 gallons had been added (1,000 gallons were intended to be added). Cooling water was started to the cooling coil to regain the weight factor reading, which had been lost. The weight factor began increasing signifying a probable leak in the cooling coil. Operation became more erratic. A distinct rumbling was heard in C-cell. Cooling water was put to wide open. As the weight factor rose, an alpha monitor in the dissolver pot cooling water discharge sounded indicating gamma activity in the discharge water. The dissolver temperature decreased and cooling water was shut off. A second and third rumbling were heard from C-cell at about 15 minute intervals. Liquid level dropped in the dissolver and rose in the sump. 3,000 gallons of solution were subsequently removed from the sump.

REDOX Dissolver Incident Comprehensive Report

Harmon, M.K. 9/13/60
Priority Value = 2

About five hours the cell block was removed and the cell inspected. The dissolver lid was detected laying upside-down on the dissolver but no other visible damage was evident. The uranium reaction resumed about seven hours later noted by raising temperatures. 1,500 gallons of water were added followed by a vigorous reaction and dissolver pressurization. At 10:00 am on April 19, the cell block was again removed for cell inspection and to replace the dissolver lid. High canyon activity readings were given so work was halted so no further contamination would be spread.

This report, originally released as a secret report, provides details of the incident, operational loss of control indicators, dissolver examination and evaluations, recovery plans and recommendations, and system deficiencies. The report provides little material specific description. Without any material specific details, other than production and operation oriented, the report becomes as little value to the SNF work scope.

Recent Zirconium Fire Experience At Hanford and the General Zirconium Fire Problem

Zima, G,E, 9/29/60
Priority Value = 2

This paper reviews recent fire experience in zirconium (Zr-2) process tube installations at Hanford's C-Reactor. Zr-2 process tubes require ex-reactor trimming and machining prior to installation. The paper supports zirconium ignition with small particles: chips, turnings, pieces of zirconium. It provides the size of zirconium ball of turnings, about 1.5 inches in diameter, that ignited and could not be extinguished with water. Turning sizes are not given nor are any other descriptions of the turned zirconium, such as: continuous, broke into pieces of X length as it was machined, etc. Here is no mention of any particulates being formed. The paper demonstrates zirconium is pyrophoric and the pyrophoricity is enhanced through hydrogen ion capture from water. This paper provides little for N-Fuels U-Zr-2 reactions or increased reactivity from UH3 formation.

Zirconium and Uranium Fire at Oxide Burner

Pensinger, D.L. (a) 9/4/64
Priority Value = 3

This reference documents a drum of uranium/zirconium turnings spontaneous ignition and fire. The drum was on a pallet with four other drums of turnings that were delivered to the 303L oxide burner facility. The drums came from the HL Specialty Shops. Prior to this time the drums had been stored in the 306 building barrel storage area without a liquid covering. The drum lids were removed, one drum at a time, until four lids were off. After all lids were removed the technician would fill the drums with water to cover the turnings in preparation for feeding the turnings to the oxide burner. As the technician removed the fifth drum lid, the drum ignited with a "swoosh". The technician dropped the lid back on the drum and covered the drum with a fire barrel. None of the other four drums on the pallet ignited or burned.

All drums were suspected of being 30-gallon drums, since only four 55-gallon drums will fit on a standard 40 in. X 48 in. pallet. The drums were filled with the turnings on June 23, 1964. It is reported that the drum contained 70 pounds of .947% enriched uranium and zirconium turnings.

This has been the only report discovered that has given age of turnings, weight of turnings, drum size, exact storage area and condition, generator, and that the drum contained enriched turnings and no fines.

N-Reactor Fuels Process Significant Events 1960 - 1966

Cornell, D.L. 8/29/66
Priority Value = 2

Only Appendix III of the document (pages 51 and 52) was found. It contains a few sentence summation of each of the 300 Area uranium fuel fabrication related incidents from 12/11/62 to 5/20/66 . Neither the WSU Technical Library nor the DOE Public Reading Room has a copy of the document.

The appendix lists 13 reported incidents of which six may be of interest to SNF Program. However, the 13 reported events appear not to be a complete listing because Pensinger (1964b) reports a 7/23/64 U/Zr fire outside the oxide burner. D.L. Cornell was also on distribution for the Pensinger (1964b) letter.

The six incidents of interest include: four oxide burner fires (8/6/63, 9/3/64, 1/27/65, and 5/20/66); an exhaust duct fire (1/9/63); and the belt sander igniting U/Zr fines (5/27/64). Pensinger (1964a) reports on the 9/3/64 incident at the oxide burner (see Pensinger 1964a write-up). Of the other three oxide burner fires, two involved U/Zr fines fires in drums and the third incident involved accumulated uranium chips that spontaneously ignited in a crack at the oxide burner pad. There is no mention of the amount of uranium in the drums nor if they contained fines and turnings/chips. There is also no information given on how long the durms had been filled, or where or how they had been stored. The 8/6/63 event does indicate it was a 30-gallon drum covered with coolant and water. The other two events deal with fines and soot (assumed to be uranium) ignited spontaneously or , in the case of the belt sander, by inadequate coolant flow due to a broken copper water feed line. Both cite poor house-keeping as the reason for accumulation of fines, dust, or soot.

Collectively, these incidents provide little in defining bounding circumstances for uranium metal ignition or fires.

The Ignition of Uranium

Baker, L., JG Schnizlein, JD Bingle 2/28/66
Priority Value = 3

The paper explores and supports previous data on the ignition of pure uranium, ANL uranium (beta-quenched uranium supplied by Argonne National Laboratory), and BMI uranium ("as-cast" uranium supplied by Battelle Memorial Institute). The tests were conducted in air and several gas mixtures (oxygen enriched, oxygen-helium, oxygen-air) and confirmed the ignition temperature was very close to 600 ° C. for an 8.5 mm cube of uranium heated in a 1-inch ID Mullite reactor. The uranium purity of the samples ranged from 75 ppm impurities (high purity uranium) to 250 ppm impurities in the ANL and BMI uranium.

Also tested were smaller samples of uranium metal in the form of wires and foils. Ignition temperatures decreased with sample size. The testing, conducted on a series of cubes, wires, and foils with specific areas of 0.3 to 120 cm^2/g , yielded an irregular decrease in ignition temperature from 640 to 315 ° C in oxygen. It was concluded that uranium ignitions in air and oxygen are thermal ignitions which can be explained in terms of a balance of heat losses and heat generated by the oxidation reactions. Also, larger specimens, especially in cylindrical form, do not ignite in a well-defined manner in air.

The paper presents data that a uranium metal burn in air differs greatly from a burn in oxygen. The burn characteristics of uranium in air show a thermocycle effect until the uranium cube is consumed while uranium in an oxygen atmosphere continues to burn at white heat until the uranium sample is consumed. The uranium burn in air thermocycles from about 700° to 1100°C while the uranium in oxygen burn will exceed 2,000°C.

The text provides specific sample dimensions; specific area; and resultant ignition temperatures, burn characteristics, thermocycle nature , and burn temperatures. The text also supports helium deluge as a means of terminating uranium burn experiments.

Shear-Leach Processing of N-Reactor Fuel--Cladding Fires

Schulz, W.W. **2/15/72**
Priority Value = 3

A significant fraction of the spent (1000 and 3000 MWD/MTU) N-fuel elements sent to West Valley NFS in 1967-68 for reprocessing arrived in an unexpectedly broken/corroded condition. (In this reference the corrosion product was assumed, but not analyzed, to be uranium dioxide.) At the time of shipment from Hanford the fuel was reported to be uncorroded, unruptured, and intact. At receipt at West Valley much of the fuel was found to be broken/corroded. Nineteen instances of ignition occurred at some time during processing at NFS; 14 during processing in the dissolvers; 4 on defueled cladding in ambient air in the receiving bins during the dumping operation, and one on pieces of defueled cladding when accidentally dropped on the receiving canyon deck.

The dissolver fires were not directly visually observed but were indicated by large holes burned through the dissolver basket walls. It was concluded that the cause of the fires was the accelerated reaction of the nitric acid in the dissolvers with the broken/corroded fuel. This accelerated reaction resulted in ignition of the fuel pieces near the top of the dissolver and the consequent burn through the dissolver walls. It was concluded that the initiator of ignition of the material near the top of the dissolver basket was mechanical shock due to metal-to-metal contact. This resulted from the turbulence/shaking induced by the rapid dissolution reaction in the lower part of the dissolver.
The bin fires were visually observed and had the physical appearance of "burning charcoal". It was concluded that ignition was due to mechanical shocking of zirconium hydride and/or uranium hydride near the 'sensitized' weld-bead end caps of the fuel cladding. This judgement was supported by subsequent electric spark ignition testing of the sensitized Zircaloy cladding, which showed it to be prone to violent ignition, desribed as "detonations". The Zircaloy sensitization resulted from the chemical extraction of the uranium and/or beryllium from the Zircaloy, resulting in a porous metal matrix with a high surface area per unit volume.

It was found during the study of these events that dipping sensitized Zircaloy cladding in aqueous caustic solution de-sensitized the material.

Shear-Leach Processing of N-Reactor Fuel--Cladding Fires

Schulz, W.W. **2/15/72**

Priority Value = 3

Key points/unknowns:

- Fuel element corrosion resulted in dramatic increase in chemical reactivity in the dissolver compared to uncorroded fuel
- 'Sensitization' of Zircaloy due to removal of uranium and/or beryllium from weld zone
- Ignition at top of dissolver due to metal-to-metal contact; i.e., mechanically induced
- Ignition in bins caused by mechanical shock of uranium/zirconium hydride in air
- Unknown relative role of 'sensitized' zirconium versus uranium hydride

Summary of Some Incidents Involving Uranium Fires

Brown, V. 5/1976
Priority Level = 2

Magnox fuel elements which had been stored for four months in sealed bottles which had leaked dissolved unusually vigorously and rapidly in the dissolver trays during processing at Sellafield. The consequent rapid exothermic reaction rate in the nitric acid caused failure of the dissolver's internal cooling coils and seals and thereby flooded the fuel with the cooling water. This in turn resulted in a hydrogen buildup from the rapid corrosion of the uranium metal, which then resulted in a hydrogen/air explosion that separated and inverted the dissolver lid. When the dissolver was subsequently being drained the upper half of the fuel in the trays was exposed to air and dried out, and the fuel ignited. The fuel ignition was attributed to sudden exposure of uranium hydride, which had formed due to corrosion of the fuel in the leaking storage cans, to the air.

Key points/unknowns:

- Fuel was more corroded than normal due to the four months of water storage
- Corroded fuel was more chemically reactive in dissolver than uncorroded fuel
- Sudden exposure of uranium hydride to air caused fuel ignition at ambient temperature
- Drying of hydrided fuel in the upper part of the dissolver made it more prone to ignition
- Unknown whether first ignition of hydrogen-air mix was thermally or mechanically initiated

Summary of Some Incidents Involving Uranium Fires

Brown, V. 5/1976
Priority Level = 2

A Bradwell reactor Magnox fule element, in what was supposed to be a sealed storage can delivered to Berkeley labs for examination, ignited in air at ambient temperature during de-bottling. When the bottle was opened water was observed in the bottle along with particulate material assumed to be corrosion product. The bottle had apparently leaked during storage and/or transport, allowing corrosion of the fuel element inside. This observation was shortly followed by self-sparking and ignition of the fuel element. Examination of the can after removal of the fuel element showed internal surface corrosion had occured. It was concluded that the fuel element had ignited due to sudden exposure to air of uranium hydride which had formed as a result of the corrosion.

Key points/unknowns:
- Fuel corroded in a closed environment, forming uranium hydride
- Ignition due to sudden exposure of uranium hydride to air
- Unknown whether ignition thermally or mechanically initiated

An aluminum 'crimped can' storage container for Chinon reactor metallic uranium spent fuel elements, supposedly sealed, exploded during transfer from the storage pond to the decanning pond. No specific explanation of the accident sequence was provided but it was concluded that hydrogen buildup due to uranium corrosion and subsequent reaction with leaking air was the cause. A subsequent investigation showed that unirradiated fuel elements corroded readily inside sealed cans containing demineralised water until the gas in the can became 100% hydrgogen. The investigation also showed that irradiated fuel (6000 MWD/T) reacted so rapidly in pH 11.5 pond water that it noticeably swelled and formed a powdery corrosion product that ignited readily when dried.

Key points/unknowns:
- Unknown whether corrosion product hydride played role in ignition
- Unknown initiator of transfer can ignition

Analysis of the Safety and Technical Performance of the UNC Nuclear Industries Concretion Process

Moore, R.H. 8/25/82
Priority Value = 3

Summary

At Hanford, three instances have occurred wherein concreted uranium billets, sealed in cans, have autoignited.

The UNC concretion process has been reviewed to determine the reason for billet deformation and can splitting, to evaluate the hazard of further operation of the process and for shipment of materials on hand, and to recommend for, or against, resumption of operations.

It has been found that billet deformation and can splitting results from the use of a high temperature curing cycle, which causes substantial oxidation of uranium. This produces high volume, incompressible oxides that places the concrete in direct tension at forces sufficient to rapture the concrete. The resulting expansion splits the cans at a vertical crimped seam.

Early Experience 1971 - 1979

The Concretion Process supplanted the "Oxide Process" in 1971 due to difficulties in control of dust contamination with the latter. At the onset of the Concretion Process, lathe turnings were crudely mixed with saw fines in a ration of about 3:1, which approximates the ratio in which they are produced. These materials were not accurately weighed but were dumped out of the 30-gallon drums in which they had been stored under water, and into which they had originally been weighed. The mixture of metals was combined in a rotary cement mixer with masonry cement of composition shown in the text. Cement and water were simply added until a mix of proper consistency for pouring resulted. The mix was poured into metal cans of 0.97 CF volume (3 cans per batch). The cans were allowed to stand in air for seven days to allow the cement to cure. Lids were installed, taped for sealing, and the cans were packed in wooden crates, 2 cans to a crate, and stored until shipped.

On August 8, 1977 six recently concreted billets were found to have split open during the 7-day curing process. In the absence of other combustibles, there was no fire. The heat of the burning metals, however, reduced the billets to powder.

On July 23, 1979 a fire occurred in crated billets in the 3712 warehouse building. The fire was concluded to have centered in 12 crated billets, which were the most recently processed material stored in the warehouse. The curing process was stated to have generated sufficient heat to disrupt the integrity of the concrete billet, exposing uranium. The investigation also disclosed that these billets contained a higher weight of fines (over 100 lbs) than typical of recent experience.

On March 13, 1982 a fire occurred involving 12 concreted billets in the 303-K building. These were 97 hrs. into the final stage of the high temperature curing cycle that was operating at 61°C (142° F). These billets were found to have been placed on wooden pallets in violation of normal procedures. These became involved in the fire and very probably caused propagation of uranium autoignition from billet to billet.

Pacific Northwest Laboratories began an investigation on June 28, 1982.

- All billets in metal cans have swelled or distorted so as to split the cans. The side seams are open, often more than an inch in width.
- Many billets in plastic cans exhibit swelling and distortion. The plastic material stretches to accommodate the distortion and does not rupture.
- This problem has led UNC to go to the use of polyethylene cans (165 mil wall thickness).
- It appears that swelling and distortion of the cement billets results from reaction of uranium metal (and zirconium metal) with moisture.
- All of these reactions are exothermic and lead to products (oxides) whose volume greatly exceeds the volume, by as much as three times, of the metals from which they are derived.

E.A. Weakley has stated that these billets weigh only about 120 lbs. total. They contain on average about 40 lbs of uranium. A rough calculation shows this would occupy a volume of about 0.034 ft' so the remaining volume (0.97-0.034=0.936 ft^3) is cement weighing only 80 lbs. In short, the cement has a density of only 1.37 g/cc instead of the expected 2.0-2.2. This low density is due to the extreme porosity revealed by the photomicrographs. These gas bubbles had to form during mixing and casting, and prior to the initial set of the cement. They comprise an estimated 36 percent of billet volume, i.e., 0.34 ft^3. Conventional masonry cement would contain 2-6% porosity due to air entraimnent. It would be reasonable to conclude the gas responsible for most of the bubble formation is hydrogen. Approximately 0.0008 pound moles of H_2 would be produced by reaction of only about 0.095 lb. of uranium. This amount of reaction could conceivably occur during mixing, pouring, and initial setting time (apx. 1.5 hours total).

Photomicrographs in the text are very revealing. Very small particles of uranium are extensively oxidized. Extensive cracking of the concrete near these particles is also clear. These are very small cracks but they must be very large in number. Oxidation has produced cracking in the cement. Small particles of metal show extensive oxidation. The smaller particles react much more rapidly and completely than the larger particles. Detailed inspection of these photos shows that most of the small particles of metal have completely oxidized.

The swelling of billets and splitting of cans is due to the internal stresses generated in the cement by reaction of the metals with water or hydration. Such swelling did not occur when the billets were not subjected to elevated temperature curing, as in the 1971 - 1979 period.

Safety Aspects of Procedural Changes

Prior to 1979, the billets produced retained a high degree of integrity, probably contained fewer cracks than those now being produced, but were demonstrably capable of ignition at temperatures below 66° C (150° F). The present process with its high temperature curing cycle, essentially a "bum test," yields a product that will not be likely to autoignite unless exposed to higher temperatures than those used in the curing cycle. Further, and this is most important, a substantial fraction of the uranium and zirconium will have already converted to oxide. Higher temperatures will be required to ignite the remaining and less reactive materials. Should ignition occur, the temperature rise within the billet will be substantially less than would be the case if no pre-oxidation had occurred.

The controlled curing cycle that entails heating over a 26 day interval to about 150° F will inevitably involve the possibility of autoignition of a billet. The phenomenon of autoignition differs from the slow process of oxidation occurring during the curing cycle. The latter appears to be a diffusion controlled reaction with water vapor diffusing through the cement. Autoignition appears to occur when the temperature reaches a level high enough to trigger a reaction between the metals and water of hydration. The metals and water bound as water of hydration are in direct contact and the reaction proceeds as a solid-solid reaction, and at a much higher rate than the diffusion controlled reaction. Reaction with oxygen from air plays only a minor role after the cement has disintegrated.

The controlled bum tests on special experimental billets, as well as on production billets show only one billet (no fines present) could withstand a temperature of 93°C (200°F). At temperatures as low as 63°C (145°F) the test results showed two autoignitions in eight tests. One of these was a billet containing 2 lbs of unmixed fines in the middle of the billet. The other was a heavy fines to chips ratio billet cured only 5 days at 39°C.

It would be possible to significantly reduce the hazard in this process by eliminating the processing of saw fines. "Chips only" billets that have undergone the complete curing cycle presently in place, and that are limited to no more than 50 lbs of uranium total per billet, would be much safer to process.

Material Stored Under Water in Drums

When finely divided uranium reacts with water, both $U0_2$ and H_2 form. The latter can react with additional uranium to form uranium hydride; however, a hydrogen pressure exceeding one atmosphere is required. This process tends to disintegrate the metal to yield still finer metal particles - which are even more reactive.

U and Zr saw fines from the oldest stored drum (01/12/82), the newest stored drum (06/28/82), and two intermediate dates (03/09/82 and 05/03/82) were sampled and screened. The four samples were wet screened from +40 mesh to -100 mesh. As suspected, both uranium and zirconium are concentrated in the fines with increased time of storage. If present as finely divided uranium metal, this would represent and even greater hazard. The data shows these stored wastes continue to undergo reaction and change under these conditions of storage.

The high temperature curing cycle produces substantial conversion of metal to oxide. The oxide occupies at least twice the volume of the metal from which it is derived, and is incompressible. Formation of the oxides causes the distortion of the billets and splitting of metal cans.

Air oxidation only becomes a factor if the rate of reaction of metal with water, including water of hydration, becomes rapid, as in the case of autoignition, so as to disintegrate the concrete structure.

Laboratory Studies of Shear/Leach Processing of Zircaloy Clad Metallic Uranium Reactor Fuel

Swanson, J.L., et al 12/85
Priority Value = 2

The document summarizes several aspects of shear/leach documentation dealing with the processing of N-Fuels. Several chapters contain very complete reference sections, particularly chapters 6, 7, and 9. The text summarizes the results of the cited literature in each chapter. Most of the text deals with dissolution of N-fuels but later chapters provide some generalized statements concerning uranium porosity and pyrophoricity, nothing quantitative.

Several dissolution curves are given for 3M to 9M HNO_3 at several temperatures. The results conclude the dissolution of the uranium produces a roughened surface having an area 3 to 4-fold higher that the initial as-cut area. No correlation is given to water reactions of broken fuel in the basins and postulated surface area increase due to hydrogen embrittlement or hydride attack.

Near the end of dissolution, black solids flaked off cladding at what would be the Zr/U interface. The solids were about 6 to 8 mm in diameter and were analyzed to contain equal weights of U and Zr. One specimen did flash when induced by a spark from a Tesla coil while others did not. These reactant solid remains were observed after dissolution of unirradiated fuel. No mention was ever made of observing the black solids flakes on fuel stored in the basins. Solbrig, et al, 12/94, reports that UH_3 is a loose, fine, black particulate.

Zirconium and uranium can react rapidly with either oxygen, nitrogen, or mixtures of these gases. Cited literature reports that fire extinguishing properties of argon with burning uranium is effective while nitrogen gives an initial intensification of the burning uranium. Therefore, nitrogen is not recommended.

The text discussed the reaction of unreacted UH_3 and finely divided UO_2 with nitric acid to produce possible run-away reactions at dissolution. The text mentions only hydride production as a possible cause of cladding rupture while in storage. No quantitative values are given.

Corrosion of Reactor Grade Uranium in Aqueous Solutions Relevant to Storage and Transport

Tyfield, S.P. **4/88**
Priority Value = 4

The aqueous corrosion of Magnox uranium fuel has been studied to ensure safe storage and transportation. The corrosion rate of the irradiated uranium fuel is related to temperature and to the degree of irradiation swelling. The spallation of the corrosion products, the formation of uranium hydride, and the release of fission and activation products is reported.

The study was to measure the corrosion rate of uranium fuel in terms of hydrogen evolved as a function of irradiation swelling, temperature, fuel elemental composition, and water chemistry. The examination of the release of fission and activation products to solution during uranium corrosion was conducted. Both unirradiated and irradiated uranium samples were tested. Irradiated samples were 7mm x 5mm x 2mm while unirradiated fuel samples were sections of the fuel rod weighing about 7 g.

The corrosion kinetics were studied using Magnox fuel storage pond water, approximately pH 11.5 (0.2 kg/m^3 sodium hydroxide) and transport flask water (storage pond water with 1 kg/m^3 fluoride added as a corrosion inhibitor).

The results showed that the aqueous corrosion of irradiated reactor grade uranium is generally similar to that of unirradiated fuel but with two significant differences. First, the rate of irradiated uranium fuel corrosion is enhanced, relative to surface area. This enhancement is the result of the increase in the reaction surface area with the extent of irradiated induced swelling Second, the aqueous corrosion of irradiated is accompanied by release of fission and activation products in solution, notably Cs-137, Cs-134, and Sr-90. Measuring the release of the radionuclides to solution provides a convenient and sensitive method assessing the corrosion rate of irradiated fuel.

The constant uranium corrosion rate noted in this study, in the presence of water and sodium hydroxide, occurs at the thin adherent film of the uranium fuel. The thin film is considered to disrupt above a certain thickness, due to stresses built up with growth, thereby producing an outer friable corrosion product. Hydroxide ions, rather than oxide anions or water molecules, are considered to be the mobile species in the adherent oxide.

Recent Studies Related to HeadEnd Fuel Processing at the Hanford PUREX Plant

Swanson, J.L. **8/88**
Priority Value = 1

During 1986-87 operating problems were experienced in the processing of N-fuel elements which had been stored underwater for longer periods than usual prior to shipment to the PUREX plant. It was found that fuel which showed extensive corrosion reacted much more vigorously in the dissolvers than fuel which had much shorter water storage times and consequently less corrosion. The high reaction rates with the dissolver nitric acid resulted in foaming, overheating, and dissolver control difficulties.

It was noted that at comparable burnup values, corroded fuel displayed significantly enhanced chemical reactivity compared to uncorroded fuel. This enhanced reactivity of the corroded N-fuel was ascribed to an enhanced effective surface area-to-volume ratio resulting from the corrosion process.

Key points/unknowns:

- For equal burnup values, corroded fuel is significantly more reactive in nitric acid than uncorroded fuel
- Rapid dissolution rate made control of dissolvers difficult
- Enhanced effective surface area was invoked as source of increased chemical reactivity, not hydride
- Unknown whether any of the fuel dried out during transfer to, or residence in, dissolver

An Assessment of the Potential for Energetic Uranium Hydride Reactions Occurring During K-Basin Irradiated Fuel Handling Activities

Schmidt, J.P. 8/14/91
Priority Level = 1

Document Purpose - To document an evaluation of a potential finding from a PHA for K Basin - " A potential energetic reaction may occur when canisters of fuel are opened or the fuel processed in the case where hydration of the uranium in the canister has occurred". "The existing SAR does not address this potential event. This assessment has been conducted to determine if the event merits consideration as an event whose consequences could challenge the existing safety envelope."

"The assessment ...reviews applicable operational experience associated with storage facility handling of irradiated Hanford production reactor metallic uranium fuel." Based on this experience, judgements are made that such a reaction occurring as a result of underwater fuel handling activities ... is extremely unlikely."

"Uranium hydride (UH_3) can also be formed during the reaction. Generally this occurs to a limited degree where the hydrogen can escape. When it cannot, the hydrogen may actually accelerate the corrosion process and promote the formation of hydride as well as oxide. UH_3 formed in the corrosion reaction is normally oxidized by water at low temperatures but this reaction can be inhibited by oxide layer protection of the hydride[2]. Thus both oxides and hydrides may be present in the corrosion products formed by aqueous corrosion of the uranium."

([2]- reactor Handbook, Second Edition, Volume I , Materials, Interscience Publishers, Inc. New York, 1960, pp. 127-133.)

" While the extent of hydride which can be present in such degraded fuel has not ben quantitatively determined, it is known to be present to some extent. This is based on extensive hot cell examinations conducted over the years and the metallographic and visual identification of the presence of uranium hydride. Further, extensive underwater and hotcell handling of fuel has involved the complete spectrum of corrosion damage described. Thus it is believed the handling experience to date covers the maximum range of potential hydride concentrations in such fuel."

" In 1986, approximately 4000 canisters of such fuel (K-East open topped storage) were dumped from the storage canisters onto a sorting table"... ' None of this handling produced any observable indication suggesting that an energetic oxidation of potentially present uranium hydride occurred."

" the fuel in K-West is stored in sealed containers which by design allow the venting of oxidation reaction products at ambient storage pressures (~16' of H_2O)."..." "...have been stored in 105-KW Basin since 1981 and over 1000 MTU (~6300 lids) of fuel stored in K|MK I canisters have been shipped for reprocessing. These lids removal operations involved the introduction and exposure of the contained fuel to air. Observations indicate that the lid removal process did not result in oxidation of the uranium hydrides present which produced any observable results to operators or

An Assessment of the Potential for Energetic Uranium Hydride Reactions Occurring During K-Basin Irradiated Fuel Handling Activities

Schmidt, J.P. 8/14/91
Priority Level = 1

facility supervision."

"Examination typically included a comprehensive visual examination followed by extensive sectioning and metallographic examinations of selected areas to investigate the failure mechanisms. Based on visual attributes, failed elements which had been stored and shipped in rupture cans (sealed cans) were believed to frequently exhibit uranium hydride in the corrosion products. Sectioning occurred by water cooled abrasive wheel cutting. In no instance, where such fuel had received the 30 day or greater cooling period, did any observable indications of a uranium hydride oxidation reaction occur. These sectioning activities frequently involved areas where corrosion product existed between the cladding and uncorroded uranium fuel."

Conclusions:

> The percentage of uranium hydrides formed under various storage conditions would not be expected to change markedly with time and experience to date would appear to bound the range of hydride content that could be expected to occur. Thus the likelihood of uranium hydride reactions during underwater fuel storage and handling activities would not be to change relative to experience to date.

B30 Bottled Fuel Opening Option Study

Fisher, D., S. Knight 4/ 1993
Priority Level 4

Five 'bottles' containing Magnox spent fuel were examined at Sellafield. Four of the bottles contained intact (bottle numbers 1 and 2) or sectioned (bottle numbers 4 and 5) Tokai Mura fuel elements and one contained BNFL fuel element debris (bottle number 3). Bottles 1, 2, and 3 were made of stainless steel, bottles 4 and 5 of aluminum. Bottle 1 showed considerable evidence of external corrosion and the interior was moist, although there was no standing water. The fuel element inside was intact although there was significant evidence of corrosion. Bottle 2 was heavily corroded,with a through-wall hole seemingly corroded through at the top. The interior was wet, but with no observable standing water. The fuel element inside showed no significant corrosion. Bottle 3 showed no significant external corrosion. It contained approximately one half of a fuel element's worth of sectioned fuel. Upon opening the bottle a quantity of water was released from the interior. The fuel element section inside was heavily corroded and swollen, making retrieval difficult. Bottle 4 was in good condition with only slight surface corrosion. The nine sections of fuel in the bottle were also in good condition and no water was present. None of the contents of these four bottles showed evidence of pyrophoric behavior.

Bottle 5 contained a fuel element in two sections. The exterior of the bottle was extensively corroded. When opened in air and tipped to remove the fuel element sections, the second fuel section ignited. The burn was suppressed, and the fuel cooled, by means of an argon purge. But when the argon purge was stopped the fuel ignited again upon re-exposure to air. The argon purge was resumed and the burning stopped. After cooling again, a controlled amount of oxygen was introduced into the argon to stabilize the fuel. After this the fuel was re-exposed to air and again re-ignited. After another argon purge a second controlled oxygen stabilization successfully inerted the fuel. The fuel was then examined and two types of powder, one white (associated with the first section of fuel to be removed) and one black (associated with the second section of fuel to be removed), were found adhering to or near the element sections. The black powder (uranium hydride?) ignited when separated and exposed to air.

B30 Bottled Fuel Opening Option Study

Fisher, D., S. Knight 4/ 1993
Priority Level 4

Key points/unknowns:

- Corrosion in sealed containers caused uranium hydride buildup
- Uranium hydride source of pyrophoricity
- Unknown whether ignition was thermally or mechanically ('tipping') induced
- Why didn't the fuel in bottles 1 and 3 show pyrophoric behavior similar to bottle 5?
- Why didn't the fuel element in bottle 2 corrode?
- Why did the first 'controlled oxygen inerting' of the bottle 5 fuel not prevent re-ignition, whereas the second one did (in spite of uranium hydride powder still being present)?
- Unknown quantity of oxygen in the argon during 'passivation'

Regarding the Chemistry of Metallic Uranium Stored in Steel Drums

Wood, D.H., et al 7/26/93
Priority level = 1

In 1993 at Lawrence Livermore National Laboratory a 55-gallon drum containing sections of *unirradiated*, iron-clad, uranium alloy fuel elements experienced a "mild explosion" while being opened. The drum had been in storage at LLNL for about 5 years. The drum was one of 25 of a shipment of this type of fuel and was the only one which showed any pyrophoric behavior when handled.

The drum exploded while being 'tapped' open to unloose a sticky ring seal at the top of the drum, and at the approximate moment that ambient air entered the drum. After the initial explosion it was observed that the fuel itself had ignited and was burning vigorously with a yellow-orange flame. Within moments the lid of the drum was loosely replaced, suppressing the flames but leaving the contents emitting smoke. Three hours later the lid was clamped and sealed. After 83 days the drum gas was sampled and found to be 75% nitrogen and 25% hydrogen. Upon reopening and exposure to air the fuel once again spontaneously ignited, but the contents did not 'explode'.

An analysis of the event concluded that it was caused by the ignition of uranium hydride upon sudden exposure to air. The hydride resulted from corrosion of the exposed uranium metal surfaces of the (sectioned) fuel elements during storage. A bag of dessicant placed in the drum to scavenge moisture during storage was found to be substantially dry. The water source for the corrosion was moisture contained in the plywood spacers used to hold and separate the cardboard fuel container tubes. (Dessicant packages in the other 24 drums were later found to have adequately scavenged the moisture released from the plywood in those drums.) The corrosion in the oxygen-free environment had resulted in the buildup of both uranium hydride powder corrosion product and hydrogen gas in the sealed drum. When the drum was tapped open, the sudden exposure of the contents to air ignited the uranium hydride powder - which may have become suspended due to the mechanical tapping action. This in turn ignited the newly-formed hydrogen-air mixture, causing the explosion. Since replacement of the lid prevented the burn from going to completion , the remaining uranium hydride later ignited when re-exposed to air.

Regarding the Chemistry of Metallic Uranium Stored in Steel Drums

Wood, D.H., et al 7/26/93
Priority level = 1

Ironically, the absence of pyrophoric reactions in the other 24 drums was ascribed to the lack of a good seal by their lids. The small amounts of oxygen which leaked into the drums during their long storage may have effectively passivated the exposed uranium surfaces.

Key points/unknowns:

- Ignition ocurred spontaneously at ambient temperature due to sudden exposure of uranium hydride to air
- Hydrides formed due to moisture corrosion of uranium metal in a sealed system
- Small amounts of air leakage to other 24 drums may have passivated surfaces
- The dessicant bag didn't work in the sealed environment of the drum which exploded

Pyrophoricity of Uranium in Long-Term Storage Environments

Solbrig, C.W., et al 12/94
Priority Value = 2

At ORNL in 1992, a uranium metal foil was sealed with atmospheric air in a small bottle. After a period of time the water vapor and air inside the bottle were completely consumed, leaving the bottle containing uranium metal, uranium dioxide, uranium hydride, and the residual nitrogen from the air. Upon re-exposure to air at ambient temperature the uranium hydride ignited, causing the uranium metal to reach its ignition point and burn.

Key points/unknowns:
- All oxygen and moisture in the air consumed by corrosion of the foil in sealed system
- Sudden exposure of hydride to air causes ignition at ambient temperature
- Uranium burns to completion, reaction self-sustaining

At Fernald in 1992, two lids on drums containing depleted uranium metal spontaneously blew off. The drums were originally sealed in air. The explosions were blamed on a failure of the venting system of the drums, resulting in the accumulation of a hydrogen-oxygen mixture inside. The hydrogen was the product of corrosion of the uranium metal with the moisture in the drum air. Uranium hydride exposure was not thought to have been the ignition source; rather the ignition initiator was assumed to be a spark, although the source of the spark was not identified.

Key points/unknowns:
- lack of venting identified as cause of hydrogen explosion but not as cause of corrosion and/or hydride formation
- spark was identified as ignition initiator

Pyrophoricity of Uranium in Long-Term Storage Environments

Solbrig, C.W., et al 12/94
Priority Value = 2

In 1985 at Argonne National Laboratory, Zero Power Physics Reactor (ZPPR) fuel plates were found to be severely corroding in their storage canisters. The ZPPR fuel is uranium metal clad in stainless steel in the form of 1/16" thick plates, but the cladding is vented such that the uranium fuel is in communication with the storage canister atmosphere. The initial storage container atmosphere was air. An attempt to halt the corrosion by placing bags of dessicant in the containers failed because the uranium had a greater affinity for the moisture that the dessicant. In 1991-2, the containers were flushed with dry air, then evacuated, to halt corrosion. But upon inspection in 1993 more corrosion was observed and several instances of 'flashing' of the fuel occurred when the containers were opened. The flashing was found to be the spontaneous ignition of uranium hydride powder which became suspended due to the mechanical disturbance associated with opening the containers. The uranium hydride resulted from corrosion due to the canisters not vacuum tight and leaking air over the three years. When the canister atmosphere was examined in 1992 it was found to be mostly nitrogen (with the balance hydrogen) at atmospheric pressure.

Key points/unknowns:

- Uranium metal scavenges moisture better than dessicant
- Fuel consumed all leaking oxygen until nitrogen at atmospheric pressure attained in container
- 'Flashing' identified as igniting uranium hydride powder

A Summary of BNFL's Experience in the Storage and Handling of Spent Metallic Fuel - Addendum: Summary of Reference Paper Contents

BNFL 4/95
Priority Value = 3/4

Three Magnox fuel elements ignited in air at ambient temperature while in a transfer tray. The cause of the ignition was identified as contact friction between the elements.

Key points/unknowns:
- Friction identified as ignition initiator
- Unknown chemistry of elements

It was concluded that the cause of ignition of a Magnox fuel rod in cave B38 was the exposure of uranium hydride in the corrosion product to air. Reference states that 'badly corroded unirradiated uranium can catch fire in air and that this can happen even though no heat is being generated by friction'.

Key points/unknowns:
- Heavy corrosion identified as source of pyrophoric behavior
- Thermally-induced ignition at ambient temperature
- Irradiation swelling of rod not given

'Sparking' was observed on Tokai Mura Magnox fuel from cans which had leaked during pool storage. The sparking resulted from the exposure of a film of uranium hydride on the fuel - formed as a result of corrosion inside the cans - to air.

Key points/unknowns:
- Sparking blamed on exposure uranium hydride film to air
- Water leak was source of moisture for corrosion

A Summary of BNFL's Experience in the Storage and Handling of Spent Metallic Fuel - Addendum: Summary of Reference Paper Contents

BNFL 4/95
Priority Value = 3/4

Four instances of spontaneous ignition in ambient air of Magnox spent fuel, which had irradiation swelling in excess of 9%, occurred. Two of these occurred when sections of fuel were heated in vacuum at 350C to drive off hydrogen, then subsequently cooled and exposed to air. The other two occurred when sections that had been immersed in water were stored in sealed, air-filled containers for 12 days, then exposed to air.

Key points/unknowns:

- Elements were significantly irradiation swollen
- Heating to 350C in vacuum made the elements more pyrophoric
- Corrosion in sealed containers made the elements more pyrophoric
- Unkown degree of corrosion/hydride

During decanning operations for Magnox fuel in cave B30 at Windscale in July 1979, an element became jammed in a 'splitter'. In attempting to unjam the element, friction heating caused a hot piece of material to drop to the tray below the splitter. The tray contained pieces of fuel which then ignited. The resulting fuel fire could not be extinguished and was allowed to burn out. It was found afterward that the material which burned was primarily Magnox cladding, but some uranium burned as well. The source of ignition was determined to be uranium hydride.

Key points/unknowns:

- Ignition initiated by friction heating from de-jamming effort
- Burn could not be extinguished
- Cladding burned preferentially to uranium

APPENDIX C IGMCO FORTRAN SOURCE CODE FOR IGNITION ANALYSIS OF FUEL BASKETS

```
PROGRAM IGMCO
C
C     DRIVER/SUBROUTINE VERSION
C
C     IGNITION TEMPERATURE FOR FUEL IN AN MCO
C     SINGLE MCO - CONVECTS AND RADIATES TO AMBIENT
C     RODLIKE GEOMETRY, INTERNAL RADIATION BY T**3 DT/DR
C
C     "PEARCE" KINETICS FROM HANFORD + MULTIPLIER
C     MULTIPLIER CAN ACCOUNT FOR FAILURE FRACTION, SWELLING,
C          PRESENCE OF POROUS SURFACE LAYER, ETC.
C     EXTERNAL HEAT TRANSFER INDEPENDENT OF LENGTH
C
C     MAJOR PROGRAM SECTIONS:
C     1.0  DECLARATIONS & CONSTANTS
C     2.0  CASE INPUTS
C     3.0  LOOP OVER RADIUS - INACTIVE
C     4.0  LOOP OVER PARTICLE SIZE, MOISTURE - PARTLY ACTIVE
C     5.0  PICK FUEL T & REACTION SOURCE & T AT MCO RADIUS
C     6.0  NEWTON LOOP FOR AMBIENT T
C     7.0  SEARCH FOR MAXIMUM
C     8.0  CASE OUTPUT
C
C     ------------------------------------------------------------
C     1.0  DECLARATIONS & CONSTANTS
C     ------------------------------------------------------------
C
      IMPLICIT REAL (A-H, K-Z)
      INTEGER NDP, NPS
      CHARACTER*1 ACON
C
C     VECTOR AND ARRAY DEFINITIONS:
C
C     TAMS(,)  AMBIENT TEMPERATURE AT IGNITION (DPV,PPSTV) CASES
C     ACON(,)  CONVERGENCE INDICATOR CHARACTER: > OR < OR BLANK
C     TFSAV(,)  FUEL TEMPERATURE AT IGNITION SAVED DETAILED PRINT
C     TSSAV(,)  OUTER SURFACE T AT IGNITION
C     TRSAV(,)  MCO SURFACE T AT IGNITION
C     QRSAV(,)  CHEMICAL SOURCE AT IGNITION
C     CONSAV(,) CONVERGENCE CHECK: SOURCE-SINK AT IGNITION
C     DPV()     VECTOR OF PARTICLE SIZES FOR LOOP
C               -NOTE- CURRENTLY PARTIALLY USED, DESIRED FEWER CASES
C               ! HERE USED AS A/V MULTIPLIER ON NOMINAL VALUE
C     PPSTV()   VECTOR OF STEAM PRESSURE FOR LOOP
C               -NOTE- CURRENTLY BYPASSED, DESIRED FEWER CASES
C
      PARAMETER (NTA=25,  NDP=7,  NPS=4)
      DIMENSION  TAMS(NDP,NPS), ACON(NDP,NPS), TFSAV(NDP,NPS),
     &           TSSAV(NDP,NPS),TRSAV(NDP,NPS), QRSAV(NDP,NPS),
     &          CONSAV(NDP,NPS)
      DIMENSION DPV(NDP), PPSTV(NPS)
C     PARTICLE DIAMETER -- A/V MULTIPLIER HERE
      DATA DPV /1.E0, 0.75E0, 0.45E0, 0.25E0, 0.1E0, 0.05E0, 0.014E0/
C     STEAM PRESSURE: 0, 2 KPA, AND SAT AT: 30 C, 50 C
C     !! PPSTV IN KPA
      DATA PPSTV /0.E0, 2.E0, 4.2E0, 12.3E0/
C     UNIVERSAL CONSTANTS
      DATA TKO /273.15/
C
      OPEN (UNIT=12, STATUS='UNKNOWN', FORM='FORMATTED',
     &      FILE='FOR012.DAT', ERR=1234)
      OPEN (UNIT=13, STATUS='UNKNOWN', FORM='FORMATTED',
     &      FILE='FOR013.DAT', ERR=1234)
C
C  SIMPLE CONSTANT GAS PROPERTIES: AIR
C
```

```
C  KG    GAS THERMAL CONDUCTIVITY W/M/K
C  NUG   GAS VISCOSITY (MU/RHO)  M^2/S
C  ALG   GAS THERMAL DIFFUSIVITY M^2/S
      KG= 0.030
      NUG= 26.4E-6
      ALG= 38.3E-6
C
C     PICK 30 CM OUTER RADIUS
C
      XL= 0.30E0
C
C     ------------------------------------------------------------
C     2.0  ESTABLISH CASE INPUTS
C     ------------------------------------------------------------
C
C     PHI= POROSITY
C     QV= VOLUMETRIC POWER W/M^3
C     HIN= ZERO TO CALCULATE, ELSE INPUT W/M^2/K
C     FEAC= MULTIPLIER DESCRIBED BELOW
C     KSL= EFFECTIVE DISTRIBUTED THERMAL CONDUCTIVITY W/M/K
C     EPS= OVERALL EMISSIVITY -INSIDE MCO-
C     RIN= INNER RADIUS FOR FUEL IN MCO
C     XGAP= GAP THICKNESS MCO TO VAULT TUBE
C     XTUBE= VAULT WALL THICKNESS
C     AOV0= NOMINAL A/V; WILL LOOP OVER MULTIPLIER; 1/M
C     FRAD= RADIATION DISTANCE FACTOR
C           <1 XRAD = FRAD*XL  USE FOR RODS:  1/FRAD = # SERIES PATHS
C                              DEFAULT IS 4 SERIES PATHS FOR MCO
C           >1 XRAD = FRAD*DP  USE FOR BEDS, ACCOUNTS FOR REFLECTIONS
C                              DEFAULT IS 3 USING PHI=0.4, EPS=0.7:
C                              LAM = 1 - 1.21 (1 - (1-PHI)**2/3)
C                              FRAD= (1 + LAM/EPS)/(1 - LAM)
C     EPGAP  OVERALL EMISSIVITY OF MCO-TUBE GAP
C     EPOUT  OVERALL EMISSIVITY OF OUTER TUBE-AIR
C
C
C     DEFAULT VALUES HERE FOR RODS IN AN MCO
C     FOR FUEL FRAGMENTS THESE ARE APPROPRIATE DEFAULTS:
C     PHI= 0.40  KSL=0.20 TO 0.30  FRAD=3.0  RIN=0.20  AOV0=1000
C
      CALL GETIN (  QV,  PHI, FEAC,   HIN,   KSL, EPS, RIN, XTUBE,
     &            XGAP, AOV0, FRAD, EPGAP, EPOUT)

C
C     ------------------------------------------------------------
C     4.0 TOP OF LOOP OVER PARTICLE SIZE, MOISTURE
C         LOOP OVER STEAM PRESSURE INACTIVE, PICK 2 KPA VALUE
C         LOOP OVER PARTICLE SIZE SELECTS EQUIVALENT DP GIVEN A/V
C     ------------------------------------------------------------
C
      DO 4100 IPS=2,2
      PPST= PPSTV(IPS)
      DO 4000 IDP=1,7
      AOV= AOV0*DPV(IDP)
      DP= 6.E0/AOV
C
C     AREA MULTIPLIER ACCOUNTS FOR ENHANCED SURFACE AREA
C      FOR REACTION OF A POROUS POWDER VS HEAT TRANSFER AREA
C      = 2 TO 6 * # GRAIN DISTANCES INWARD EFFECTIVELY EXPOSED
C     KINETIC RATE MULTIPLIER ACCOUNTS FOR EITHER:
C       ACTUAL RATE UNCERTAINTY
C       VOLUME FRACTION OF REACTING MATERIAL
C       SWELLING EFFECT, ETC.
C
      FARX= FEAC * 6.E0*(1.E0 - PHI)/DP
C
      CALL TIGMCO (
     &     QV,   PHI,   HIN,   KSL,   EPS,  RIN, XTUBE,
     &   XGAP,  FRAD, EPGAP, EPOUT,    KG,  NUG,  ALG,
     &     XL,  FARX,  PPST,    DP,
     &    TCL,    TR,    TS,  TAMB,    QR,  SORC,  ERR, ITIG)
```

```
C
C     SAVE OUTPUT
C
      TAMS(IDP,IPS)= TAMB - TKO
      TFSAV(IDP,IPS)= TCL - TKO
      TSSAV(IDP,IPS)= TS - TKO
      TRSAV(IDP,IPS)= TR - TKO
      QRSAV(IDP,IPS)= QR
      CONSAV(IDP,IPS)= ERR
      IF (ITIG .EQ. 1) THEN
C     CASE WHERE LOWER THAN FIRST GUESS
        ACON(IDP,IPS)= '<'
      ELSEIF (ITIG .EQ. 2) THEN
C     CASE OF CONVERGENCE
        ACON(IDP,IPS)= ' '
      ELSEIF (ITIG .EQ. 3) THEN
C     CASE OF T HIGHER THAN LAST GUESS
        ACON(IDP,IPS)= '>'
      ELSE
C     UNCONVERGED, MESSAGE ALREADY PRINTED
        GOTO 1234
      ENDIF
C
C --- BOTTOM OF LOOP OVER DP,PPST, ETC
 4000 CONTINUE
 4100 CONTINUE
C
C     ------------------------------------------------------------
C     6.0  CASE OUTPUT
C     ------------------------------------------------------------
C
C     HERE ASSUMES ONE PPST VALUE
C
      WRITE (*,4001) PHI,QV,FEAC,HIN,EPS,KSL,RIN,XL,XGAP,XTUBE,FRAD
      WRITE (12,4001)PHI,QV,FEAC,HIN,EPS,KSL,RIN,XL,XGAP,XTUBE,FRAD
      WRITE (*,4002) PPST
      WRITE (12,4002) PPST
 4001 FORMAT(//,' ***** Ignition of fuel in MCO ***** ',/,
     & '   Porosity=       ',F8.3,'       Power W/m^3= ',F8.2,/,
     & '   Kin. Rate Mult= ',F8.3,'     Hin (<0 calc)= ',1PE9.2,/,0P,
     & '   Emissivity=     ',F8.3,'      Therm. cond.= ',F8.3,/,
     & '   Inner radius=   ',F8.4,'    Outer radius = ',F8.4,/,
     & '   Gap thickness=  ',F8.6,'  Outer wall thick= ',F8.4,/,
     & '   Frad <1 rods, >1 rubble: ',F8.4,/)
 4002 FORMAT(' ------------------------------------------------',/,
     &'   Ambient ignition T and profiles in C for Pst = ',F6.2,' kPa'/,
     &'    A/V',T12,'Tamb',T22,'Tsur',T32,'Tmco',T42,'Tmax',T52,'Qchem',
     &     T62,'Error',/)
C
      J=2
      DO 4020 IDP=1,7
      AOV= AOV0*DPV(IDP)
      WRITE (*,4008) AOV,ACON(IDP,J),TAMS(IDP,J),TSSAV(IDP,J),
     &  TRSAV(IDP,J),TFSAV(IDP,J),QRSAV(IDP,J),CONSAV(IDP,J)
      WRITE (12,4008)AOV,ACON(IDP,J),TAMS(IDP,J),TSSAV(IDP,J),
     &  TRSAV(IDP,J),TFSAV(IDP,J),QRSAV(IDP,J),CONSAV(IDP,J)
 4020 CONTINUE
 4008 FORMAT('  ',F7.1,T10,A1,4(F7.2,3X),F7.1,3X,1PE9.2)
C --- BOTTOM OF CASE LOOP
 5000 CONTINUE
C --- OUTSIDE ALL LOOPS
 1234 WRITE (*,666)
  666 FORMAT(' Attaboy, Marty')
      END

      SUBROUTINE TIGMCO (
     &     QV,    PHI,    HIN,    KSL,    EPS,   RIN, XTUBE,
     &   XGAP,  FRAD, EPGAP, EPOUT,     KG,   NUG,  ALG,
     &     XL,  FARX,  PPST,     DP,
     &    TCL,     TR,     TS,   TAMB,     QR,  SORC,  ERR, ITIG)
C
```

```
      IMPLICIT REAL (A-H,K-Z)
      INTEGER NTA
      PARAMETER (NTA=25,  NDP=7,  NPS=4)
      DIMENSION TAM(NTA),TU(NTA)
      DATA PI /3.14159E0/, GRAV /9.81E0/, SIGMA /5.67E-8/
C
C     TAM()   AMBIENT TEMPERATURES SAVED DURING SEARCH FOR MAXIMUM
C     TU()    FUEL TEMPERATURES SAVED DURING SEARCH FOR MAXIMUM
C             -NOTE- MORE VALUES SAVED THAN OPTIMALLY NECESSARY,
C              SO DEBUGGING/PLOTTING OF LOCAL BEHAVIOR IS EASIER
C
C
C     EXIT CONDITION CODE:
C     ITIG: 1  TIG < LOWER BOUND
C     ITIG: 2  TIG FOUND
C     ITIG: 3  TIG > UPPER BOUND
C
      ITIG= 0
      TCL= 273.
      TR=  273.
      TS=  273.
      TAMB=273.
      QR=  0.E0
      SORC= 0.E0
      ERR= 0.E0
C
C     TOP OF LOOP OVER PARTICLE TEMPERATURE
C
C     FOR A GIVEN PPST,DP,XL MAY RUN PAST THIS POINT SEVERAL TIMES
C     START WITH LOW,COARSE RANGE OF FUEL TEMPERATURE FOR IGNITION
C     COME BACK HERE IF HIGHER RANGES OR FINE RANGES ARE DESIRED
C     FIRST GET THE CORRECT COARSE RANGE, THEN FINE RANGES
C     SEE TESTS AFTER NEWTON LOOP BOTTOM
C
C     TLOW:  LOW END OF RANGE TO INVESTIGATE
C            MAY BE RESET AT END OF LOOP OVER THE RANGE
C     DT:    INCREMENT OF RANGE, MAY ALSO BE RESET AT END OF LOOP
C     IRANGE: RANGE COUNTER
C     FINE:   FINE RANGE COUNTER
C
      TLOW= 273.E0
      DT=10.
      IRANGE=0
      IFINE=0
 999  CONTINUE
      IIT=10
      DO 3000 IT=1,IIT
C
C     ---------------------------------------------------------
C     3.0  FUEL T, REACTION SOURCE, MCO WALL TEMPERATURE
C     ---------------------------------------------------------
C
      TCL= TLOW + DT*FLOAT(IT-1)
      TU(IT)=TCL
C
C     GIVEN FUEL T, GET REACTION POWER, THEN
C       1) SOLVE FOR TEMPERATURE AT MCO RADIUS
C       2) ITERATE TO SOLVE FOR TUBE AND AMBIENT TEMPERATURES
C
C     MCGILLIVRAY CORRELATION FOR MOIST AIR
C     RATE IN MG O2/CM^2 MIN IS CONVERTED TO W/M^2
C     VIA 10^-6/10^-4/60 = 0.01/60  WHERE 3.4E7 IS HEAT OF REACTION
C      RD= EXP(11.093 - 8077.0/TCL)
C      RK1= EXP(7.831 - 6432.0/TCL)
C      RK2= EXP(-15.208 + 5237.0/TCL)
C      RR= RD + RK1*PPST/(1.0 + RK2*PPST)
C      QR= FARX * 3.4E7 * RR * 0.01/60.0
C
C!!!MARV
C     RATE LAW USED BY MARV THURGOOD IN MG/CM^2/HR CONVERT BY 0.01/3600
C
```

```
      RR= 10.E0**(7.364 - 3016./TCL)
      QR= FARX * 1.67E7 * RR * 0.01/3600.0
C
C     TOTAL SOURCE:
      SORC= QV*(1.E0 - PHI) + QR
C
C     TEMPERATURE TR AT RADIUS R=XL:
C     ROA = (r=R)/(r=a) = outer/inner radii ratio; AOR2 = a^2/R^2
C     XRAD= EFFECTIVE DISTANCE BETWEEN RADIATION SHIELDS
C         = RADIUS/# OF SHIELDS
C
      ROA= XL/RIN
      AOR2= RIN*RIN/XL/XL
      SIGEP= SIGMA*EPS
      SIGEP1= SIGMA*EPGAP
      SIGEP2= SIGMA*EPOUT
      IF (FRAD .LT. 1.E0) THEN
        XRAD= FRAD*XL
      ELSE
        XRAD= FRAD*DP
      ENDIF
      CRAD= 4.E0*SIGEP*XRAD
      TR= FTR(TCL,SORC,XL,KSL,CRAD,ROA,AOR2,IOK)
      TR4= TR**4.E0
C
C     ---------------------------------------------------------
C     4.0  NEWTON LOOP FOR AMBIENT TEMPERATURE
C     ---------------------------------------------------------
C
C     -- FIRST MUST GUESS VALUES, INITIALIZE HEAT XFER COEFF --
C
C     HEAT FLUX AT RADIUS XL:
      QFLUX= (SORC*XL/2.E0) * (1.E0 - AOR2)
C     GAP CONDUCTANCE
      HGAP= KG/XGAP
C     -- ESTIMATED TEMPERATURE AFTER GAP --
      HRR= 4.E0*SIGEP1*TR**3.E0
      TS= TR - QFLUX/(HGAP + HRR)
C     OUTER RADIUS NEEDED FOR OUTER FLUX
      XLS= XL + XGAP + XTUBE
C
C     CYLINDER: VERTICAL FLAT PLATE NATURAL CONVECTION
C     APPROXIMATE GAS PROPERTIES AT PARTICLE TEMPERATURE
C     H0 IS HEAT TRANSFER COEFFICIENT LACKING (DELTA-T)**POWER
C
C     IF HIN = 0 CALCULATE & USE RADIATION - SINGLE MCO CASE
C     IF HIN > 0 USE INPUT VALUE, NO RADIATION - VAULT CASE
C
      BETA= 1.E0/TS
      IF (HIN .LE. 0.001) THEN
C          HORIZONTAL UPWARD SURFACE COMMENTED OUT
C          H0= 0.1*KG*(GRAV*BETA/NUG/ALG)**0.33333
C          HEXP= 0.333333E0
C          VERTICAL FLAT PLATE USED
        H0= 0.062*KG*(GRAV*BETA/NUG/ALG)**0.33333
        HEXP= 0.333333E0
      ELSE
        H= HIN
        H0= 3.E0*HIN
        DH= 0.E0
      ENDIF
C
C      WRITE (*,31) T, SORC-QR, QR
C  31  FORMAT(' T = ',F6.1,' VOL HT = ',1PE10.3,'  CHEM HT = ',E10.3)
C
C     MAX H IS WITHOUT RADIATION, YIELDS MIN SOLUTION VALUE
C     BUT LET MIN GO AT LEAST 1 K BELOW MAX
C     -- AMBIENT TEMPERATURE GUESS ONLY IF HIN=0 --
      IF (HIN .LE. 0.001E0) THEN
        HRS= 4.E0*SIGEP2*TS**3.E0
        TMIN= TS - 2.E0*QFLUX/HRS
```

```
        TAMB= MAX(TS-3.0, (TS+TMIN)/2.E0)
      ELSE
        TMIN= TR - 2.E0*QFLUX/(HGAP + HRR)
      ENDIF
C
C     IN NEWTON LOOP, PUT TS EQUATIONS FIRST, TAMB LAST,
C         SINCE TAMB IS DIRECTLY FOUND FOR HIN = 0
C
      DO 1000 I=1,20
      TSOLD= TS
      TS4= TS**4.E0
      HRR= SIGEP1*(TR4 - TS4)/(TR - TS)
      DHRR= SIGEP1*((TR*TR + TS*TS) + 2.E0*TS*(TR + TS))
      F= -QFLUX + (HGAP+HRR)*(TR - TS)
      FP= -(HGAP+HRR) + (TR-TS)*DHRR
      DELS= -F/FP
      TS= TS + DELS
      IF (TS .GE. TR) TS= (TSOLD + TR)/2.E0
      IF (TS .LE. TMIN) TS= (TSOLD + TMIN)/2.E0
      IF (HIN .GT. 0.001E0) THEN
C     --- TAMB FOUND DIRECTLY
        QFLUXS= QFLUX * XL/XLS
        TAMB= TS - QFLUXS/HIN
        SINK= QFLUXS*XLS/XL * 2.E0/XL/(1.E0 - AOR2)
        IF (ABS(DELS/TR) .LE. 1.E-5) GOTO 1100
      ELSE
C     --- ALSO SOLVE FOR TAMB
        IF (TAMB .GE. TS)
     &    TAMB= TS - QFLUX/(4.E0*SIGEP2*TS**3.E0) * XL/XLS
        TOLD= TAMB
        H= H0*(TS - TAMB)**HEXP
        DH= -HEXP*H/(TS -TAMB)
        HRS= SIGEP2*(TS4 - TAMB**4.E0)/(TS - TAMB)
        DHRS= SIGEP2*((TS*TS + TAMB*TAMB) + 2.E0*TAMB*(TS + TAMB))
        G= -QFLUX*(XL/XLS) + (H + HRS)*(TS - TAMB)
        GP= -(H + HRS) + (TS-TAMB)*(DH + DHRS)
        DELA= -G/GP
        TAMB= TAMB + DELA
        IF (TAMB .LE. TMIN) TAMB= (TOLD + TMIN)/2.E0
        IF (TAMB .GE. TS) TAMB= (TS + TMIN)/2.E0
        QFLUXS= (H+HRS)*(TS-TAMB)
        SINK= QFLUXS*XLS/XL * 2.E0/XL/(1.E0 - AOR2)
        IF (ABS((TAMB-TOLD)/TR) + ABS((TS-TSOLD)/TR) .LE. 1.E-5)
     &      GO TO 1100
      ENDIF
C
C      IF (IDBG.GE.1) THEN
C      WRITE (*,33) I,TAMB,DEL,F
C  33  FORMAT(' ',I2,'  ',F8.3,'  ',F8.4,' ',1PE10.3)
C      ENDIF
 1000 CONTINUE
C     CONVERGENCE FAILS HERE
      WRITE (*,1010) TOLD,TAMB,TSOLD,TS
      WRITE (*,1011) TMIN,TR,TCL,QFLUX
 1010 FORMAT(' CONVERGENCE FAILS: ',/,
     &   '  TOLD = ',F9.3, ' TAMB= ',F9.3,'   TSO=',F9.3,'  TS=',F9.3)
 1011 FORMAT('  TMIN = ',F9.3,'  TR ',F9.3,'  T=',F9.3,'  Q=',F12.3)
C      WRITE (*,1110) T, TAMB, SORC, SINK, I
      GO TO 660
C
 1100 CONTINUE
C      WRITE (*,1110) TCL, TAMB, SORC, SINK, I
 1110 FORMAT(
     & ' T= ',F8.2,'  TAMB= ',F8.2,'  SORC= ',1PE10.3,'  SINK= ',E10.3,
     & '  ',0P,I2)
C
C     CONVERGED; NOW SEE IF MAXIMUM FOUND
C
C     ---------------------------------------------------------
C     5.0  SEARCH FOR MAXIMUM
C     ---------------------------------------------------------
```

```
C
      TAM(IT)= TAMB
C
C     CASE WHERE MAX IS LOWER THAN FIRST GUESS - JUST QUIT
C
      IF (IT .EQ. 2 .AND. TAMB .LT. TAM(1)) THEN
        ITIG= 1
        WRITE (*,2011) TLOW,DP*1.E6,PPST,XL*1000.,H
 2011 FORMAT(' Ignition temperature below starting value',F5.1,/,
     & ' DP=',F4.1,'  PPST=',F6.1,'   XL=',F4.1,'   H=',F5.2)
        WRITE (*,1110) TCL, TAMB, SORC, QFLUX, I
        GOTO 660
      ENDIF
C
C     CASE WHERE MAX FOUND - GO BACK FOR FINER RANGE
C
      IF (IT.GE.3 .AND. TAM(IT) .LT. TAM(IT-1)) THEN
        IFINE=IFINE+1
        IF (IFINE .GE. 3) THEN
          ITIG= 2
          ERR= (SINK - SORC)/SORC
          GO TO 660
        ENDIF
        TLOW= TU(IT-2)
        DT= (TU(IT) - TU(IT-2))/10.
C DIAGNOSTIC TO ENSURE CONVERGING CORRECTLY
        WRITE (13,2040) DP*1.E6,PPST,TAM(IT-2),TAM(IT-1),TAM(IT)
 2040   FORMAT(' DP= ',F6.2,' PST= ',F6.1,' T RANGE:',3(F7.3,3X))
        GOTO 999
      ENDIF
C
C     MAX NOT YET FOUND - CHECK A HIGHER RANGE
C
      IF (IT .EQ. IIT .AND. TAM(IT) .GT. TAM(IT-1)) THEN
        IRANGE=IRANGE+1
        IF (IRANGE .GE. 5) THEN
          ITIG= 2
          ERR= (SORC - SINK)/SORC
          GO TO 660
        ENDIF
        TLOW= TU(IT-1)
        GO TO 999
      ENDIF
C --- BOTTOM OF LOOP OVER FUEL T - SHOULD BREAK ABOVE
 3000 CONTINUE
C --- GET TO 660 WHEN CONVERGED ON AN IGNITION TEMPERATURE
  660 CONTINUE
      RETURN
      END

      FUNCTION FTR(T,SORC,XL,KSL,CRAD,ROA,AOR2,IOK)
      IMPLICIT REAL (A-H,K-Z)
C
C     GET TR = TEMPERATURE OF MCO WALL
C     FIRST GUESS BY CONSTANT RADIATIVE CONDUCTIVITY METHOD
C       I.E. SOLUTION WITH CONSTANT KEFF
      KEFF= KSL + CRAD*(T-5.E0)**3.E0
      TQ= (SORC*XL*XL/2.E0) * ((1.E0 - AOR2)/2.E0 - AOR2*LOG(ROA))
     &    / KSL
      TMAX= T
      TMIN= T - TQ
      TR= T - TQ*KSL/KEFF
      CEFF= CRAD/4.E0/KSL
      T4= T**4E0
      IOK=0
  100 CONTINUE
      TOLD= TR
      IOK=IOK+1
      G= T - TR + CEFF*(T4 - TR**4.E0) - TQ
      DG= -1.E0 - 4.E0*CEFF*TR**3.E0
      DEL= -G/DG
```

```
      TR= TR + DEL
      TR= MIN(TR, (TOLD+TMAX)/2.E0)
      TR= MAX(TR, (TOLD+TMIN)/2.E0)
      IF (ABS(DEL)/T .LE. 1.E-5) GOTO 200
      IF (IOK .LE. 10) GOTO 100
      IF (ABS(DEL)/T .LE. 1.E-4) GOTO 200
      WRITE (*,110) T,TR,DEL,TMAX,TMIN,TQ
 110  FORMAT('  Failure to find MCO temperature ',/,
     &    ' Tcl = ',F10.4,'   Tmco= ',F10.4,'   Del= ',F10.5,/,
     &    ' Tmx = ',F10.4,'   Tmin= ',F10.4,'   Tq = ',F10.5)
      STOP
 200  CONTINUE
      FTR= TR
      RETURN
      END

      SUBROUTINE GETIN
     &           ( QV,    PHI, FEAC,   HIN,   KSL, EPS, RIN, XTUBE,
     &            XGAP, AOV0, FRAD, EPGAP, EPOUT)
      IMPLICIT REAL (A-H,K-Z)
C
      QV= 2000.0
      PHI= 0.57
      FEAC= 1.0
      HIN= 0.0E0
      KSL= 0.12
      EPS= 0.70
      RIN= 0.04
      XTUBE= 0.0254/2.E0
      XGAP= 0.0254
      AOV0= 220.E0
      FRAD= 0.25E0
      EPGAP= 0.70
      EPOUT= 0.70
C!!!MARV
C     DEFAULT VALUES CHANGED FOR MARV THURGOOD HE-FILLED MCO
C     XGAP CHANGED TO REPRESENT MCO WALL
C
      QV= 1875.
      FEAC= 3.2
      HIN= 1.E5
      KSL= 1.0
      RIN= 0.02
      XGAP= 5.E-5
      EPGAP= 1.E3
C
 100  CONTINUE
      WRITE (*,20) PHI,QV,FEAC,KSL,HIN,EPS,AOV0,RIN,XTUBE,XGAP,FRAD,
     &             EPGAP,EPOUT
   20 FORMAT(' Current values: ',/,
     & '     1 PHI= ',F8.2,'     2 QV = ',F8.2,'     3 FEA=  ',F5.3,/,
     & '     4 KSL= ',F8.3,'     5 HIN= ',1PE9.2,0P,'     6 EPS=  ',F5.3,/,
     & '     7 AOV= ',F8.3,'     8 RIN= ',F8.3,'     9 TUBE= ',F8.3,/,
     & '    10 GAP= ',F8.6,'    11 FRAD=',F8.3,' <1 rods >1 rubble',/,
     & '    12 EGAP=',F8.4,'    13 EOUT=',F8.3,/,
     & '     HIN=0 means calculate & use radiation, ',
     &          'else constant with no radiation',/,
     & '     Enter 0,0 if OK else index,value: ',$)
      READ (*,*) IND,VAL
      IF (IND .LE. 0) GO TO 200
      IF (IND .EQ. 1) PHI=VAL
      IF (IND .EQ. 2) QV=VAL
      IF (IND .EQ. 3) FEAC=VAL
      IF (IND .EQ. 4) KSL=VAL
      IF (IND .EQ. 5) HIN=VAL
      IF (IND .EQ. 6) EPS=VAL
      IF (IND .EQ. 7) AOV0=VAL
      IF (IND .EQ. 8) RIN=VAL
      IF (IND .EQ. 9) XTUBE=VAL
      IF (IND .EQ. 10) XGAP=VAL
      IF (IND .EQ. 11) FRAD=VAL
```

```
      IF (IND .EQ. 12) EPGAP=VAL
      IF (IND .EQ. 13) EPOUT=VAL
      IF (IND .GE. 14) GO TO 200
      GOTO 100
 200  CONTINUE
C
      RETURN
      END



SUBROUTINE TIGMCO (
     &     QV,    PHI,    KSL,    EPS,    RIN,
     &   XGAP,  FRAD, EPGAP, EPOUT,     KG,
     &     XL,  FARX,  PPST,     DP,
     &    TCL,     TR,  TAMB,     QR,  SORC,  ERR, ITIG)
C
      IMPLICIT REAL (A-H,K-Z)
      INTEGER NTA
      PARAMETER (NTA=25,  NDP=7,  NPS=4)
      DIMENSION TAM(NTA),TU(NTA)
      DATA PI /3.14159E0/, GRAV /9.81E0/, SIGMA /5.67E-8/
C
C     TAM()   AMBIENT TEMPERATURES SAVED DURING SEARCH FOR MAXIMUM
C     TU()    FUEL TEMPERATURES SAVED DURING SEARCH FOR MAXIMUM
C             -NOTE- MORE VALUES SAVED THAN OPTIMALLY NECESSARY,
C              SO DEBUGGING/PLOTTING OF LOCAL BEHAVIOR IS EASIER
C
C
C     EXIT CONDITION CODE:
C     ITIG: 1  TIG < LOWER BOUND
C     ITIG: 2  TIG FOUND
C     ITIG: 3  TIG > UPPER BOUND
C
      ITIG= 0
      TCL= 273.
      TR=  273.
      TS=  273.
      TAMB=273.
      QR=  0.E0
      SORC= 0.E0
      ERR= 0.E0
C
C     TOP OF LOOP OVER PARTICLE TEMPERATURE
C
C     FOR A GIVEN PPST,DP,XL MAY RUN PAST THIS POINT SEVERAL TIMES
C     START WITH LOW,COARSE RANGE OF FUEL TEMPERATURE FOR IGNITION
C     COME BACK HERE IF HIGHER RANGES OR FINE RANGES ARE DESIRED
C     FIRST GET THE CORRECT COARSE RANGE, THEN FINE RANGES
C     SEE TESTS AFTER NEWTON LOOP BOTTOM
C
C     TLOW:  LOW END OF RANGE TO INVESTIGATE
C            MAY BE RESET AT END OF LOOP OVER THE RANGE
C     DT:    INCREMENT OF RANGE, MAY ALSO BE RESET AT END OF LOOP
C     IRANGE: RANGE COUNTER
C     FINE:   FINE RANGE COUNTER
C
      TLOW= 273.E0
      DT=10.
      IRANGE=0
      IFINE=0
 999  CONTINUE
      IIT=10
      DO 3000 IT=1,IIT
C
C     ---------------------------------------------------------
C     3.0  FUEL T, REACTION SOURCE, MCO WALL TEMPERATURE
C     ---------------------------------------------------------
C
      TCL= TLOW + DT*FLOAT(IT-1)
```

```
      TU(IT)=TCL
C
C     GIVEN FUEL T, GET REACTION POWER, THEN
C       1) SOLVE FOR TEMPERATURE AT MCO RADIUS
C       2) ITERATE TO SOLVE FOR TUBE AND AMBIENT TEMPERATURES
C
C     MCGILLIVRAY CORRELATION FOR MOIST AIR
C     RATE IN MG O2/CM^2 MIN IS CONVERTED TO W/M^2
C     VIA 10^-6/10^-4/60 = 0.01/60  WHERE 3.4E7 IS HEAT OF REACTION
C      RD= EXP(11.093 - 8077.0/TCL)
C      RK1= EXP(7.831 - 6432.0/TCL)
C      RK2= EXP(-15.208 + 5237.0/TCL)
C      RR= RD + RK1*PPST/(1.0 + RK2*PPST)
C      QR= FARX * 3.4E7 * RR * 0.01/60.0
C
C!!!MARV
C     RATE LAW USED BY MARV THURGOOD IN MG/CM^2/HR CONVERT BY 0.01/3600
C
      RR= 10.E0**(7.364 - 3016./TCL)
      QR= FARX * 1.67E7 * RR * 0.01/3600.0
C
C     TOTAL SOURCE:
      SORC= QV*(1.E0 - PHI) + QR
C
C     TEMPERATURE TR AT RADIUS R=XL:
C     ROA = (r=R)/(r=a) = outer/inner radii ratio; AOR2 = a^2/R^2
C     XRAD= EFFECTIVE DISTANCE BETWEEN RADIATION SHIELDS
C         = RADIUS/# OF SHIELDS
C
      ROA= XL/RIN
      AOR2= RIN*RIN/XL/XL
      SIGEP= SIGMA*EPS
      IF (FRAD .LT. 1.E0) THEN
        XRAD= FRAD*XL
      ELSE
        XRAD= FRAD*DP
      ENDIF
      CRAD= 4.E0*SIGEP*XRAD
      TR= FTR(TCL,SORC,XL,KSL,CRAD,ROA,AOR2,IOK,ERR)
C
C     HEAT FLUX AT RADIUS XL:
      QFLUX= (SORC*XL/2.E0) * (1.E0 - AOR2)
C     GAP CONDUCTANCE
      HGAP= KG/XGAP
C     -- ESTIMATED TEMPERATURE AFTER GAP I.E. MCO WALL --
      TAMB= TR - QFLUX/HGAP
C
C     CONVERGED; NOW SEE IF MAXIMUM FOUND
C
C     ---------------------------------------------------------------
C     5.0  SEARCH FOR MAXIMUM
C     ---------------------------------------------------------------
C
      TAM(IT)= TAMB
C
C     CASE WHERE MAX IS LOWER THAN FIRST GUESS - JUST QUIT
C
      IF (IT .EQ. 2 .AND. TAMB .LT. TAM(1)) THEN
        ITIG= 1
        WRITE (13,2011) TLOW,DP*1.E6,PPST,XL*1000.
        WRITE (13,1110) TCL, TAMB, SORC, QFLUX
        GOTO 660
      ENDIF
 2011 FORMAT(' Ignition temperature below starting value',F5.1,/,
     & ' DP=',F4.1,'  PPST=',F6.1,'   XL=',F4.1)
 1110 FORMAT(
     & ' T= ',F8.2,'  TAMB= ',F8.2,'  SORC= ',1PE10.3,'  FLUX= ',E10.3)
C
C     CASE WHERE MAX FOUND - GO BACK FOR FINER RANGE
C
      IF (IT.GE.3 .AND. TAM(IT) .LT. TAM(IT-1)) THEN
```

```
        IFINE=IFINE+1
        IF (IFINE .GE. 3) THEN
          ITIG= 2
          GO TO 660
        ENDIF
        TLOW= TU(IT-2)
        DT= (TU(IT) - TU(IT-2))/10.
C DIAGNOSTIC TO ENSURE CONVERGING CORRECTLY
        WRITE (13,2040) DP*1.E6,PPST,TAM(IT-2),TAM(IT-1),TAM(IT)
 2040   FORMAT(' DP= ',F6.2,' PST= ',F6.1,' T RANGE:',3(F7.3,3X))
        GOTO 999
      ENDIF
C
C     MAX NOT YET FOUND - CHECK A HIGHER RANGE
C
      IF (IT .EQ. IIT .AND. TAM(IT) .GT. TAM(IT-1)) THEN
        IRANGE=IRANGE+1
        IF (IRANGE .GE. 5) THEN
          ITIG= 2
          GO TO 660
        ENDIF
        TLOW= TU(IT-1)
        GO TO 999
      ENDIF
C --- BOTTOM OF LOOP OVER FUEL T - SHOULD BREAK ABOVE
 3000 CONTINUE
C --- GET TO 660 WHEN CONVERGED ON AN IGNITION TEMPERATURE
  660 CONTINUE
      RETURN
      END

      FUNCTION FTR(T,SORC,XL,KSL,CRAD,ROA,AOR2,IOK,ERR)
      IMPLICIT REAL (A-H,K-Z)
C
C     GET TR = TEMPERATURE OF MCO WALL
C     FIRST GUESS BY CONSTANT RADIATIVE CONDUCTIVITY METHOD
C       I.E. SOLUTION WITH CONSTANT KEFF
      KEFF= KSL + CRAD*(T-5.E0)**3.E0
      TQ= (SORC*XL*XL/2.E0) * ((1.E0 - AOR2)/2.E0 - AOR2*LOG(ROA))
     &    / KSL
      TMAX= T
      TMIN= T - TQ
      TR= T - TQ*KSL/KEFF
      CEFF= CRAD/4.E0/KSL
      T4= T**4E0
      IOK=0
  100 CONTINUE
      TOLD= TR
      IOK=IOK+1
      G= T - TR + CEFF*(T4 - TR**4.E0) - TQ
      DG= -1.E0 - 4.E0*CEFF*TR**3.E0
      DEL= -G/DG
      TR= TR + DEL
      TR= MIN(TR, (TOLD+TMAX)/2.E0)
      TR= MAX(TR, (TOLD+TMIN)/2.E0)
      IF (ABS(DEL)/T .LE. 1.E-5) GOTO 200
      IF (IOK .LE. 10) GOTO 100
      IF (ABS(DEL)/T .LE. 1.E-4) GOTO 200
      WRITE (13,110) T,TR,DEL,TMAX,TMIN,TQ
  110 FORMAT('  Failure to find MCO temperature ',/,
     &    ' Tcl = ',F10.4,'   Tmco= ',F10.4,'   Del= ',F10.5,/,
     &    ' Tmx = ',F10.4,'   Tmin= ',F10.4,'   Tq = ',F10.5)
      STOP
  200 CONTINUE
      ERR= DEL/TR
      FTR= TR
      RETURN
      END
```

APPENDIX D SSTEMP FORTRAN SOURCE CODE FOR IGNITION ANALYSIS OF FUEL BASKETS

```
C-----------------------------------------------------------------------
      PROGRAM SSTEMP
C
C  THIS PROGRAM COMPUTES THE STEADY STATE FUEL TEMPERATURES IN THE
C  MCO
C
C-----------------------------------------------------------------------
      IMPLICIT REAL (A-H, K-Z)
      DIMENSION VOLHS(15),RHO(15),CPHS(15),ASHS(15,2),AHSOX(15,2),
     @   EHSO(15),EHSI(15)
      DIMENSION IFROM(27),ITO(27),XLCOND(15,15),VIEWF(15,15)
      DIMENSION QDECAY(15),QOX(15),QRAD(15,15),QCOND(15,15),QNET(15),
     @          QTOTAL(15),QCON(15)
      DIMENSION BRAD(15),TFUEL(15)
C CONSTANTS
      DATA SIGMA/5.67E-8/
C
C READ IN THE INPUT DECK
C
      OPEN (UNIT=5,FILE='SSTEMP.DAT',STATUS='OLD',IOSTAT=IERRX)
      IF (IERRX .GT. 0) THEN
         WRITE(*,*) 'INPUT ERROR !'
         STOP
      ENDIF
C READ THE RUN CONTROL INPUT
      READ(5,*)
      READ(5,*) LAMDA, QV, TMCO, KG, NFO2, PPST, PR
C READ THE HEAT SINK DATA INPUT
      READ(5,*)
      DO 50 I=1,15
         READ(5,*) VOLHS(I),RHO(I),CPHS(I),ASHS(I,1),ASHS(I,2),
     @             AHSOX(I,1),AHSOX(I,2),EHSO(I),EHSI(I)
   50 CONTINUE
C READ THE HEAT TRANSFER PATH DATA INPUT
      READ(5,*)
      DO 60 IPATH=1,27
         READ(5,*) IFROM(IPATH),ITO(IPATH),XLCOND1,VIEWF1
         XLCOND(IFROM(IPATH),ITO(IPATH))=XLCOND1
         VIEWF(IFROM(IPATH),ITO(IPATH))=VIEWF1
   60 CONTINUE
C FILL IN REST OF THE VIEW FACTOR MATRIX
      DO 70 I=1,15
         DO 75 J=I+1,15
            VIEWF(J,I)=VIEWF(I,J)*ASHS(I,2)/ASHS(J,2)
   75    CONTINUE
   70 CONTINUE
      DO 80 I=1,15
         SUM=0.E0
         DO 85 J=1,15
            SUM=SUM+VIEWF(I,J)
   85    CONTINUE
         VIEWF(I,I)=1.E0-SUM
   80 CONTINUE
```

```
C
C GUESS THE TEMPERATURES AND THE RADIOSITIES
C
      DO 100 I=1,14
         QDECAY(I)=VOLHS(I)*QV
         TFUEL(I)=TMCO+40.
         IF (I/2*2 .EQ. I) THEN
            BRAD(I)=50.E0
         ELSE
            BRAD(I)=0.E0
         ENDIF
  100 CONTINUE
      BRAD(15)=50.E0
      TFUEL(15)=TMCO
C
C  ITERATE
C
 1000 CONTINUE
C
C  INITIALIZE THE TOTAL HEAT SOURCE
C
      DO 200 I=1,14
         QTOTAL(I)=QDECAY(I)
         QCON(I)=0.E0
  200 CONTINUE
      QTOTAL(15)=0.E0
      QCON(15)=0.E0
C
C  FOR EACH OF THE 28 HEAT TRANSFER PATHS, DETERMINE THE CONDUCTION HEAT
C  TRANSFER RATE
C
      DO 300 IPATH=1,27
         I=IFROM(IPATH)
         J=ITO(IPATH)
         QCOND(I,J)=KG/XLCOND(I,J)*VIEWF(I,J)*ASHS(I,2)*
     @              (TFUEL(I)-TFUEL(J))
         QTOTAL(I)=QTOTAL(I)-QCOND(I,J)
         QCON(I)=QCON(I)+QCOND(I,J)
         QTOTAL(J)=QTOTAL(J)+QCOND(I,J)
         QCON(J)=QCON(J)-QCOND(I,J)
  300 CONTINUE
C
C  FOR EACH OF THE 7 FUEL OUTER ELEMENTS AND THE MCO WALL, DETERMINE THE
C  NEW GUESS FOR THE RADIOSITY
C
      DO 400 I=2,14,2
         SUMBF=0.E0
         DO 410 J=1,15
            SUMBF=SUMBF+BRAD(J)*VIEWF(I,J)
  410    CONTINUE
         BRAD(I)=EHSO(I)*SIGMA*TFUEL(I)**4.0+(1.E0-EHSO(I))*SUMBF
  400 CONTINUE
      I=15
      SUMBF=0.E0
      DO 430 J=1,15
         SUMBF=SUMBF+BRAD(J)*VIEWF(I,J)
  430 CONTINUE
```

```
      BRAD(I)=EHSO(I)*SIGMA*TFUEL(I)**4.0+(1.E0-EHSO(I))*SUMBF
C
C  ONCE THE RADIOSITY IS KNOWN, DETERMINE THE NET HEAT LOSS DUE TO RADIATION
C
      DO 500 I=2,14,2
         QNET(I)=ASHS(I,2)*(EHSO(I)*SIGMA*TFUEL(I)**4.E0-
     @                      EHSO(I)*BRAD(I))/(1.E0-EHSO(I))
         QTOTAL(I)=QTOTAL(I)-QNET(I)
  500 CONTINUE
      I=15
      QNET(I)=ASHS(I,2)*(EHSO(I)*SIGMA*TFUEL(I)**4.E0-
     @                   EHSO(I)*BRAD(I))/(1.E0-EHSO(I))
      QTOTAL(I)=QTOTAL(I)-QNET(I)
C
C  FOR EACH OF THE 7 FUEL ASSEMBLIES, DETERMINE THE RADIATION HEAT TRANSFER
C  RATE BETWEEN THE INNER AND THE OUTER ELEMENTS
C
      DO 600 I=1,13,2
         J=I+1
         QRAD(I,J)=(ASHS(I,2)+ASHS(J,1))/2.E0*SIGMA*(TFUEL(I)**4.E0-
     @      TFUEL(J)**4.E0)/(1/EHSO(I)+1/EHSI(J)-1.E0)
         QTOTAL(I)=QTOTAL(I)-QRAD(I,J)
         QTOTAL(J)=QTOTAL(J)+QRAD(I,J)
  600 CONTINUE
C
C  FOR EACH OF THE 14 FUEL ELEMENTS, DETERMINE THE CORROSION POWER
C
C  WHEN OXYGEN IS PRESENT,
C
C     1.  U (METAL) + O2   --->   UO2,  3.4E7 J PER KG OF OXYGEN
C
C  IN OXYGEN FREE ENVIRONMENT,
C
C     1.  U (METAL) + 2 H2O   --->   UO2 + 2 H2, 1.67E7 J PER KG OF OXYGEN
C
      DO 700 I=1,14
         QOX(I)=0.E0
         DO 710 ISIDE=1,2
C USE PEARCE CORRELATION
            ILAW=0
            KCORRO= WRXUO(ILAW,TFUEL(I),NFO2,PPST,PR,1)
C WEIGHT GAIN RATE OF THE URANIUM METAL DUE TO OXIDATION
            WO2U=KCORRO*AHSOX(I,ISIDE)
            IF (NFO2 .GT. 1.E-3) THEN
               QOX(I)=QOX(I)+3.4E7*WO2U
            ELSE
               QOX(I)=QOX(I)+1.67E7*WO2U
            ENDIF
  710    CONTINUE
         QTOTAL(I)=QTOTAL(I)+QOX(I)
  700 CONTINUE
C
C  FOR EACH OF THE 14 FUEL ELEMENTS, DETERMINE THE NEW GUESS FOR THE TEMP
C
      ERRMAX=0.E0
      DO 800 I=1,14
         TFUEL(I)=TFUEL(I)+QTOTAL(I)/(RHO(I)*VOLHS(I)*CPHS(I)*LAMDA)
```

```
          IF (ABS(QTOTAL(I)) .GT. ERRMAX) ERRMAX=ABS(QTOTAL(I))
  800 CONTINUE
      WRITE(*,*) 'ERRMAX=',ERRMAX
      IF (ERRMAX .GT. 0.01) GOTO 1000
C
C  WRITE THE OUTPUT
C
      OPEN (UNIT=6,FILE='SSTEMP.OUT',STATUS='UNKNOWN',IOSTAT=IERRX)
      WRITE(*,910) QV,TMCO,KG,NFO2,PPST,PR,
     @(TFUEL(I),I=1,13,2),TFUEL(15),
     @(TFUEL(I),I=2,14,2),TFUEL(15),
     @(QDECAY(I)+QDECAY(I+1),I=1,13,2),0.E0,
     @(QOX(I)+QOX(I+1),I=1,13,2),0.E0,
     @(QCON(I),I=2,14,2),QCON(15),
     @(QNET(I),I=2,14,2),QNET(15),
     @(QTOTAL(I)+QTOTAL(I+1),I=1,13,2),QTOTAL(15)
      WRITE(6,910) QV,TMCO,KG,NFO2,PPST,PR,
     @(TFUEL(I),I=1,13,2),TFUEL(15),
     @(TFUEL(I),I=2,14,2),TFUEL(15),
     @(QDECAY(I)+QDECAY(I+1),I=1,13,2),0.E0,
     @(QOX(I)+QOX(I+1),I=1,13,2),0.E0,
     @(QCON(I),I=2,14,2),QCON(15),
     @(QNET(I),I=2,14,2),QNET(15),
     @(QTOTAL(I)+QTOTAL(I+1),I=1,13,2),QTOTAL(15)
  910 FORMAT(1X,35X,'----------'/
     @1X,        35X,'SSTEMP 1.0'/
     @1X,        35X,'----------'//
     @1X,        37X,'Inputs'/
     @1X,3x,'Qv (W/m^3)    Tmco (K)     kg (W/m/C)     nfo2',
     @1X,'     Pst (Pa)     P (Pa)'/
     @1X,3X,F8.1,7X,F5.1,9X,F5.3,7X,F5.3,3X,F9.1,5X,F9.1//
     @1X,37X,'Outputs'/
     @19X,'fuel-1 fuel-2 fuel-3 fuel-4 fuel-5 fuel-6 fuel-7 MCO wall'/
     @19x,'------ ------ ------ ------ ------ ------ ------ --------'/
     @1X,'inner elem temp   ',7(F5.1,2X),F7.1/
     @1X,'outer elem temp   ',7(F5.1,2X),F7.1/
     @1X,'decay power       ',7(F5.1,2X),F7.1/
     @1X,'corrosion power   ',7(F5.1,2X),F7.1/
     @1X,'conduction loss   ',7(F5.1,2X),F7.1/
     @1X,'radiation loss    ',7(F5.1,2X),F7.1/
     @1X,'net energy source ',7(F5.3,2X),F7.3//
     @1X,20X,'* all temperatures are in Kelvin and power in watts')
      STOP
      END
```

APPENDIX E IGMCOFIN FORTRAN SOURCE CODE FOR IGNITION ANALYSIS OF SCRAP BASKETS WITHOUT FINS

```
PROGRAM IGMCOFIN
C
C     DRIVER/SUBROUTINE VERSION !!! debug version !!!
C
C     SCRAP BASKET WITH FIN MODEL
C
C     VARIATION ON IGMCOMC - MONTE CARLO CALC
C     TO PLOT SEPARATE EFFECTS OF MULTIPLIER, KGAS, PPST
C
C
C     IGNITION TEMPERATURE FOR FUEL IN AN MCO AT CVD
C       I.E. CONSTANT WALL TEMPERATURE
C     SCRAP GEOMETRY, INTERNAL RADIATION BY T**3 DT/DR
C
C     "PEARCE" KINETICS FROM HANFORD + MULTIPLIER
C     MULTIPLIER CAN ACCOUNT FOR FAILURE FRACTION, SWELLING,
C          PRESENCE OF POROUS SURFACE LAYER, ETC.
C     EXTERNAL HEAT TRANSFER INDEPENDENT OF LENGTH
C
C     SURFACE AREA AND SCRAP VOID FRACTION ARE CORRELATED
C     EVAPORATION TERM EXPLICITLY CONSIDERED
C
C     MAJOR PROGRAM SECTIONS:
C     1.0  DECLARATIONS & CONSTANTS
C     2.0  LOOP TO SELECT PARTICULAR CASE
C     3.0  CASE INPUTS
C     4.0  IGNITION TEMPERATURE
C     5.0  STATISTICS AND OUTPUT
C
C     ------------------------------------------------------------
C     1.0  DECLARATIONS & CONSTANTS
C     ------------------------------------------------------------
C
C
      IMPLICIT REAL (A-H, K-Z)
      PARAMETER (INARX=100)
      DIMENSION ARX(INARX),TIGSAV(INARX,4),TMXSAV(INARX,4)
      DATA TKO /273.15/
C
C     OUTPUT FILES:
C     12  DIRECT VALUES FROM EACH CASE
C     13  ERROR MESSAGES AND PROOF MAXIMUM FOUND
C     14  PLOT OUTPUT
C
       OPEN (UNIT=12, STATUS='UNKNOWN', FORM='FORMATTED',
     &       FILE='FOR012.DAT', ERR=1234)
       OPEN (UNIT=13, STATUS='UNKNOWN', FORM='FORMATTED',
     &       FILE='FOR013.DAT', ERR=1234)
       OPEN (UNIT=14, STATUS='UNKNOWN', FORM='FORMATTED',
     &       FILE='FOR014.DAT', ERR=1234)
C
C     ------------------------------------------------------------
C     2.0  ESTABLISH CASE INPUTS
```

```
C     ------------------------------------------------------------
C
C     GET PARAMETER DISTRIBUTION VALUES
C
C     QLOW   DECAY POWER LOW VALUE
C     QMID   DECAY POWER MID VALUE
C     QUPP   DECAY POWER HIGH VALUE
C     PHILO  POROSITY LOW VALUE
C     PHIDL  POROSITY RANGE
C     FEAMN  RATE LAW MULTIPLIER MIN VALUE
C     FEAMX  RATE LAW MULTIPLIER HAX VALUE
C     IRDIS  0=UNIFORM, 1=LOG-UNIFORM RATE LAW DISTRIBUTION
C     EPSLO  INTERNAL EMISSIVITY LOW VALUE
C     EPSDL  INTERNAL EMISSIVITY RANGE
C     EGPLO  GAP EMISSIVITY LOW VALUE
C     EGPDL  GAP EMISSIVITY RANGE
C     ALO    REACTION AREA LOW VALUE
C     AHI    REACTION AREA HIGH VALUE
C     IADIS  0=UNIFORM, 1=LOG-UNIFORM AREA DISTRIBUTION
C     DLO    SCRAP SIZE LOW DIAMETER
C     DHI    SCRAP SIZE HIGH DIAMETER
C     IDDIS  0=UNIFORM, 1=LOG-UNIFORM DIAMETER (SIZE) DISTRIBUTION
C     PSLO   STEAM PRESSURE IN KPA - LOW
C     PSHI   STEAM PRESSURE IN KPA - HIGH
C     IPDIS  0=UNIFORM, 1=LOG-UNIFORM PRESSURE DISTRIBUTION
C     NULO   NUSSELT NUMBER FOR CONVECTION -LO
C     NUDL   NUSSELT NUMBER FOR CONVECTION - RANGE TO HIGH
C     WEVLO  LOW BOUND AVERAGE EVAPORATION RATE KG/S DURING CVD
C     WEVDL  RANGE IN AVERAGE EVAPORATION RATE
C  -- CONSTANT VALUES
C     RIN     INNER RADIUS FOR FUEL IN MCO
C     XL      OUTER RADIUS OF FUEL, INNER RADIUS OF MCO
C     XGAP    BASKET-MCO WALL GAP THICKNESS
C     KRAT    MCO GAS THERMAL CONDUCTIVITY - RATIO KBED/KGAS
C     HFG     WATER LATENT HEAT OF EVAPORATION J/KG
C     VBAS    BASKET VOLUME M^3
C     KFIN    FIN CONDUCTIVITY
C     TFIN    FIN THICKNESS
C     FSEC    SECTOR FRACTION OF CIRCLE
C     FFIN    SECTOR FRACTION FOR PERIPHERAL FIN
C
      CALL GETVAR (
     &      QLOW,  QMID,  QUPP, PHILO, PHIDL, FEAMN, FEAMX, IRDIS,
     &     EPSLO, EPSDL, EGPLO, EGPDL,   ALO,   AHI, IADIS,
     &       DLO,   DHI, IDDIS,  PSLO,  PSHI, IPDIS,  NULO,  NUDL,
     &     WEVLO, WEVDL,
     &       RIN,    XL,  XGAP,  KRAT,   HFG,  VBAS,
     &      KFIN,  TFIN,  FSEC,  FFIN)
C
C     SETUP REACTING AREA & RATE MULTIPLIER RANGE
C
C     INARX  # OF SEPARATE CASES FOR COMBINED AREA AND RATE MULTIPLIER
C     TIGSAV SAVED OUTPUT FOR LATER PLOTTING
C
      ARXLO= ALO*FEAMN
      ARXHI= AHI*FEAMX
      DELARX= (ARXHI-ARXLO) / FLOAT(INARX-1)
```

```
      DO 100 JJ=1, INARX
         ARX(JJ)= ARXLO + FLOAT(JJ-1)*DELARX
 100  CONTINUE
C
C
C
      IDBG=1
C
C     PHI      POROSITY
C     QV       VOLUMETRIC POWER W/M^3
C     HIN      ZERO TO CALCULATE, ELSE INPUT W/M^2/K
C     FEAC     MULTIPLIER DESCRIBED BELOW
C     KSL      EFFECTIVE DISTRIBUTED THERMAL CONDUCTIVITY W/M/K
C     EPS      OVERALL EMISSIVITY -INSIDE MCO-
C     RIN      INNER RADIUS FOR FUEL IN MCO
C     XL       OUTER RADIUS OF FUEL, INNER RADIUS OF MCO
C     XGAP     BASKET-MCO WALL GAP THICKNESS
C     KGAP     MCO GAS THERMAL CONDUCTIVITY
C     EGAP     EFFECTIVE OVERALL EMISSIVITY IN GAP 1/(1/E1 + 1/E2 -1)
C     AOV0     NOMINAL A/V 1/M
C     FRAD     RADIATION DISTANCE FACTOR
C              <1 XRAD = FRAD*XL  USE FOR RODS:  1/FRAD = # SERIES PATHS
C                                 DEFAULT IS 4 SERIES PATHS FOR MCO
C              >1 XRAD = FRAD*DP  USE FOR BEDS, ACCOUNTS FOR REFLECTIONS
C                                 DEFAULT IS 3 USING PHI=0.4, EPS=0.7:
C                                 LAM = 1 - 1.21 (1 - (1-PHI)**2/3)
C                                 FRAD= (1 + LAM/EPS)/(1 - LAM)
C
C     BED THERMAL CONDUCTIVITY MODEL OPTIONS:
C         KRAT < 0.01, USE DEFAULT GASES AND POROSITY MODEL
C         KRAT > 0.01, KBED = KRAT * KGAS, CONVECTION IS IGNORED
C
C
C
C     DEFAULT VALUES HERE FOR RODS IN AN MCO
C     FOR FUEL FRAGMENTS THESE ARE APPROPRIATE DEFAULTS:
C     PHI= 0.40  KSL=0.20 TO 0.30  FRAD=3.0  RIN=0.20  AOV0=1000
C
C
C     OVERRIDE CASE INPUTS SELECTIVELY
C     SUBROUTINE USED BELOW WAS FOR MONTE CARLO ANALYSIS
C     HERE EXPECT DETERMINISTIC VALUES
C
C     LAST TWO LINES OF 'GETIN' ARE THE OUTPUTS
C     CAN ONLY ASSIGN GAS PROPERTIES INSIDE DETERMINISTIC LOOP
C     RATE MULTIPLIER SET = 1, INFORMATION CONVEYED BY AOV0
C
C
C      CALL GETIN (NSAM,
C     &      QLOW,  QMID,  QUPP, PHILO, PHIDL, FEAMN, FEAMX, IRDIS,
C     &     EPSLO, EPSDL, EGPLO, EGPDL,   ALO,   AHI, IADIS,
C     &       DLO,   DHI, IDDIS,  PSLO,  PSHI, IPDIS,  NULO,  NUDL,
C     &     WEVLO, WEVDL,
C     &       RIN,    XL,  XGAP,  KGAS,   HFG,  VBAS,
C     &        QV,   PHI,  FEAC,   KSL,   EPS,   NUS,
C     &      KGAP,  EGAP,  AOV0,  FRAD,    DP,  PPST,  QVEV)
C
```

```
      QV= QLOW
      PHI= PHILO
      FEAC= 1.E0
      EPS= EPSLO
      NUS= NULO
      EGAP= EGPLO
      LAM= 1.E0 - 1.21E0*(1.E0-(1.E0-PHI))**(2.E0/3.E0)
      FRAD= (1.E0 + LAM/EPS)/(1.E0-LAM)
      DP= DLO
      QVEV= 0.E0
      KHEL= 0.17E0
      KSTM= 0.022E0
C
      WRITE (*,51) QV,PHI,EPS,NUS,EGAP,DP
      WRITE (*,55) KHEL,KHEL,KSTM,KSTM, PSLO,PSHI,PSLO,PSHI
   51 FORMAT(//,
     &       ' ** IGNITION TEMPERATURE VARIATION ** ',//,
     &       ' QV  = ',F9.2,'    PHI  = ',F9.4,/,
     &       ' EPS = ',F9.4,'    NUS  = ',F9.4,/,
     &       ' EGAP= ',F9.4,'    DP   = ',F9.6,/)
   55 FORMAT(' COLUMNS FOR INDICATED COMBINATIONS OF',/,
     &       ' GAS THERMAL CONDUCTIVITY, I.E. HE AND H2O, W/M/K',/,
     &       ' AND VARIOUS STEAM PRESSURES IN KPA',/,
     &       ' ROWS FOR PRODUCT OF AREA*RATE MULTIPLIER, M^2',//,
     &       ' A*Frx',T10,'K:', T15,4(F6.3,6X),/,
     &              T10,'P:', T15,4(F6.3,6X),/)
   59 FORMAT(' ',F8.4,T15,4(F6.2,6X))
C
C
C     ------------------------------------------------------------
C     3.0  LOOP OVER AREA*MULTIPLIER AND VARIOUS PRESSURE/GAS
C     ------------------------------------------------------------
C
C
C     !!! NOTE FOR LOOP OVER AREA*MULTIPLIER:
C         A/V IS ONLY USED FOR REACTING AREA LATER
C         BUT MUST BE DIVIDED HERE BY (1-PHI) TO PRESERVE ARX
C
C
      DO 777 ISAM= 1,INARX
      AOV0= ARX(ISAM) / VBAS / (1.E0 - PHI)
C
      DO 766 JSAM=1,4
C
      IF (JSAM .EQ. 1) THEN
          KGAS= KHEL
          PPST= PSLO
      ELSEIF (JSAM .EQ. 2) THEN
          KGAS= KHEL
          PPST= PSHI
      ELSEIF (JSAM .EQ. 3) THEN
          KGAS= KSTM
          PPST= PSLO
      ELSE
          KGAS= KSTM
          PPST= PSHI
      ENDIF
```

```
C
      IF (KRAT .LE. 0.01E0) THEN
      KSL= KGAS / (1.E0 - (1.E0-PHI)**0.3333E0)
     &     + KGAS*(NUS-1.E0)
      ELSE
      KSL= KRAT*KGAS
      ENDIF
      KGAP= KGAS
C
C     ------------------------------------------------------------
C     4.0  IGNITION TEMPERATURE
C     ------------------------------------------------------------
C
      CALL TIGMCO (
     &     QV,   PHI,   KSL,   EPS,   RIN,  FRAD,
     &     XL,  FEAC,  AOV0,  PPST,    DP,  QVEV,
     &   XGAP,  KGAP,  EGAP,  IDBG,
     &   KFIN,  TFIN,  FSEC,  FFIN,
     &    TCL,    TR,  TAMB,    QR,  SORC, QFLUX,  ERR, ITIG)
C
C     SAVE OUTPUT IN C
C
      TAMB= TAMB - TKO
      TCL= TCL - TKO
      TR= TR - TKO
C
C     ------------------------------------------------------------
C     OPTIONAL CASE OUTPUT
C     ------------------------------------------------------------
C
      IF (IDBG .EQ. 1) THEN
      WRITE (12,4001) PHI, QV, FEAC,KSL, EPS,EGAP, RIN,XL,
     %                XGAP,KGAP, DP,PPST, NUS, FRAD
      WRITE (12,4002)
      WRITE (12,4003) AOV0,TAMB,TR,TCL,SORC,QFLUX,ERR
      ENDIF
 4001 FORMAT(//,' ***** Ignition of fuel in MCO ***** ',/,
     & '   Porosity=       ',F8.3,'       Power W/m^3= ',F8.2,/,
     & '   Kin. Rate Mult= ',F8.3,'      Therm. cond.= ',F8.4,/,
     & '   Emissivity=     ',F8.4,'        Gap emiss.= ',F8.4,/,
     & '   Inner radius=   ',F8.5,'     Outer radius = ',F8.5,/,
     & '   Gap thickness=  ',F8.6,'    Gap therm cond= ',F8.4,/,
     & '   Diameter=       ',F8.6,'        Psteam Kpa= ',F8.3,/,
     & '   Nusselt=        ',F8.4,/,
     & '   Frad <1 rods, >1 rubble: ',F8.4,/)
 4002 FORMAT(
     &'   Ambient ignition T and profiles in C for Pst =1 kPa',/,
     &'    A/V',T12,'Tamb',T22,'Tmin',T32,'Tmax',T42,'Qsor',
     &     T52,'Qflux',T62,'Error',/)
 4003 FORMAT('  ',F7.1,T10, 3(F7.2,3X), F8.2,2X, F7.1,3X, 1PE9.2)
C
C --- BOTTOM OF CASE CALCULATION
C
C --- SAVE IGNITION TEMPERATURE FOR EACH CASE
C
      TIGSAV(ISAM,JSAM)= TAMB
      TMXSAV(ISAM,JSAM)= TCL
```

```
C
C --- END OF CASE LOOPS
C
 766  CONTINUE
      WRITE (*,59) ARX(ISAM),(TIGSAV(ISAM,JJ),JJ=1,4)
      IF (MOD(ISAM,10) .EQ. 0) WRITE (*,'('' '')')
 777  CONTINUE
C
C --- OUTSIDE ALL LOOPS
C
C
C     ------------------------------------------------------------
C     5.0  PLOT
C     ------------------------------------------------------------
C
C --- GRAPHIC FILE - CUT OUT VALUES BELOW 0 C AND ABOVE 250 C
C
      WRITE (14, '('' 5'')')
      WRITE (14, '('' '')')
      WRITE (14, '('' '')')
      WRITE (14, '('' MCO Ignition Results'')')
      WRITE (14, '(3X,''Arx '',10X,''He-8'',10X,''He-16'',
     &                          10X,''St-8'',10X,''St-16'')')
      WRITE (14, '(3X,''m^2 '',10X,''C   '',10X,''C    '',
     &                          10X,''C   '',10X,''C    '')')
      WRITE (14, '('' '')')
      WRITE (14, '('' '')')
      DO 790 II=1,INARX
      DO 788 JJ=1,4
      TIGSAV(II,JJ)= MAX(0.E0, MIN(250.E0, TIGSAV(II,JJ)))
 788  CONTINUE
      WRITE (14, '('' '',5(G13.4,2X))')
     &      ARX(II),(TIGSAV(II,JJ),JJ=1,4)
 790  CONTINUE
C
 1234 WRITE (*,666)
  666 FORMAT(' Attaboy, Marty')
      END

      SUBROUTINE TIGMCO (
     &     QV,   PHI,   KSL,   EPS,   RIN,  FRAD,
     &     XL,  FEAC,  AOV0,  PPST,    DP,  QVEV,
     &   XGAP,  KGAP,  EGAP,  IDBG,
     &   KFIN,  TFIN,  FSEC,  FFIN,
     &    TCL,    TR,  TAMB,    QR,  SORC, QFLUX,  ERR, ITIG)
C
C     IGNITION TEMPERATURE OF FUEL IN A SCRAP BASKET
C     FIXED MCO WALL TEMPERATURE = TAMB = IGNITION TEMP.
C
      IMPLICIT REAL (A-H,K-Z)
      INTEGER NTA
      PARAMETER (NTA=25,  NDP=7,  NPS=4)
      DIMENSION TAM(NTA),TU(NTA)
      DATA SIGMA /5.67E-8/
      DATA PI /3.14159E0/
C
C     TAM()   AMBIENT TEMPERATURES SAVED DURING SEARCH FOR MAXIMUM
```

```
C     TU()     FUEL TEMPERATURES SAVED DURING SEARCH FOR MAXIMUM
C              -NOTE- MORE VALUES SAVED THAN OPTIMALLY NECESSARY,
C               SO DEBUGGING/PLOTTING OF LOCAL BEHAVIOR IS EASIER
C
C
C     EXIT CONDITION CODE:
C     ITIG: 1  TIG < LOWER BOUND
C     ITIG: 2  TIG FOUND
C     ITIG: 3  TIG > UPPER BOUND
C
      ITIG= 0
      TCL= 273.
      TR=  273.
      TAMB=273.
      QR=  0.E0
      SORC= 0.E0
      QFLUX= 0.E0
      ERR= 0.E0
C
C     KINETIC RATE MULTIPLIER ACCOUNTS FOR EITHER:
C       ACTUAL RATE UNCERTAINTY
C       VOLUME FRACTION OF REACTING MATERIAL
C       SWELLING EFFECT, ETC.
C
      FARX= FEAC * (1.E0 - PHI)*AOV0
C
C     DERIVED FIN QUANTITIES
C
C     MFIN  'M' IN FIN EQUATION
C     LFIN  'L' IN FIN EQUATION = LENGTH OF PERIPHERAL FIN SECTION
C            STARTING FROM RADIAL FIN TO ITS END OR HALF OF SECTOR!
C     HEFF   THETA/Q" RATIO: PERIPHERAL FIN DELTA-T / HEAT FLUX
C            I.E. EFFECTIVE HEAT TRANSFER COEFFICIENT
C
      HGAP= KGAP/XGAP
      MFIN= SQRT(HGAP/KFIN/TFIN)
      THETA1= 2.E0*PI*FSEC
      THETA2= 2.E0*PI*FFIN
      LFIN= XL*THETA2
      HEFF= LFIN / SQRT(HGAP*KFIN*TFIN) / TANH(MFIN*LFIN)
C
C
C     TOP OF LOOP OVER PARTICLE TEMPERATURE
C
C     FOR A GIVEN PPST,DP,XL MAY RUN PAST THIS POINT SEVERAL TIMES
C     START WITH LOW,COARSE RANGE OF FUEL TEMPERATURE FOR IGNITION
C     COME BACK HERE IF HIGHER RANGES OR FINE RANGES ARE DESIRED
C     FIRST GET THE CORRECT COARSE RANGE, THEN FINE RANGES
C     SEE TESTS AFTER NEWTON LOOP BOTTOM
C
C     TLOW:  LOW END OF RANGE TO INVESTIGATE
C            MAY BE RESET AT END OF LOOP OVER THE RANGE
C     DT:    INCREMENT OF RANGE, MAY ALSO BE RESET AT END OF LOOP
C     IRANGE: RANGE COUNTER
C     FINE:   FINE RANGE COUNTER
C
      TLOW= 273.E0
```

```
      DT=10.
      IRANGE=0
      IFINE=0
  999 CONTINUE
      IIT=10
      DO 3000 IT=1,IIT
C
C     ------------------------------------------------------------
C     3.0  FUEL T, REACTION SOURCE, MCO WALL TEMPERATURE
C     ------------------------------------------------------------
C
      TCL= TLOW + DT*FLOAT(IT-1)
      TU(IT)=TCL
C
C     GIVEN FUEL T, GET REACTION POWER, THEN
C       1) SOLVE FOR TEMPERATURE AT MCO RADIUS
C       2) ITERATE TO SOLVE FOR TUBE AND AMBIENT TEMPERATURES
C
C     MCGILLIVRAY CORRELATION FOR MOIST AIR
C     RATE IN MG O2/CM^2 MIN IS CONVERTED TO W/M^2
C     VIA 10^-6/10^-4/60 = 0.01/60  WHERE 3.4E7 IS HEAT OF REACTION
C      RD= EXP(11.093 - 8077.0/TCL)
C      RK1= EXP(7.831 - 6432.0/TCL)
C      RK2= EXP(-15.208 + 5237.0/TCL)
C      RR= RD + RK1*PPST/(1.0 + RK2*PPST)
C      QR= FARX * 3.4E7 * RR * 0.01/60.0
C
C
C     RATE LAW: PEARCE U-H2O BELOW 350 C, PPST IN KPA
C     LAW UNITS OF MG/CM^2/HR CONVERT BY 0.01/3600 TO KG/M^2/S
C
C     HEAT OF REACTION IS PER KG O2 WEIGHT SINCE
C      CORRELATIONS ARE FOR WEIGHT GAIN PER AREA PER TIME
C
C     REACTION ENERGIES ARE:
C
C     U + O2 = UO2           DH= 1085E3 J/G.MOL
C                              = 3.4E7 J/KG OXYGEN GAINED
C                                USE THIS IF O2 IS REACTING
C
C     H2 + 1/2 O2 = H2O      DH= 241E3 J/G.MOL
C
C     U + 2H2O = UO2 + 2H2   DH= 1085 - 2*241 = 603 J/G.MOL
C                              = 1.67E7 J/KG H2O LOST
C                              = 1.88E7 J/KG O2 GAINED
C
      ARG= 4.33E0 - 2144.E0/TCL
      RR= 10.E0**(ARG) * SQRT(PPST)
      QR= FARX * 1.88E7 * RR * 0.01/3600.0
C
C     TOTAL SOURCE:
C
C     ABANDON WHEN SOURCE < 100 W/M^3, BY EXPERIENCE IGNITION CAN'T HAPPEN
C
      SORC= QV*(1.E0 - PHI) + QR - QVEV
C
      IF (SORC .LE. 100.E0) THEN
```

```
      ITIG= 3
      TCL= 773.
      TR=  773.
      TAMB=773.
      ERR= 0.E0
      QFLUX= (SORC*XL/2.E0) * (1.E0 - (RIN*RIN)/(XL*XL))
      GOTO 660
      ENDIF
C
C     TEMPERATURE TR AT RADIUS R=XL:
C     AOR = (r=A)/(r=r) = inner/outer radii ratio; AOR2 = a^2/R^2
C     XRAD= EFFECTIVE DISTANCE BETWEEN RADIATION SHIELDS
C         = RADIUS/# OF SHIELDS
C
C     FOR FIN, NEED EFFECTIVE INSERT RADIUS TO REPLACE RIN
C     FIRST GET RADIAL FIN DELTA-T AND EQUIVALENT PLANAR DELTA-T RATIO
C
C
      FRFIN= SORC*THETA1 / (KFIN*TFIN)
      DTRFIN= FRFIN/6.E0 * (XL*XL*XL - RIN*RIN*(3.E0*XL - 2.E0*RIN))
      DTPLAN= SORC*XL*XL/2.E0/KSL
      DELTA= DTRFIN/DTPLAN
      RHO1= SQRT( (1.E0 - 2.E0*DELTA)
     &           /(2.E0*THETA1*THETA1 + 1.E0) )
      DO 2020 JJJ=1,8
      RHO1= SQRT( (1.E0 - 2.E0*DELTA)
     &           /(2.E0*THETA1*THETA1 + 1.E0 - 2.E0*LOG(RHO1)) )
 2020 CONTINUE
      AOR= RHO1
      RINEF= AOR*XL
C
      SIGEP= SIGMA*EPS
      XRAD= FRAD*DP
      CRAD= 4.E0*SIGEP*XRAD
      TR= FTR(TCL,SORC,XL,KSL,CRAD,AOR,IOK1,ERR1)
C
C     HEAT FLUX AT RADIUS XL: FULL POWER GOES INTO FIN !!!
C
      QFLUX= (SORC*XL/2.E0) * (1.E0 - RIN*RIN/(XL*XL))
C
C     ESTIMATED TEMPERATURE AFTER GAP I.E. MCO WALL
C      TAMB= FTS(TR,QFLUX,EGAP,KGAP,XGAP,IOK2,ERR2)
C
C     FOR FINNED BASKET, ADD DROP ALONG PERIPHERAL FIN
C     TEXTBOOK SOLUTION FOR FIN INSULATED AT ITS TIP
C     ALL BASKET POWER GOES INTO BASE OF FIN
C
      DTPFIN= QFLUX * HEFF
      TAMB= TR - DTPFIN
      ERR2= 0.E0
C
      ERR= ABS(ERR1)+ABS(ERR2)
C
C     CONVERGED; NOW SEE IF MAXIMUM FOUND
C
C     ------------------------------------------------------------
C     5.0  SEARCH FOR MAXIMUM
```

```
C     ------------------------------------------------------------
C
      TAM(IT)= TAMB
C
C     CASE WHERE MAX IS LOWER THAN FIRST GUESS - JUST QUIT
C
      IF (IT .EQ. 2 .AND. TAMB .LT. TAM(1)) THEN
        ITIG= 1
        WRITE (13,2011) TLOW,DP*1.E6,PPST,XL*1000.
        WRITE (13,1110) TCL, TAMB, SORC, QFLUX
        GOTO 660
      ENDIF
 2011 FORMAT(' Ignition temperature below starting value',F5.1,/,
     & ' DP=',F4.1,'  PPST=',F6.1,'   XL=',F4.1)
 1110 FORMAT(
     & ' T= ',F8.2,'  TAMB= ',F8.2,'  SORC= ',1PE11.3,'  FLUX= ',E10.3)
C
C     CASE WHERE MAX FOUND
C       GO BACK FOR FINER RANGE OR
C       ON THIRD TRY DECLARE CONVERGED
C     FOR DEBUG, DIAGNOSTIC TO ENSURE CONVERGING CORRECTLY
C
      IF (IT.GE.3 .AND. TAM(IT) .LT. TAM(IT-1)) THEN
        IF (IDBG .EQ. 1)
     &  WRITE (13,2040) AOV0,SORC,QFLUX,TAM(IT-2),TAM(IT-1),TAM(IT)
        IFINE=IFINE+1
        TLOW= MIN( TU(IT-2), TU(IT))
        DT= ABS(TU(IT) - TU(IT-2))/10.
        TERR= MAX( ABS(TU(IT-1) - TU(IT)),
     &             ABS(TU(IT-1) - TU(IT-2)) )
        IF (TERR. LE. 0.05E0 .OR. IFINE .GE. 3) THEN
          ITIG= 2
          GO TO 660
        ELSE
          GOTO 999
        ENDIF
      ENDIF
 2040 FORMAT(' A/V=',F6.2,'   Q/V=',F7.1,'   Q/A=',F8.2,
     &       '   T RANGE:',3(F7.3,3X))
C
C     MAX NOT YET FOUND - CHECK A HIGHER RANGE
C
      IF (IT .EQ. IIT .AND. TAM(IT) .GT. TAM(IT-1)) THEN
        IRANGE=IRANGE+1
        IF (IRANGE .GE. 5) THEN
          ITIG= 2
          GO TO 660
        ENDIF
        TLOW= TU(IT-1)
        GO TO 999
      ENDIF
C --- BOTTOM OF LOOP OVER FUEL T - SHOULD BREAK ABOVE
 3000 CONTINUE
C --- GET TO 660 WHEN CONVERGED ON AN IGNITION TEMPERATURE
  660 CONTINUE
      RETURN
      END
```

```
      FUNCTION FTR(TCL,SORC,XL,KSL,CRAD,AOR,IOK,ERR)
      IMPLICIT REAL (A-H,K-Z)
C
C     GET TR = TEMPERATURE OF SCRAP BASKET OUTER RADIUS
C
C     FIRST GUESS BY CONSTANT RADIATIVE CONDUCTIVITY METHOD
C       I.E. SOLUTION WITH CONSTANT KEFF
C
      AOR2= AOR*AOR
      KEFF= KSL + CRAD*(TCL-5.E0)**3.E0
      TQ= (SORC*XL*XL/2.E0) * ((1.E0 - AOR2)/2.E0 + AOR2*LOG(AOR))
     &    / KSL
      TMAX= TCL
      TMIN= TCL - TQ
      TR= TCL - TQ*KSL/KEFF
      CEFF= CRAD/4.E0/KSL
      T4= TCL**4.E0
      IOK=0
  100 CONTINUE
      TOLD= TR
      IOK=IOK+1
      G= TCL - TR + CEFF*(T4 - TR**4.E0) - TQ
      DG= -1.E0 - 4.E0*CEFF*TR**3.E0
      DEL= -G/DG
      TR= TR + DEL
      TR= MIN(TR, (TOLD+TMAX)/2.E0)
      TR= MAX(TR, (TOLD+TMIN)/2.E0)
      IF (ABS(DEL)/TCL .LE. 1.E-5) GOTO 200
      IF (IOK .LE. 10) GOTO 100
      IF (ABS(DEL)/TCL .LE. 1.E-4) GOTO 200
      WRITE (13,110) TCL,TR,DEL,TMAX,TMIN,TQ
  110 FORMAT('  Failure to find MCO temperature ',/,
     &    ' Tcl = ',F10.4,'   Tmco= ',F10.4,'   Del= ',F10.5,/,
     &    ' Tmx = ',F10.4,'   Tmin= ',F10.4,'   Tq = ',F10.5)
      STOP
  200 CONTINUE
      ERR= DEL/TR
      FTR= TR
      RETURN
      END

      FUNCTION FTS(TR,QFLUX,EGAP,KGAP,XGAP,IOK,ERR)
      IMPLICIT REAL (A-H,K-Z)
      DATA SIGMA /5.67E-8/
C
C     GET TS = TEMPERATURE OF MCO WALL
C     FIRST GUESS USING TR FOR HRAD
C
      HGAP= KGAP/XGAP
      HEFF= 4.E0*SIGMA*EGAP*(TR-1.E0)**3.E0 + HGAP
      TS= TR - QFLUX/HEFF
      TMAX= TR
      TMIN= TR - QFLUX/HGAP
      TMIN= MAX(10.E0, TMIN)
      SIGEP= SIGMA*EGAP
      TR4= TR**4.E0
```

```
      IOK=0
  100 CONTINUE
      TOLD= TS
      IOK=IOK+1
      G= -QFLUX + SIGEP*(TR4 - TS**4.E0) + HGAP*(TR - TS)
      DG= -4.E0*SIGEP*TS**3.E0 - HGAP
      DEL= -G/DG
      TS= TS + DEL
      TS= MIN(TS, (TOLD+TMAX)/2.E0)
      TS= MAX(TS, (TOLD+TMIN)/2.E0)
      IF (ABS(DEL)/TR .LE. 1.E-5) GOTO 200
      IF (IOK .LE. 10) GOTO 100
      IF (ABS(DEL)/TR .LE. 1.E-4) GOTO 200
      WRITE (13,110) TR,TS,DEL,TMAX,TMIN,QFLUX
  110 FORMAT('  Failure to find MCO wall temperature ',/,
     &    ' TR  = ',F10.4,'   Tmco= ',F10.4,'   Del= ',F10.5,/,
     &    ' Tmx = ',F10.4,'   Tmin= ',F10.4,'   q" = ',F10.5)
      STOP
  200 CONTINUE
      ERR= DEL/TS
      FTS= TS
      RETURN
      END

      SUBROUTINE GETVAR (
     &      QLOW,  QMID,  QUPP, PHILO, PHIDL, FEAMN, FEAMX, IRDIS,
     &     EPSLO, EPSDL, EGPLO, EGPDL,   ALO,   AHI, IADIS,
     &       DLO,   DHI, IDDIS,  PSLO,  PSHI, IPDIS,  NULO,  NUDL,
     &     WEVLO, WEVDL,
     &       RIN,    XL,  XGAP,  KRAT,   HFG,  VBAS,
     &      KFIN,  TFIN,  FSEC,  FFIN)
      IMPLICIT REAL (A-H,K-Z)
      CHARACTER*11 LABDIS(2)
      DATA LABDIS /'Uniform    ','Log-Uniform'/
C
C     GET MONTE CARLO INPUTS FROM FILE
C
      OPEN (UNIT=11, STATUS='UNKNOWN', FORM='FORMATTED',
     &      FILE='FOR011.DAT')
C
C     LINES WITH A NON-BLANK IN FIRST COLUMN ARE COMMENTS
C     VARIABLES ARE FOUND IN ORDER
C
      QLOW= RREAD(11)
      QMID= RREAD(11)
      QUPP= RREAD(11)
      PHILO= RREAD(11)
      PHIDL= RREAD(11)
      FEAMN= RREAD(11)
      FEAMX= RREAD(11)
      IRDIS= IREAD(11)
      EPSLO= RREAD(11)
      EPSDL= RREAD(11)
      EGPLO= RREAD(11)
      EGPDL= RREAD(11)
      ALO= RREAD(11)
      AHI= RREAD(11)
```

```
      IADIS= IREAD(11)
      DLO= RREAD(11)
      DHI= RREAD(11)
      IDDIS= IREAD(11)
      PSLO= RREAD(11)
      PSHI= RREAD(11)
      IPDIS= IREAD(11)
      NULO= RREAD(11)
      NUDL= RREAD(11)
      WEVLO= RREAD(11)
      WEVDL= RREAD(11)
      RIN= RREAD(11)
      XL= RREAD(11)
      XGAP= RREAD(11)
      KRAT= RREAD(11)
      HFG= RREAD(11)
      VBAS= RREAD(11)
      KFIN= RREAD(11)
      TFIN= RREAD(11)
      FSEC= RREAD(11)
      FFIN= RREAD(11)
      IRDIS= MAX(1, MIN(0, IRDIS))
      IADIS= MAX(1, MIN(0, IADIS))
      IDDIS= MAX(1, MIN(0, IDDIS))
      IPDIS= MAX(1, MIN(0, IPDIS))
C
      CLOSE (11)
C
      WRITE (*,100)
     &  QLOW,  QMID,  QUPP, PHILO, PHIDL, LABDIS(IRDIS), FEAMN, FEAMX,
     &  EPSLO, EPSDL, EGPLO, EGPDL, LABDIS(IADIS),  ALO,  AHI
      WRITE (12,100)
     &  QLOW,  QMID,  QUPP, PHILO, PHIDL, LABDIS(IRDIS), FEAMN, FEAMX,
     &  EPSLO, EPSDL, EGPLO, EGPDL, LABDIS(IADIS),  ALO,  AHI
      WRITE (13,100)
     &  QLOW,  QMID,  QUPP, PHILO, PHIDL, LABDIS(IRDIS), FEAMN, FEAMX,
     &  EPSLO, EPSDL, EGPLO, EGPDL, LABDIS(IADIS),  ALO,  AHI
      WRITE (*,102)
     &  LABDIS(IDDIS),100.*DLO,100.*DHI,  LABDIS(IPDIS), PSLO,  PSHI,
     &  NULO,   NUDL, WEVLO, WEVDL
      WRITE (12,102)
     &  LABDIS(IDDIS),100.*DLO,100.*DHI,  LABDIS(IPDIS), PSLO,  PSHI,
     &  NULO,   NUDL, WEVLO, WEVDL
      WRITE (13,102)
     &  LABDIS(IDDIS),100.*DLO,100.*DHI,  LABDIS(IPDIS), PSLO,  PSHI,
     &  NULO,   NUDL, WEVLO, WEVDL
      WRITE (*,104) RIN,    XL,   XGAP,  KRAT,  HFG, VBAS
      WRITE (12,104) RIN,    XL,   XGAP,  KRAT,  HFG, VBAS
      WRITE (13,104) RIN,    XL,   XGAP,  KRAT,  HFG, VBAS
      WRITE (*,105) KFIN,  TFIN,  FSEC,  FFIN
      WRITE (12,105) KFIN,  TFIN,  FSEC,  FFIN
      WRITE (13,105) KFIN,  TFIN,  FSEC,  FFIN
C
 100  FORMAT(' ***** DETERMINISTIC IGNITION TEMPERATURE *****',//,
     &       ' Decay Power Distribution',/,
     &       '    Qlo=   ',F6.1,'   Qmid= ',F6.1,'   Qhi= ',F6.1,/,
     &       ' Scrap Porosity Distribution',/,
```

```
     &        '    Philo= ',F6.4,'    Del= ',F6.4,/,
     &        ' Rate Multiplier Distribution ',A11,/,
     &        '    Min  = ',F6.3,'    Max= ',F6.3,/,
     &        ' Internal Emissivity Distribution',/,
     &        '    Epslo= ',F6.4,'    Del= ',F6.4,/,
     &        ' Gap Emissivity Distribution',/,
     &        '    Egplo= ',F6.4,'    Del= ',F6.4,/,
     &        ' Reaction Area Distribution ',A11,/,
     &        '    Alo  = ',F6.4,'    Ahi= ',F6.4)
 102  FORMAT(
     &        ' Scrap Size Distribution (cm) ',A11,/,
     &        '    Dlo  = ',F6.3,'    Dhi= ',F6.3,/,
     &        ' Steam Pressure Distribution (kPa) ',A11,/,
     &        '    Pslo = ',F6.3,'   Pshi= ',F6.3,/,
     &        ' Nusselt Number for convection',/,
     &        '    Nulo = ',F6.3,'    Del= ',F6.3,/,
     &        ' Evaporation rate kg/hr',/,
     &        '    Wevlo= ',F6.3,'    Del= ',F6.3)
 104  FORMAT(
     &        ' Constant Values',/,
     &        '    Rin  = ',F8.5,'   Rout= ',F8.5,/,
     &        '    Gap  = ',F8.5,'   Krat= ',F8.5,/,
     &        '    Hfg  = ',F9.1,'   Vbas= ',F8.5,/,
     &        ' Note krat < 0 uses default k-bed model',/,
     &        '      krat > 0.01 sets k-bed = kgas * krat',/)
 105  FORMAT(
     &        '    Kfin = ',F8.3,'   Tfin= ',F8.5,/,
     &        '    Fsec = ',F8.5,'   Ffin= ',F8.5,//)
C
      RETURN
      END

      REAL FUNCTION RREAD (IUNIT)
C
C     GET A REAL VALUE FROM A LINE WITH A BLANK FIRST COLUMN
C     SKIP LINES WITH NON-BLANK FIRST COLUMNS
C
      CHARACTER*1 LINE,BLANK
      DATA BLANK /' '/
      VALUE= 0.E0
 100  CONTINUE
      READ (IUNIT,'(A)',END=200) LINE
      IF (LINE .NE. BLANK) GOTO 100
      BACKSPACE (IUNIT)
      READ (IUNIT,*) VALUE
 200  CONTINUE
      RREAD= VALUE
      RETURN
      END

      INTEGER FUNCTION IREAD (IUNIT)
C
C     GET AN INTEGER FROM A LINE WITH A BLANK FIRST COLUMN
C     SKIP LINES WITH NON-BLANK FIRST COLUMNS
C
      CHARACTER*1 LINE,BLANK
      DATA BLANK /' '/
```

```
      IVALUE= 0
  100 CONTINUE
      READ (IUNIT,'(A)',END=200) LINE
      IF (LINE .NE. BLANK) GOTO 100
      BACKSPACE (IUNIT)
      READ (IUNIT,*) IVALUE
  200 CONTINUE
      IREAD= IVALUE
      RETURN
      END

      SUBROUTINE GETIN (NSAM,
     &      QLOW,  QMID,  QUPP, PHILO, PHIDL, FEAMN, FEAMX, IRDIS,
     &     EPSLO, EPSDL, EGPLO, EGPDL,   ALO,   AHI, IADIS,
     &       DLO,   DHI, IDDIS,  PSLO,  PSHI, IPDIS,  NULO,  NUDL,
     &     WEVLO, WEVDL,
     &       RIN,    XL,  XGAP,  KGAS,   HFG,  VBAS,
     &        QV,   PHI,  FEAC,   KSL,   EPS,   NUS,
     &      KGAP,  EGAP,  AOV0,  FRAD,    DP,  PPST, QVEV)
      INTEGER NSAM
      IMPLICIT REAL (A-H,K-Z)
      SAVE
C
C     RANDOM SEED IS INITIALIZED ON FIRST PASS ONLY
C
      DATA IDUM /0/
C
C     DEFAULT VALUES CHANGED FOR MARV THURGOOD HE-FILLED MCO
C     COMMENTED-OUT VALUES ARE SUPERSEDED BY DISTRIBUTIONS
C
C     SCRAP BASKET OUTER RADIUS GIVEN 22.625 INCH DIAMETER
C     GAP BASED ON 23 INCH MCO INNER DIAMETER
C     HE CONDUCTIVITY SELECTED FOR 50 C - CONSERVATIVE
C     GAP EMISSIVITY GIVEN 0.7 FOR SURFACES, ROUNDED DOWN
C
C      QV= 1875.
C      PHI=  0.40
C      FEAC= 3.2
C      KSL= 1.0
C      RIN= 0.02
C      XL= 0.287E0
C      XGAP= 0.00476E0
C      KGAP= 0.16E0
C      EGAP= 0.50E0
C      AOV0= 54.E0 / 0.17
C
C --- RANDOM VARIABLES ---
C
C     DECAY POWER
C
      CALL TRIANG(QLOW,QMID,QUPP,QTRI)
      QV=QTRI
C
      PHI= PHILO + PHIDL*RANDOM(IDUM)
      IF (IRDIS .EQ. 0) THEN
          FEAC= FEAMN + (FEAMX - FEAMN)*RANDOM(IDUM)
      ELSE
```

```
          FEAC= FEAMN * (FEAMX/FEAMN)**RANDOM(IDUM)
        ENDIF
        EPS= EPSLO + EPSDL*RANDOM(IDUM)
        EGAP= EGPLO  + EGPDL*RANDOM(IDUM)
        NUS= NULO + NUDL*RANDOM(IDUM)
C
C       MODIFY CONDUCTIVITY USING VOID FRACTION AND NUSSELT #
C
        KSL= KGAS / (1.E0 - (1.E0-PHI)**0.3333E0)
       &      + KGAS*(NUS-1.E0)
        KGAP= KGAS
C
C       AREA PER UNIT VOLUME BY RANDOM AREA
C
C       CORRELATE AREA WITH FUEL VOLUME FRACTION
C       AREA RANGE APPLIES TO MIN VOID FRACTION
C
        IF (IADIS .EQ. 0) THEN
            ARX= ALO + (AHI - ALO)*RANDOM(IDUM)
        ELSE
            ARX= ALO * (AHI/ALO)**RANDOM(IDUM)
        ENDIF
        ARX= ARX * (1.E0 - PHI) / (1.E0 - PHILO)
        AOV0= ARX/VBAS
C
C       RADIATION FACTOR IS DERIVED
C
        LAM= 1.E0 - 1.21E0*(1.E0-(1.E0-PHI)**(2.E0/3.E0))
        FRAD= (1.E0 + LAM/EPS)/(1.E0-LAM)
C
C       PARTICLE DIAMETER
C
        IF (IDDIS .EQ. 0) THEN
            DP= DLO + (DHI - DLO)*RANDOM(IDUM)
        ELSE
            DP= DLO * (DHI/DLO)**RANDOM(IDUM)
        ENDIF
C
C       STEAM PRESSURE
C
        IF (IPDIS .EQ. 0) THEN
            PPST= PSLO + (PSHI - PSLO)*RANDOM(IDUM)
        ELSE
            PPST= PSLO * (PSHI/PSLO)**RANDOM(IDUM)
        ENDIF
C
C       EVAPORATION VOLUMETRIC POWER, FROM KG/HR TO W/M^3
C
        WEV= (WEVLO + WEVDL*RANDOM(IDUM)) / 3600.E0
        QVEV= WEV * HFG / VBAS
C
C       MANUAL INPUT SECTION HERE FOR CONVENIENT CHECK OF RESULTS
C       USED WHEN # SAMPLES = 1 ON ENTRY
C
        IF (NSAM .GT. 1) RETURN
C
  100   CONTINUE
```

```
C
      WRITE (*,20) PHI,QV,FEAC,KSL,EPS,AOV0,RIN,XL,
     &             XGAP,KGAP,EGAP,FRAD,DP,PPST,NUS,QVEV
   20 FORMAT(' Current values: ',/,
     & '    1 PHI= ',F8.2,'    2 QV = ',F8.2,'    3 FEA=  ',F8.3,/,
     & '    4 KSL= ',F8.3,'    5 EPS= ',F8.4,'    6 AOV=  ',F8.2,/,
     & '    7 RIN= ',F8.4,'    8 XL=  ',F8.4,'    9 XGAP= ',F8.6,/,
     & '   10 KGAP=',F8.3,'   11 EGAP=',F8.4,'   12 FRAD= ',F8.4,/,
     & '   13  DP= ',F8.6,'   14 PPST=',F8.4,'   15   NU= ',F8.3,/,
     & '   16 QVEV=',F8.3,/,
     & '    Enter 0,0 if OK else index,value: ',$)
      READ (*,*) IND,VAL
      IF (IND .LE. 0) GO TO 200
      IF (IND .EQ. 1) PHI=VAL
      IF (IND .EQ. 2) QV=VAL
      IF (IND .EQ. 3) FEAC=VAL
      IF (IND .EQ. 4) KSL=VAL
      IF (IND .EQ. 5) EPS=VAL
      IF (IND .EQ. 6) AOV0=VAL
      IF (IND .EQ. 7) RIN=VAL
      IF (IND .EQ. 8) XL=VAL
      IF (IND .EQ. 9) XGAP=VAL
      IF (IND .EQ. 10) KGAP=VAL
      IF (IND .EQ. 11) EGAP=VAL
      IF (IND .EQ. 12) FRAD=VAL
      IF (IND .EQ. 13) DP=VAL
      IF (IND .EQ. 14) PPST=VAL
      IF (IND .EQ. 16) QVEV=VAL
      IF (IND .GE. 17) GO TO 100
      GOTO 100
  200 CONTINUE
C
      RETURN
      END

C
       FUNCTION GASDEV(IDUM)
       DATA ISET/0/
       IF (ISET.EQ.0) THEN
    1      V1=(2.0*RANDOM(IDUM)-1.0)
         V2=(2.0*RANDOM(IDUM)-1.0)
         R=V1**2.0+V2**2.0
         IF(R.GE.1.0) GO TO 1
         FAC=SQRT(-2.0*LOG(R)/R)
         GSET=V1*FAC
         GASDEV=V2*FAC
         ISET=1
       ELSE
         GASDEV=GSET
         ISET=0
       ENDIF
       RETURN
       END

       FUNCTION RANDOM(IDUM)
       DATA NCALLS /0/
       IF (NCALLS.EQ.0) THEN
```

```
        NCALLS=1
        Y=RRAND()
       ELSE
        Y=RND()
       ENDIF
       RANDOM=Y
       RETURN
       END


      SUBROUTINE TRIANG(A,B,C,X)
C*****************************************************************
C SUBROUTINE TRIANG GENERATES THE TRIANGULAR DISTRIBUTION
C
       IDUM=1
       PROBINC=1.0
       C1=C-A
       C2=(B-A)/C1
       STRTPT=0.
       N=1
       DO 10 I=1,N
        R=PROBINC*RANDOM(IDUM)+STRTPT
        IF(R.LE.C2)THEN
          X=A+SQRT(R*C1*(B-A))
        ELSE
          X=C-SQRT((1.-R)*C1*(C-B))
        ENDIF
   10  CONTINUE
       RETURN
       END
```

APPENDIX F IGMCOMC FORTRAN SOURCE CODE FOR PROBABILISTIC IGNITION ANALYSIS OF SCRAP BASKETS WITHOUT FINS

```
PROGRAM IGMCOMC
C
C     DRIVER/SUBROUTINE VERSION !!! debug version !!!
C
C     IGNITION TEMPERATURE FOR FUEL IN AN MCO AT CVD
C       I.E. CONSTANT WALL TEMPERATURE
C     SCRAP GEOMETRY, INTERNAL RADIATION BY T**3 DT/DR
C
C     "PEARCE" KINETICS FROM HANFORD + MULTIPLIER
C     MULTIPLIER CAN ACCOUNT FOR FAILURE FRACTION, SWELLING,
C          PRESENCE OF POROUS SURFACE LAYER, ETC.
C     EXTERNAL HEAT TRANSFER INDEPENDENT OF LENGTH
C
C     SURFACE AREA AND SCRAP VOID FRACTION ARE CORRELATED
C     EVAPORATION TERM EXPLICITLY CONSIDERED
C
C     MAJOR PROGRAM SECTIONS:
C     1.0  DECLARATIONS & CONSTANTS
C     2.0  MONTE CARLO LOOP
C     3.0  CASE INPUTS
C     4.0  IGNITION TEMPERATURE
C     5.0  STATISTICS AND OUTPUT
C
C     ------------------------------------------------------------
C     1.0  DECLARATIONS & CONSTANTS
C     ------------------------------------------------------------
C
C     BIN DEFINITIONS:
C     BIN JJ  GOES FROM TBIN(JJ) TO TBIN(JJ+1)
C     BIN JJ=1 INCLUDES ALL TEMPERATURES BELOW
C     BIN JJ=NBIN INCLUDES ALL TEMPERATURES ABOVE
C     TBIN(NBIN+1) IS DUMMY HIGH VALUE
C
C     TBIN   BIN TEMPERATURE DESCRIBED ABOVE
C     IBIN   # TRIALS FALLING IN BIN
C     PBIN   PROBABILITY OF TRIAL IN BIN
C     CBIN   CUMULATIVE PROBABILITY OF TRIALS
C
C
      IMPLICIT REAL (A-H, K-Z)
      INTEGER NBIN, NSAM
      PARAMETER (NBIN=40)
      DIMENSION TBIN(NBIN+1),PBIN(NBIN),CBIN(NBIN),IBIN(NBIN)
      DATA TKO /273.15/
      DATA PBIN /NBIN*0.E0/
      DATA CBIN /NBIN*0.E0/
      DATA IBIN /NBIN*0/
C
C     OUTPUT FILES:
C     12  DIRECT BIN VALUES FROM MONTE CARLO TRIALS
C     13  ERROR MESSAGES
C     14  PLOT OUTPUT
C
```

```
      OPEN (UNIT=12, STATUS='UNKNOWN', FORM='FORMATTED',
     &      FILE='FOR012.DAT', ERR=1234)
      OPEN (UNIT=13, STATUS='UNKNOWN', FORM='FORMATTED',
     &      FILE='FOR013.DAT', ERR=1234)
      OPEN (UNIT=14, STATUS='UNKNOWN', FORM='FORMATTED',
     &      FILE='FOR014.DAT', ERR=1234)
C
C     ------------------------------------------------------------
C     2.0 MONTE-CARLO ITERATION LOOP, NSAM TRIALS
C     ------------------------------------------------------------
C
C     GET PARAMETER DISTRIBUTION VALUES
C
C     QLOW   DECAY POWER LOW VALUE
C     QMID   DECAY POWER MID VALUE
C     QUPP   DECAY POWER HIGH VALUE
C     PHILO  POROSITY LOW VALUE
C     PHIDL  POROSITY RANGE
C     FEAMN  RATE LAW MULTIPLIER MIN VALUE
C     FEAMX  RATE LAW MULTIPLIER HAX VALUE
C     IRDIS  0=UNIFORM, 1=LOG-UNIFORM RATE LAW DISTRIBUTION
C     EPSLO  INTERNAL EMISSIVITY LOW VALUE
C     EPSDL  INTERNAL EMISSIVITY RANGE
C     EGPLO  GAP EMISSIVITY LOW VALUE
C     EGPDL  GAP EMISSIVITY RANGE
C     ALO    REACTION AREA LOW VALUE
C     AHI    REACTION AREA HIGH VALUE
C     IADIS  0=UNIFORM, 1=LOG-UNIFORM AREA DISTRIBUTION
C     DLO    SCRAP SIZE LOW DIAMETER
C     DHI    SCRAP SIZE HIGH DIAMETER
C     IDDIS  0=UNIFORM, 1=LOG-UNIFORM DIAMETER (SIZE) DISTRIBUTION
C     PSLO   STEAM PRESSURE IN KPA - LOW
C     PSHI   STEAM PRESSURE IN KPA - HIGH
C     IPDIS  0=UNIFORM, 1=LOG-UNIFORM PRESSURE DISTRIBUTION
C     NULO   NUSSELT NUMBER FOR CONVECTION -LO
C     NUDL   NUSSELT NUMBER FOR CONVECTION - RANGE TO HIGH
C     WEVLO  LOW BOUND AVERAGE EVAPORATION RATE KG/S DURING CVD
C     WEVDL  RANGE IN AVERAGE EVAPORATION RATE
C  -- CONSTANT VALUES
C     RIN     INNER RADIUS FOR FUEL IN MCO
C     XL      OUTER RADIUS OF FUEL, INNER RADIUS OF MCO
C     XGAP    BASKET-MCO WALL GAP THICKNESS
C     KGAS    MCO GAS THERMAL CONDUCTIVITY
C     HFG     WATER LATENT HEAT OF EVAPORATION J/KG
C     VBAS    BASKET VOLUME M^3
C
      CALL GETVAR (
     &      QLOW,  QMID,  QUPP, PHILO, PHIDL, FEAMN, FEAMX, IRDIS,
     &     EPSLO, EPSDL, EGPLO, EGPDL,   ALO,   AHI, IADIS,
     &       DLO,   DHI, IDDIS,  PSLO,  PSHI, IPDIS,  NULO,  NUDL,
     &     WEVLO, WEVDL,
     &       RIN,    XL,  XGAP,  KGAS,   HFG,  VBAS)
C
C     SETUP BINS AND SUMS FOR STATISTICS
C
      DO 100 JJ=1, NBIN
         TBIN(JJ)= 25.E0 + 5.E0 * FLOAT(JJ-1)
```

```
 100  CONTINUE
      TBIN(NBIN+1)= 1000.E0
      TSUM= 0.E0
      T2SUM= 0.E0
C
C     INQUIRE FOR # OF TRIALS
C     POSITIVE MEANS MONTE CARLO AS USUAL
C     NEGATIVE MEANS DEBUG OUTPUT
C     ZERO MEANS INPUT ALL VALUES MANUALLY
C
      WRITE (*,'('' Enter # Monte Carlo Trials -> '',$)')
      READ (*,*) NSAM
      IF (NSAM .LT. 0) THEN
          NSAM= -NSAM
          IDBG= 1
      ELSEIF (NSAM .LE. 1) THEN
          NSAM= 1
          IDBG= 1
      ELSE
          IDBG= 0
      ENDIF
      WRITE (12,'(/,'' '',1PE10.3,''  Samples'',/)') NSAM
      WRITE (13,'(/,'' '',1PE10.3,''  Samples'',/)') NSAM
C
      DO 777 ISAM= 1,NSAM
      IF (MOD(FLOAT(ISAM-1),1.E4) .EQ. 0.E0)
     &    WRITE (*,'('' Trial count: '',I8)') ISAM
C
C     ------------------------------------------------------------
C     3.0  ESTABLISH CASE INPUTS
C     ------------------------------------------------------------
C
C     PHI      POROSITY
C     QV       VOLUMETRIC POWER W/M^3
C     HIN      ZERO TO CALCULATE, ELSE INPUT W/M^2/K
C     FEAC     MULTIPLIER DESCRIBED BELOW
C     KSL      EFFECTIVE DISTRIBUTED THERMAL CONDUCTIVITY W/M/K
C     EPS      OVERALL EMISSIVITY -INSIDE MCO-
C     RIN      INNER RADIUS FOR FUEL IN MCO
C     XL       OUTER RADIUS OF FUEL, INNER RADIUS OF MCO
C     XGAP     BASKET-MCO WALL GAP THICKNESS
C     KGAP     MCO GAS THERMAL CONDUCTIVITY
C     EGAP     EFFECTIVE OVERALL EMISSIVITY IN GAP 1/(1/E1 + 1/E2 -1)
C     AOV0     NOMINAL A/V 1/M
C     FRAD     RADIATION DISTANCE FACTOR
C              <1 XRAD = FRAD*XL  USE FOR RODS:  1/FRAD = # SERIES PATHS
C                                 DEFAULT IS 4 SERIES PATHS FOR MCO
C              >1 XRAD = FRAD*DP  USE FOR BEDS, ACCOUNTS FOR REFLECTIONS
C                                 DEFAULT IS 3 USING PHI=0.4, EPS=0.7:
C                                 LAM = 1 - 1.21 (1 - (1-PHI))**2/3
C                                 FRAD= (1 + LAM/EPS)/(1 - LAM)
C
C     DEFAULT VALUES HERE FOR RODS IN AN MCO
C     FOR FUEL FRAGMENTS THESE ARE APPROPRIATE DEFAULTS:
C     PHI= 0.40  KSL=0.20 TO 0.30  FRAD=3.0  RIN=0.20  AOV0=1000
C
      CALL GETIN (NSAM,
```

```
     &      QLOW,  QMID,  QUPP, PHILO, PHIDL, FEAMN, FEAMX, IRDIS,
     &     EPSLO, EPSDL, EGPLO, EGPDL,   ALO,   AHI, IADIS,
     &       DLO,   DHI, IDDIS,  PSLO,  PSHI, IPDIS,  NULO,  NUDL,
     &     WEVLO, WEVDL,
     &       RIN,    XL,  XGAP,  KGAS,   HFG,  VBAS,
     &        QV,   PHI,  FEAC,   KSL,   EPS,   NUS,
     &      KGAP,  EGAP,  AOV0,  FRAD,    DP,  PPST,  QVEV)
C
C
C     ------------------------------------------------------------
C     4.0  IGNITION TEMPERATURE
C     ------------------------------------------------------------
C
      CALL TIGMCO (
     &     QV,   PHI,   KSL,   EPS,   RIN,  FRAD,
     &     XL,  FEAC,  AOV0,  PPST,    DP,  QVEV,
     &   XGAP,  KGAP,  EGAP,  IDBG,
     &    TCL,    TR,  TAMB,    QR,  SORC, QFLUX,  ERR, ITIG)
C
C     SAVE OUTPUT IN C
C
      TAMB= TAMB - TKO
      TCL= TCL - TKO
      TR= TR - TKO
C
C     ------------------------------------------------------------
C     OPTIONAL CASE OUTPUT
C     ------------------------------------------------------------
C
      IF (IDBG .EQ. 1) THEN
      WRITE (12,4001) PHI, QV, FEAC,KSL, EPS,EGAP, RIN,XL,
     %               XGAP,KGAP, DP,PPST, NUS, FRAD
      WRITE (12,4002)
      WRITE (12,4003) AOV0,TAMB,TR,TCL,SORC,QFLUX,ERR
      ENDIF
 4001 FORMAT(//,' ***** Ignition of fuel in MCO ***** ',/,
     & '   Porosity=       ',F8.3,'       Power W/m^3= ',F8.2,/,
     & '   Kin. Rate Mult= ',F8.3,'      Therm. cond.= ',F8.4,/,
     & '   Emissivity=     ',F8.4,'        Gap emiss.= ',F8.4,/,
     & '   Inner radius=   ',F8.5,'     Outer radius = ',F8.5,/,
     & '   Gap thickness=  ',F8.6,'    Gap therm cond= ',F8.4,/,
     & '   Diameter=       ',F8.6,'        Psteam Kpa= ',F8.3,/,
     & '   Nusselt=        ',F8.4,/,
     & '   Frad <1 rods, >1 rubble: ',F8.4,/)
 4002 FORMAT(
     &'   Ambient ignition T and profiles in C for Pst =1 kPa',/,
     &'    A/V',T12,'Tamb',T22,'Tmin',T32,'Tmax',T42,'Qsor',
     &     T52,'Qflux',T62,'Error',/)
 4003 FORMAT('  ',F7.1,T10,4(F7.2,3X),F7.1,3X,1PE9.2)
C
C --- BOTTOM OF CASE CALCULATION
C
C --- KEEP SCORE OF MONTE CARLO TRIALS AND ACCUMULATE SUMS
C
C     BOTTOM BIN GETS ANY TRIALS THAT FALL BELOW IT
C     TOP BIN GETS ANY TRIALS THAT FALL ABOVE IT
C     LEAVE LOOP WHEN BIN FOUND
```

```
C      FALL OUT OF LOOP IF TRIAL IN LAST BIN
C
       DO 770 J=1, NBIN-1
          IF (TAMB .LT. TBIN(J+1)) THEN
             IBIN(J)=IBIN(J)+1
             GOTO 772
          ENDIF
 770   CONTINUE
       IBIN(NBIN)= IBIN(NBIN)+1
 772   CONTINUE
C
       TSUM= TSUM + TAMB
       T2SUM= T2SUM + TAMB*TAMB
C
C --- END OF MONTE CARLO TRIAL LOOP
C
 777   CONTINUE
C
C --- OUTSIDE ALL LOOPS
C
       IF (NSAM .LE. 1) GOTO 1234
C
C      ------------------------------------------------------------
C      5.0  MONTE CARLO STATISTICS
C      ------------------------------------------------------------
C
       WRITE (12,'('' '')')
C --- MEAN AND STANDARD DEVIATION
       TBAR= TSUM / FLOAT(NSAM)
       TVAR= (FLOAT(NSAM)*T2SUM - TSUM*TSUM) /
      &      (FLOAT(NSAM)*FLOAT(NSAM-1))
       TSIG= SQRT(TVAR)
       WRITE ( *,'('' Tave= '',F7.2,''   Deviation= '',F7.3)') TBAR,TSIG
       WRITE (12,'('' Tave= '',F7.2,''   Deviation= '',F7.3)') TBAR,TSIG
C --- PROBABILITY DENSITY FUNCTION
       DO 780 JJ=1,NBIN
          PBIN(JJ)= FLOAT(IBIN(JJ))/FLOAT(NSAM)
 780   CONTINUE
C --- CUMULATIVE DISTRIBUTION FUNCTION
       CBIN(1)=PBIN(1)
       DO 782 JJ=2,NBIN
          CBIN(JJ)=CBIN(JJ-1) + PBIN(JJ)
 782   CONTINUE
C --- REPORT
       WRITE (12,'('' '')')
       WRITE (12,4012)
       DO 784 JJ=1, NBIN
          WRITE (12,4014) JJ,TBIN(JJ),IBIN(JJ),PBIN(JJ),CBIN(JJ)
 784   CONTINUE
4012   FORMAT (T3,'Bin', T12,'Tlow', T22,'Count', T30,'Frequency',
      &        T45,'Cumulative Freq.',/)
4014   FORMAT (T3,I3, T10,F7.2, T20,I7, T30,1PE10.3, T45,E10.3)
C
C --- GRAPHIC FILE
C
       WRITE (14, '('' 3'')')
       WRITE (14, '('' '')')
```

```
      WRITE (14, '('' '')')
      WRITE (14, '('' MCO Ignition Results'')')
      WRITE (14, '(3X,''Tbin'',10X,''Pbin'',10X,''Cbin'')')
      WRITE (14, '(3X,''C   '',10X,''    '',10X,''    '')')
      WRITE (14, '('' '')')
      WRITE (14, '('' '')')
      DO 790 JJ=1,NBIN-1
      WRITE (14, '('' '',5(G13.4,2X))')
     &      (TBIN(JJ)+TBIN(JJ+1))/2.E0, PBIN(JJ), CBIN(JJ)
 790  CONTINUE
      WRITE (14, '('' '',5(G13.4,2X))')
     &      TBIN(NBIN), PBIN(NBIN), CBIN(NBIN)
C
 1234 WRITE (*,666)
  666 FORMAT(' Attaboy, Marty')
      END

      SUBROUTINE TIGMCO (
     &     QV,   PHI,   KSL,   EPS,   RIN,  FRAD,
     &     XL,  FEAC,  AOV0,  PPST,    DP,  QVEV,
     &   XGAP,  KGAP,  EGAP,  IDBG,
     &    TCL,    TR,  TAMB,    QR,  SORC, QFLUX,  ERR, ITIG)
C
C     IGNITION TEMPERATURE OF FUEL IN A SCRAP BASKET
C     FIXED MCO WALL TEMPERATURE = TAMB = IGNITION TEMP.
C
      IMPLICIT REAL (A-H,K-Z)
      INTEGER NTA
      PARAMETER (NTA=25,  NDP=7,  NPS=4)
      DIMENSION TAM(NTA),TU(NTA)
      DATA SIGMA /5.67E-8/
C
C     TAM()   AMBIENT TEMPERATURES SAVED DURING SEARCH FOR MAXIMUM
C     TU()    FUEL TEMPERATURES SAVED DURING SEARCH FOR MAXIMUM
C             -NOTE- MORE VALUES SAVED THAN OPTIMALLY NECESSARY,
C              SO DEBUGGING/PLOTTING OF LOCAL BEHAVIOR IS EASIER
C
C
C     EXIT CONDITION CODE:
C     ITIG: 1  TIG < LOWER BOUND
C     ITIG: 2  TIG FOUND
C     ITIG: 3  TIG > UPPER BOUND
C
      ITIG= 0
      TCL= 273.
      TR=  273.
      TAMB=273.
      QR=  0.E0
      SORC= 0.E0
      QFLUX= 0.E0
      ERR= 0.E0
C
C     KINETIC RATE MULTIPLIER ACCOUNTS FOR EITHER:
C       ACTUAL RATE UNCERTAINTY
C       VOLUME FRACTION OF REACTING MATERIAL
C       SWELLING EFFECT, ETC.
C
```

```
      FARX= FEAC * (1.E0 - PHI)*AOV0
C
C
C     TOP OF LOOP OVER PARTICLE TEMPERATURE
C
C     FOR A GIVEN PPST,DP,XL MAY RUN PAST THIS POINT SEVERAL TIMES
C     START WITH LOW,COARSE RANGE OF FUEL TEMPERATURE FOR IGNITION
C     COME BACK HERE IF HIGHER RANGES OR FINE RANGES ARE DESIRED
C     FIRST GET THE CORRECT COARSE RANGE, THEN FINE RANGES
C     SEE TESTS AFTER NEWTON LOOP BOTTOM
C
C     TLOW:  LOW END OF RANGE TO INVESTIGATE
C            MAY BE RESET AT END OF LOOP OVER THE RANGE
C     DT:    INCREMENT OF RANGE, MAY ALSO BE RESET AT END OF LOOP
C     IRANGE: RANGE COUNTER
C     FINE:   FINE RANGE COUNTER
C
      TLOW= 273.E0
      DT=10.
      IRANGE=0
      IFINE=0
 999  CONTINUE
      IIT=10
      DO 3000 IT=1,IIT
C
C     ---------------------------------------------------------
C     3.0  FUEL T, REACTION SOURCE, MCO WALL TEMPERATURE
C     ---------------------------------------------------------
C
      TCL= TLOW + DT*FLOAT(IT-1)
      TU(IT)=TCL
C
C     GIVEN FUEL T, GET REACTION POWER, THEN
C       1) SOLVE FOR TEMPERATURE AT MCO RADIUS
C       2) ITERATE TO SOLVE FOR TUBE AND AMBIENT TEMPERATURES
C
C     MCGILLIVRAY CORRELATION FOR MOIST AIR
C     RATE IN MG O2/CM^2 MIN IS CONVERTED TO W/M^2
C     VIA 10^-6/10^-4/60 = 0.01/60  WHERE 3.4E7 IS HEAT OF REACTION
C      RD= EXP(11.093 - 8077.0/TCL)
C      RK1= EXP(7.831 - 6432.0/TCL)
C      RK2= EXP(-15.208 + 5237.0/TCL)
C      RR= RD + RK1*PPST/(1.0 + RK2*PPST)
C      QR= FARX * 3.4E7 * RR * 0.01/60.0
C
C
C     RATE LAW: PEARCE U-H2O BELOW 350 C, PPST IN KPA
C     LAW UNITS OF MG/CM^2/HR CONVERT BY 0.01/3600 TO KG/M^2/S
C
C!! WAS USED BY COOPER,THURGOOD   RR= 10.E0**(7.364 - 3016./TCL)
C
      ARG= 4.33E0 - 2144.E0/TCL
      RR= 10.E0**(ARG) * SQRT(PPST)
      QR= FARX * 3.4E7 * RR * 0.01/3600.0
C
C     TOTAL SOURCE:
C
```

```
C     ABANDON WHEN SOURCE < 100 W/M^3, BY EXPERIENCE IGNITION CAN'T HAPPEN
C
      SORC= QV*(1.E0 - PHI) + QR - QVEV
C
      IF (SORC .LE. 100.E0) THEN
      ITIG= 3
      TCL= 773.
      TR=  773.
      TAMB=773.
      ERR= 0.E0
      QFLUX= (SORC*XL/2.E0) * (1.E0 - AOR2)
      GOTO 660
      ENDIF
C
C     TEMPERATURE TR AT RADIUS R=XL:
C     ROA = (r=R)/(r=a) = outer/inner radii ratio; AOR2 = a^2/R^2
C     XRAD= EFFECTIVE DISTANCE BETWEEN RADIATION SHIELDS
C         = RADIUS/# OF SHIELDS
C
      ROA= XL/RIN
      AOR2= RIN*RIN/XL/XL
      SIGEP= SIGMA*EPS
      XRAD= FRAD*DP
      CRAD= 4.E0*SIGEP*XRAD
      TR= FTR(TCL,SORC,XL,KSL,CRAD,ROA,AOR2,IOK1,ERR1)
C
C     HEAT FLUX AT RADIUS XL:
      QFLUX= (SORC*XL/2.E0) * (1.E0 - AOR2)
C     ESTIMATED TEMPERATURE AFTER GAP I.E. MCO WALL
      TAMB= FTS(TR,QFLUX,EGAP,KGAP,XGAP,IOK2,ERR2)
C
      ERR= ABS(ERR1)+ABS(ERR2)
C
C     CONVERGED; NOW SEE IF MAXIMUM FOUND
C
```

```
C     ------------------------------------------------------------
C     5.0  SEARCH FOR MAXIMUM
C     ------------------------------------------------------------
C
      TAM(IT)= TAMB
C
C     CASE WHERE MAX IS LOWER THAN FIRST GUESS - JUST QUIT
C
      IF (IT .EQ. 2 .AND. TAMB .LT. TAM(1)) THEN
        ITIG= 1
        WRITE (13,2011) TLOW,DP*1.E6,PPST,XL*1000.
        WRITE (13,1110) TCL, TAMB, SORC, QFLUX
        GOTO 660
      ENDIF
 2011 FORMAT(' Ignition temperature below starting value',F5.1,/,
     & ' DP=',F4.1,'  PPST=',F6.1,'   XL=',F4.1)
 1110 FORMAT(
     & ' T= ',F8.2,'  TAMB= ',F8.2,'  SORC= ',1PE10.3,'  FLUX= ',E10.3)
C
C     CASE WHERE MAX FOUND
C       GO BACK FOR FINER RANGE OR
C       ON THIRD TRY DECLARE CONVERGED
C     FOR DEBUG, DIAGNOSTIC TO ENSURE CONVERGING CORRECTLY
C
      IF (IT.GE.3 .AND. TAM(IT) .LT. TAM(IT-1)) THEN
        IF (IDBG .EQ. 1)
     &  WRITE (13,2040) AOV0,SORC,QFLUX,TAM(IT-2),TAM(IT-1),TAM(IT)
        IFINE=IFINE+1
        TLOW= MIN( TU(IT-2), TU(IT))
        DT= ABS(TU(IT) - TU(IT-2))/10.
        TERR= MAX( ABS(TU(IT-1) - TU(IT)),
     &             ABS(TU(IT-1) - TU(IT-2)) )
        IF (TERR. LE. 0.05E0 .OR. IFINE .GE. 3) THEN
          ITIG= 2
          GO TO 660
        ELSE
          GOTO 999
        ENDIF
      ENDIF
 2040 FORMAT(' A/V=',F6.2,'   Q/V=',F6.1,'   Q/A=',F6.2,
     &       '   T RANGE:',3(F7.3,3X))
C
C     MAX NOT YET FOUND - CHECK A HIGHER RANGE
C
      IF (IT .EQ. IIT .AND. TAM(IT) .GT. TAM(IT-1)) THEN
        IRANGE=IRANGE+1
        IF (IRANGE .GE. 5) THEN
          ITIG= 2
          GO TO 660
        ENDIF
        TLOW= TU(IT-1)
        GO TO 999
      ENDIF
C --- BOTTOM OF LOOP OVER FUEL T - SHOULD BREAK ABOVE
 3000 CONTINUE
C --- GET TO 660 WHEN CONVERGED ON AN IGNITION TEMPERATURE
  660 CONTINUE
```

```
      RETURN
      END

      FUNCTION FTR(TCL,SORC,XL,KSL,CRAD,ROA,AOR2,IOK,ERR)
      IMPLICIT REAL (A-H,K-Z)
C
C     GET TR = TEMPERATURE OF SCRAP BASKET OUTER RADIUS
C
C     FIRST GUESS BY CONSTANT RADIATIVE CONDUCTIVITY METHOD
C       I.E. SOLUTION WITH CONSTANT KEFF
C
      KEFF= KSL + CRAD*(TCL-5.E0)**3.E0
      TQ= (SORC*XL*XL/2.E0) * ((1.E0 - AOR2)/2.E0 - AOR2*LOG(ROA))
     &    / KSL
      TMAX= TCL
      TMIN= TCL - TQ
      TR= TCL - TQ*KSL/KEFF
      CEFF= CRAD/4.E0/KSL
      T4= TCL**4.E0
      IOK=0
  100 CONTINUE
      TOLD= TR
      IOK=IOK+1
      G= TCL - TR + CEFF*(T4 - TR**4.E0) - TQ
      DG= -1.E0 - 4.E0*CEFF*TR**3.E0
      DEL= -G/DG
      TR= TR + DEL
      TR= MIN(TR, (TOLD+TMAX)/2.E0)
      TR= MAX(TR, (TOLD+TMIN)/2.E0)
      IF (ABS(DEL)/TCL .LE. 1.E-5) GOTO 200
      IF (IOK .LE. 10) GOTO 100
      IF (ABS(DEL)/TCL .LE. 1.E-4) GOTO 200
      WRITE (13,110) TCL,TR,DEL,TMAX,TMIN,TQ
  110 FORMAT('  Failure to find MCO temperature ',/,
     &    ' Tcl = ',F10.4,'   Tmco= ',F10.4,'   Del= ',F10.5,/,
     &    ' Tmx = ',F10.4,'   Tmin= ',F10.4,'   Tq = ',F10.5)
      STOP
  200 CONTINUE
      ERR= DEL/TR
      FTR= TR
      RETURN
      END

      FUNCTION FTS(TR,QFLUX,EGAP,KGAP,XGAP,IOK,ERR)
      IMPLICIT REAL (A-H,K-Z)
      DATA SIGMA /5.67E-8/
C
C     GET TS = TEMPERATURE OF MCO WALL
C     FIRST GUESS USING TR FOR HRAD
C
      HGAP= KGAP/XGAP
      HEFF= 4.E0*SIGMA*EGAP*(TR-1.E0)**3.E0 + HGAP
      TS= TR - QFLUX/HEFF
      TMAX= TR
      TMIN= TR - QFLUX/HGAP
      TMIN= MAX(10.E0, TMIN)
      SIGEP= SIGMA*EGAP
```

```
      TR4= TR**4.E0
      IOK=0
  100 CONTINUE
      TOLD= TS
      IOK=IOK+1
      G= -QFLUX + SIGEP*(TR4 - TS**4.E0) + HGAP*(TR - TS)
      DG= -4.E0*SIGEP*TS**3.E0 - HGAP
      DEL= -G/DG
      TS= TS + DEL
      TS= MIN(TS, (TOLD+TMAX)/2.E0)
      TS= MAX(TS, (TOLD+TMIN)/2.E0)
      IF (ABS(DEL)/TR .LE. 1.E-5) GOTO 200
      IF (IOK .LE. 10) GOTO 100
      IF (ABS(DEL)/TR .LE. 1.E-4) GOTO 200
      WRITE (13,110) TR,TS,DEL,TMAX,TMIN,QFLUX
  110 FORMAT('  Failure to find MCO wall temperature ',/,
     &    ' TR  = ',F10.4,'   Tmco= ',F10.4,'   Del= ',F10.5,/,
     &    ' Tmx = ',F10.4,'   Tmin= ',F10.4,'   q" = ',F10.5)
      STOP
  200 CONTINUE
      ERR= DEL/TS
      FTS= TS
      RETURN
      END

      SUBROUTINE GETVAR (
     &      QLOW,  QMID,  QUPP, PHILO, PHIDL, FEAMN, FEAMX, IRDIS,
     &     EPSLO, EPSDL, EGPLO, EGPDL,   ALO,   AHI, IADIS,
     &       DLO,   DHI, IDDIS,  PSLO,  PSHI, IPDIS,  NULO,  NUDL,
     &     WEVLO, WEVDL,
     &       RIN,    XL,  XGAP,  KGAS,   HFG,  VBAS)
      IMPLICIT REAL (A-H,K-Z)
      CHARACTER*11 LABDIS(2)
      DATA LABDIS /'Uniform    ','Log-Uniform'/
C
C     GET MONTE CARLO INPUTS FROM FILE
C
      OPEN (UNIT=11, STATUS='UNKNOWN', FORM='FORMATTED',
     &      FILE='FOR011.DAT')
C
C     LINES WITH A NON-BLANK IN FIRST COLUMN ARE COMMENTS
C     VARIABLES ARE FOUND IN ORDER
C
      QLOW= RREAD(11)
      QMID= RREAD(11)
      QUPP= RREAD(11)
      PHILO= RREAD(11)
      PHIDL= RREAD(11)
      FEAMN= RREAD(11)
      FEAMX= RREAD(11)
      IRDIS= IREAD(11)
      EPSLO= RREAD(11)
      EPSDL= RREAD(11)
      EGPLO= RREAD(11)
      EGPDL= RREAD(11)
      ALO= RREAD(11)
      AHI= RREAD(11)
```

```
      IADIS= IREAD(11)
      DLO= RREAD(11)
      DHI= RREAD(11)
      IDDIS= IREAD(11)
      PSLO= RREAD(11)
      PSHI= RREAD(11)
      IPDIS= IREAD(11)
      NULO= RREAD(11)
      NUDL= RREAD(11)
      WEVLO= RREAD(11)
      WEVDL= RREAD(11)
      RIN= RREAD(11)
      XL= RREAD(11)
      XGAP= RREAD(11)
      KGAS= RREAD(11)
      HFG= RREAD(11)
      VBAS= RREAD(11)
      IRDIS= MAX(1, MIN(0, IRDIS))
      IADIS= MAX(1, MIN(0, IADIS))
      IDDIS= MAX(1, MIN(0, IDDIS))
      IPDIS= MAX(1, MIN(0, IPDIS))
C
      CLOSE (11)
C
      WRITE (*,100)
     &  QLOW,  QMID,  QUPP, PHILO, PHIDL, LABDIS(IRDIS), FEAMN, FEAMX,
     &  EPSLO, EPSDL, EGPLO, EGPDL, LABDIS(IADIS),  ALO,  AHI
      WRITE (12,100)
     &  QLOW,  QMID,  QUPP, PHILO, PHIDL, LABDIS(IRDIS), FEAMN, FEAMX,
     &  EPSLO, EPSDL, EGPLO, EGPDL, LABDIS(IADIS),  ALO,  AHI
      WRITE (13,100)
     &  QLOW,  QMID,  QUPP, PHILO, PHIDL, LABDIS(IRDIS), FEAMN, FEAMX,
     &  EPSLO, EPSDL, EGPLO, EGPDL, LABDIS(IADIS),  ALO,  AHI
      WRITE (*,102)
     &  LABDIS(IDDIS),100.*DLO,100.*DHI,  LABDIS(IPDIS), PSLO,  PSHI,
     &  NULO,   NUDL, WEVLO, WEVDL
      WRITE (12,102)
     &  LABDIS(IDDIS),100.*DLO,100.*DHI,  LABDIS(IPDIS), PSLO,  PSHI,
     &  NULO,   NUDL, WEVLO, WEVDL
      WRITE (13,102)
     &  LABDIS(IDDIS),100.*DLO,100.*DHI,  LABDIS(IPDIS), PSLO,  PSHI,
     &  NULO,   NUDL, WEVLO, WEVDL
      WRITE (*,104) RIN,    XL,   XGAP,  KGAS,  HFG, VBAS
      WRITE (12,104) RIN,    XL,   XGAP,  KGAS,  HFG, VBAS
      WRITE (13,104) RIN,    XL,   XGAP,  KGAS,  HFG, VBAS
C
 100  FORMAT(' ***** MONTE CARLO IGNITION TEMPERATURE *****',//,
     &       ' Decay Power Distribution',/,
     &       '    Qlo=   ',F6.1,'   Qmid= ',F6.1,'   Qhi= ',F6.1,/,
     &       ' Scrap Porosity Distribution',/,
     &       '    Philo= ',F6.4,'    Del= ',F6.4,/,
     &       ' Rate Multiplier Distribution ',A11,/,
     &       '    Min  = ',F6.3,'    Max= ',F6.3,/,
     &       ' Internal Emissivity Distribution',/,
     &       '    Epslo= ',F6.4,'    Del= ',F6.4,/,
     &       ' Gap Emissivity Distribution',/,
     &       '    Egplo= ',F6.4,'    Del= ',F6.4,/,
```

```
     &        ' Reaction Area Distribution ',A11,/,
     &        '    Alo  = ',F6.4,'    Ahi= ',F6.4)
 102  FORMAT(
     &        ' Scrap Size Distribution (cm) ',A11,/,
     &        '    Dlo  = ',F6.3,'    Dhi= ',F6.3,/,
     &        ' Steam Pressure Distribution (kPa) ',A11,/,
     &        '    Pslo = ',F6.3,'   Pshi= ',F6.3,/,
     &        ' Nusselt Number for convection',/,
     &        '    Nulo = ',F6.3,'    Del= ',F6.3,/,
     &        ' Evaporation rate kg/hr',/,
     &        '    Wevlo= ',F6.3,'    Del= ',F6.3)
 104  FORMAT(
     &        ' Constant Values',/,
     &        '    Rin  = ',F8.5,'   Rout= ',F8.5,/,
     &        '    Gap  = ',F8.5,'   Kgas= ',F8.5,/,
     &        '    Hfg  = ',F9.1,'   Vbas= ',F8.5)
C
      RETURN
      END

      REAL FUNCTION RREAD (IUNIT)
C
C     GET A REAL VALUE FROM A LINE WITH A BLANK FIRST COLUMN
C     SKIP LINES WITH NON-BLANK FIRST COLUMNS
C
      CHARACTER*1 LINE,BLANK
      DATA BLANK /' '/
      VALUE= 0.E0
 100  CONTINUE
      READ (IUNIT,'(A)',END=200) LINE
      IF (LINE .NE. BLANK) GOTO 100
      BACKSPACE (IUNIT)
      READ (IUNIT,*) VALUE
 200  CONTINUE
      RREAD= VALUE
      RETURN
      END

      INTEGER FUNCTION IREAD (IUNIT)
C
C     GET AN INTEGER FROM A LINE WITH A BLANK FIRST COLUMN
C     SKIP LINES WITH NON-BLANK FIRST COLUMNS
C
      CHARACTER*1 LINE,BLANK
      DATA BLANK /' '/
      IVALUE= 0
 100  CONTINUE
      READ (IUNIT,'(A)',END=200) LINE
      IF (LINE .NE. BLANK) GOTO 100
      BACKSPACE (IUNIT)
      READ (IUNIT,*) IVALUE
 200  CONTINUE
      IREAD= IVALUE
      RETURN
      END

      SUBROUTINE GETIN (NSAM,
```

```
     &       QLOW,   QMID,   QUPP, PHILO, PHIDL, FEAMN, FEAMX, IRDIS,
     &      EPSLO, EPSDL, EGPLO, EGPDL,   ALO,   AHI, IADIS,
     &        DLO,    DHI, IDDIS,  PSLO,  PSHI, IPDIS,  NULO,  NUDL,
     &      WEVLO, WEVDL,
     &        RIN,     XL,  XGAP,  KGAS,   HFG,  VBAS,
     &         QV,    PHI,  FEAC,   KSL,   EPS,   NUS,
     &       KGAP,  EGAP,  AOV0,  FRAD,    DP,  PPST, QVEV)
      INTEGER NSAM
      IMPLICIT REAL (A-H,K-Z)
      SAVE
C
C     RANDOM SEED IS INITIALIZED ON FIRST PASS ONLY
C
      DATA IDUM /0/
C
C     DEFAULT VALUES CHANGED FOR MARV THURGOOD HE-FILLED MCO
C     COMMENTED-OUT VALUES ARE SUPERSEDED BY DISTRIBUTIONS
C
C     SCRAP BASKET OUTER RADIUS GIVEN 22.625 INCH DIAMETER
C     GAP BASED ON 23 INCH MCO INNER DIAMETER
C     HE CONDUCTIVITY SELECTED FOR 50 C - CONSERVATIVE
C     GAP EMISSIVITY GIVEN 0.7 FOR SURFACES, ROUNDED DOWN
C
C      QV= 1875.
C      PHI=  0.40
C      FEAC= 3.2
C      KSL= 1.0
C      RIN= 0.02
C      XL= 0.287E0
C      XGAP= 0.00476E0
C      KGAP= 0.16E0
C      EGAP= 0.50E0
C      AOV0= 54.E0 / 0.17
C
C --- RANDOM VARIABLES ---
C
C     DECAY POWER
C
      CALL TRIANG(QLOW,QMID,QUPP,QTRI)
      QV=QTRI
C
      PHI= PHILO + PHIDL*RANDOM(IDUM)
      IF (IRDIS .EQ. 0) THEN
          FEAC= FEAMN + (FEAMX - FEAMN)*RANDOM(IDUM)
      ELSE
          FEAC= FEAMN * (FEAMX/FEAMN)**RANDOM(IDUM)
      ENDIF
      EPS= EPSLO + EPSDL*RANDOM(IDUM)
      EGAP= EGPLO  + EGPDL*RANDOM(IDUM)
      NUS= NULO + NUDL*RANDOM(IDUM)
C
C     MODIFY CONDUCTIVITY USING VOID FRACTION AND NUSSELT #
C
      KSL= KGAS / (1.E0 - (1.E0-PHI)**0.3333E0)
     &     + KGAS*(NUS-1.E0)
      KGAP= KGAS
C
```

```
C     AREA PER UNIT VOLUME BY RANDOM AREA
C
C     CORRELATE AREA WITH FUEL VOLUME FRACTION
C     AREA RANGE APPLIES TO MIN VOID FRACTION
C
      IF (IADIS .EQ. 0) THEN
          ARX= ALO + (AHI - ALO)*RANDOM(IDUM)
      ELSE
          ARX= ALO * (AHI/ALO)**RANDOM(IDUM)
      ENDIF
      ARX= ARX * (1.E0 - PHI) / (1.E0 - PHILO)
      AOV0= ARX/VBAS
C
C     RADIATION FACTOR IS DERIVED
C
      LAM= 1.E0 - 1.21E0*(1.E0-(1.E0-PHI))**(2.E0/3.E0)
      FRAD= (1.E0 + LAM/EPS)/(1.E0-LAM)
C
C     PARTICLE DIAMETER
C
      IF (IDDIS .EQ. 0) THEN
          DP= DLO + (DHI - DLO)*RANDOM(IDUM)
      ELSE
          DP= DLO * (DHI/DLO)**RANDOM(IDUM)
      ENDIF
C
C     STEAM PRESSURE
C
      IF (IPDIS .EQ. 0) THEN
          PPST= PSLO + (PSHI - PSLO)*RANDOM(IDUM)
      ELSE
          PPST= PSLO * (PSHI/PSLO)**RANDOM(IDUM)
      ENDIF
C
C     EVAPORATION VOLUMETRIC POWER, FROM KG/HR TO W/M^3
C
      WEV= (WEVLO + WEVDL*RANDOM(IDUM)) / 3600.E0
      QVEV= WEV * HFG / VBAS
C
C     MANUAL INPUT SECTION HERE FOR CONVENIENT CHECK OF RESULTS
C     USED WHEN # SAMPLES = 1 ON ENTRY
C
      IF (NSAM .GT. 1) RETURN
C
 100  CONTINUE
C
      WRITE (*,20) PHI,QV,FEAC,KSL,EPS,AOV0,RIN,XL,
     &             XGAP,KGAP,EGAP,FRAD,DP,PPST,NUS,QVEV
   20 FORMAT(' Current values: ',/,
     & '     1 PHI= ',F8.2,'     2 QV = ',F8.2,'     3 FEA=  ',F8.3,/,
     & '     4 KSL= ',F8.3,'     5 EPS= ',F8.4,'     6 AOV=  ',F8.2,/,
     & '     7 RIN= ',F8.4,'     8 XL=  ',F8.4,'     9 XGAP= ',F8.6,/,
     & '    10 KGAP=',F8.3,'    11 EGAP=',F8.4,'    12 FRAD= ',F8.4,/,
     & '    13  DP= ',F8.6,'    14 PPST=',F8.4,'    15   NU= ',F8.3,/,
     & '    16 QVEV=',F8.3,/,
     & '     Enter 0,0 if OK else index,value: ',$)
      READ (*,*) IND,VAL
```

```
      IF (IND .LE. 0) GO TO 200
      IF (IND .EQ. 1) PHI=VAL
      IF (IND .EQ. 2) QV=VAL
      IF (IND .EQ. 3) FEAC=VAL
      IF (IND .EQ. 4) KSL=VAL
      IF (IND .EQ. 5) EPS=VAL
      IF (IND .EQ. 6) AOV0=VAL
      IF (IND .EQ. 7) RIN=VAL
      IF (IND .EQ. 8) XL=VAL
      IF (IND .EQ. 9) XGAP=VAL
      IF (IND .EQ. 10) KGAP=VAL
      IF (IND .EQ. 11) EGAP=VAL
      IF (IND .EQ. 12) FRAD=VAL
      IF (IND .EQ. 13) DP=VAL
      IF (IND .EQ. 14) PPST=VAL
      IF (IND .EQ. 16) QVEV=VAL
      IF (IND .GE. 17) GO TO 100
      GOTO 100
 200  CONTINUE
C
      RETURN
      END

C
       FUNCTION GASDEV(IDUM)
       DATA ISET/0/
       IF (ISET.EQ.0) THEN
  1       V1=(2.0*RANDOM(IDUM)-1.0)
         V2=(2.0*RANDOM(IDUM)-1.0)
         R=V1**2.0+V2**2.0
         IF(R.GE.1.0) GO TO 1
         FAC=SQRT(-2.0*LOG(R)/R)
         GSET=V1*FAC
         GASDEV=V2*FAC
         ISET=1
       ELSE
         GASDEV=GSET
         ISET=0
       ENDIF
       RETURN
       END

       FUNCTION RANDOM(IDUM)
       DATA NCALLS /0/
       IF (NCALLS.EQ.0) THEN
        NCALLS=1
        Y=RRAND()
       ELSE
        Y=RND()
       ENDIF
       RANDOM=Y
       RETURN
       END


      SUBROUTINE TRIANG(A,B,C,X)
C*****************************************************************
```

```
C SUBROUTINE TRIANG GENERATES THE TRIANGULAR DISTRIBUTION
C
      IDUM=1
      PROBINC=1.0
      C1=C-A
      C2=(B-A)/C1
      STRTPT=0.
      N=1
      DO 10 I=1,N
       R=PROBINC*RANDOM(IDUM)+STRTPT
       IF(R.LE.C2)THEN
         X=A+SQRT(R*C1*(B-A))
       ELSE
         X=C-SQRT((1.-R)*C1*(C-B))
       ENDIF
   10 CONTINUE
      RETURN
      END
```

APPENDIX G MATHCAD FILE FOR HYDRIDE LAYER TRANSIENTS

HYDRIDE LAYER IMPACT ON DAMAGED FUEL IGNITION POTENTIAL

Investigate transient behavior of a hydride layer on damaged fuel. The layer is thin and depletes, but it carries a large amount of surface area which can heat up the bulk fuel and "boost" the metal surface reaction.

By: Martin G. Plys, Fauske & Associates, Inc. 16W070 West 83rd St. Burr Ridge IL 60521 Phone (630)887-5207
For: Darrel R. Duncan Hanford Spent Nuclear Fuel Project Phone (509) 372-1013.
August 1998 **File ig-hyd-lay-tran-3-short 6 pages**

1.0 Constant Values

Hydride layer:

Hydride layer density, kg/m^3 $\rho_l := 8000$

Hydride fraction in layer $f_h := 0.25$

Weight gain ratio: $\mu := \frac{29}{241}$

Area per unit volume: $A_v := 4 \cdot 10^6$

Hydride multiplier with a 10 micron layer:

$F_{ho} := f_h \cdot A_v \cdot 10^{-5}$ $F_{ho} = 10$

Fuel:

Fuel half-thickness, m $b := 0.0045$

Fuel density, kg/m^3 $\rho_f := 19000$

Fuel heat capacity, J/kg/K $c_f := 120$

Fuel thermal conductivity, damaged, W/m/K $k_f := 20$

$\alpha_f := k_f \cdot (\rho_f \cdot c_f)^{-1}$ $C_f := \rho_f \cdot c_f \cdot b$

Rate law multiplier, fuel: $F_f := 10$

Reaction rate law, Pearce oxygen-free:

Heat of reaction, J/kgO2 $\Delta H := 1.67 \cdot 10^7$

Rate pre-exponential, kgO2/m^2/s $k_o := 0.05939$

Rate activation energy, K $T_E := 4936.7$

Conversion: $T_k := 273.15$

Fuel heat transfer parameters:

Stefan-Boltzmann const. $\sigma := 5.67 \cdot 10^{-8}$

Overall emissivity, parallel plates of e=0.7. $\varepsilon := 0.5$

Convective hxfer k/d, W/m^2, where k=0.03 is steam, account for H2 by doubling, and d = 2 cm average $h_e := \frac{0.06}{0.02}$

Adiabatic temperature rise, 10 micron layer: $\Delta T_{ad} := \frac{\rho_l \cdot f_h \cdot 10^{-5}}{\rho_f \cdot b} \cdot \frac{\Delta H \cdot \mu}{c_f}$ $\Delta T_{ad} = 3.917$

Nodalization of undamaged element and coefficients for finite-difference solution:

Length of element: $L_e := 0.66$

Damage length: $L_d := 0.1$

Intact length: $L_i := L_e - L_d$ $L_i = 0.56$

Number of nodes: $J := 6$

First node size for fine gradient at damaged end: $\Delta x_o := 0.025$

Ratio of node sizes, increasing geometrically from damaged end

$r := 2$ $r := \text{root}\left[r^J - \frac{L_i}{\Delta x_o} \cdot (r - 1) - 1, r\right]$ $r = 1.532$

Establish node sizes: $j := 0..J - 1$ $\Delta x_j := \Delta x_o \cdot r^j$ $\sum_j \Delta x_j = 0.56$ Nodes sum to intact length

First node coefficients: $A_0 := 2 \quad C_0 := 2\cdot\left[1 + \Delta x_2\cdot(\Delta x_1)^{-1}\right]^{-1} \quad B_0 := -(A_0 + C_0)$

Last node coefficients: $A_{J-1} := 2\cdot\left[1 + \Delta x_{J-2}\cdot(\Delta x_{J-1})^{-1}\right]^{-1} \quad C_{J-1} := 0 \quad B_{J-1} := -A_{J-1}$

Middle node values: $j := 1..J-2 \quad A_j := 2\cdot\left[1 + \Delta x_{j-1}\cdot(\Delta x_j)^{-1}\right]^{-1}$

$C_j := 2\cdot\left[1 + \Delta x_{j+1}\cdot(\Delta x_j)^{-1}\right]^{-1} \quad B_j := -(A_j + C_j)$

Analogue of Fourier number: $j := 0..J-1 \quad Fo_j := \alpha_f\cdot(\Delta x_j)^{-2}$

$\Delta x^T = (0.025\ 0.038\ 0.059\ 0.09\ 0.138\ 0.211)$

$A^T = (2\ \ 1.21\ \ 1.21\ \ 1.21\ \ 1.21\ \ 1.21) \qquad C^T = (0.79\ \ 0.79\ \ 0.79\ \ 0.79\ \ 0.79\ \ 0)$

2.0 Functions

Overall heat transfer, sum of loss to gas and conduction to infinitely long element, multiplier "s" for adiabatic case

$fh(T_a, s) := s\cdot\left(h_e + 4\cdot\sigma\cdot\varepsilon\cdot T_a^3\right) \qquad fh(323, 1) = 6.821$

Rate law including depletion, kgO2/m^2/sec - Pearce correlation, spherical particle model. Test for 50 C, saturated conditions.

$fmdot(T, p) := k_o\cdot\sqrt{p}\cdot\exp\left(\frac{-T_E}{T}\right) \qquad fmdot(323, 12) = 4.738\times 10^{-8}$

Depletion function: change of fraction reacted alpha

$$f\alpha dot(\alpha, T, p) := \begin{cases} 0 & \text{if } \alpha \geq 1 \\ \frac{A_v}{\mu\cdot\rho_1}\cdot(fmdot(T,p))\cdot(1-\alpha)^{\frac{2}{3}} & \text{otherwise} \end{cases}$$

Temperature derivative for damaged end. Power in from hydride layer and surface oxidation, power out by convection from surface and axial conduction to undamaged rod portion

Test: expect over 10^-3 when rate law multipliers are 10 + 10

$fTdot(0, 323, 12, 323, 0, 10, 10, 323) = 1.542\times 10^{-3}$

$$fTdot(\alpha, T, p, T_a, s, F_f, F_h, TF0) := \begin{cases} w \leftarrow fmdot(T, p) \\ h \leftarrow fh(T_a, s) \\ F \leftarrow F_f \ \text{ if } \alpha \geq 1 \\ F \leftarrow F_f + F_h\cdot(1-\alpha)^{\frac{2}{3}} \ \text{ otherwise} \\ q_{el} \leftarrow \frac{b}{L_d}\cdot\frac{k_f\cdot(T - TF0)}{0.5\cdot\Delta x_0} \\ \frac{1}{C_f}\cdot\left[F\cdot w\cdot\Delta H - h\cdot(T - T_a) - q_{el}\right] \end{cases}$$

Function for derivative of intact fuel temperature TF with J elements from 0 to J-1. 'To' is the end value at x=0, insulated at the end after point J-1, 'Ta' is the temperature for convection, 's' is the view factor to cooler elements. This is an explicit solution of the finite difference equation because Mathcad won't provide the timestep it uses during integration, so an implicit derivative cannot be calculated.

$$\begin{aligned}
&\text{fTFdot}(T_o, T_a, s, TF) := \\
&\quad Bo \leftarrow fh(T_a, s)\cdot C_f^{-1} \\
&\quad Tdot_0 \leftarrow Fo_0\cdot(A_0\cdot T_o + B_0\cdot TF_0 + C_0\cdot TF_1) - Bo\cdot(TF_0 - T_a) \\
&\quad \text{for } j \in 1..J-2 \\
&\quad\quad Tdot_j \leftarrow Fo_j\cdot(A_j\cdot TF_{j-1} + B_j\cdot TF_j + C_j\cdot TF_{j+1}) - Bo\cdot(TF_j - T_a) \\
&\quad Tdot_{J-1} \leftarrow Fo_{J-1}\cdot(A_{J-1}\cdot TF_{J-2} + B_{J-1}\cdot TF_{J-1}) - Bo\cdot(TF_{J-1} - T_a) \\
&\quad Tdot
\end{aligned}$$

Test for step change in end boundary temperature:

$j := 0..J-1 \quad TF_j := 323 \quad T_a := 323 \quad T_o := 333 \quad \text{fTFdot}(T_o, T_a, 1, TF)^T = (0.281\ 0\ 0\ 0\ 0\ 0)$

Test for step change in ambient temperature:

$j := 0..J-1 \quad TF_j := 323 \quad T_a := 322 \quad T_o := 323$

$$\text{fTFdot}(T_o, T_a, 1, TF)^T = \left(-6.61\times 10^{-4}\ \ -6.61\times 10^{-4}\ \ -6.61\times 10^{-4}\ \ -6.61\times 10^{-4}\ \ -6.61\times 10^{-4}\ \ -6.61\times 10^{-4}\right)$$

Overall derivative of state vector. State variables of vector X by index are: 0=reacted fraction, 1=temperature of damaged end, 2=ambient steam pressure, 3= ambient temperature for heat transfer, 4=Surface heat transfer multiplier, use 0 for adiabatic, otherwise choose a value that represents the view factor to cooler fuel elements, 5=Rate law multiplier for metal surface, use 0 to ignore, 10 is nominal, 6=Rate law multiplier for hydride with zero depletion, nominal 10 to 12. Trick: some of these have zero derivatives; this allows the function to be evaluated parametrically. Values from 7 to 7+J-1 are temperatures of the undamaged element.

$$\begin{aligned}
&D(t, X) := \\
&\quad \alpha \leftarrow X_0 \\
&\quad T \leftarrow X_1 \\
&\quad p \leftarrow X_2 \\
&\quad T_a \leftarrow X_3 \\
&\quad s \leftarrow X_4 \\
&\quad F_f \leftarrow X_5 \\
&\quad F_h \leftarrow X_6 \\
&\quad TF \leftarrow \text{submatrix}(X, 7, 7+J-1, 0, 0) \\
&\quad TFdot \leftarrow \text{fTFdot}(T, T_a, s, TF) \\
&\quad X1 \leftarrow \left(\text{f}\alpha\text{dot}(\alpha, T, p)\ \ \text{fTdot}(\alpha, T, p, T_a, s, F_f, F_h, TF_0)\ \ 0\ 0\ 0\ 0\ 0\right)^T \\
&\quad Xdot \leftarrow \text{stack}(X1, TFdot)
\end{aligned}$$

3.0 INTEGRATE FOR SPECIFIC INITIAL CONDITIONS.

No surface hydride, 10 X Metal multiplier, 75 C and 12 kPa, get expected steady axial delta-T

$\alpha_o := 1 \quad T_o := 80 + T_k \quad p := 12 \quad T_a := 75 + T_k \quad s := 0.3 \quad F_f := 10 \quad F_h := 10 \quad j := 0..J-1 \quad TF_j := T_a + 2$

$X := \text{stack}\left(\left(\alpha_o \;\; T_o \;\; p \;\; T_a \;\; s \;\; F_f \;\; F_h\right)^T, TF\right)$

$Y := \text{Rkadapt}(X, 0, 8000, 100, D) \quad i := 0..100 \quad t_i := \left(Y^{\langle 0 \rangle}\right)_i$

$T_i := \left(Y^{\langle 2 \rangle}\right)_i - T_a \quad \alpha_i := \left(Y^{\langle 1 \rangle}\right)_i \quad T1_i := \left(Y^{\langle 8 \rangle}\right)_i - T_a \quad T3_i := \left(Y^{\langle 10 \rangle}\right)_i - T_a \quad T6_i := \left(Y^{\langle 13 \rangle}\right)_i - T_a$

$Bfin := \sqrt{fh\left(T_a + 2, 1\right) \cdot s \cdot b^{-1} \cdot k_f^{-1}} \qquad Qfin := \dfrac{k_f \cdot \left(T_{100} - T1_{100}\right)}{0.5 \cdot \Delta x_o}$

$dTfin := \dfrac{Qfin}{k_f \cdot Bfin} \cdot \dfrac{\cosh\left(Bfin \cdot L_i\right) - 1}{\sinh\left(Bfin \cdot L_i\right)} \qquad dTfin = 3.588 \qquad T_{100} - T6_{100} = 3.562$

Steady-state axial temperature difference: Exact solution agrees, about 3.6 C

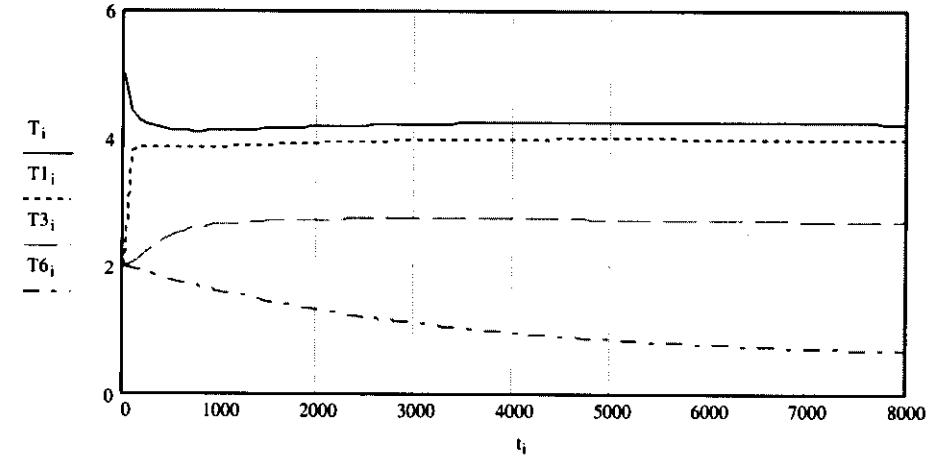

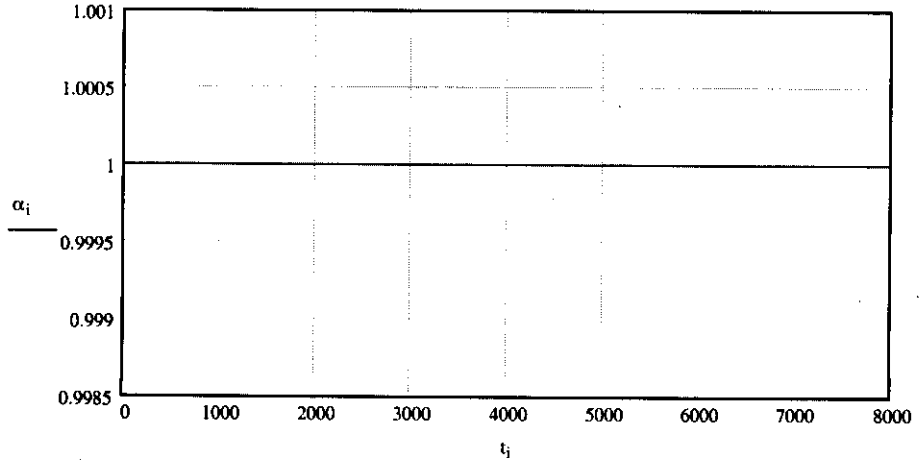

4.0 Multiple Cases, Use same time vector as above. $i := 0..100 \quad t_i := (Y^{\langle 0 \rangle})_i$

View factor for central element = 0.52, but this is for the external perimeter only, so s=0.26 applies.

Case 1: 75 C, 12 kPa, F=10+12

$\alpha_o := 0 \quad T_o := 75 + T_k \quad p := 12 \quad T_a := 75 + T_k \quad s := 0.26 \quad F_f := 10 \quad F_h := 12 \quad j := 0..J-1 \quad TF_j := T_a$

$X := \text{stack}\left((\alpha_o \ T_o \ p \ T_a \ s \ F_f \ F_h)^T, TF\right) \quad Y := \text{Rkadapt}(X, 0, 8000, 100, D) \quad T_{i,0} := (Y^{\langle 2 \rangle})_i - T_a$

Case 2: 75 C, 12 kPa, F=10+60

$\alpha_o := 0 \quad T_o := 75 + T_k \quad p := 12 \quad T_a := 75 + T_k \quad s := 0.26 \quad F_f := 10 \quad F_h := 60 \quad j := 0..J-1 \quad TF_j := T_a$

$X := \text{stack}\left((\alpha_o \ T_o \ p \ T_a \ s \ F_f \ F_h)^T, TF\right) \quad Y := \text{Rkadapt}(X, 0, 8000, 100, D) \quad T_{i,1} := (Y^{\langle 2 \rangle})_i - T_a$

Depletion time for this case: $(Y^{\langle 1 \rangle})_{30} = 0.959 \quad t_{30} = 2.4 \times 10^3$

Case 3: 75 C, 4 kPa, F=10+12

$\alpha_o := 0 \quad T_o := 75 + T_k \quad p := 4 \quad T_a := 75 + T_k \quad s := 0.26 \quad F_f := 10 \quad F_h := 12 \quad j := 0..J-1 \quad TF_j := T_a$

$X := \text{stack}\left((\alpha_o \ T_o \ p \ T_a \ s \ F_f \ F_h)^T, TF\right) \quad Y := \text{Rkadapt}(X, 0, 8000, 100, D) \quad T_{i,2} := (Y^{\langle 2 \rangle})_i - T_a$

Case 4: 75 C, 12 kPa, F=22+60

$\alpha_o := 0 \quad T_o := 75 + T_k \quad p := 12 \quad T_a := 75 + T_k \quad s := 0.26 \quad F_f := 22 \quad F_h := 60 \quad j := 0..J-1 \quad TF_j := T_a$

$X := \text{stack}\left((\alpha_o \ T_o \ p \ T_a \ s \ F_f \ F_h)^T, TF\right) \quad Y := \text{Rkadapt}(X, 0, 8000, 100, D) \quad T_{i,3} := (Y^{\langle 2 \rangle})_i - T_a$

Case 5: 75 C, 12 kPa, F=10+120

$\alpha_o := 0 \quad T_o := 75 + T_k \quad p := 12 \quad T_a := 75 + T_k \quad s := 0.26 \quad F_f := 10 \quad F_h := 120 \quad j := 0..J-1$

$X := \text{stack}\left((\alpha_o \ T_o \ p \ T_a \ s \ F_f \ F_h)^T, TF\right) \quad Y := \text{Rkadapt}(X, 0, 8000, 100, D) \quad T_{i,4} := (Y^{\langle 2 \rangle})_i - T_a$

Fig. 8-1Temperature Rise During Hydride Layer Reaction for Various Ambient Temperatures, Steam Partial Pressures, and Metal Rate Multipliers. F= x + y means the initial rate law multiplier F is the sum of a sustained term 'x' from internal hydride or any other reason, and a depleting term 'y' due to the surface hydride. Curves arranged top to bottom by peak value in order listed below figure.

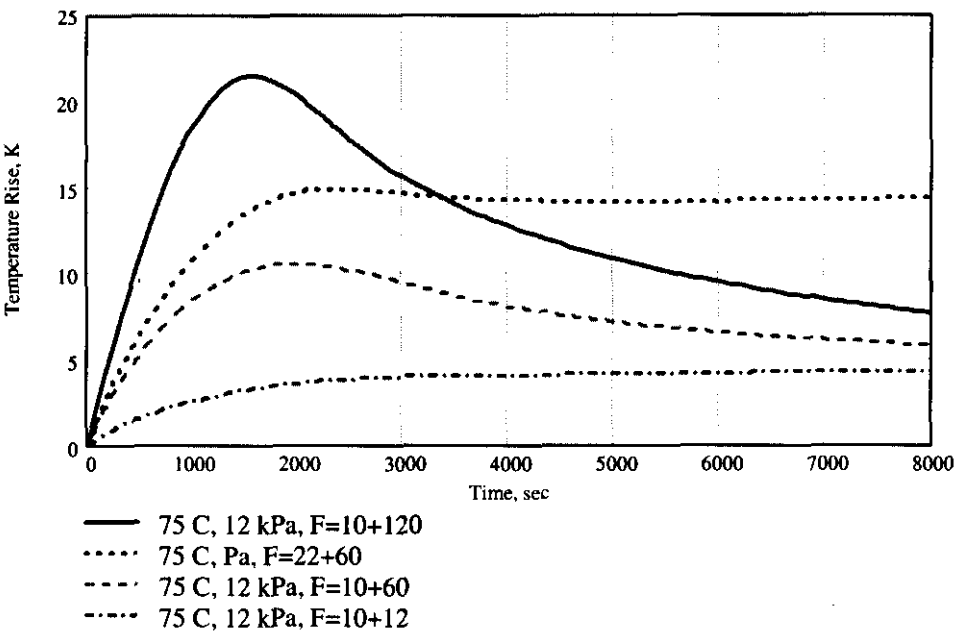

APPENDIX H HANSF RESULTS FOR CASE VC1A22

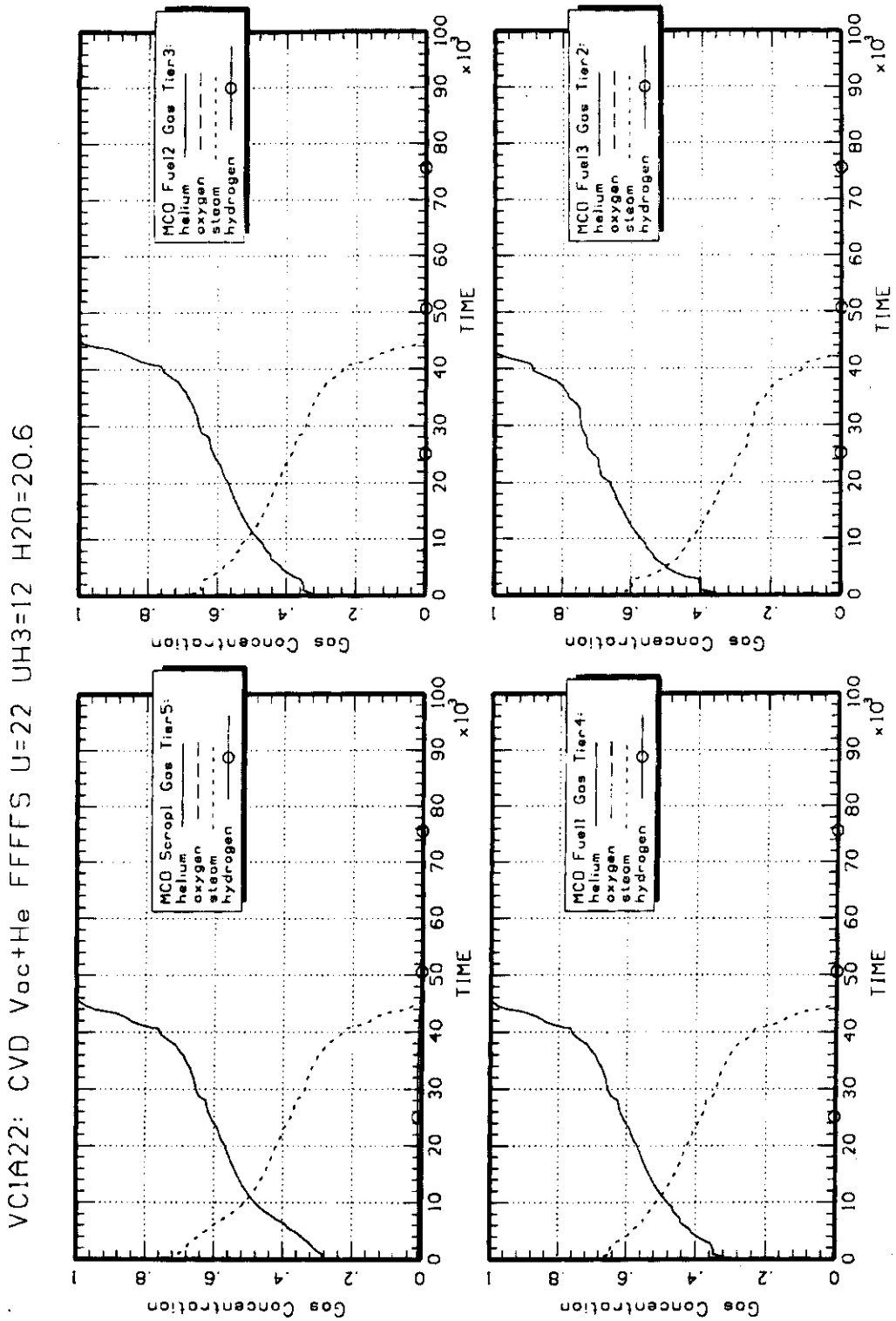

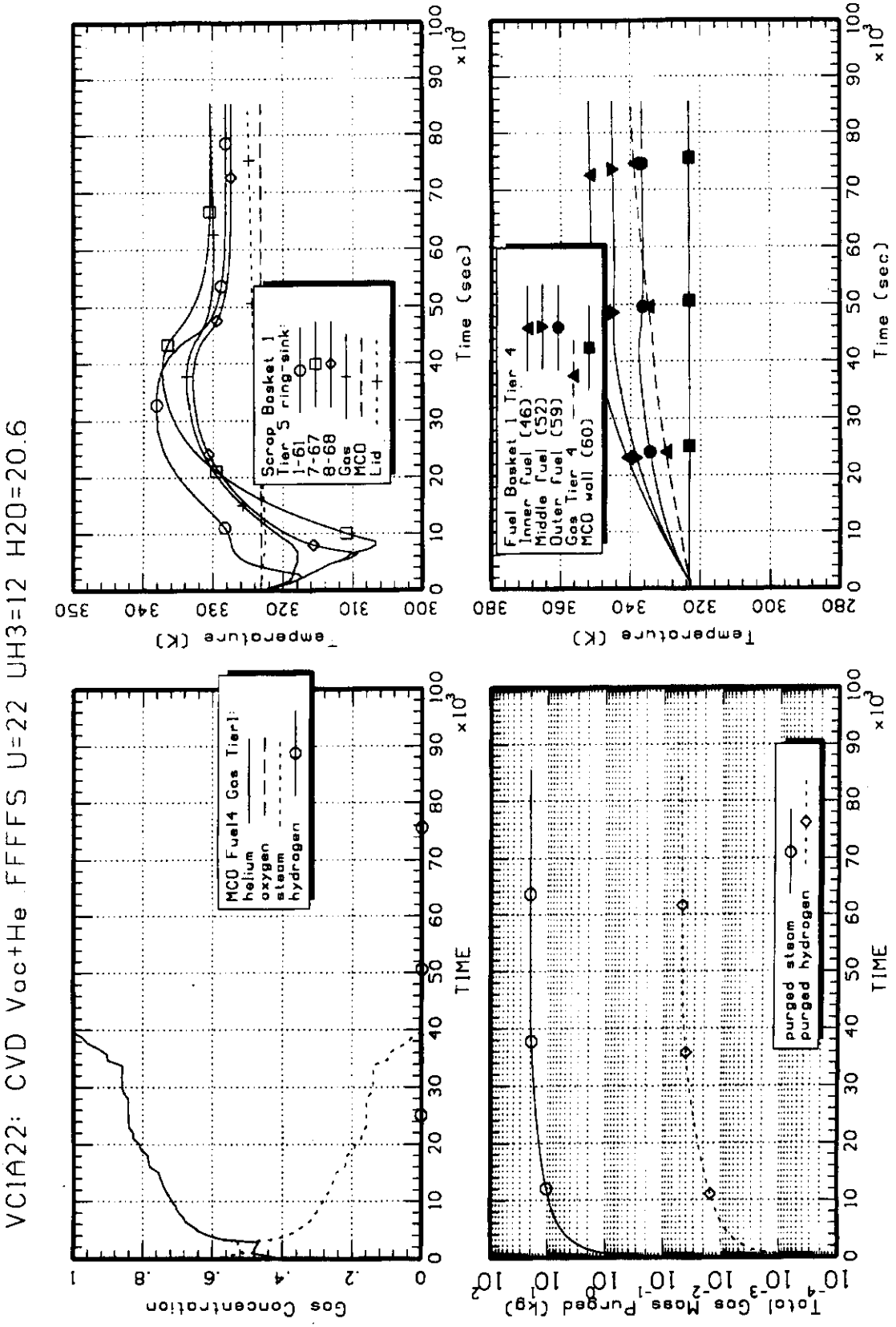
VC1A22: CVD Vac+He FFFFS U=22 UH3=12 H2O=20.6
Scrap Basket 1
Tier 5 ring-sink
1-61
7-67
8-68
Gas
MCO
Lid
Temperature (K)
Time (sec)
Fuel Basket 1 Tier 4
Inner Fuel (46)
Middle Fuel (52)
Outer Fuel (59)
Gas Tier 4
MCO wall (60)
Temperature (K)
Time (sec)
MCO Fuel4 Gas Tier1
helium
oxygen
steam
hydrogen
Gas Concentration
TIME
purged steam
purged hydrogen
Total Gas Mass Purged (kg)
TIME

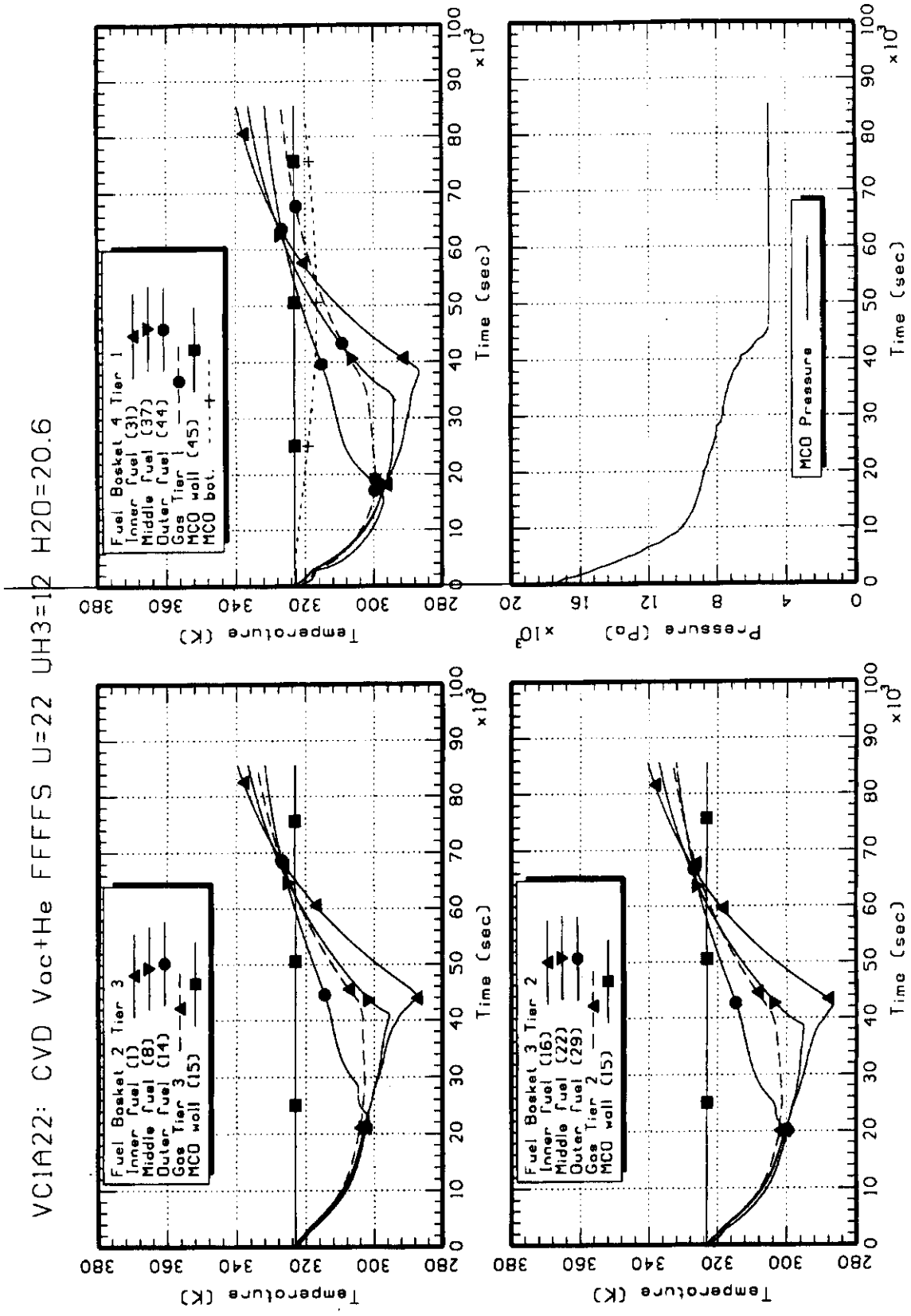
VC1A22: CVD Voc+He FFFFS U=22 UH3=12 H2O=20.6
Fuel Basket 4 Tier 1
Inner Fuel (31)
Middle Fuel (37)
Outer Fuel (44)
Gas Tier 1
MCO wall (45)
MCO bot.
Temperature (K)
Time (sec)
MCO Pressure
Pressure (Pa) x10^3
Fuel Basket 2 Tier 3
Inner Fuel (1)
Middle Fuel (8)
Outer Fuel (14)
Gas Tier 3
MCO wall (15)
Fuel Basket 3 Tier 2
Inner Fuel (16)
Middle Fuel (22)
Outer Fuel (29)
Gas Tier 2
MCO wall (15)

APPENDIX I HANSF RESULTS FOR CASE VC1AR50

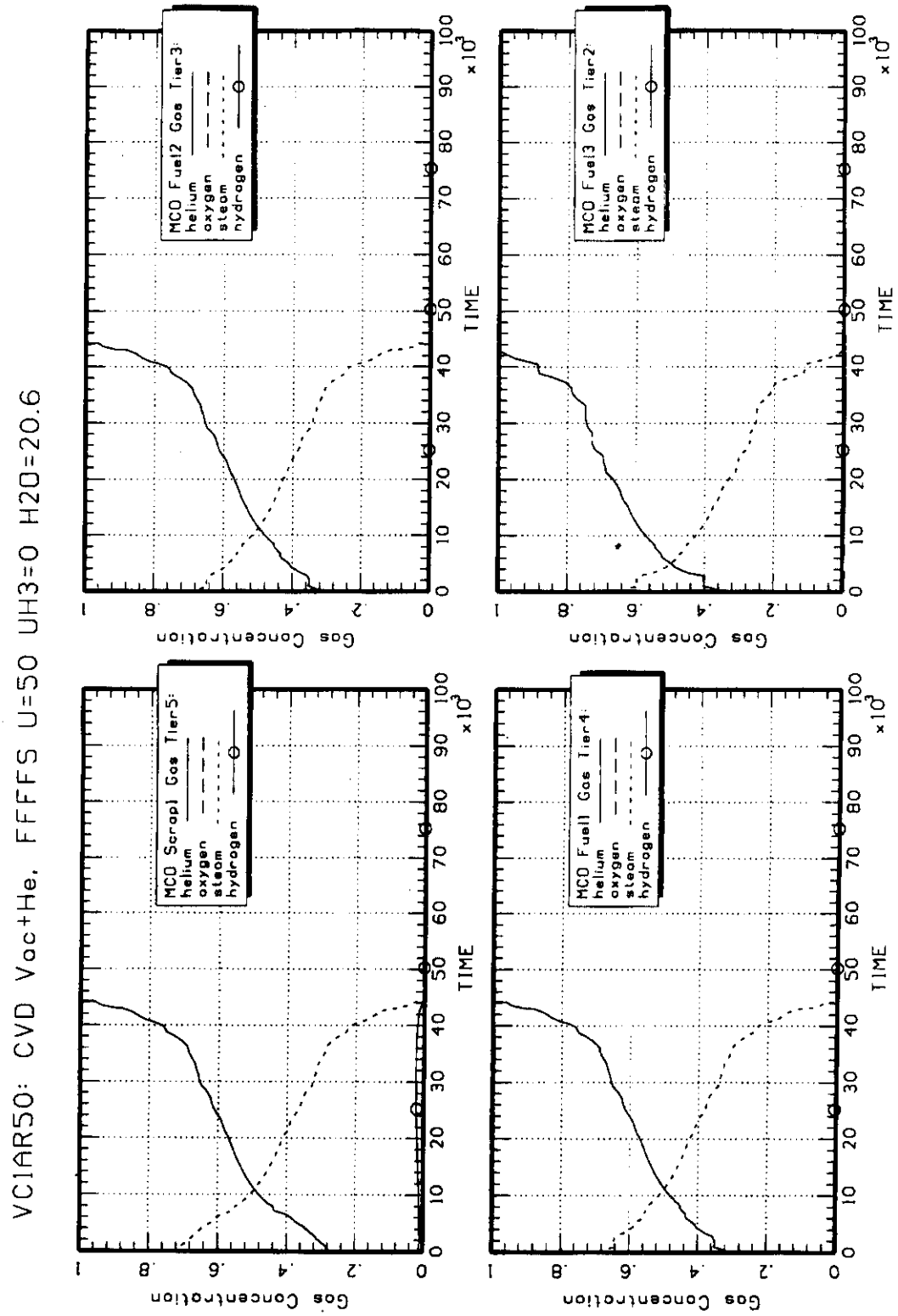

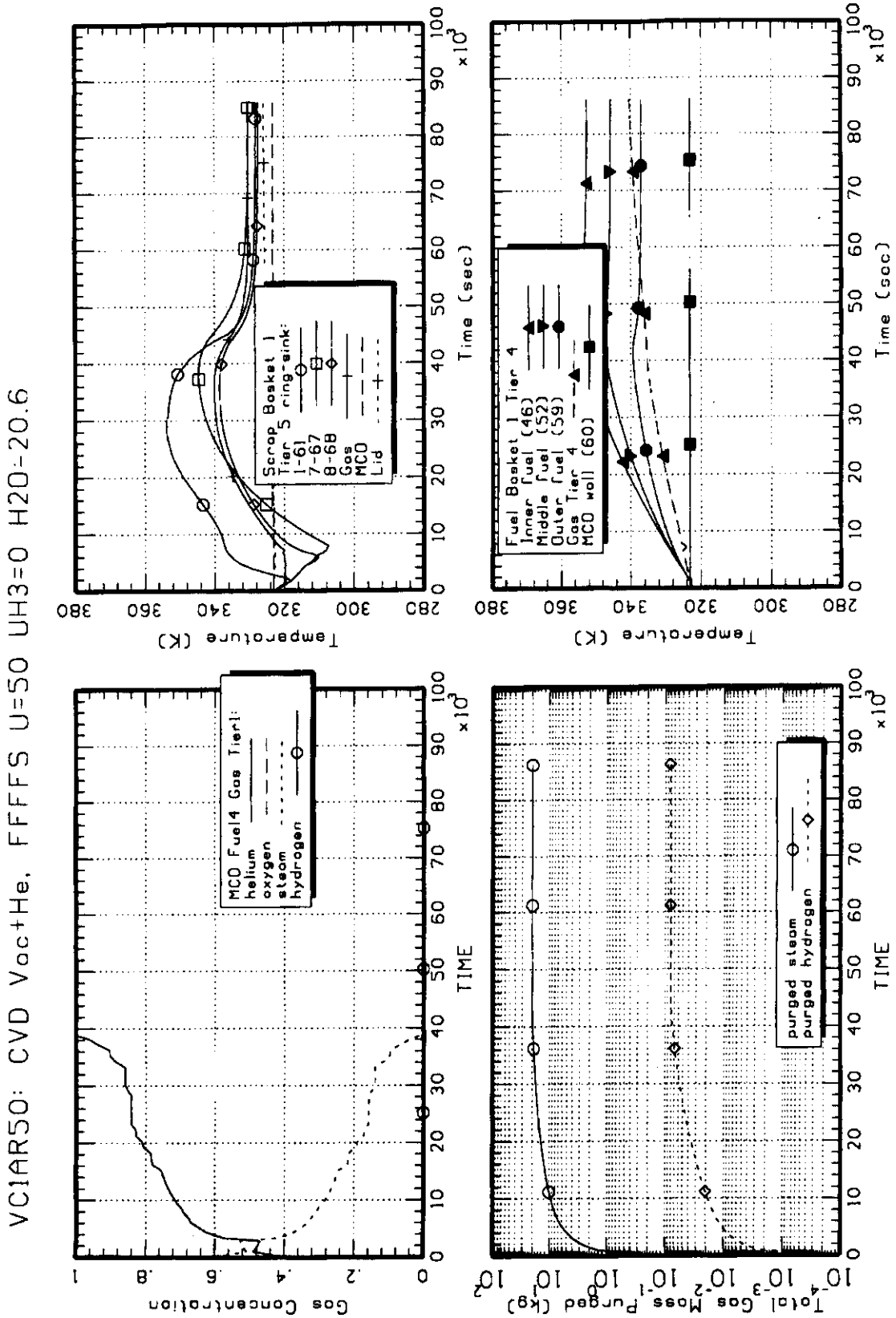
VC1AR50: CVD Vac+He, FFFFS U=50 UH3=0 H2O=20.6
Temperature (K)
Time (sec)
Scrap Basket 1
Tier 5 ring-sink
1-61
7-67
8-68
Gas
MCO
Lid
Fuel Basket 1 Tier 4
Inner Fuel (46)
Middle Fuel (52)
Outer Fuel (59)
Gas Tier 4
MCO wall (60)
Gas Concentration
TIME
MCO Fuel4 Gas Tier1
helium
oxygen
steam
hydrogen
Total Gas Mass Purged (kg)
purged steam
purged hydrogen

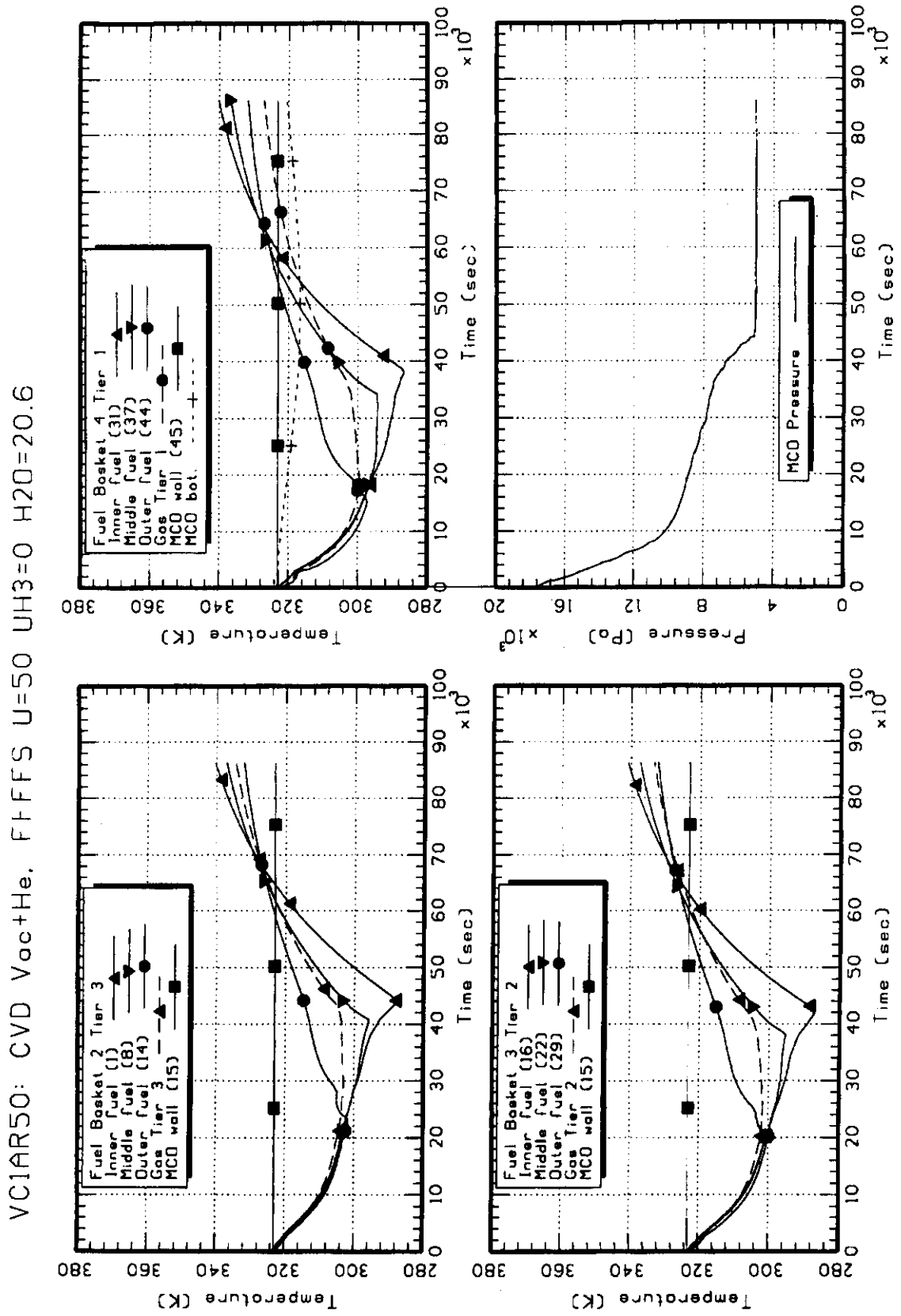
VC1AR50: CVD Vac+He, FHFFS U=50 UH3=0 H2O=20.6
Fuel Basket 4 Tier 1
Inner Fuel (31)
Middle Fuel (37)
Outer Fuel (44)
Gas Tier 1
MCO wall (45)
MCO bot.
Temperature (K)
Time (sec)
MCO Pressure
Pressure (Pa)
Fuel Basket 2 Tier 3
Inner Fuel (1)
Middle Fuel (8)
Outer Fuel (14)
Gas Tier 3
MCO wall (15)
Fuel Basket 3 Tier 2
Inner Fuel (16)
Middle Fuel (22)
Outer Fuel (29)
Gas Tier 2
MCO wall (15)

APPENDIX J MATHCAD FILES FOR CHAPTER 9 EXAMPLES

Constant Reaction Rate Theory Application for 50 gallon drums with U metal scrap

By Martin G. Plys, Fauske & Associates, Inc. 16W070 West 83rd Street
Burr Ridge IL 60521 USA 630-323-8750 plys@fauske.com
For Darrel R. Duncan Hanford Spent Nuclear Fuel Project 509-372-1013
June 2000 File ig-drums-powder.mcd

Cases for 50 gallon drums in storage, McGillivray kinetics x 3 for humid air:

Height and radius, m: $L := 0.89 \quad R := 0.29$

Kinetic parameters: $\xi := 3 \quad k_o := 10.95 \quad T_E := 8077$

Heat of reaction: $\Delta H_o := 3.4 \cdot 10^7$

Porosity and thermal conductivity: $\phi := 0.4 \quad k := 0.5$

Loop over temperature $i := 0..80 \quad Tam_i := 293 + i$

$Tr_i := T_E \cdot (Tam_i)^{-1} \quad TC_i := Tam_i - 273$

Isolated drum: $f := 0.065$ $\quad dpI_i := \dfrac{6 \cdot (1-\phi) \cdot L^2 \cdot f \cdot \xi \cdot k_o \cdot Tr_i \cdot \Delta H_o}{2 \cdot k \cdot Tam_i \cdot \exp(Tr_i - 1)}$

Side-by-side: $f := 0.170$ $\quad dpS_i := \dfrac{6 \cdot (1-\phi) \cdot L^2 \cdot f \cdot \xi \cdot k_o \cdot Tr_i \cdot \Delta H_o}{2 \cdot k \cdot Tam_i \cdot \exp(Tr_i - 1)}$

$AvI_i := \dfrac{6 \cdot (1-\phi)}{dpI_i} \quad dpI := 1000\, dpI$

$AvS_i := \dfrac{6 \cdot (1-\phi)}{dpS_i} \quad dpS := 1000\, dpS$

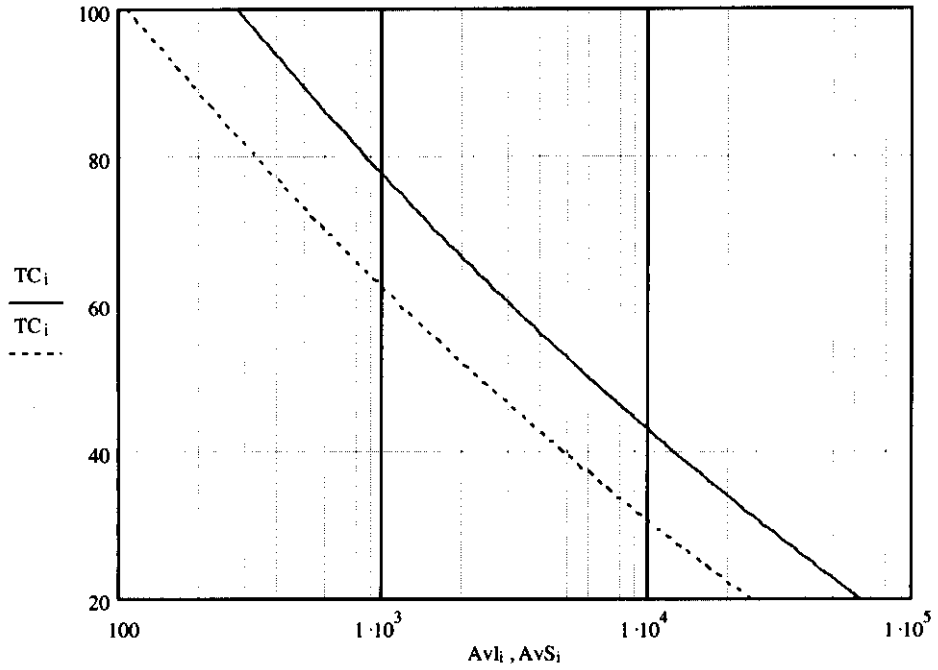
100
80
60
40
20
TC_i
TC_i
100
1·10^3
1·10^4
1·10^5
Avl_i , AvS_i

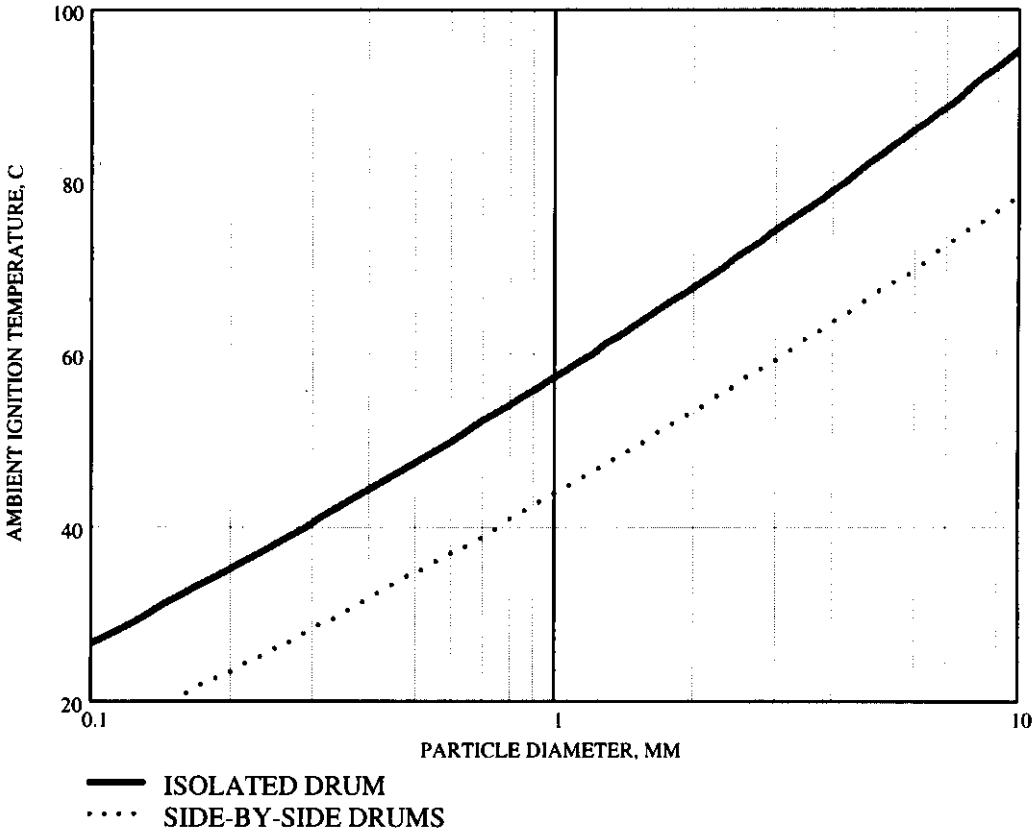
AMBIENT IGNITION TEMPERATURE, C
100
80
60
40
20
0.1
1
10
PARTICLE DIAMETER, MM
ISOLATED DRUM
SIDE-BY-SIDE DRUMS

Evaluate Hartmann's UH3 experience:

Useful values: $T_k := 273.15$ $Ce10 := \ln(10.0)$ $Ce10 = 2.303$

Convert mg/cm^2/hr to kg/m^2/s: $Cmk := 10^{-6} \cdot 10^{4} \cdot 3600^{-1}$ $Cmk = 2.778 \times 10^{-6}$

Ritchie parameters, original source: $koR75 := Cmk\, 10^{13.8808}$ $koR75 = 2.111 \times 10^{8}$

$TER75 := Ce10 \cdot 5769.6$ $TER75 = 1.328 \times 10^{4}$

External h accounts for rad: $h_e := 5$ Porosity $\phi := 0.4$

Internal k accounts for air; $k_b := 0.4$ Enthalpy $\Delta H := 3.4 \cdot 10^{7}$

Particle diameter: $d := 1.85 \cdot 10^{-6}$

FK parameter:

$$fB(k_o, T_E, L, T) := \frac{\frac{6 \cdot (1 - \phi)}{d} \cdot L^2 \cdot k_o \cdot \Delta H \cdot \left(\frac{T_E}{T}\right)}{2 \cdot \left(\frac{k_b}{1 + \frac{2 \cdot k_b}{h_e \cdot L}}\right) \cdot T \cdot \exp\left(\frac{T_E}{T} - 1\right)}$$

$i := 0..9$ $L_i := 0.001 \cdot (1 + i)$ $Tg := 310$ $T_k := 273$

McGillivray Dry: $Tdry_i := root\left(fB\left(10.95, 8077, L_i, Tg\right) - 1, Tg\right) - T_k$

McGillivray Wet, rate * 3: $Twet_i := root\left(fB\left(3 \cdot 10.95, 8077, L_i, Tg\right) - 1, Tg\right) - T_k$

Ritchie: $TRit_i := root\left(fB\left(koR75, TER75, L_i, Tg\right) - 1, Tg\right) - T_k$

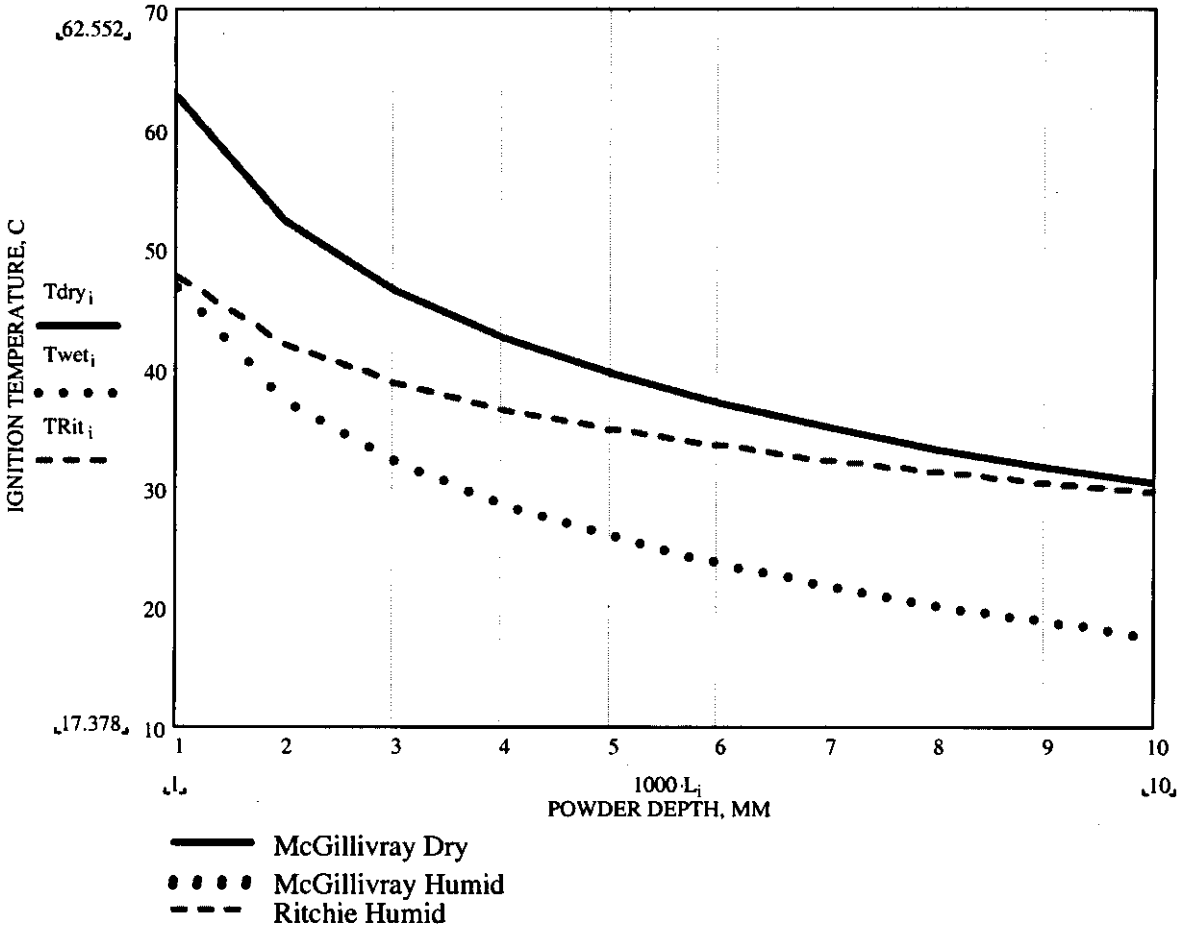
62.552
70
60
50
40
30
20
17.378
10
IGNITION TEMPERATURE, C
Tdry_i
Twet_i
TRit_i
1
2
3
4
5
6
7
8
9
10
L_1
1000·L_i
L_10
POWDER DEPTH, MM
McGillivray Dry
McGillivray Humid
Ritchie Humid

SNF-6781
KEVO

APPENDIX K
QUALITY ASSURANCE DOCUMENTS

Included here are:

1. Calculation Note Cover Sheet.
2. Authorship and Reviewer Table.
3. Calculation Note Methodology Checklist.

SNF-6781
REV 0

FAUSKE & ASSOCIATES, INC.

CALCULATION NOTE COVER SHEET

SECTION TO BE COMPLETED BY AUTHOR(S):

Calc-Note Number FAI/00-39 Revision Number 0

Title Uranium Pyrophoricity Phenomena and Prediction

Project Hanford Spent Nuclear Fuel Project Project No. or Shop Order DESH02

Purpose: Present a topical reference on the phenomena and prediction of uranium pyrophoricity for the Hanford SNFP with specific applications to SNFP processes and situations.

Results Summary: See Chapter 9.

References of Resulting Reports, Letters, or Memoranda (Optional)

Author(s): Name (Print or Type)	Signature	Completion Date
Martin G. Plys	M. Plys	6/15/00
Boro Malinovic	Boro Malinovic	6/23/00
Michael Epstein	Michael Epstein	6/23/00

SECTION TO BE COMPLETED BY VERIFIER(S):

Verifier(s): Name (Print or Type)	Signature	Completion Date
Boro Malinovic		
Martin G. Plys	M. Plys	6/15/00

Method of Verification: Design Review ____, Independent Review or Alternate Calculations X, Testing ____

Other (specify) ____

SECTION TO BE COMPLETED BY MANAGER:

Responsible Manager: Name (Print or Type)	Signature	Approval Date
Martin G. Plys	M. Plys	6/22/00

Section	Author	Reviewer
1	Martin Plys	Boro Malinovic
2	Martin Plys	Boro Malinovic
3	Michael Epstein	Martin Plys
4	Michael Epstein	Martin Plys
5.1	Martin Plys	Boro Malinovic
5.2 - 5.6	Michael Epstein	Martin Plys
6	Martin Plys	Boro Malinovic
7.1	Martin Plys	Boro Malinovic
7.2	Boro Malinovic	Martin Plys
8.1, 8.2	Martin Plys	Boro Malinovic
8.3	Boro Malinovic	Martin Plys
9	Martin Plys	Boro Malinovic
10	Michael Epstein, Martin Plys	Boro Malinovic
App. A	Martin Plys	Boro Malinovic
App. B	N/A	N./A
App. C, D, E, F, G	Martin Plys	Boro Malinovic
App. H, I	Boro Malinovic	Martin Plys
App. J	Martin Plys	Boro Malinovic
App. K	N/A	N/A

SNF-6781
REV 0

CALCULATION NOTE METHODOLOGY CHECKLIST

CHECKLIST TO BE COMPLETED BY AUTHOR(S) (CIRCLE APPROPRIATE RESPONSE)

1. Is the subject and/or the purpose of the design analysis clearly stated? ... (YES) • NO
2. Are the required inputs and their sources provided? ... (YES) • NO • N/A
3. Are the assumptions clearly identified and justified? ... (YES) • NO • N/A
4. Are the methods and units clearly identified? ... (YES) • NO • N/A
5. Have the limits of applicability been identified? ... (YES) • NO • N/A
   (Is the analysis for a 3 or 4 loop plant or for a single application.)
6. Are the results of literature searches, if conducted, or other background data provided? ... (YES) • NO • N/A
7. Are all the pages sequentially numbered and identified by the calculation note number? ... (YES) • NO
8. Is the project or shop order clearly identified? ... (YES) • NO
9. Has the required computer calculation information been provided? ... (YES) • NO • N/A
10. Were the computer codes used under configuration control? Listings Provided → HANSF ... (YES) • NO • (N/A)
11. Were the computer code(s) used applicable for modeling the physical and/or computational problems identified? ... (YES) • NO • N/A
    (Is the correct computer code being used for the intended purpose.)
12. Are the results and conclusions clearly stated? ... (YES) • NO
13. Are Open Items properly identified ... YES • NO • (N/A)
14. Were approved Design Control practices followed without exception? ... YES • NO • (N/A)
    (Approved Design Control practices refers to guidance documents within NSD that state how the work is to be performed, such as how to perform a LOCA analysis.)
15. Have all related contract requirements been met? ... (YES) • NO • N/A

NOTE: If **NO** to any of the above, Page Number containing justification: _____